

Project Summary Report

Data for Thermophysical Properties of Humid Gases in Power Cycles[†]

DOE/NETL Interagency Agreement DE-AI26-06NT4295

Performing Agency:
Thermophysical Properties Division
National Institute of Standards and Technology
325 Broadway
Boulder, CO 80305

Allan H. Harvey[‡]
Mark O. McLinden
Richard A. Perkins

June 20, 2011

Project Duration: July 1, 2006 to May 31, 2010

[†] Contribution of the National Institute of Standards and Technology. Not subject to copyright in the United States.

[‡] Corresponding author; tel: 303-497-3555; a.harvey@boulder.nist.gov

EXECUTIVE SUMMARY

This report summarizes the results of work performed under DOE/NETL Interagency Agreement DE-AI26-06NT42957, which began in July 2006 and ended May 31, 2010. This report is organized by the three primary tasks as described in the Statement of Work (Attachment B to the Interagency Agreement). More detailed technical expositions of the work will be presented in publications in the scientific literature, which we will supply when they are ready for publication.

The key objectives for this work were to:

- (1) Use results of first-principles quantum mechanics to develop a description of the thermodynamics of humid gases in power cycles.
- (2) Validate the thermodynamic description by high-accuracy density measurements at high temperatures.
- (3) Measure the thermal conductivity of key water-nitrogen and water-CO₂ mixtures at conditions relevant to power cycles.

We produced a potential-energy surface for the water-carbon dioxide pair and used this to calculate second virial coefficients over a large temperature range with uncertainties better than all but the most precise experimental data. These results, together with previous results (not funded by this project) have been incorporated into software for accurate calculation of thermodynamic properties of humid gases containing H₂O with Ar, O₂, N₂, CH₄, CO, and CO₂ at any composition. The existing framework of the NIST REFPROP software [1] was used, and this software will be provided separately to DOE.

To validate the theoretical results, we developed in conjunction with this project (but with NIST funds) a new experimental apparatus to perform high-accuracy density measurements on the water-nitrogen and water-CO₂ systems at temperatures of 500 K, 560 K, and 620 K. Although considerable experimental difficulties were encountered, the measurements yielded virial coefficients consistent with the theoretical results.

For thermal conductivity, measurements are essential because no good theoretical approach is available for this property. Because water's electrical conductivity is problematic for the traditional DC (direct current) implementation of the transient hot-wire technique, an AC (alternating current) version of the apparatus was developed. Thermal conductivity measurements of mixtures of (N₂ or CO₂) with water have been completed for two compositions each at temperatures of 500 K to 740 K. The density dependence of the mixture thermal conductivity falls between those of the pure components at a fixed temperature.

INTRODUCTION AND APPROACH

Innovative power cycles (such as IGCC and oxyfuel) are being developed for production of electric power with higher efficiency and reduced environmental impact, including the possibility of CO₂ sequestration. For optimizing the design of these systems, it is important to have accurate values of the thermophysical properties (density, heat capacity, thermal conductivity, etc.) of the fluid mixtures in the turbines and other parts of these cycles. These mixtures have a large water content, along with other gases such as nitrogen and carbon dioxide; they are at high temperatures where thermodynamic data are scarce, but the pressures are only moderately high. Typical approaches such as ideal-gas thermodynamics or common engineering equations of state are inaccurate for such systems, primarily due to the presence of water. Therefore, it is necessary to develop alternative modeling approaches, supplemented by selected high-temperature experimental measurements.

The description of the thermodynamic properties is developed here at the level of the second virial coefficient, which is the first-order correction to the ideal-gas law. The key parameters are the “cross” second virial coefficients representing interactions between one water molecule and one gas molecule. Our approach is to use computational quantum mechanics to develop accurate surfaces describing the potential energy between the molecules, from which the virial coefficients can be calculated with high accuracy.

In order to validate our theoretical results, we measured the key water-nitrogen and water-CO₂ systems at high temperatures. The high temperatures are necessary because adsorption renders the measurements nearly impossible below about $T = 500$ K, but few laboratories have the capability for precision densimetry at high temperatures. We developed such a capability in conjunction with this work. The instrument is known as a “single-sinker magnetic-suspension densimeter” operating on the Archimedes or buoyancy principle. By knowing the sinker volume and comparing the apparent weight while it is immersed in the gas mixture to the known mass of the sinker, the density is determined.

We have developed parallel capability for measuring the thermal conductivities of these mixtures at high temperatures; in this case the measurements are essential because no good theoretical approach is available for this property. The measurements use the transient hot-wire method, which has become the method of choice for high-accuracy thermal conductivity measurements. Because water’s electrical conductivity is problematic for the traditional DC implementation of this technique, an AC version of the apparatus has been developed.

1. THERMODYNAMIC MODELING (TASK 1)

The goal of this task was to produce accurate models (including nonideal gas effects) for the thermodynamics of gaseous mixtures commonly found in the post-combustion portions of power cycles. The main components of such mixtures would be H₂O, CO₂, and N₂, with the interactions involving H₂O being most important for the nonideality.

A theoretically rigorous way of describing gas-phase nonideality is the virial expansion, which gives a series of corrections to the ideal gas as a function of the molar density ρ :

$$\frac{P}{\rho RT} = 1 + B\rho + C\rho^2 + \dots \quad (1.1)$$

In Eq. (1.1), the second virial coefficient B represents interactions between pairs of molecules, the third virial coefficient C represents three-molecule interactions, and so forth. Other key thermodynamic properties such as enthalpies, entropies, heat capacities, and fugacity coefficients can be obtained by appropriate manipulation of Eq. (1.1). For pressures up to at least 5 MPa, and up to 10 MPa at higher temperatures, sufficient accuracy can be obtained by truncating Eq. (1.1) after the B term. The second virial coefficient for the mixture B_m is a mole-fraction sum of contributions from all pairs of species in the system:

$$B_m = \sum_i \sum_j x_i x_j B_{ij} \quad (1.2)$$

For the terms in Eq. (1.2) where $i = j$, B_{ij} is simply a pure-component property and is known with high accuracy for the fluids of interest here. However, there is a serious lack of “cross” second-virial-coefficient data for unlike water-gas pairs due to the difficulty of the required experiments. Obtaining accurate cross second virial coefficients for water-gas pairs is therefore the key to modeling the thermodynamics of these systems with quantitative accuracy.

For the H₂O-N₂ pair, an earlier project at NIST made use of computational chemistry to produce B_{ij} for this pair over a wide temperature range. The accuracy is comparable to that of the best experiments, but the temperature range covered (100 K to 3000 K) is much wider, encompassing the range of interest for combustion turbines. This work has been published by Tulegenov et al. [2] The results of this work were described by the equation

$$B_{12}(T) = c_1(T^*)^{-0.24} + c_2(T^*)^{-1.06} + c_3(T^*)^{-3.22}, \quad (1.3)$$

where $T^* = T/(100 \text{ K})$, B_{12} and the c_i have units of $\text{cm}^3 \text{ mol}^{-1}$, and $c_1 = 67.595$, $c_2 = -249.83$, and $c_3 = -204.38$.

The second virial coefficients from Eq. (1.3) are in good agreement with the limited experimental data [3-13] available both for $B_{12}(T)$ and for the quantity $\phi = B - T(dB/dT)$, as shown in Figures 1.1 and 1.2; see Tulegenov et al. [2] for details.

For theory-based calculation of the influence of H₂O-CO₂ interactions on the thermodynamic properties, NIST contracted in the present project with the Chemistry Department at the University of Nottingham (Dr. Richard Wheatley, Principal Investigator), to supply a high-quality potential-energy surface for the molecular pair, and interaction second virial coefficients $B_{12}(T)$ calculated from that surface. The results of this work were delivered to NIST in December 2009, with analysis and verification of the results and their uncertainties performed during 2010.

The results for the H₂O-CO₂ system are described by the equation

$$B_{12}(T) = c_1(T^*)^{-0.126} + c_2(T^*)^{-1.34} + c_3(T^*)^{-3.75} + c_4(T^*)^{-7.6}, \quad (1.4)$$

where $T^* = T/(100 \text{ K})$, B_{12} and the c_i have units of cm³ mol⁻¹, and $c_1 = 47.54$, $c_2 = -658.04$, $c_3 = -3969.1$, $c_4 = -24225$.

The second virial coefficients from Eq. (1.4) are in good agreement with the limited experimental data [14-19] available both for $B_{12}(T)$ and for the quantity $\phi = B - T(dB/dT)$. Figures 1.3 and 1.4 show these comparisons, which give us confidence that the theoretical results should be reliable at higher temperatures (turbine conditions). We note, however, that the uncertainty at the low end of the temperature range of Fig. 1.3 is larger than we might hope and larger than that for the H₂O-N₂ system; this is because of the larger number of atoms and electrons in CO₂ (rendering the quantum calculations more difficult) and the relatively greater strength of the H₂O-CO₂ interaction. The details of this work are reported by Wheatley and Harvey [20].

Previous work at NIST (with academic collaborators) has produced similar results for H₂O with argon [21], methane [22], oxygen [23], and carbon monoxide [24]. These can also be incorporated in the thermodynamic calculations in order to deal with their possible presence in combustion gases.

To make these new data accessible for the calculation of thermodynamic properties of humid gases, it was decided to use the existing framework of the NIST REFPROP software [1]. REFPROP contains a mixture thermodynamic model that reduces to the available high-accuracy equations of state at the pure-component limits. For the nonaqueous components of combustion gases, the mixture interaction parameters have already been optimized in previous work on

natural gas, air, etc. Therefore, only the parameters for interactions involving water were optimized here. The procedure involved generating mixture second virial coefficients for each pair over a range of temperatures, and then adjusting the binary mixing parameters within REFPROP to reproduce those coefficients.

The REFPROP calculations for these properties have been implemented as a spreadsheet plug-in with functions to call for various properties. This is being provided separately to DOE, with documentation adapted from the existing REFPROP documentation.

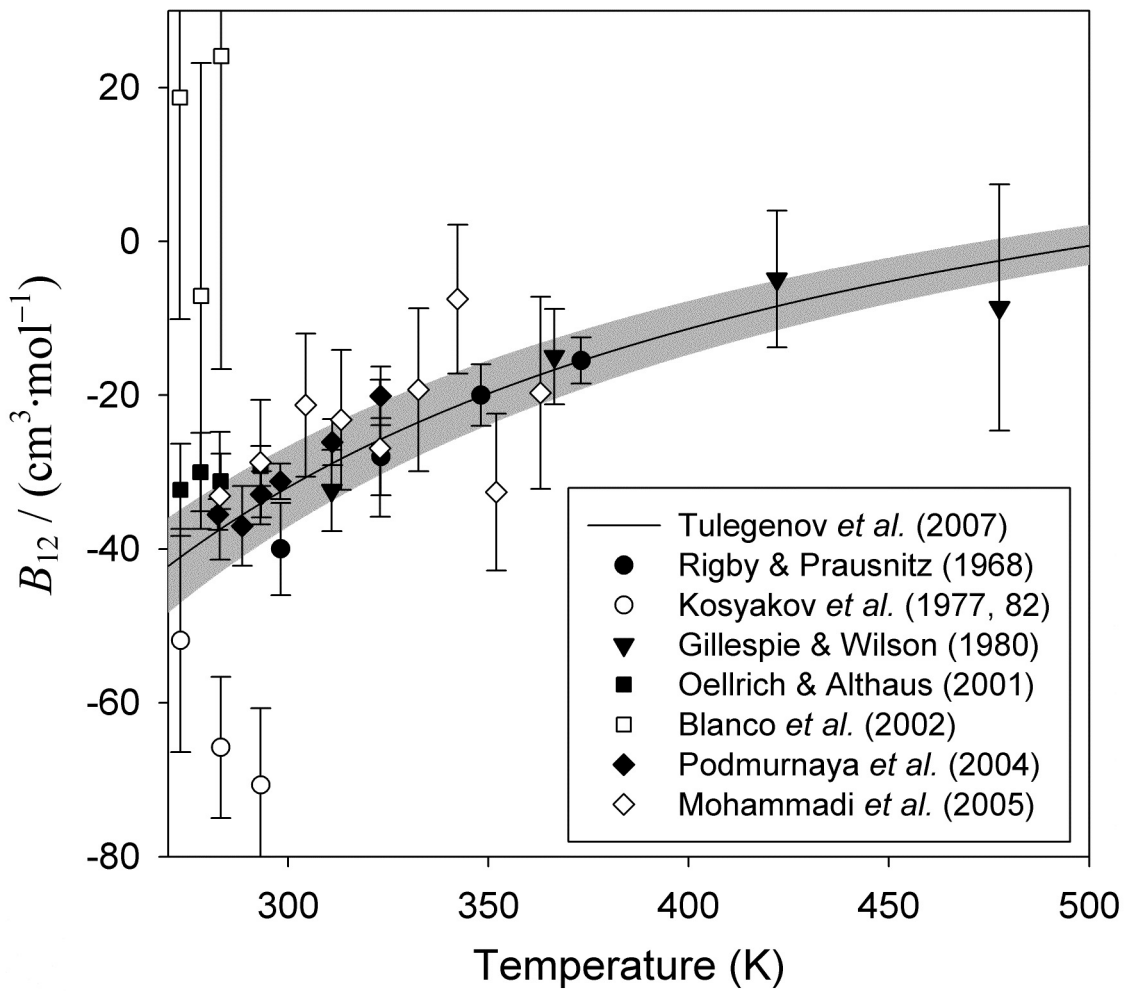


Figure 1.1. Comparison of $B_{12}(T)$ predicted from theory to available experimental data for the $\text{H}_2\text{O}/\text{N}_2$ binary; shading and error bars represent expanded ($k=2$) uncertainty approximately equivalent to a 95% confidence level.

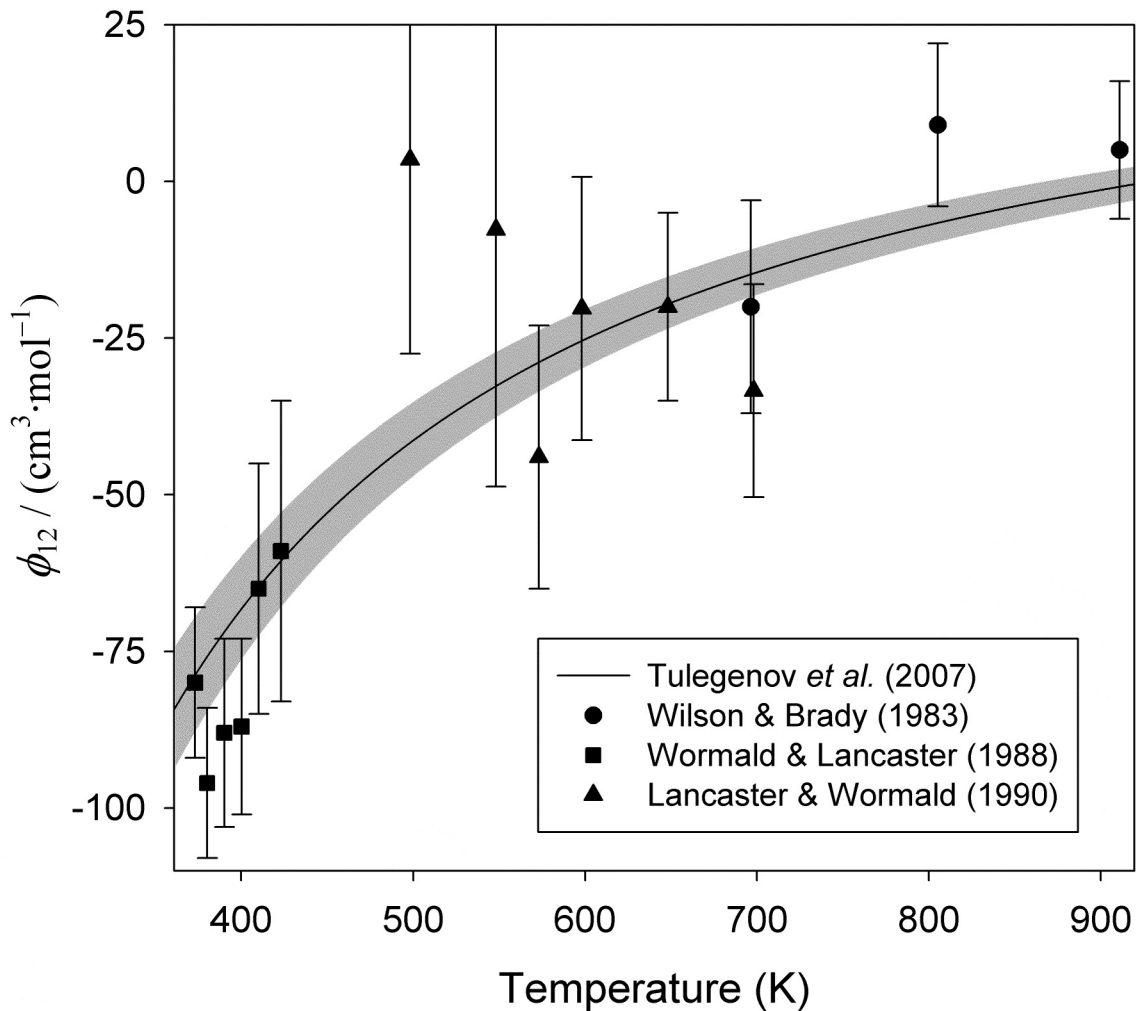


Figure 1.2. Comparison of $\phi = B - T(dB/dT)$ predicted from theory to available experimental data for the $\text{H}_2\text{O}/\text{N}_2$ binary; shading and error bars as in Fig. 1.1

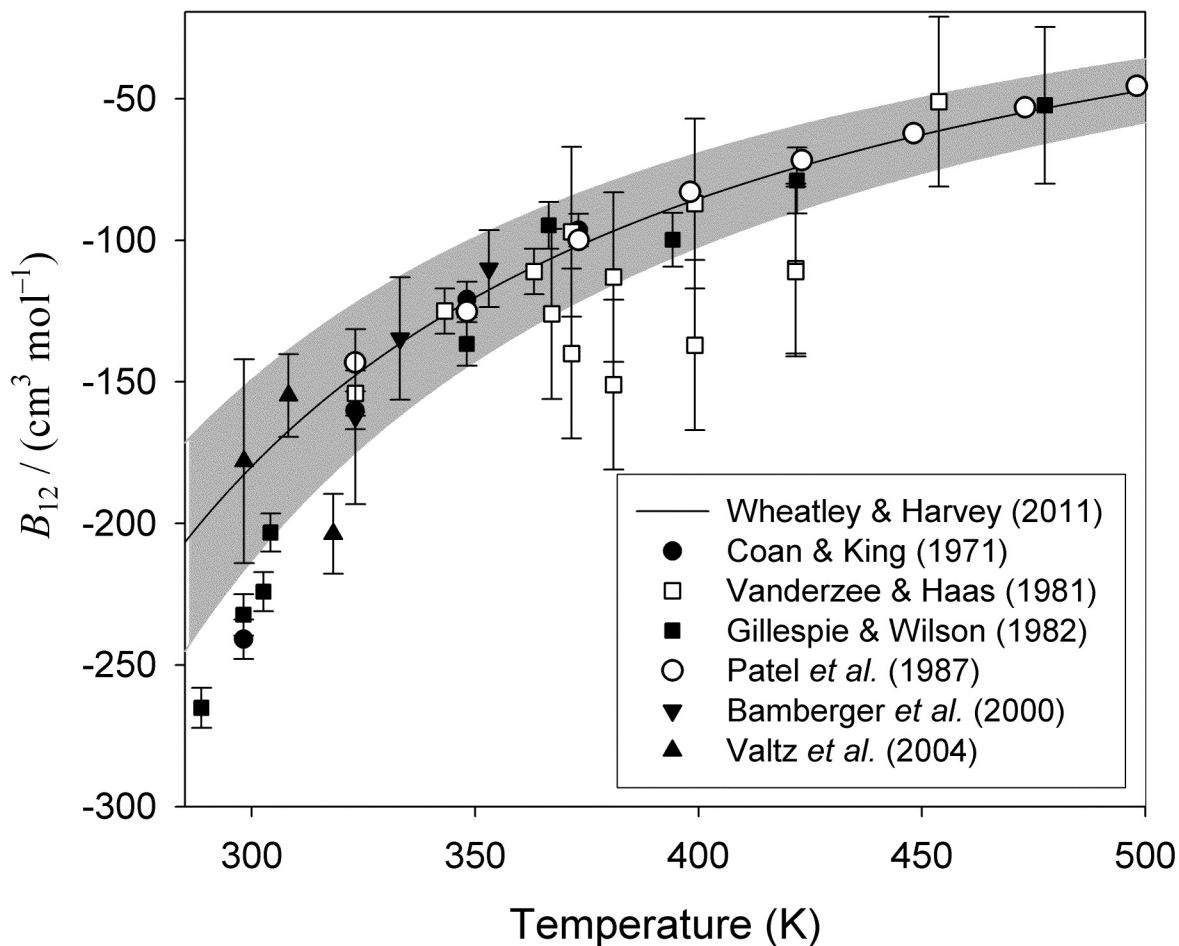


Figure 1.3. Comparison of $B_{12}(T)$ predicted from theory to available experimental data for the $\text{H}_2\text{O}/\text{CO}_2$ binary; shading and error bars represent expanded ($k=2$) uncertainty approximately equivalent to a 95% confidence level.

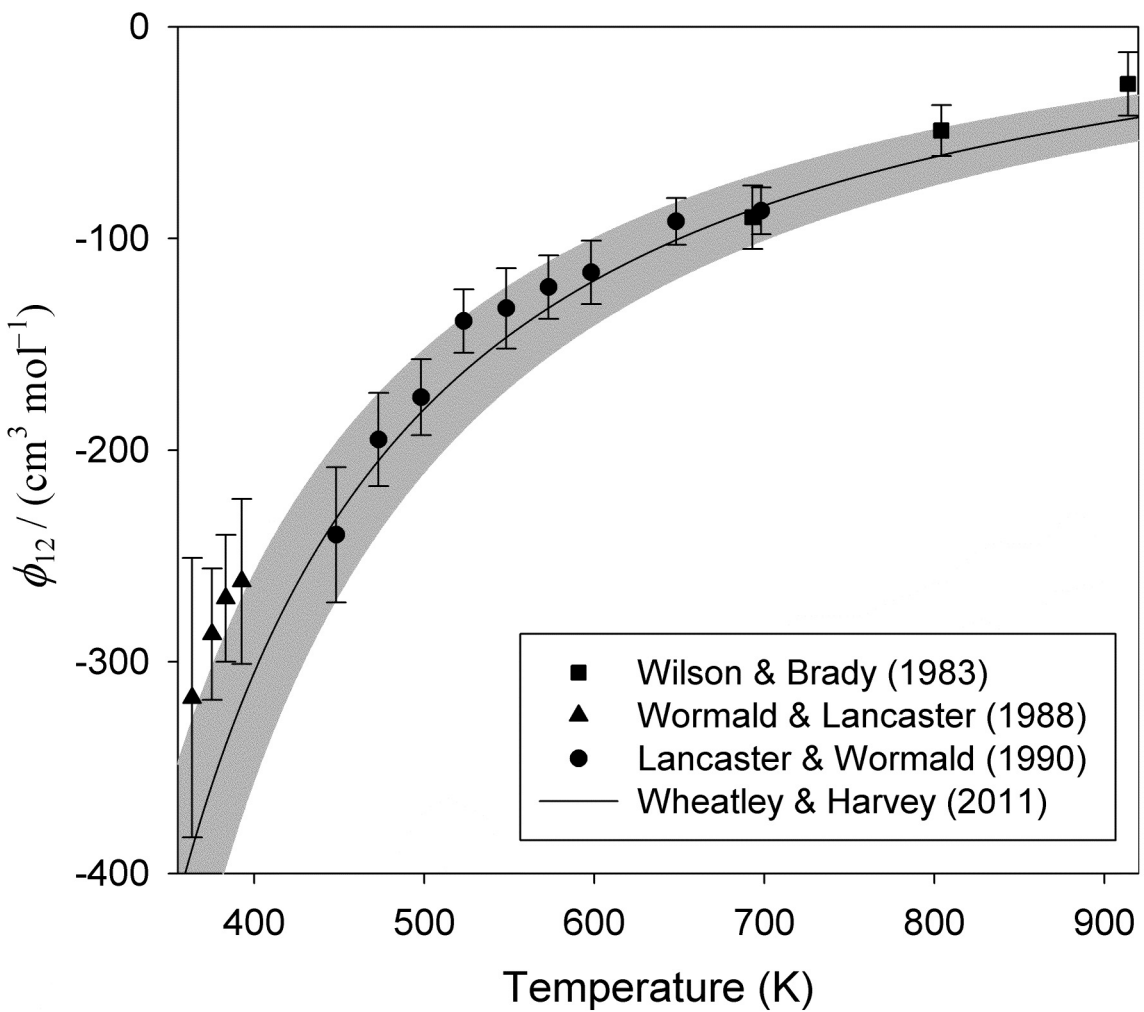


Figure 1.4. Comparison of $\phi = B - T(dB/dT)$ predicted from theory to available experimental data for the $\text{H}_2\text{O}/\text{CO}_2$ binary; shading and error bars as in Fig. 1.3

2. EXPERIMENTAL VALIDATION OF THERMODYNAMICS (TASK 2)

To validate the theoretical results, we developed in conjunction with this project a new experimental apparatus to perform high-accuracy density measurements on the key water-nitrogen and water-CO₂ systems at high temperatures. The high temperatures are necessary because adsorption renders the measurements nearly impossible below about 500 K, but few laboratories have the capability for precision densimetry at high temperatures. The instrument is known as a “single-sinker magnetic-suspension densimeter.” The apparatus (which was developed with NIST funds) and measurements using it are described in this section.

Measurements were carried out on the water-nitrogen and water-CO₂ systems at temperatures of 500 K, 560 K, and 620 K. Although the sinker (the key measuring element of the densimeter) was damaged (i.e., gained mass due to oxidation) during the measurements, an analysis compensating for the damage yields virial coefficients consistent with the theoretical results.

2.1 Measuring Principle of the Densimeter

The present measurements utilized a single-sinker densimeter with a magnetic suspension coupling. This type of instrument applies the Archimedes (buoyancy) principle to provide an absolute determination of the density. This general type of instrument is described by Wagner and Kleinrahm [25]. Briefly, a sinker is weighed with a high-precision balance while it is immersed in a fluid of unknown density. The fluid density ρ (on a mass basis) is given by

$$\rho = \frac{m - W}{V} , \quad (2.1)$$

where m and V are the sinker mass and volume and W is the balance reading. A magnetic suspension coupling transmits, to the balance, the weight of the sinker across a coupling housing, which separates the fluid from the atmosphere. The coupling consists of an electromagnet (in air) and a permanent magnet (in the fluid). The permanent magnet is linked with a lifting device to pick up the sinker for weighing. In addition to the sinker, two calibration masses (designated “tare” and “cal”) are also weighed in separate weighings, providing a calibration of the balance.

With proper design, the efficiency of this force transmission is nearly one, but the coupling will be influenced by nearby magnetic materials, external magnetic fields, and the magnetic properties of the fluid being measured. These give rise to a “force transmission error” (FTE) that must be accounted for to realize the full accuracy of this technique [26]. Eq. (2.1) does not include the force transmission error—it must be modified to yield the correct density.

Three distinct weighings were carried out for each density determination:

- (1) the sinker together with the “tare” mass,
- (2) the “cal” mass, with the sinker on its rest and the permanent magnet in suspension, and
- (3) the “tare” mass with the sinker on its rest and the permanent magnet in suspension.

Weighings (1) and (2) define the fluid density, and weighings (2) and (3) provide a calibration of the balance. The “tare” and “cal” masses are also serve to more nearly equalize the total load on the balance during weighings (1) and (2) and thereby minimize errors due to balance nonlinearity effects. The balance reading for each of the weighings was a result of a summation of the loads on the balance as follows:

$$W_1 = \alpha \left[\phi \left\{ m_s + m_{p\text{-mag}} - \rho_{\text{fluid}} (V_s + V_{p\text{-mag}}) \right\} + m_{e\text{-mag}} + m_{\text{tare}} - \rho_{\text{air}} (V_{e\text{-mag}} + V_{\text{tare}}) \right] \quad (2.2)$$

$$W_2 = \alpha \left[\phi \left\{ m_{p\text{-mag}} - \rho_{\text{fluid}} V_{p\text{-mag}} \right\} + m_{e\text{-mag}} + m_{\text{cal}} - \rho_{\text{air}} (V_{e\text{-mag}} + V_{\text{cal}}) \right] \quad (2.3)$$

$$W_3 = \alpha \left[\phi \left\{ m_{p\text{-mag}} - \rho_{\text{fluid}} V_{p\text{-mag}} \right\} + m_{e\text{-mag}} + m_{\text{tare}} - \rho_{\text{air}} (V_{e\text{-mag}} + V_{\text{tare}}) \right] \quad (2.4)$$

where:

α = balance calibration factor

ϕ = coupling factor

ρ_{fluid} = mass density of fluid under test

ρ_{air} = mass density of ambient air (or purge gas) in the balance chamber

V = volume

m = mass

W = balance reading

subscripts: s: sinker

cal: (heavier) calibration mass

tare: (lighter) calibration mass

p-mag: permanent magnet (in fluid), includes the lifting device

e-mag: electromagnet (in air), includes linkage to the balance.

The coupling factor ϕ accounts for the efficiency of the magnetic suspension coupling; it is a multiplier applied to the loads that are held in suspension by the coupling. The balance calibration factor α applies to the total load on the under-pan weighing hook of the balance. The key assumptions implicit in Eqs. (2.2–2.4) are that (a) the force transmitted to the balance by the magnetic suspension coupling is proportional to the suspended load; the proportionality factor, or coupling factor ϕ , is directly related to the FTE; (b) all quantities (and in particular α , ϕ , and ρ_{fluid}) are constant over the several minutes needed for a complete density determination; and (c) the balance reading is linear with the applied load.

Equations (2.3) and (2.4) are solved for the balance calibration factor:

$$\alpha = \frac{W_2 - W_3}{(m_{\text{cal}} - m_{\text{tare}}) - \rho_{\text{air}}(V_{\text{cal}} - V_{\text{tare}})} , \quad (2.5)$$

and Eqs. (2.2) and (2.3) are solved for the fluid density:

$$\rho_{\text{fluid}} = \frac{\phi m_s + (m_{\text{tare}} - m_{\text{cal}}) - (W_1 - W_2)/\alpha - \rho_{\text{air}}(V_{\text{tare}} - V_{\text{cal}})}{\phi V_s} . \quad (2.6)$$

Equation (2.6) yields the fluid density in terms of directly measured quantities, except that the coupling factor is unknown. McLinden et al. [26] demonstrate that ϕ is composed of an “apparatus contribution” ϕ_0 and a fluid-specific contribution:

$$\phi = \phi_0 + \varepsilon_\rho \frac{\chi_s}{\chi_{s0}} \frac{\rho_{\text{fluid}}}{\rho_0} , \quad (2.7)$$

where χ_s is the specific magnetic susceptibility of the fluid, $\rho_0 = 1000 \text{ kg}\cdot\text{m}^{-3}$ and $\chi_{s0} = 10^{-8} \text{ m}^3\cdot\text{kg}^{-1}$ are reducing constants, and ε_ρ is an apparatus-specific constant. The constant ε_ρ was obtained from a calibration with nitrogen, as discussed in Section 2.5.2.

The apparatus contribution to the force transmission error, ϕ_0 , is ordinarily obtained by weighing the sinker with the coupling in an evacuated measuring cell. It can be determined from Eq. (2.6) with ($\rho_{\text{fluid}} = 0$):

$$\phi_0 = \frac{-(m_{\text{tare}} - m_{\text{cal}}) + (W_1 - W_2)/\alpha + \rho_{\text{air}}(V_{\text{tare}} - V_{\text{cal}})}{m_s} . \quad (2.8)$$

2.2 Densimeter Description

A photograph of the entire densimeter is shown as Figure 2.1. It consists of the following key components:

- the sinker, which, together with a balance, the magnetic suspension coupling, and a mechanism to pick up the sinker, constitute the density measuring system;
- a measuring cell (pressure vessel) that contains the sinker and the fluid of interest;
- a thermostat system incorporating fluid cooling and electrical heating;
- pressure- and temperature-measuring instruments;
- a computer, which controls the entire system and records the experimental data; and
- auxiliary systems, such as a sample charging manifold and a vacuum system.

Each of these key components is now described in turn.

2.2.1 Density System and Measuring Cell

The density system, including the measuring cell (pressure vessel), sinker, and magnetic suspension coupling, was manufactured by Rubotherm GmbH¹. The density system is depicted in Figure 2.2, and is briefly described here.

The sinker was made of single-crystal silicon ($\rho = 2329 \text{ kg}\cdot\text{m}^{-3}$), and it had a nominal mass of 15.068 g to give a volume of 6.470 cm³ at ambient conditions. The sinker was contained within a measuring cell designed for pressures up to 50 MPa. The sinker was picked up with a “lifting hook” fabricated of a nickel-chromium alloy (UNS N06625; Inconel 625®); the lifting hook was weighed along with the sinker and was effectively part of the sinker. The total mass and volume of the sinker plus lifting hook were 17.276 g and 6.709 cm³ at ambient conditions.

Isolation of the fluid sample from the balance was accomplished with a magnetic suspension coupling. The central elements of the coupling are two magnets, one on each side of a nonmagnetic, pressure-separating wall. The top magnet, which is an electromagnet with a ferrite core, is outside the pressure vessel and is suspended from the under-pan weighing hook of the balance. The bottom magnet, which is a permanent magnet, is inside the measuring cell, completely immersed in the sample fluid, and is held in a freely suspended state by the electromagnet. A position sensor is also part of the coupling, and the stable suspension is maintained by means of a feedback control circuit making fine adjustments in the electromagnet current. A “lifting device” connected to the permanent magnet engages the “lifting hook” to weigh the sinker. The weight of the sinker is thus transmitted to the balance (Sartorius CC111), which had a total capacity of 111 g and an electronic range of 31 g; its resolution was 1 µg. The balance was enclosed by a plastic draft hood to improve the stability of the weighings. The magnetic suspension coupling/balance combination is stable and repeatable at the level of a few micrograms to yield a resolution in density of 0.001 kg·m⁻³.

2.2.2 Thermostat and Temperature System

The thermostat provides a uniform and controlled temperature environment for the fluid sample and magnetic suspension coupling. The thermostat is a vacuum-insulated, and a detailed diagram of the thermostat and density system is shown as Figure 3. Multiple layers of active (heated or cooled) and passive shields are used.

¹ Certain trade names and products are identified only to adequately document the experimental equipment and procedure. This does not constitute a recommendation or endorsement of these products by the National Institute of Standards and Technology, nor does it imply that the products are necessarily the best available for the purpose.

The innermost element, which includes the measuring cell and magnetic suspension coupling, is controlled within 5 mK of a constant temperature with an uncertainty in temperature of 20 mK. The measuring cell comprises upper and lower parts; both have close-fitting copper sleeves to decrease temperature gradients.

The next two levels of the thermostat are the inner and outer shields. The inner shield attaches to the top of the upper copper sleeve of the measuring cell; it is maintained at the cell temperature. The outer sleeve surrounds the measuring cell and inner shield and is maintained at a temperature 0.5 to 1 K cooler than that of the measuring cell. The temperature is constant to within 50 mK. Both the inner and outer shields are electrically heated and also have fluid channels to allow operation at below-ambient temperatures by flowing a fluid from a temperature-controlled circulating bath. (In the present work, all measurements were carried out at elevated temperatures, and the cooling channels were used only to quickly cool the system between isotherms). The shields were fabricated primarily from lengths of standard copper pipe. The top disk of the outer shield was fabricated from dispersion-strengthened copper (UNS C15725; Glidcop AL25®); this material possesses nearly the same thermal conductivity as pure copper, but it retains its strength at high temperatures.

The outer shield is surrounded by four passive radiation shields of thin stainless steel foil. The outermost element of the thermostat is the vacuum can. The vacuum system consists of an oil diffusion pump plus liquid nitrogen cold trap backed by a mechanical vacuum pump. Feedthroughs for the electrical connections and fluid lines are made through a “feedthrough collar” located just above the top of the shields.

Magnetic materials will affect the magnetic suspension coupling. The acceptable materials vary with the distance from the coupling. In the immediate vicinity of the magnets, only materials with a low magnetic susceptibility can be used. The measuring cell is constructed of a nickel–molybdenum–chromium alloy (UNS N10242; Haynes 242®). This material is slightly magnetic and results in a force transmission error that is large compared to that for the typical alloys used for magnetic suspension couplings (e.g., beryllium copper); this is discussed further in section 2.5. This alloy was selected because of its high strength and corrosion resistance at temperatures up to 800 K. Within about 1 m of the coupling, copper, aluminum, and brass can be used, and small quantities of stainless steel are acceptable. At distances beyond about 1 m from the coupling, carbon steel and other ferromagnetic materials will not disturb the coupling. It is important, however, to keep strong permanent magnets at a distance of at least 2 m.

Care has been taken to construct the thermostat of nonmagnetic materials. The inner and outer shields are copper, and the vacuum chamber, balance plate (which forms the top of the vacuum chamber), and base plate are aluminum. The screws are type 316 or A286 stainless steel. The fluid fittings are type 316 stainless steel; these were tested before installation to verify that they were minimally magnetic. The mechanical vacuum pump, which is made largely of steel and has a large motor, is located about 2 m from the apparatus. Steel gas cylinders are located at a similar distance.

Temperatures were measured with a variety of probes, depending on the required accuracy. The sample temperature requires the highest accuracy, and this temperature was measured by a $25\ \Omega$ long-stem standard platinum resistance thermometer (SPRT) (Rosemount model 162CE) in a thermowell in the lower measuring cell at the same level as the sinker. This “cell SPRT,” which measured the temperature reported in the p - ρ - T results, was measured with an AC resistance bridge (ASL model F700). The $25\ \Omega$ reference resistor for the bridge (Tinsley type 5685A) was thermostatted at $36.0 \pm 0.1\ ^\circ\text{C}$ in a small enclosure.

The heat to the measuring cell and shields was controlled using the output of small $100\ \Omega$ PRTs read by a nanovoltmeter (Keithley model 2002 with a model SCAN-2001 scanning card). They have a short-term stability of $10\ \text{mK}$, however the absolute temperature does not need to be known accurately. The temperatures of the room and the balance enclosure were also measured with $100\ \Omega$ PRTs read by the nanovoltmeter. The temperatures of the pressure transducers were measured with their internal quartz thermometers and internal circuitry.

The humidity inside the draft hood was read by a thin-film, capacitance-type humidity transmitter (Vaisala model PTU303).

2.2.3 Pressure Measuring System

The pressure of the sample was measured with a vibrating-quartz-crystal-type pressure transducer with a full-scale range of $69\ \text{MPa}$ (Paroscientific model 9000-10K-105). The transducer was in direct communication with the sample—the transducer was water filled, but no differential pressure diaphragm was used. The atmospheric pressure was read by a vibrating-quartz-crystal-type pressure transducer (Paroscientific model 6000-30A).

2.2.4 Control System and Measurement Sequence

Measurements were made along isotherms starting at the highest pressure. A computer program written in Visual Basic 6 provides three main functions. The PC automates and controls the experiment, provides data logging of all the instrument readings, and serves as a PID controller for the electric heaters on the cell and shields.

All the instruments were scanned once each minute through either the serial RS-232 ports or an IEEE-488 interface. Temperatures were controlled by the modified PID algorithm of Hust *et al.* [27] implemented in the control program. A running average and standard deviation of the temperatures and pressures were computed for the preceding eight readings. When these were within preset tolerances of the set-point conditions, a weighing sequence was triggered.

Weighings were made in the order: tare weight; sinker + tare weight; calibration weight; sinker + tare weight; calibration weight; sinker + tare weight; and tare weight for a total of seven weighings—two or three repetitions for each of the weighings outlined by Eqs. (2.2–2.4). The weighing design is symmetrical with respect to time, and this will tend to cancel any drift in the temperature or pressure. The weighings were spaced 60 to 90 seconds apart to give adequate time for the sinker to be picked up (or a calibration mass to be placed on the balance pan) and to allow the magnetic suspension coupling and balance to reach a stable weight.

The temperatures and pressures were recorded between each weighing and also before the first weighing and after the final weighing. The resistances of the thermometers, temperature and pressure periods of the pressure transducers, and individual balance readings were written to a file; more than 300 individual instrument readings were recorded for each density determination. The calibrations for the various instruments were applied to the raw data, and the multiple readings were averaged in a separate analysis program.

Multiple replicate determinations of density were made at each (T, p) state point. The control program then prompted the operator to vent the sample to the next pressure on the isotherm. Following every isotherm, the cell was vented to atmospheric pressure and the measuring cell was filled with pure nitrogen or carbon dioxide and several further density determinations were made. Ordinarily, a vacuum measurement would be carried out to determine the ϕ_0 that appears in Eq. (2.6). In this apparatus, however, the very small diameter of the filling capillary would require a very long time to thoroughly evacuate the cell, and any leak in that line might result in a significant pressure. We determined that measurements at atmospheric pressure (as measured by the very accurate barometer) would yield a known density (from an equation of state) of lower uncertainty than assuming that the density was “zero” with a (possibly imperfect) vacuum. The equation for ϕ_0 is thus modified to

$$\phi_0 = \frac{-(m_{\text{tare}} - m_{\text{cal}}) + (W_1 - W_2)/\alpha + \rho_{\text{air}}(V_{\text{tare}} - V_{\text{cal}})}{(m_s - \rho_{\text{atm}}V_s)} - \varepsilon_\rho \frac{\chi_s \rho_{\text{atm}}}{\chi_{s0} \rho_0}, \quad (2.9)$$

where ρ_{atm} is the fluid density at the temperature of the measuring cell and atmospheric pressure as calculated by an equation of state (Span *et al.* [28] for nitrogen or Span and Wagner [29] for

carbon dioxide). It will be seen below that ϕ_0 is required in the calibrations needed to determine the parameter ε_ρ , but ε_ρ is required in the above equation for ϕ_0 . The fluid-specific term (second term on right-hand side of Eq. (2.9)), is very small (order of 10^{-6}) at atmospheric pressure, however, and an approximate value of ε_ρ suffices in the calibration.

2.3 Experimental Samples

The nitrogen used here was “UHP grade” (Scott Specialty Gases) with a stated purity of 99.9995 mol %. The carbon dioxide was “research grade” (Scott Specialty Gases) with a certified purity of 99.9972 mol %. Deionized water was degassed by boiling for 10 minutes prior to storage in an evacuated piston pump with wetted parts of 316 stainless steel and poly-tetrafluoroethane (PTFE). The mixtures were prepared gravimetrically, as described in Section 4.

2.4 Measured p - ρ - T Data

Measurements were carried out along isotherms at nominal temperatures of 500 K, 560 K, and 620 K on binary mixtures of N₂/H₂O and CO₂/H₂O; two or three mixture compositions were measured at each temperature for each system. In addition, pure nitrogen was measured at nominal temperatures of 400 K, 500 K, 560 K, and 620 K, and pure carbon dioxide was measured at $T = 500$ K; the pure-fluid measurements followed the mixture measurements and were used to calibrate the instrument. For each isotherm, measurements were made at eight to ten pressures, with at least four replicates at each pressure. Figure 2.4 depicts the data points measured.

2.5 Calibrations and Uncertainty

2.5.1 Transducer Calibrations

The reported temperature was determined with the measuring-cell SPRT, which was calibrated on ITS-90 in the temperature range from (273 to 693 K) by using fixed-point cells (water triple point, tin freezing point, and zinc freezing point). The expanded uncertainty ($k = 2$) in the temperature instrumentation itself was 4 mK. A calibration at the water triple point following the mixture measurements showed a resistance change equivalent to 9 mK in temperature. This observed drift in the PRT, along with temperature gradients in the measuring cell and short-term oscillations in the cell temperature, increase the overall temperature uncertainty to 20 mK.

The pressure transducer was calibrated by use of a piston gauge. The expanded uncertainty ($k = 2$) of the pressure measurement is $(52 \times 10^{-6} \cdot p + 2.0)$ kPa), including the calibration, hydrostatic head correction, and drift in the transducer.

The masses of the sinker and lifting hook were determined with a double-substitution weighing design [30] using ASTM class 1 standard masses and a Mettler AX205 balance (capacity 205 g, resolution 10 μg). The uncertainty of the object masses at the time of calibration is estimated to be 20 μg . The volumes were determined at 293.15 K and atmospheric pressure by use of a hydrostatic comparator. This technique is described by Bowman et al., [31, 32] and our implementation of this technique is described in reference [33]. These volumes were adjusted for temperature with linear thermal expansion data for silicon from Swenson [34] and for Inconel (lifting hook) from Smithells [35]. The volumes of the sinker and hook were adjusted for pressure effects using literature values for the bulk modulus.

Because of changes in the sinker mass and volume (due to oxidation) as the experiments proceeded, these uncertainties must be increased significantly. Based on the variation of mass with time and the standard deviation of sinker mass observed for replicate points in the analysis described in Section 2.4, the estimated expanded uncertainty in sinker mass is 150 μg . The sinker volume was assumed to change at the same rate as the mass, resulting in a volume uncertainty of 0.010 %.

2.5.2 Determination of the Parameter ϕ_0

The parameter ϕ_0 , which characterizes the apparatus contribution of force transmission error, was determined from the measurements on pure nitrogen and pure carbon dioxide at atmospheric pressure carried out after the mixture measurements. The weighing data were combined with the densities computed from an equation of state (Span et al. [28] for nitrogen or Span and Wagner [29] for carbon dioxide) and Eq. (2.9). The resulting values of ϕ_0 are shown in Figure 2.5. This parameter is a function of temperature, but it is highly repeatable for a given temperature. The standard deviations for replicate determinations of ϕ_0 at the various temperatures ranged from 0.78×10^{-6} at $T = 560$ K to 1.80×10^{-6} at $T = 400$ K.

2.5.3 Determination of the Parameter ε_ρ

In most magnetic suspension densimeters, the value of ε_ρ in Eq. (2.7) (the parameter characterizing the fluid-specific portion of the force transmission error) is on the order of 50×10^{-6} or less, and the fluid-specific effect is small. Because the measuring cell and coupling housing of our densimeter were constructed of a slightly magnetic nickel alloy, ϕ_0 differed significantly from 1 and ε_ρ was much larger. McLinden et al. [26] describe a technique to determine ε_ρ that involves measurements on several gases with varying values of the specific magnetic susceptibility with two different sinkers of greatly different densities (e.g., silicon and tantalum); such tests are extremely time-consuming because the densimeter must be substantially disassembled to install the different sinkers. McLinden et al. [26] also describe an alternate and

much simpler approach that would ordinarily require measurements on oxygen (a highly paramagnetic fluid). Because of the large magnetic effects in the present densimeter, the measurements with pure nitrogen that were carried out after completion of the mixture tests could be used to determine ε_ρ through the equation

$$\varepsilon_\rho = \left[\frac{\rho_{\phi=\phi_0} - \rho_{\text{EOS}}}{\rho_{\text{EOS}}} \right] / \left[\frac{\chi_s}{\chi_{s0}} \left(\frac{\rho_{\text{EOS}}}{\rho_0} - \frac{\rho_s}{\rho_0} \right) \right], \quad (2.10)$$

where $\rho_{\phi=\phi_0}$ is the density determined by Eq. (2.6) with $\phi = \phi_0$, and ρ_{EOS} is the “true” density of the fluid at the experimental conditions given by a reliable equation of state (such as [28]). The specific magnetic susceptibility of nitrogen is taken from [36].

Figure 2.6 shows the values thus obtained. The dependencies on temperature and density are small, and we adopted the mean value of $\varepsilon_\rho = 2725 \times 10^{-6}$; the standard deviation in this value is 136×10^{-6} ; this effect results in an uncertainty of 0.03 % in density.

2.5.4 Correction for Changing Sinker Mass

After completing the measurements at the lowest pressure on a given isotherm, the mixture was vented and the cell was purged repeatedly with pure nitrogen or carbon dioxide (depending on the mixture just completed). The filling valve on the cell was then opened to atmospheric pressure and the density of the pure gas was measured to determine the parameter ϕ_0 according to Eq. (2.9). This parameter is expected to be only a function of temperature, but the calculated value was observed to drift in a systematic way over time. This led us to suspect that the sinker was being corroded by the aqueous systems being measured. Following all the measurements, we tore down the densimeter and removed the sinker for inspection.

After removal from the densimeter, the mass and volume of the sinker were redetermined according to the procedures of McLinden and Splett [33]. The mass of the (sinker + lifting hook assembly) had increased by 1.240 mg (72 ppm of its total mass) and its volume had increased by 0.000 97 cm³ (145 ppm). Compared to silicon not exposed to the aqueous mixtures, the sinker exposed to the aqueous mixtures had a dark, grayish, and somewhat rough, oxide layer on its surface. Figure 2.7 compares the sinker used here with a larger, but otherwise identical, sinker fabricated at the same time and from the same ingot of silicon. The Inconel lifting hook was not visibly affected, and its mass changed by only +7 µg, which was within the uncertainty of the mass determination.

These changes in the sinker necessitated an analysis to determine the sinker mass and volume as a function of time with the starting and ending values as boundary conditions. The basic

approach was to use the measurements on pure nitrogen and carbon dioxide (following the mixture measurements) to determine ϕ_0 as a function of temperature, i.e., the values shown in Figure 2.5. These values were then taken as known inputs to Eq. 2.9, which was solved for the sinker mass. The result was an apparent mass change of 1.369 mg, compared with an actual change of 1.240 mg. This discrepancy corresponds to an error in ϕ_0 of 6×10^{-6} , or, in other words, the assumption that ϕ_0 was a function of temperature only was in error by 6×10^{-6} . The change in sinker mass used in the final data analysis was scaled by the ratio 1.240/1.369. Figure 2.8 presents a summary of this analysis.

2.6 Determination of Virial Coefficients

The virial coefficients for the mixture at a fixed temperature T are defined by

$$p = \frac{\rho RT}{M} \left[1 + B(x) \frac{\rho}{M} + C(x) \frac{\rho^2}{M^2} \right], \quad (2.10)$$

where p is pressure, R is the molar gas constant ($8.314\ 472\ J \cdot mol^{-1} \cdot K^{-1}$), T is the temperature, and the average molar mass of the mixture M is required because we measure the density ρ on a mass basis, but the virial coefficients $B(x)$ and $C(x)$ are reported on a molar basis, by convention. Equation (2.10) was fitted to the experimental p - ρ - T data by orthogonal distance regression using the ODRPACK software [37]. (Orthogonal distance regression allows for uncertainties in both the independent and dependent variables. Ordinary least squares, in contrast, assumes that all uncertainties are in the dependent variable.)

In addition to fitting the $B(x)$ and $C(x)$, the molar mass M was also a parameter in the fit. Otherwise, an error in M (i.e., an error in the mixture composition) would result in Eq. (2.10) not approaching the ideal-gas limit, resulting in a poor fit. The composition of a binary mixture can be recovered from the fitted value of M :

$$x = \frac{M - M_2}{M_1 - M_2}, \quad (2.11)$$

where the composition x is on a molar basis and M_1 and M_2 are the molar masses of the two components. This provides a check on the composition determined by the gravimetric preparation of the mixture (described in Section 4).

The cross second virial coefficients are derived from Eq. (1.2), which, for a binary mixture, is rearranged to

$$B_{12} = \frac{B(x) - x_1^2 B_1 - x_2^2 B_2}{2x_1 x_2} . \quad (2.12)$$

The B_{12} are computed using both the compositions from the gravimetric preparation of the mixtures and those from the fit of $B(x)$ and M (Eq. 2.11).

Measurements were carried out along isotherms at nominal temperatures of 500 K, 560 K, and 620 K on binary mixtures of N₂/H₂O and CO₂/H₂O; two or three mixture compositions were measured at each temperature for each system. Table 2.1 and Figures 2.9 and 2.10 summarize the results.

The compositions determined by the gravimetric sample preparation and those extracted from the average molar mass (Eq. (2.9 and 2.10), and listed as x_{weigh} and x_{fit} , respectively, in Table 2.1) are consistent. The average difference was 0.0022 mole fraction with a standard deviation of 0.0051 mole fraction. Likewise, the cross virial coefficients computed with the two compositions were consistent and had standard deviations of the mean of the two compositions (averaged over all points) of only 1.36 cm³/mol for N₂/H₂O and 1.48 cm³/mol for CO₂/H₂O. The gravimetric compositions are believed to be the more reliable, but we adopt this variance as a conservative estimate of the standard uncertainty in the virial coefficient arising from uncertainty in the composition.

The expanded ($k = 2$) uncertainty in the cross virial coefficients is given as $U(B_{12})$ in Table 2.1. The uncertainty comprises contributions from (1) the variance in the data, which is (two times) the standard deviation in the fitted value returned by the regression software; (2) the effects of possible systematic errors in the experimental quantities, which were determined by varying all the input data by their corresponding uncertainties, re-running the regression and adding (in quadrature) the resulting difference in B ; and (3) the contribution from the composition uncertainty that was discussed above. The starting pressures for the measurements at $T = 500$ K were lower than those for the other isotherms to avoid the two-phase region; because of the limited pressure range, the variance (i.e., relative scatter) in the data was larger and was the dominant contribution to the overall uncertainty. At $T = 620$ K, the contribution from the composition uncertainty was the largest contribution. A significant contribution was the uncertainty in sinker mass resulting from the oxidation of the silicon sinker; this effect ranged from 0.14 cm³/mol to 2.56 cm³/mol for the different isotherms.

2.7 Discussion

Figures 2.9 and 2.10 compare the present values of the virial coefficient to the theoretical values as well as the literature values that overlap the temperature range of the present values. The

experimental and theoretical values are seen to be consistent within their mutual uncertainties. The present work has extended the available experimental data to higher temperatures for the CO₂/H₂O system and supplements the single literature data set for $T > 500$ K for the N₂/H₂O binary. In spite of the experimental difficulties encountered, the present values have uncertainties that are roughly comparable to the theoretical uncertainties for CO₂/H₂O and double the theoretical uncertainties for N₂/H₂O.

Table 2.1. Summary of isotherms and virial coefficients determined in this work.

T (K)	p range (MPa)	Composition (mol frac N ₂ or CO ₂)		$B(x)$	$B_{12, \text{weigh}}$	$B_{12, \text{fit}}$	$U(B_{12})$
		x_{weigh}	x_{fit}				
N₂/H₂O mixtures							
499.927	6.23 – 1.44	0.5321	0.5281	-30.6	4.8	6.2	7.3
500.222	3.95 – 1.78	0.3595	0.3601	-70.3	-4.4	-4.7	15.2
499.124	9.72 – 1.60	0.7091	0.7098	-5.7	1.5	1.3	4.2
559.771	8.01 – 1.38	0.3203	0.3152	-54.4	1.7	3.9	6.9
559.994	20.97 – 2.02	0.6993	0.6974	-0.2	3.5	4.0	3.1
619.786	25.49 – 3.02	0.6997	0.6972	4.9	6.3	6.7	3.0
619.705	20.25 – 2.17	0.3192	0.3129	-39.5	3.1	5.2	2.9
CO₂/H₂O mixtures							
500.671	4.45 – 1.21	0.4565	0.4571	-73.0	-32.2	-32.4	11.6
500.537	10.63 – 1.97	0.7159	0.7215	-45.3	-38.7	-39.9	6.2
561.428	10.63 – 1.80	0.3898	0.3929	-59.0	-21.9	-22.7	4.6
561.391	16.21 – 2.04	0.6833	0.6850	-32.1	-25.0	-25.3	3.8
619.830	15.23 – 1.99	0.7110	0.7026	-21.9	-21.2	-20.0	4.7
619.739	16.45 – 2.03	0.3647	0.3515	-51.5	-27.2	-24.4	3.2



Figure 2.1. Photo showing the high-temperature densimeter. From left to right the major components are: vacuum system; main part of densimeter with the mass-comparator balance at the top and the vacuum chamber containing the measuring cell at the bottom; instrument rack; and display for the control computer.

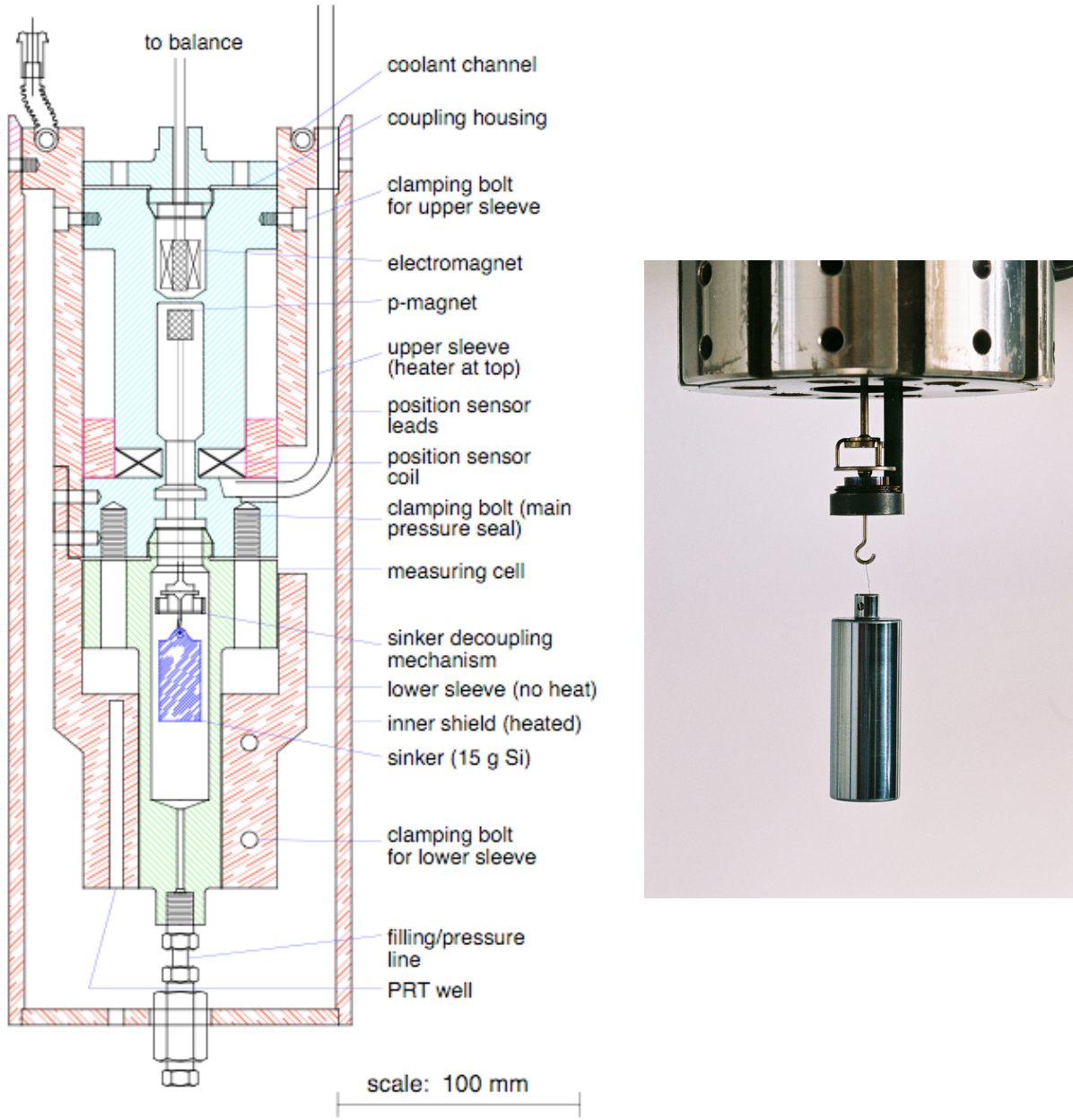


Figure 2.2. Density system; left: schematic diagram of the measuring cell, magnetic suspension coupling, and sinker; right: photo of the sinker, shown in suspension (the lower part of the measuring cell has been removed).

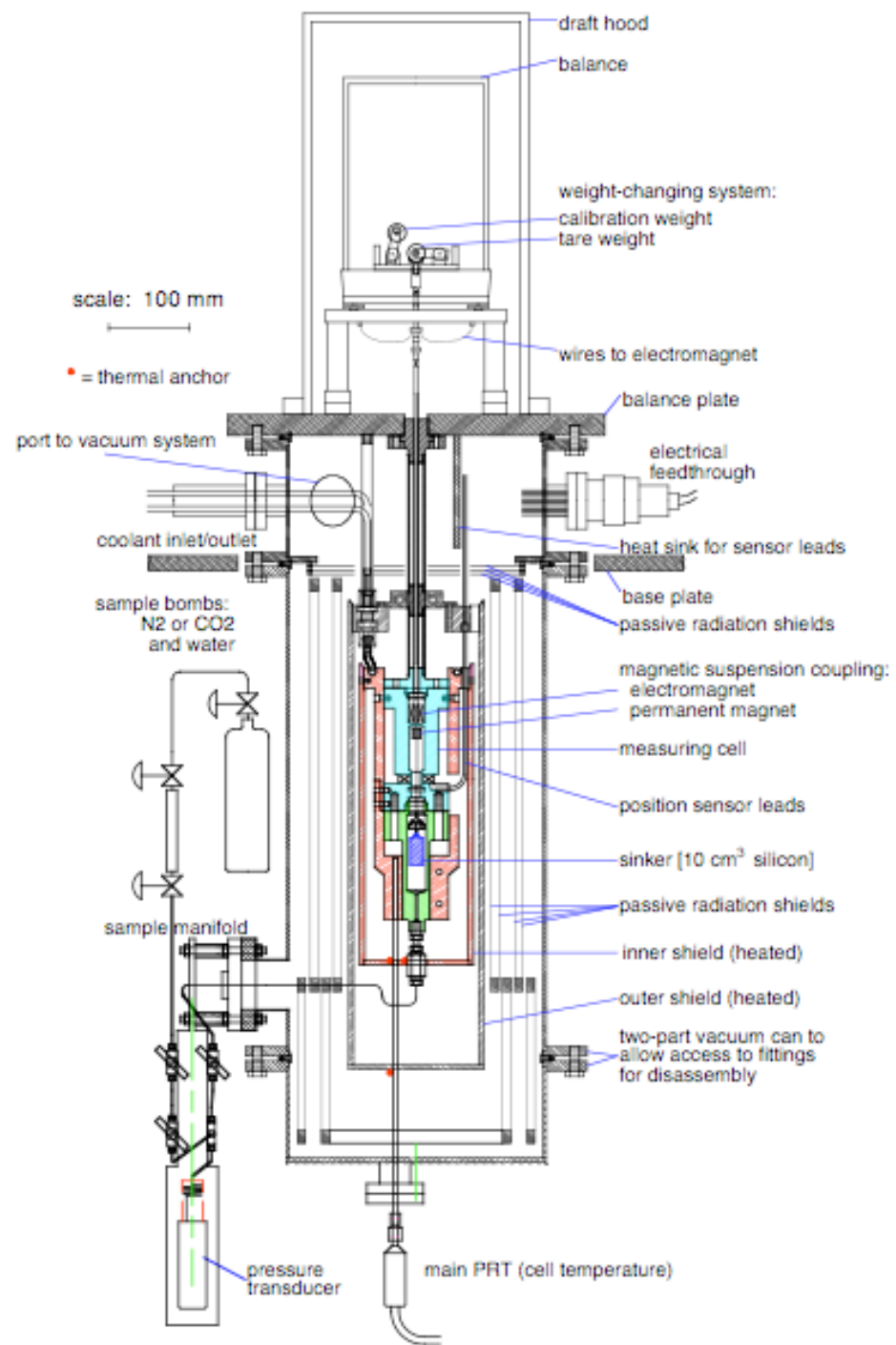


Figure 2.3. Schematic diagram of the densimeter, thermostat, and sample system.

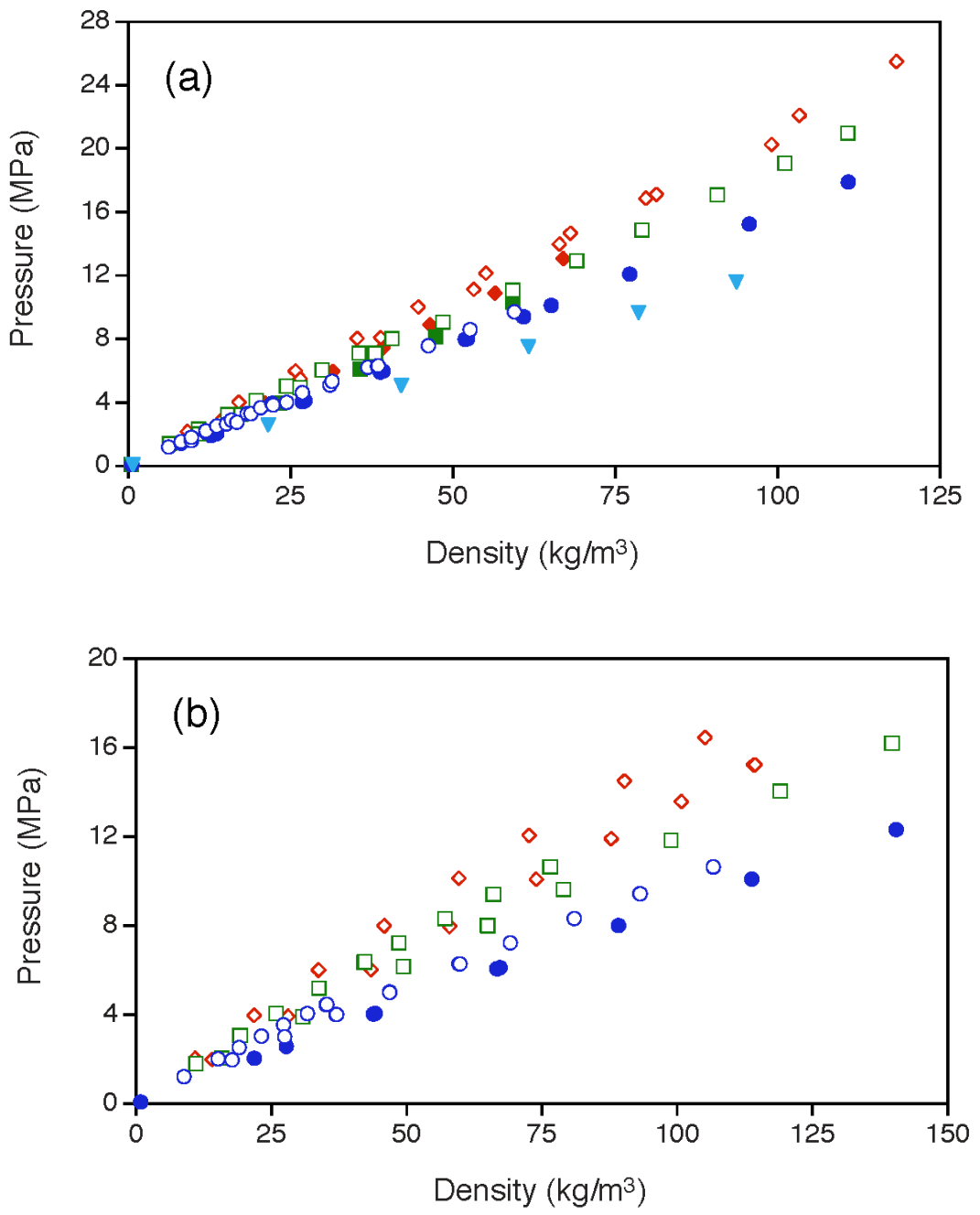


Figure 2.4. Measured p - ρ - T points on pressure-density coordinates; (a) $\text{N}_2/\text{H}_2\text{O}$ mixtures and pure N_2 and (b) $\text{CO}_2/\text{H}_2\text{O}$ mixtures and pure CO_2 . The symbols identifying the isotherms are \blacktriangledown 400 K; \bullet 500 K; \blacksquare 560 K; \blacklozenge 620 K; open symbols indicate mixtures and filled symbols indicate pure gases.

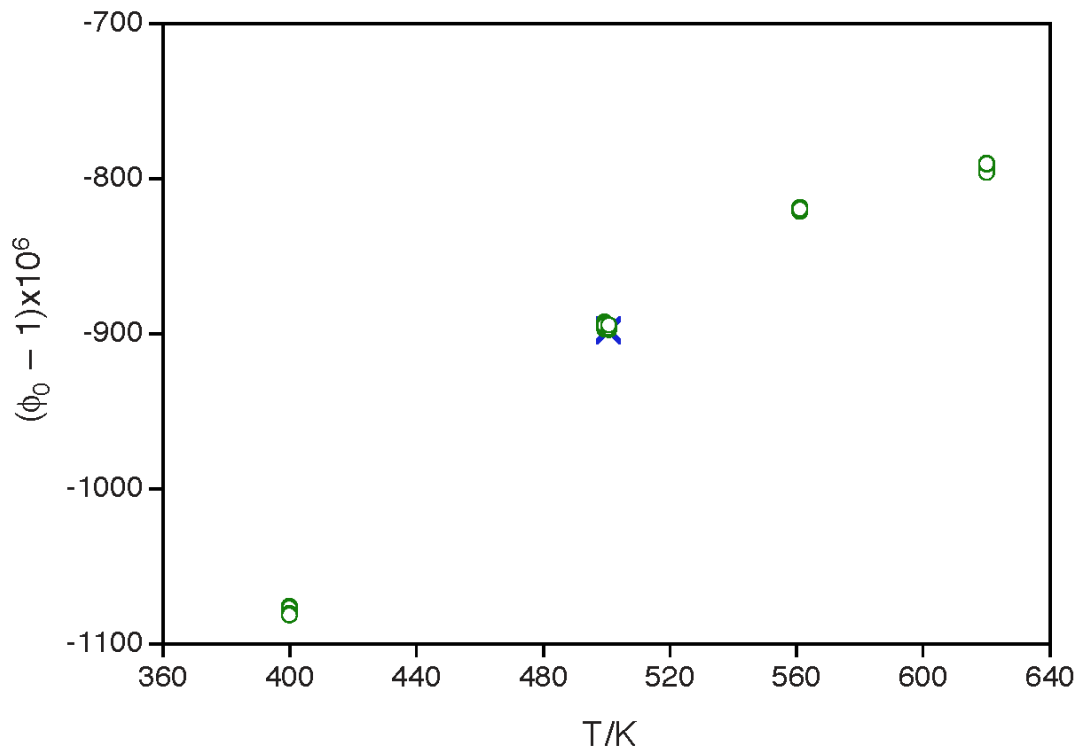


Figure 2.5. Parameter ϕ_0 determined from measurements on pure gases at atmospheric pressure;
○ measurements on pure N₂; ✕ pure CO₂.

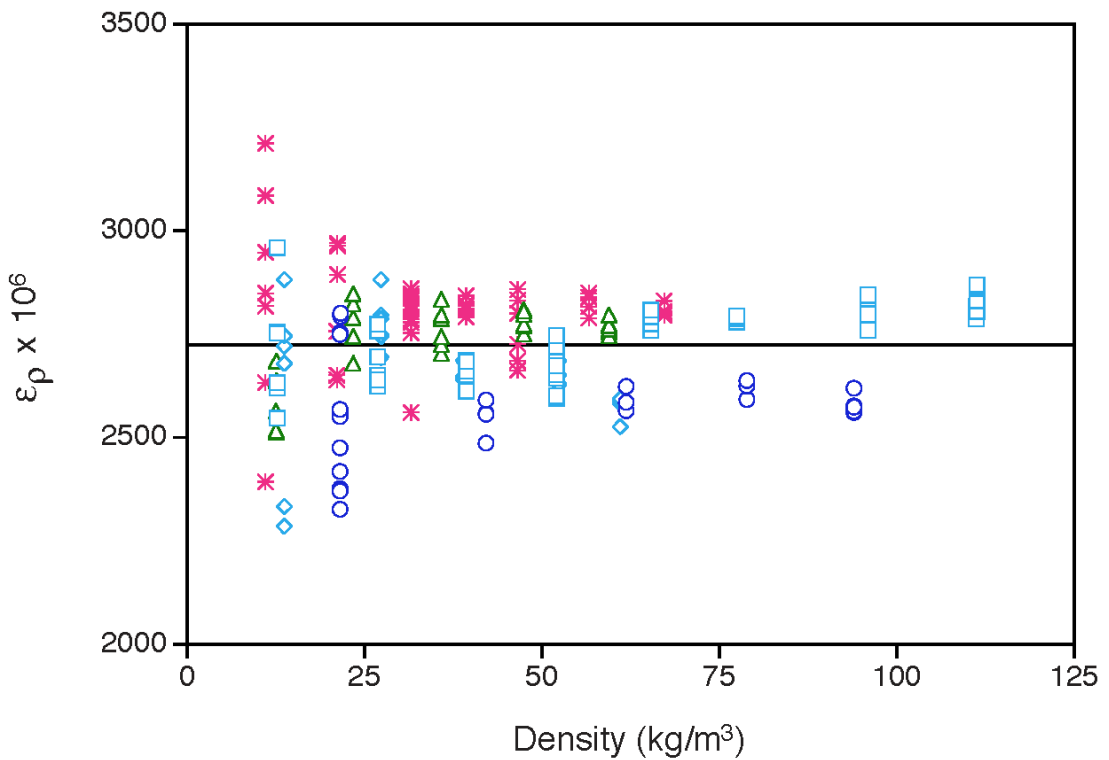


Figure 2.6. Values of the parameter ε_p determined from calibrations with nitrogen; \circ $T = 400$ K;
 \square $T = 500$ K, repetition 1; \diamond $T = 500$ K, repetition 2; \triangle $T = 560$ K; * $T = 620$ K; the
line indicates the mean value of $\varepsilon_p = 2725 \times 10^{-6}$.



Figure 2.7. Silicon sinker used in present experiments after exposure to $\text{N}_2/\text{H}_2\text{O}$ and $\text{CO}_2/\text{H}_2\text{O}$ mixtures (on left) compared to a larger sinker fabricated at the same time and from the same silicon crystal, but not exposed to the aqueous mixtures; a neutral grey photographic target is in the background.

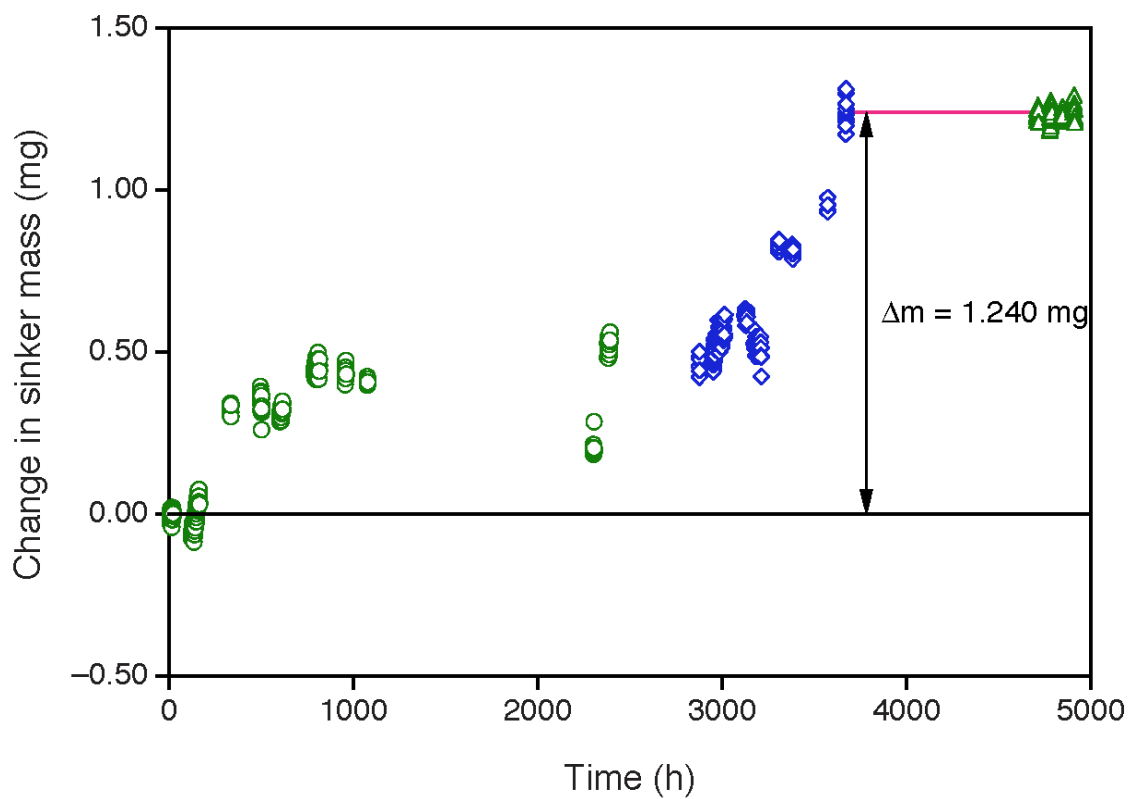


Figure 2.8. Change in sinker mass over the period January 8, 2010 to July 31, 2010;
○ measurements on $\text{N}_2/\text{H}_2\text{O}$ mixtures; ◇ $\text{CO}_2/\text{H}_2\text{O}$ mixtures; △ pure nitrogen.

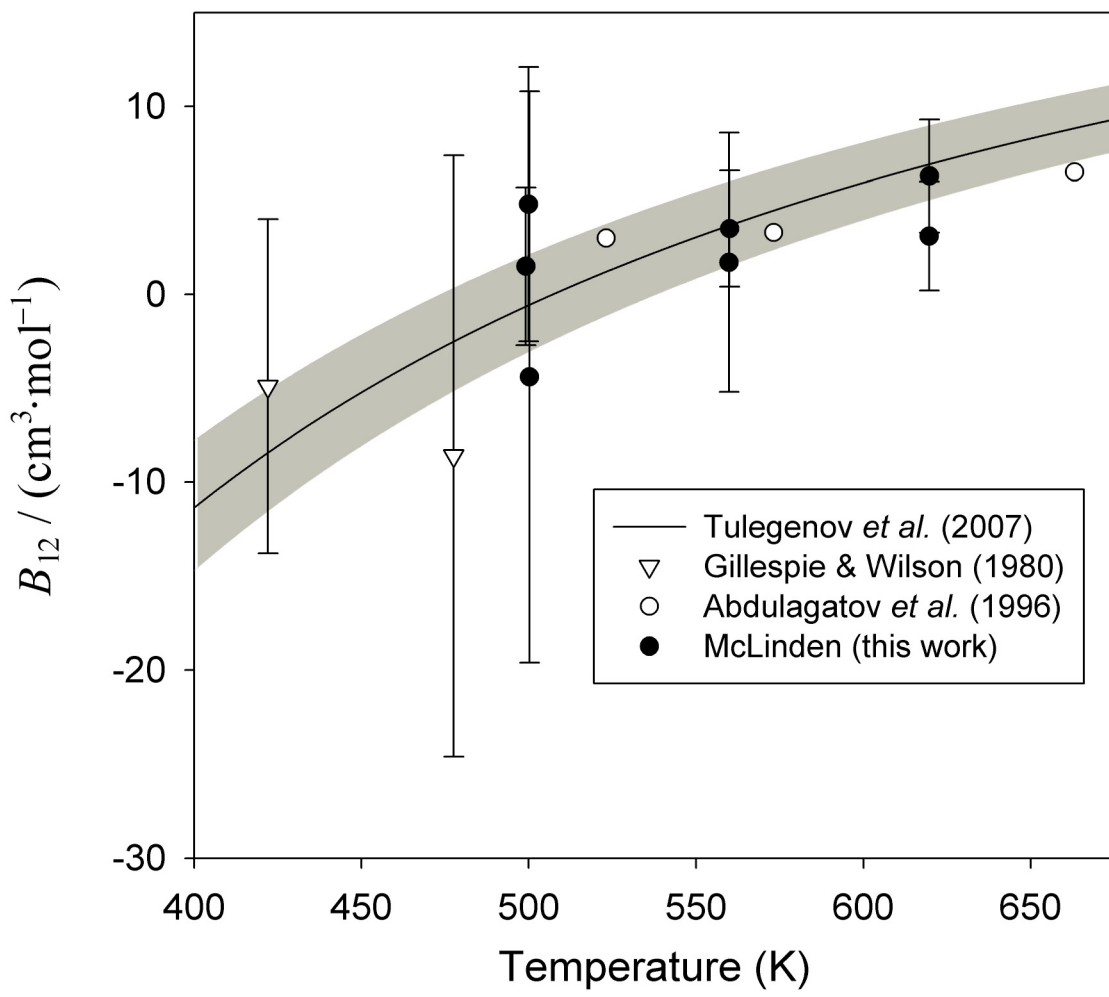


Figure 2.9. Comparison of $B_{12}(T)$ predicted from theory to present results and high-temperature literature data for the N₂/H₂O binary; shading and error bars represent expanded ($k=2$) uncertainty approximately equivalent to a 95% confidence level.

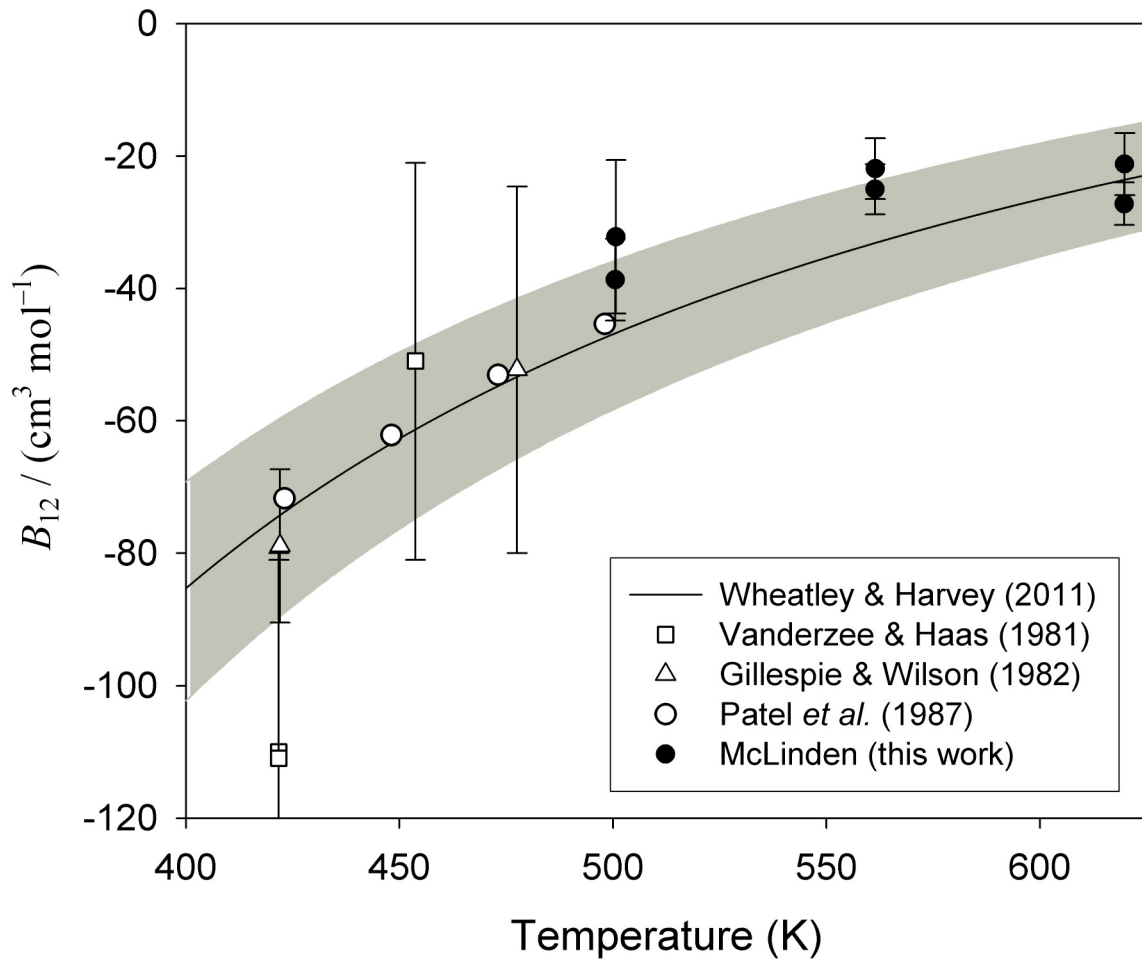


Figure 2.10. Comparison of $B_{12}(T)$ predicted from theory to present results and high-temperature literature data for the $\text{CO}_2/\text{H}_2\text{O}$ binary; shading and error bars represent expanded ($k=2$) uncertainty approximately equivalent to a 95% confidence level.

3. THERMAL CONDUCTIVITY MEASUREMENTS (TASK 3)

3.1 Measurement Technique

The measurements of thermal conductivity were obtained with a transient hot-wire instrument that has previously been described in detail [38]. During an experiment, an electrically heated wire immersed in the fluid functioned both as an electrical heat source and a resistance thermometer. Upon application of a pulse of electric energy to the wire, it (and thus the fluid surrounding it) was heated; the resulting temperature rise is a function of the thermal conductivity of the surrounding fluid. The outer cavity around the hot wire was stainless steel with a diameter of 8 mm that is formed by a stainless-steel pressure vessel that is capable of operation from 300 K to 750 K at pressures to 70 MPa in the liquid, vapor, and supercritical gas phases. The measurements on the pure nitrogen, carbon dioxide, and water were performed with bare platinum hot wires that were nominally 10 cm long with a diameter of 12.7 μm . All reported uncertainties are for a coverage factor of $k = 2$, a confidence interval of approximately 95 %.

3.1.1 Transient Measurements

The basic theory that describes the operation of the transient hot-wire instrument is given by Healy *et al.* [39]. The hot-wire cell was designed to approximate a transient line source as closely as possible, and deviations from this model are treated as corrections to the experimental temperature rise. The ideal temperature rise ΔT_{id} is given by

$$\Delta T_{\text{id}} = \frac{q}{4\pi\lambda} \left[\ln(t) + \ln\left(\frac{4a}{r_0^2 C}\right) \right] = \Delta T_w + \sum_{i=1}^{10} \delta T_i , \quad (3.1)$$

where q is the power applied per unit length, λ is the thermal conductivity of the fluid, t is the elapsed time, $a = \lambda/(\rho C_p)$ is the thermal diffusivity of the fluid, ρ is the mass density of the fluid, C_p is the isobaric specific heat capacity of the fluid, r_0 is the radius of the hot wire, $C = 1.781\dots$ is the exponential of Euler's constant, ΔT_w is the measured temperature rise of the wire, and δT_i are corrections [39] to account for deviations from ideal line-source conduction. During analysis, a line is fitted to the linear section, from 0.2 s to 1 s, of the ΔT_{id} versus $\ln(t)$ data, and the thermal conductivity is obtained from the slope of this line. Both thermal conductivity and thermal diffusivity can be determined with the transient hot-wire technique, as shown in Eq. (3.1), but only the thermal conductivity results are considered here. The experiment temperature, T_e , associated with the thermal conductivity is the average temperature of the wire over the period that was fitted to obtain the thermal conductivity.

Several corrections [39-45] that account for the finite dimensions of the wire and the concentric wall of the pressure vessel must be carefully considered. The temperature rise should always be corrected to account for the finite wire radius [39-43]. In the case of fluids with high thermal diffusivity, such as dilute gases, it is possible for the temperature rise to penetrate to the outer boundary of the fluid. The temperature rise must be corrected for the presence of the outer boundary in such cases [39-43]. A correction for axial conduction is also required for transient hot-wire cells with a single wire [44, 45]. The preferred method to deal with such corrections is to minimize them by proper design. For instance, the correction for finite wire radius can be minimized with wires of extremely small diameter ($4 \mu\text{m}$ to $7 \mu\text{m}$), and penetration of the thermal wave to the outer boundary can be eliminated by use of a cell with an outer boundary of large diameter. The correction for finite wire length could be eliminated with a more complex double-wire cell that requires about 50 cm^3 of sample [38, 39]. However, such designs were not considered optimal for the present measurements, where such extremely fine wires are too fragile, double-wire geometries are less robust and larger outer dimensions require excessive volumes at high temperatures and pressures.

Transient experiments were 1 s in duration, with 250 measurements of temperature rise as a function of elapsed time relative to the onset of wire heating. Consistency between measurements at five different applied power levels for each initial temperature and pressure confirms that convection was not a problem during the transient measurements. The parameter “STAT” reported in the data tables provides a measure of repeatability of each thermal conductivity measurement from the uncertainty (coverage factor of $k=2$) in the slope of the line fit to ideal temperature rise versus the logarithm of elapsed time (STAT = 0.001 corresponds to 0.1 %). The STAT parameter increases when the corrected temperature rise data are nonlinear due to either convection or thermal radiation. Fluid convection was normally not a problem, as indicated by consistency between measurements at different power levels and linearity over a wide range of experiment durations (STAT < 0.002). The corrections for the finite wire diameter and length [44, 45] remained less than 1 % for the measurements reported here.

Thermal radiative heat transfer between media at two different temperatures T_1 and T_2 increases in proportion to absolute temperature cubed since it is proportional to $(T_1^4 - T_2^4) \approx T^3(T_1 - T_2)$ for small temperature differences. Correction for thermal radiation during transient hot-wire measurements can be classified into three cases: (1) transparent fluid (TF), (2) opaque fluid (OF) and (3) dominated by emission from fluid (EF) [38]. In the present measurements, we have treated the fluid as transparent to thermal radiation. Significant emission of thermal radiation from the fluid would add a linear-in-time correction term to the measured temperature rise that

we have not accounted for. Thus, the presence of significant thermal radiation from fluid emission would be apparent as increasing nonlinearity in the temperature rise vs. $\ln(t)$ data as a function of experiment temperature. This nonlinearity is reflected in the parameter STAT (described above and tabulated in the Supporting Information), which is not a function of temperature during these measurements.

3.1.2 Steady-State Measurements

At very low pressures, the transient hot-wire system described above can be operated in a steady-state mode, which requires less significant corrections [46]. The working equation for the steady-state mode is based on a different solution of Fourier's law, but the geometry is still that of concentric cylinders. This equation can be solved for the thermal conductivity of the fluid, λ ,

$$\lambda = \frac{q \ln(r_2/r_1)}{2\pi(T_1 - T_2)}, \quad (3.2)$$

where q is the applied power per unit length, r_1 and T_1 are the radius and temperature, respectively, of the hot wire, and r_2 and T_2 are the radius and temperature of the cylindrical cavity enclosing the fluid and hot wire.

For the concentric-cylinder geometry described above, the total radial heat flow per unit length, q , remains constant and is not a function of the radial position. Assuming that the thermal conductivity is a linear function of temperature, such that $\lambda = \lambda_0(1 + b_\lambda T)$, it can be shown that the measured thermal conductivity is given by $\lambda = \lambda_0(1 + b_\lambda(T_1 + T_2)/2)$. Thus, the measured thermal conductivity corresponds to the value at the mean temperature of the inner and outer cylinders

$$\bar{T} = (T_1 + T_2)/2. \quad (3.3)$$

This assumption of linear temperature dependence for the thermal conductivity is valid only for experiments with small temperature differences. The density assigned to the measured thermal conductivity is calculated from an equation of state with the temperature from Eq. (3.3) and the experimentally measured pressure. An assessment of corrections during steady-state hot-wire measurements is available [46].

3.2 Hot-Wire Apparatus

The hot-wire bridge on the high-temperature thermal conductivity apparatus was modified for operation with the AC drive voltage for the measurements on mixtures containing water. The small-volume hot-wire cell for the water mixture measurements was designed to provide as much electrical insulation as possible between the lead wires inside the pressure cell that are

exposed to the sample fluid. All electrical insulators in the new cells were solid ceramic extrusions that provide moderately effective electrical insulation when immersed in electrically conducting fluids. A series of three prototype cells was constructed and tested for reliability. Shortcomings discovered during each of these tests were corrected in subsequent cells.

The final cell design had a 12.7 μm diameter platinum hot wire and 0.2 mm diameter Alumel lead wires and is shown in Figure 3.1. The pressure vessel had a volume of 5 cm^3 and is pressure rated to 117 MPa at 700 K. The Alumel lead wires entered the cell through a ceramic sealant in a compression gland and were insulated with rigid ceramic spacers. The hot wire was supported with rigid ceramic parts that also provide electrical insulation. The hot wire was tensioned by a spring arrangement at the bottom of the hot wire. The hot wires were located between the thin-ceramic support tubes, and were near the central axis of the cylindrical cavity formed by the inner wall of the pressure vessel when the wire and its support system were inserted in the pressure vessel.

The hot-wire cell was embedded in an aluminum block that was positioned inside an isothermal aluminum enclosure and is also shown in Figure 3.1. This assembly was heated in an electrical furnace that provided temperature control from ambient to over 750 K that is shown in Figure 3.2. The temperature was measured with a reference platinum resistance thermometer, located in the aluminum block that surrounds the hot-wire cell, with an uncertainty of 5 mK. The pressure was measured with a pressure transducer (0 to 70 MPa) with an uncertainty of 0.007 MPa. The filling manifold and pressure transducer had small volumes and were water-filled during measurements on the water mixtures to reduce uncertainty in the composition of the sample that would result from condensation of water from the mixture in these colder regions of the pressure system. The high-temperature hot-wire cell for the water mixtures was assembled and pressure tested. The resistance of each annealed platinum hot wire was then calibrated as a function of temperature. The first wire assembly was used for pure H_2O , N_2 and CO_2 , and for mixtures of N_2 with H_2O . The second wire assembly was used for mixtures of CO_2 with H_2O . The hot-wire cells worked well during these measurements at temperatures from 500 K to 740 K with pressures up to 40 MPa.

3.3 Measured Thermal Conductivity

The thermal conductivities of the pure components nitrogen, carbon dioxide and water were measured to establish the compositional endpoints for the mixtures of nitrogen with water and for carbon dioxide with water. Measurements for the pure materials and mixtures were

performed along five nominal isotherms at 500, 560, 620, 680, and 740 K with pressures up to 40 MPa.

The most significant uncertainty during these measurements was due to increasing electrical resistance of the platinum hot wires with elapsed time at temperatures of 740 K in water vapor or the wet-gas mixtures. The initial resistance of each hot wire was recorded at the initial equilibrium temperature and pressure for each thermal conductivity experiment. Careful analysis of the wire resistance during the measurements indicates that the derivative of the wire resistance with respect to temperature remained constant and nearly that which would be expected for pure platinum. Uncertainty in this derivative translates directly into uncertainty in the measured temperature rise of the wire during the experiments.

Two wires were used during the measurements reported here. The first wire was used for the measurements on nitrogen, carbon dioxide, water, and the mixtures of nitrogen with water. The isotherms at 740 K were the last measurements made with the first hot wire. It was decided to replace the hot wire prior to the measurements on the mixtures of carbon dioxide with water. The second hot wire was annealed and check measurements were made on nitrogen before these mixtures were measured. Again, the 740 K isotherms were the last mixture measurements for the second hot wire. After these measurements on mixtures of carbon dioxide with water, check measurements were made with the second hot wire on pure carbon dioxide and water.

We estimate the uncertainty in the present transient and steady-state measurements to be 4 % (coverage factor $k = 2$) based on consideration of the uncertainties in the fundamental measurements, heat-transfer corrections, and the calibration of the wire resistance as a function of temperature during the measurements. This uncertainty is significantly larger than our typical uncertainties, due to the relatively low density of these gas-phase measurements and the increase in the wire resistance that was observed at 740 K in water vapor and the wet-gas mixtures. The increase in wire resistance was likely due to corrosion of welded connections to the platinum hot wires or of the wires themselves at temperatures near 740 K.

3.3.1 Pure Nitrogen, Carbon Dioxide and Water

The thermal conductivity of pure nitrogen is shown in Figure 3.3 along with the values calculated with REFPROP [1], which is based on the correlation of Lemmon and Jacobsen [47], and which represents the literature data quite well. The thermal conductivity of pure carbon dioxide is shown in Figure 3.4 along with the values calculated with REFPROP, which implements the model of Vesovic et al. [48], which again represents the literature data quite well. All of the data for nitrogen and carbon dioxide are for supercritical state points at high reduced

temperatures where the critical enhancement is not significant. The thermal conductivity of pure water is shown in Figure 3.5 along with the values calculated with REFPROP, which is based on current IAPWS recommendations [49]. The data for water include both compressed liquid and supercritical gas state points. The thermal conductivity critical enhancement is quite significant for many of these measurements on pure water. For water, there was evidence of some increase in the wire resistance as a function of elapsed time at the highest temperature of 740 K. This is likely due to the corrosive nature of water at these extreme conditions.

3.3.2 Mixtures of Nitrogen and Water

Mixtures of nitrogen with water were prepared gravimetrically and handled as described in Section 4. The measured compositions are summarized in Table 3.1. Corrections for the finite dimensions of the wire and fluid outer boundary were calculated with the mixture virial model developed in this work and estimates of the mixture thermal conductivity from corresponding-states predictions with the NIST REFPROP program. The thermal conductivity data are provided in tabular form as an appendix. Figure 3.6 shows the thermal conductivity measured for the mixture isotherms near 0.3 mole fraction water with nitrogen. Figure 3.7 shows the thermal conductivity measured for the mixture isotherms near 0.6 mole fraction water with nitrogen. The thermal conductivity of this mixture system is shown at temperatures near 500 K and 680 K in Figures 3.8 and 3.9, respectively. It is apparent that the dilute-gas thermal conductivity (low pressure limit) of the mixtures is larger than the thermal conductivity of the pure components. This is likely due to the molecular interactions between the polar water and the non-polar nitrogen.

3.3.3 Mixtures of Carbon Dioxide and Water

Mixtures of carbon dioxide with water were prepared and handled as described in Section 4. The measured compositions are summarized in Table 3.2. Corrections for the finite dimensions of the wire and fluid outer boundary were calculated with the mixture virial model developed in this work and estimates of the mixture thermal conductivity from corresponding-states predictions with the NIST REFPROP program. The thermal conductivity data are provided in tabular form as an appendix. Figure 3.10 shows the thermal conductivity measured for the mixture isotherms near 0.3 mole fraction water with carbon dioxide. Figure 3.11 shows the thermal conductivity measured for the mixture isotherms near 0.6 mole fraction water with carbon dioxide. The thermal conductivity of this mixture system is shown at temperatures near 500 K and 680 K in Figures 3.12 and 3.13, respectively. It is apparent that the dilute-gas thermal conductivity (low-pressure limit) of the mixtures is larger than the thermal conductivity of the pure components. This is likely due to the molecular interactions between the polar water and the non-polar carbon dioxide.

3.4 Discussion of Results and Literature

The mixtures studied in this work are quite interesting because of the interactions between the non-polar nitrogen and carbon dioxide molecules and the polar water molecules. Our data clearly show that the thermal conductivities of the mixtures of N₂ with H₂O and CO₂ with H₂O are higher than those of the pure components in the dilute-gas limit (zero density) over this temperature range. This is very different from mixtures of similar molecules, where the mixture thermal conductivity is more ideal and the binary mixture thermal conductivity varies linearly with composition between the thermal conductivities of the pure components.

It has been reported in the literature that mixtures of molecules with significant differences in polarity exhibit positive deviations from ideal behavior, and the dilute-gas thermal conductivities of mixtures can be larger than the thermal conductivity of either pure molecule. Gruß and Schmick [50] reported this for mixtures of air with polar gases, including ammonia and water at 107 °C. Vargaftik and Timroth [51] also reported this non-ideal behavior based on their data for dilute-gas mixtures of N₂ with H₂O and CO₂ with H₂O at 338 K and 603 K. Frohn and Westerdorf [52] reported the thermal conductivities of dilute-gas mixtures of N₂ with H₂O at temperatures from 323 K to 673 K that also confirm this non-ideal behavior for the mixtures of these gases. We have not found measurements of the thermal conductivity of these mixtures at elevated pressures in the literature. Our results indicate that the density dependence of the mixture thermal conductivity falls between that of the pure components for these mixtures. There is a significant need for the development of models for the thermal conductivity of these mixtures that can account for the non-ideal behavior that has been reported in the literature and observed in the present measurements.

Table 3.1. Summary of mixtures of nitrogen with water studied in the work.

Mixture Designation	Temperature / K	Mole Frac. Water	Mole Frac. Std. Dev.
N30W701	500	0.6172	0.0028
N70W302	500	0.2497	0.0004
N30W703	560	0.6200	0.0008
N70W304	560	0.2811	0.0001
N30W705	620	0.6263	0.0007
N70W306	620	0.2881	0.0001
N30W707	680	0.6489	0.0002
N70W308	680	0.2809	0.0002
N30W709	740	0.6356	0.0009
N70W3010	740	0.2754	0.0003

Table 3.2. Summary of mixtures of carbon dioxide with water studied in the work.

Mixture Designation	Temperature / K	Mole Frac. Water	Mole Frac. Std. Dev.
C30W7011	500	0.6536	0.0026
C30W7021	500	0.6380	0.0012
C70W302	500	0.2052	0.0002
C70W3012	500	0.2363	0.0003
C30W703	560	0.5669	0.0006
C70W304	560	0.3029	0.0001
C30W705	620	0.6132	0.0002
C30W7015	620	0.6443	0.0003
C70W306	620	0.3030	0.0001
C30W707	680	0.5962	0.0001
C70W308	680	0.2596	0.0002
C30W709	740	0.5824	0.0002
C70W3010	740	0.2963	0.0002



Figure 3.1. Transient hot-wire cell and isothermal shield used in this work, shown here during assembly. The actual hot wire is located between the white ceramic insulators in the bottom assembly and is not visible at the resolution of this photo.

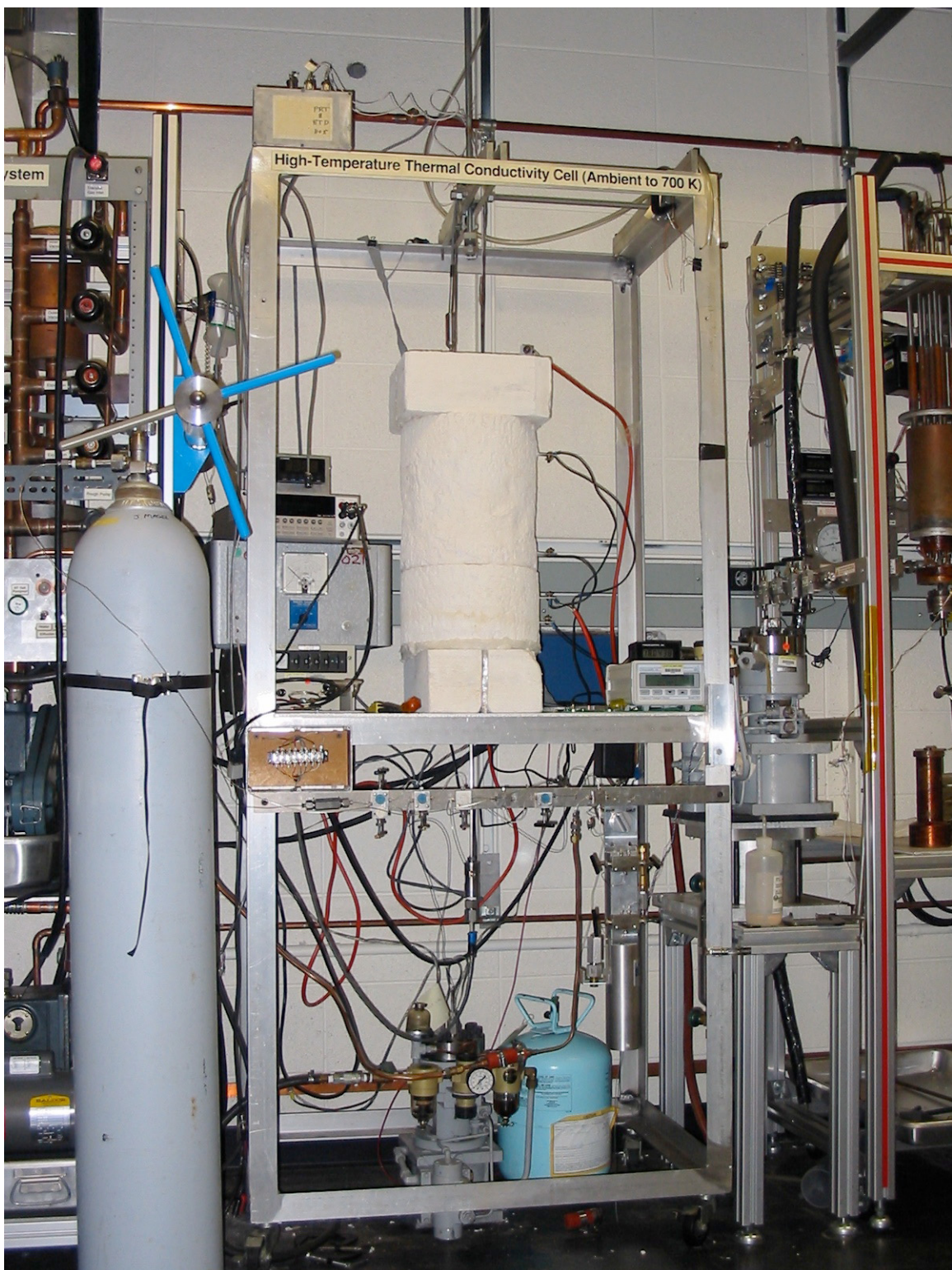


Figure 3.2. Experimental furnace and pressure manifold used during these measurements. The hot wire assembly is contained within the white ceramic furnace assembly in the center of the photo.

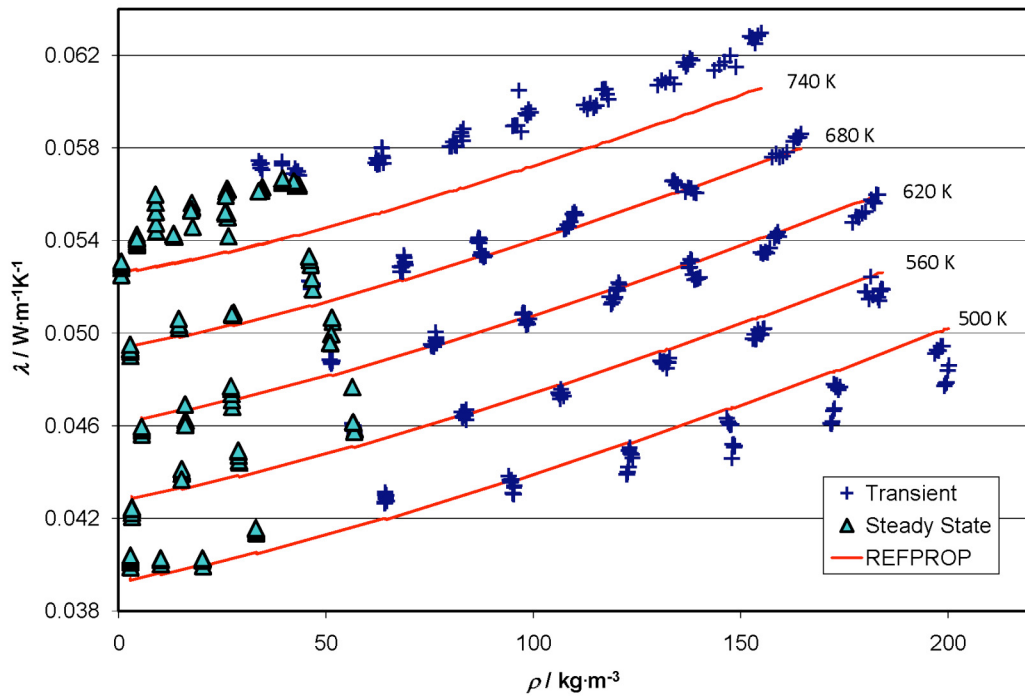


Figure 3.3. Thermal conductivity of pure nitrogen at temperatures of 500, 560, 620, 680, and 740 K with pressures up to 40 MPa.

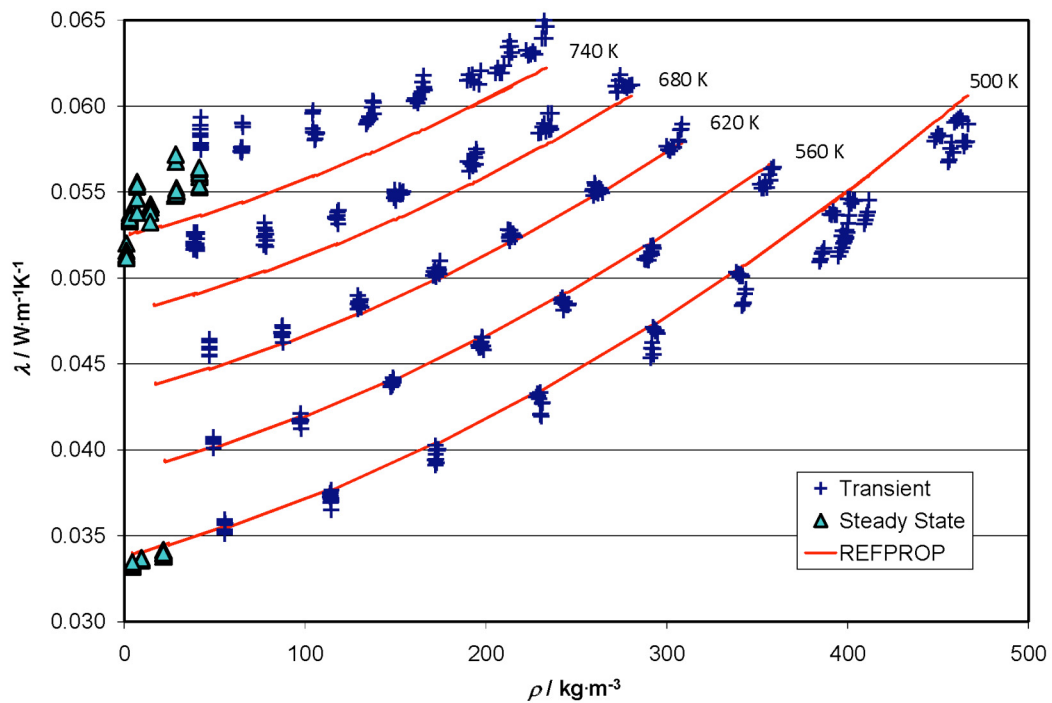


Figure 3.4. Thermal conductivity of pure carbon dioxide at temperatures of 500, 560, 620, 680, and 740 K with pressures up to 40 MPa.

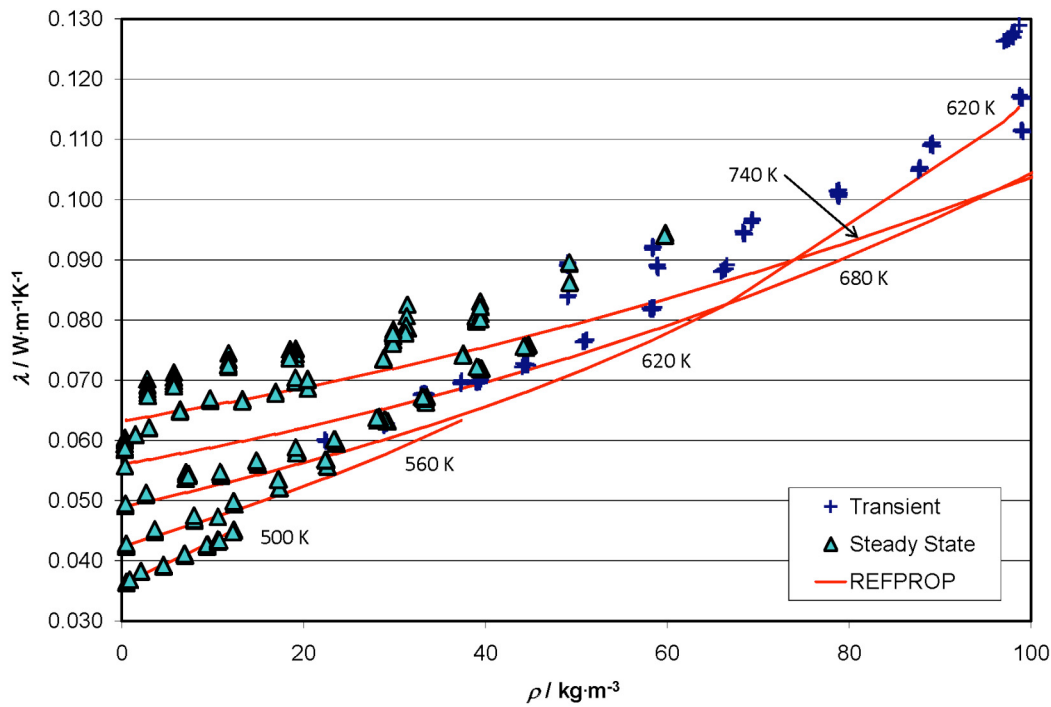


Figure 3.5. Thermal conductivity of pure water at temperatures of 500, 560, 620, 680, and 740 K with pressures up to 40 MPa. Both the model and data show strong effects of the thermal conductivity critical enhancement with crossing of the isotherms as the critical enhancement becomes more significant.

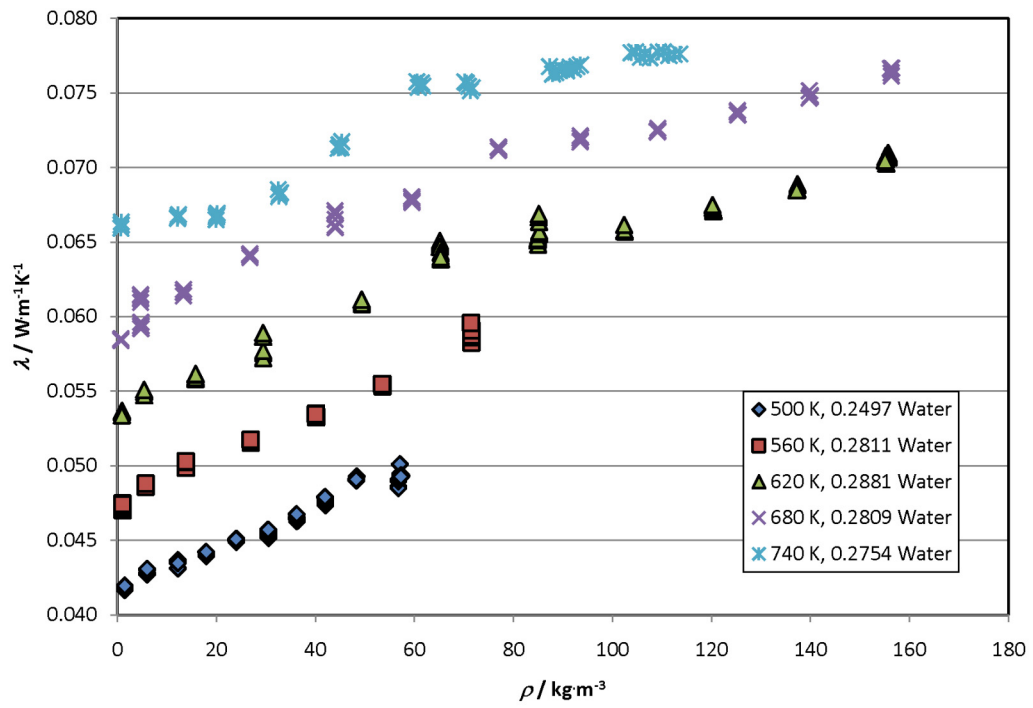


Figure 3.6. Thermal conductivity of mixtures near 0.3 mole fraction H_2O with N_2 as a function of density calculated with the mixture virial model developed in this work.

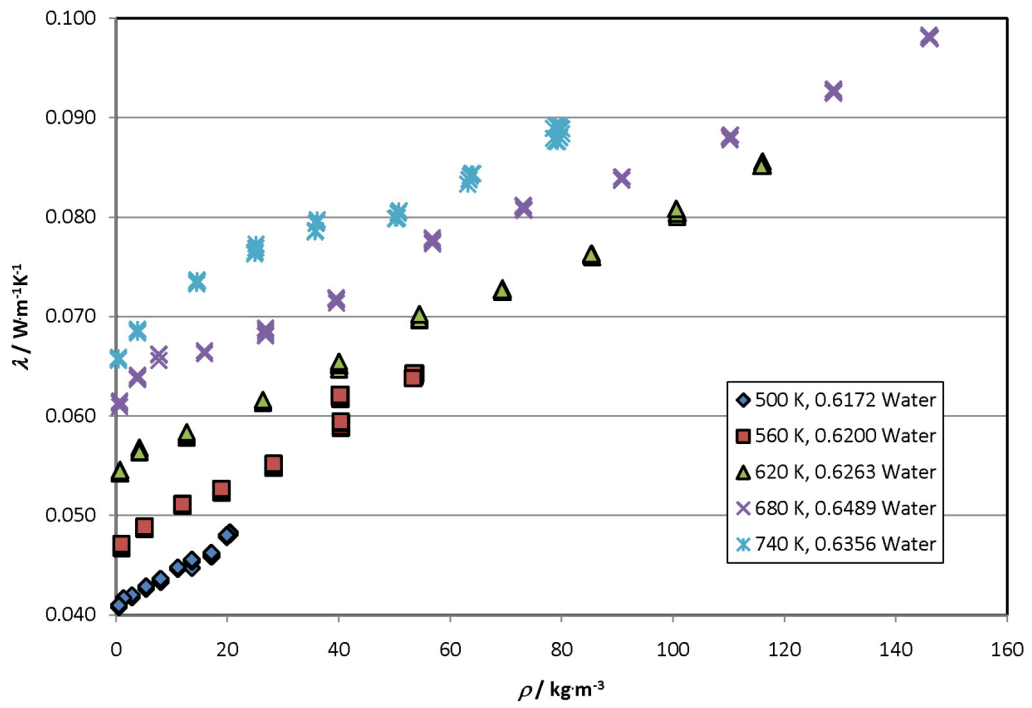


Figure 3.7. Thermal conductivity of mixtures near 0.6 mole fraction H_2O with N_2 as a function of density calculated with the mixture virial model developed in this work.

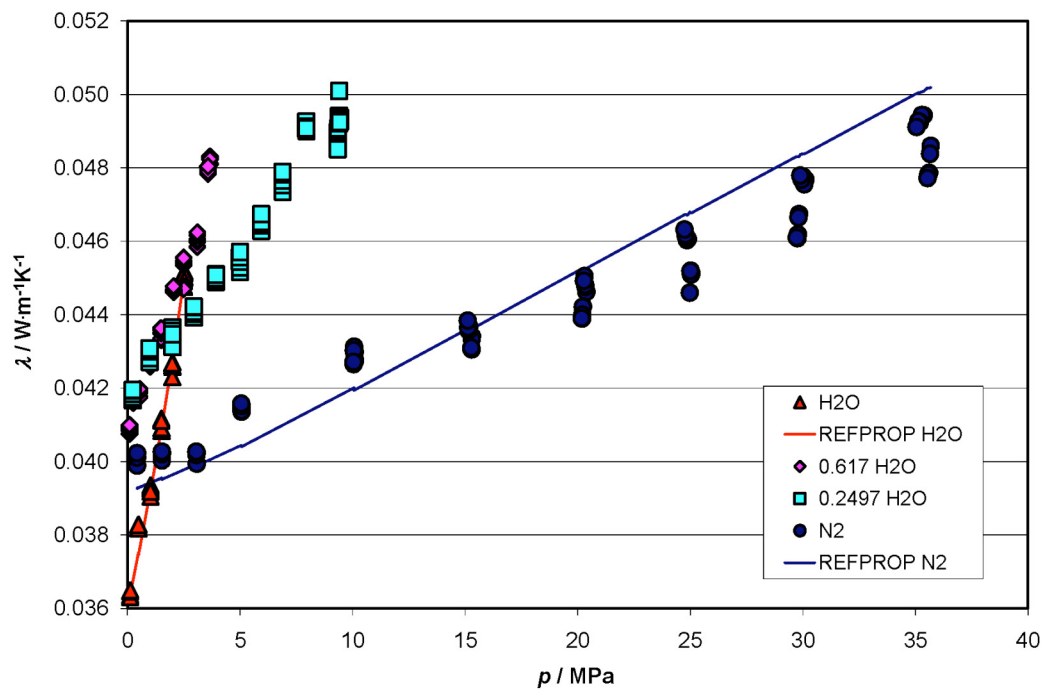


Figure 3.8. Thermal conductivity of mixtures of N₂ with H₂O measured at temperatures near 500 K as a function of pressure compared to the pure components.

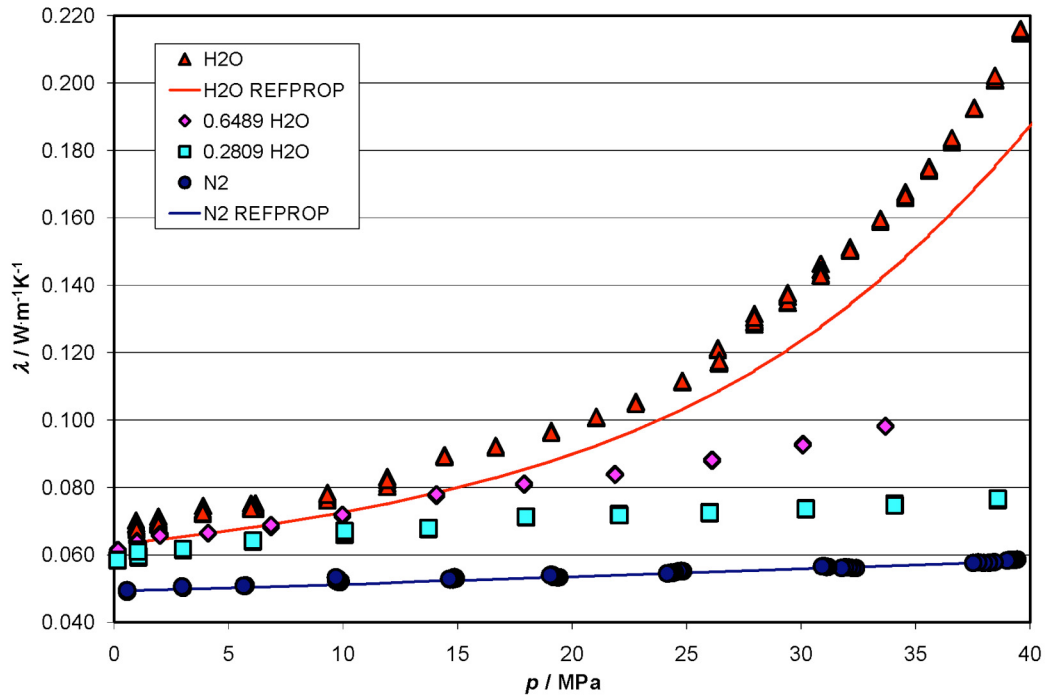


Figure 3.9. Thermal conductivity of mixtures of N_2 with H_2O measured at temperatures near 680 K as a function of pressure compared to the pure components.

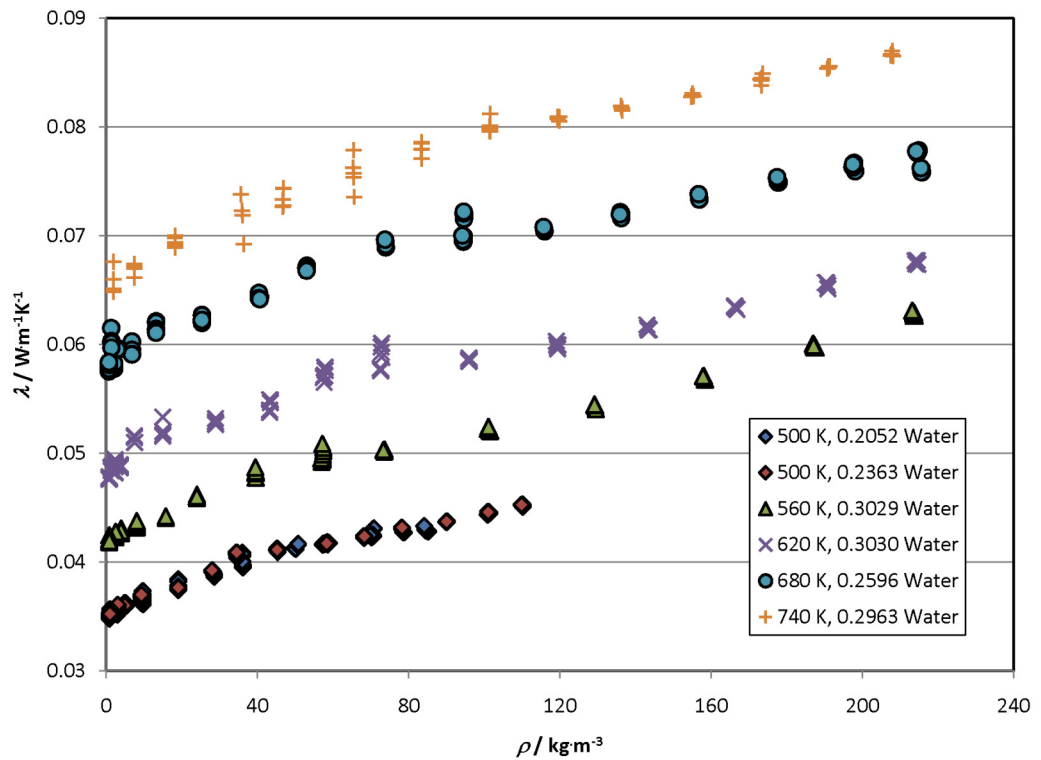


Figure 3.10. Thermal conductivity of mixtures near 0.3 mole fraction H_2O with CO_2 as a function of density calculated with the mixture virial model developed in this work.

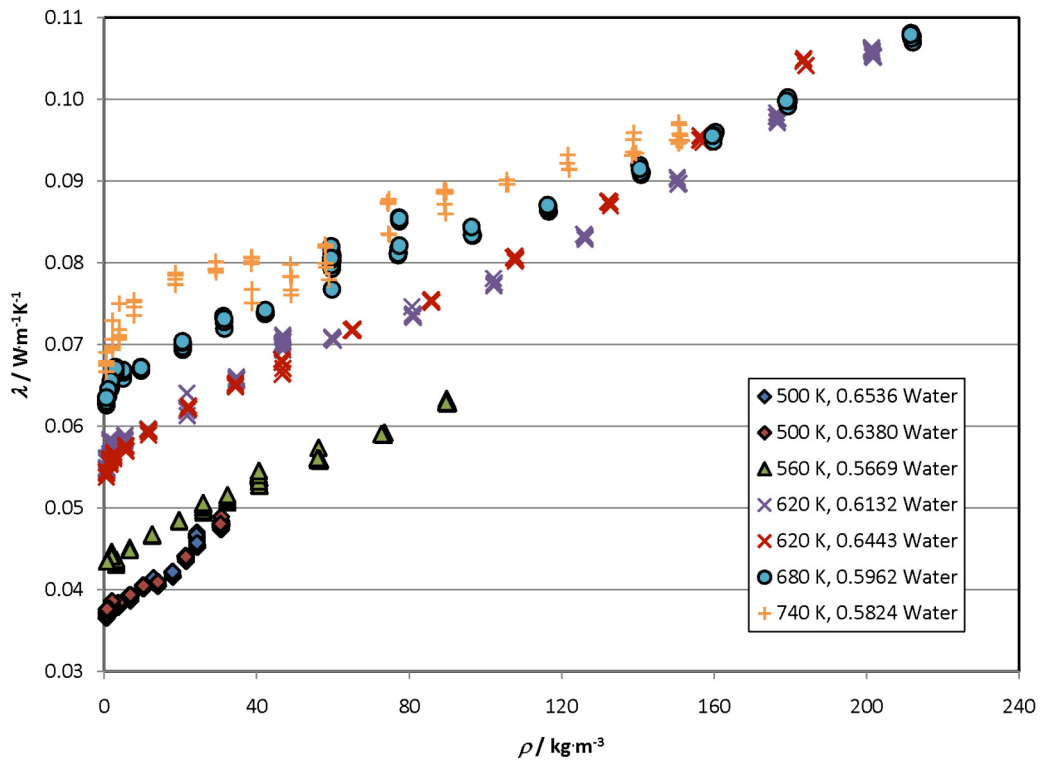


Figure 3.11. Thermal conductivity of mixtures near 0.6 mole fraction H_2O with CO_2 as a function of density calculated with the mixture virial model developed in this work.

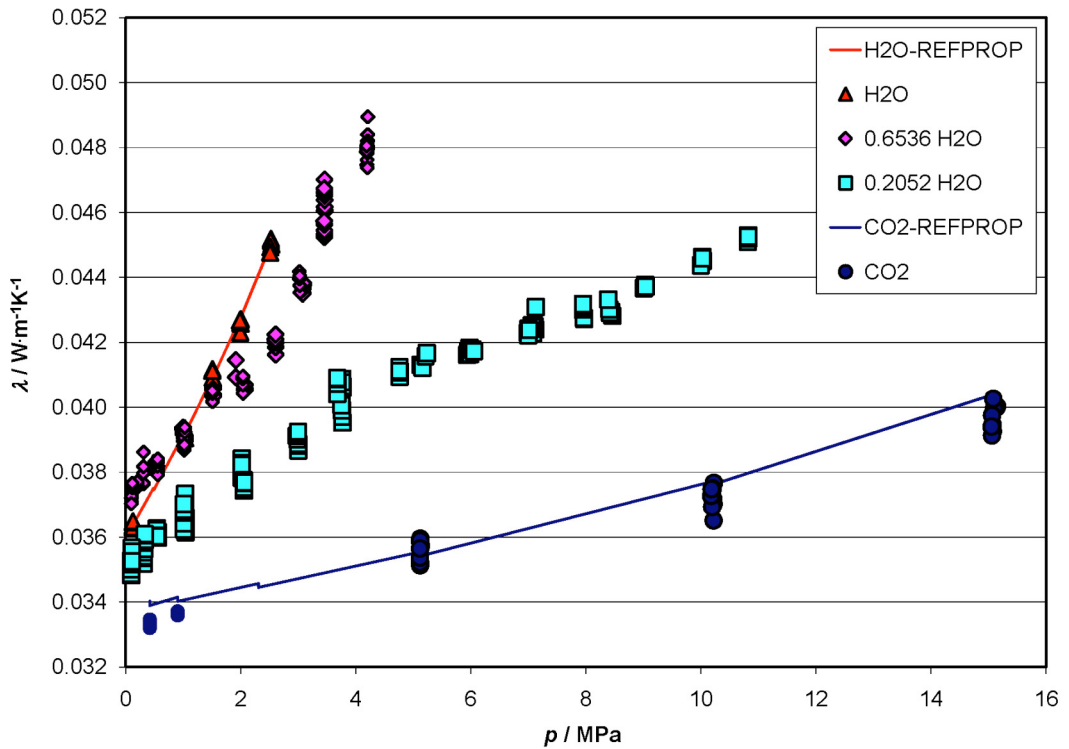


Figure 3.12. Thermal conductivity of mixtures of CO₂ with H₂O measured at temperatures near 500 K as a function of pressure compared to the pure components.

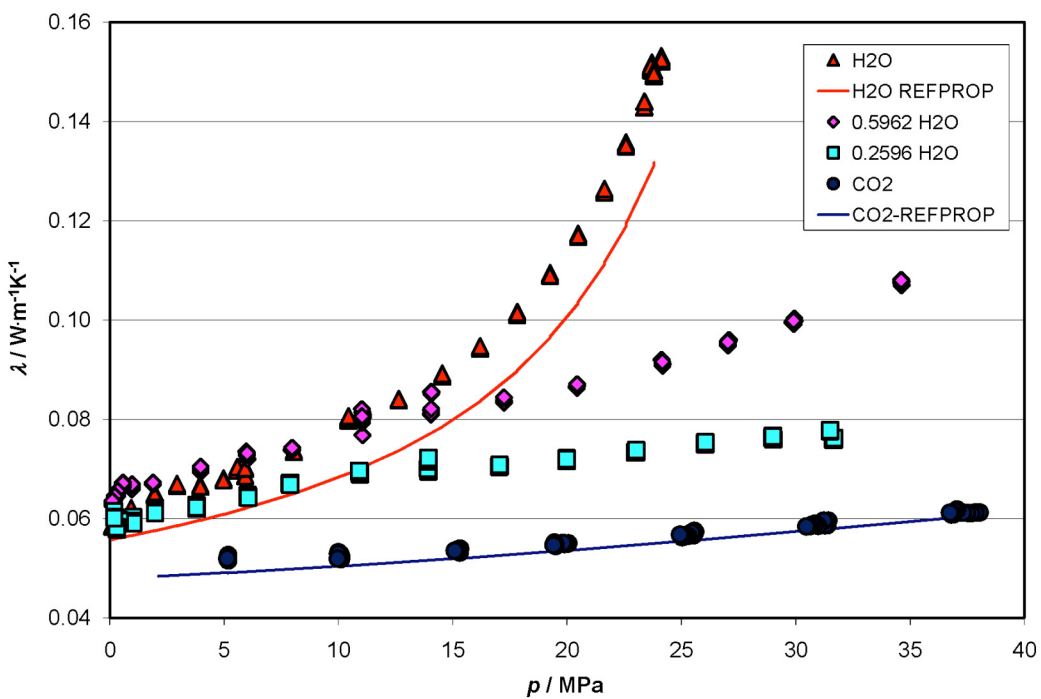


Figure 3.13. Thermal conductivity of mixtures of CO₂ with H₂O measured at temperatures near 680 K as a function of pressure compared to the pure components.

4. EXPERIMENTAL SAMPLES AND MIXTURE PREPARATION

The preparation of a sample mixture of accurately known composition was one of the key technical challenges in these measurements. Because of the extreme volatility difference between water and nitrogen or carbon dioxide, it was not feasible to prepare a homogeneous (single-phase) mixture at room temperature. Rather, the sample was prepared *in situ*, i.e., within the cell. The water and gas (nitrogen or CO₂) were contained in separate sample cylinders and loaded gravimetrically, i.e., by weight. The two cylinders were connected in series, with the nitrogen or CO₂ pushing the water ahead of it into the cell. The sample cylinders were weighed empty, after filling with the pure components, and after discharging into the measuring cell. Differences in the mass of each cylinder, before and after charging the densimeter, give the quantity of sample charged and allow the mixture composition in the apparatus to be determined accurately. This method was applied to both the density measurements (Task 2) and the thermal conductivity measurements (Task 3), with minor variations, as noted below.

4.1 Sample System

The sample cylinders are shown in Figure 4.1. The water cylinder was made up of a short length of high-pressure, type 316 stainless steel tubing with a valve at each end; its internal volume was 5.9 cm³. (For the thermal conductivity measurements, a six-port sampling valve designed for gas-chromatography applications was adapted for use as the water cylinder. One of several fixed-volume “sample loops” was attached, depending on the desired quantity of water.) The gas cylinder was a commercial pressure vessel of type 316 stainless steel (High Pressure Equipment Co. model GC-9) with an internal volume of 134.5 cm³; a valve and a pressure transducer (Omega) were also mounted to this cylinder. Two identical cylinders of each type were constructed; the “spare” cylinder served as the tare mass in a double-substitution weighing design (as described in Section 4.2). The entire sample loading and pressure system is depicted in Figure 4.2.

A major concern in handling the samples was that water could condense into the pressure transducer and filling valves (which must be maintained at near-ambient temperature), altering the composition. These “parasitic” volumes outside the measuring cell were minimized by using low-internal-volume valves designed for liquid chromatography applications and very fine capillary tubing (I.D. of 0.13 mm) for the filling/pressure tube. Since the water was injected into the sample cell first, this tube was filled with nitrogen or CO₂ after filling. The large length-to-diameter ratio of the tube provided a diffusion barrier to water migrating out of the cell.

The procedure for preparing and loading the samples was:

The water cylinder initially contained residual water and nitrogen or CO₂ at atmospheric pressure from the previous filling. The desired (approximate) quantity of water was loaded into the cylinder by volume using a manual piston pump.

The gas cylinder initially contained nitrogen or CO₂ at the pressure remaining from the previous filling. (One set of sample cylinders was dedicated to nitrogen mixtures and the other to CO₂ mixtures to minimize the chance for cross-contamination of the samples and to avoid the need to repeatedly clean and purge the cylinders.) Additional nitrogen or CO₂ was loaded using either pressure from the main supply cylinder or by use of a pneumatically driven gas compressor. The desired pressure was calculated from a mass balance written around the sample cylinders and measuring cell.

The two sample cylinders were weighed (see Section 4.2).

The sample cylinders were connected to the measuring cell as shown in Figure 4.2. The CO₂ cylinder was heated to 40 °C to boost the pressure and ensure a single-phase sample. (The critical temperature of CO₂ is 28.98 °C, and thus, it would be in a two-phase state at room temperature.)

The sinker was put in suspension and the balance reading noted (density measurements only).

The sample was loaded by operating the valves in the sequence:

- (1) V1 closed; “sample” valve to position “1” (“load”)
- (2) gas cylinder valve opened
- (3) inlet valve of water cylinder opened
- (4) outlet valve of water cylinder opened

Approximately five minutes was allowed for the sample to flow into the cell. This was monitored with the pressure transducer attached to the gas cylinder. The balance reading with the sinker in suspension was also monitored (density measurements only). As the sample flowed into the cell, the reading changed rapidly as the buoyancy force on the sinker increased; a reading that changed less than 50 µg per minute indicated that the cell pressure had equilibrated with the pressure in the gas cylinder. (Note that the main pressure transducer was not connected to the measuring cell during this time.)

The valves on the sample cylinders were closed in the reverse of the order stated above.

The line to the main pressure transducer was pressurized to the same pressure as that in the gas cylinder. This prevented flow of gas out of the cell to fill the sample lines and main pressure transducer. The sample valve was then switched to position “2” (“measure”).

The sample cylinders were disconnected and placed in the balance chamber to equilibrate in temperature.

Measurements commenced after allowing sufficient time (typically 24 hours) for diffusion to mix the sample inside the measuring cell.

The two sample cylinders were weighed again.

The water cylinder contained nitrogen or CO₂ at the filling pressure after sample loading.

After weighing the water cylinder with this gas charge, the gas was vented to atmospheric pressure, and the cylinder was weighed again. Note that residual water remained in the cylinder, but the three weighings account for the water actually loaded into the system. By not drying the cylinder before the next loading, an equilibrium water content was reached, and the water loaded into the cylinder volumetrically by the manual pump system more closely matched the water actually loaded into the measuring cell.

4.2 Weighing Design

The measurements for the sample composition are conceptually very simple: fill the water and gas sample cylinder to some initial state; connect these cylinders to the measuring cell and load in the sample; weigh the cylinders again to determine the quantities of water and gas loaded. The mass fraction of water in the mixture is then

$$x_{\text{H}_2\text{O}} = \frac{m_{\text{H}_2\text{O}}}{m_{\text{H}_2\text{O}} + m_{\text{gas}}} , \quad (4.1)$$

where $m_{\text{H}_2\text{O}}$ is the mass of water loaded into the measuring cell and m_{gas} is the mass of nitrogen or CO₂. But Eq. (4.1) must be modified to account for residual sample remaining in the cylinders and sample lines; difficulties also arise in accurately determining the masses.

The gas sample cylinder had a mass of approximately 9.3 kg, but only 2 g to 10 g of sample gas was loaded into the measuring cell. “Taring out” such a large cylinder mass requires a very high-precision balance and the proper weighing design to obtain accurate sample masses. We used a mass comparator balance (Sartorius CC10000S); it had a total capacity of 10060 g, an electronic weighing range of 60 g, a resolution of 0.1 mg, and a linearity and repeatability of 0.3 mg according to the manufacturer’s specification. The total load on the balance must be between 10 000 g and 10 060 g; additional standard masses were placed onto the balance pan to bring the total load into the weighing range. Figure 4.1 shows the sample cylinders being weighed with the mass comparator.

The effect of air buoyancy on the cylinder during the weighing can lead to significant errors if not properly accounted for. Although taking the difference of the cylinder weighings largely cancels air buoyancy effects, the density of ambient air can change by several percent over the time necessary to prepare and load the sample. The air buoyancy effect is $\rho_{\text{air}} \cdot V_{\text{cylinder}}$, or approximately 1.2 g per liter of total cylinder volume (the internal volume plus that of the cylinder itself and any valves or other fittings) at sea level (or 1.0 g/L at Boulder’s elevation,

where these measurements were conducted). The change in air buoyancy resulting from a change of just a few percent in the air density can have a significant effect.

To compensate for air buoyancy, we used the well-known technique of comparing the sample cylinder with a nearly identical “tare” or reference cylinder. The tare cylinder served as the main standard mass in a double-substitution weighing. Additional standard masses were used to make the tare cylinder weighing nearly equal to that of the sample cylinder. The double-substitution weighing design described by Harris [30] was used; this consisted of four separate weighings: (1) the tare cylinder and standard masses, (2) the sample cylinder and (possibly) different standard masses, (3) the sample cylinder and masses used in weighing 2 plus a sensitivity mass, and (4) the tare cylinder and masses used in weighing 1 plus a sensitivity mass. The use of a sensitivity mass allowed a calibration of the balance and reduced errors from balance nonlinearity. The loads on the balance for each weighing were:

$$O_1 = \alpha \left[m_{ct} + m_{sy} - \rho_{air} (V_{ct} + m_{sy}/\rho_s) - W_{zero} \right] \quad (4.2)$$

$$O_2 = \alpha \left[m_{cx} + m_{sx} - \rho_{air} (V_{cx} + m_{sx}/\rho_s) - W_{zero} \right] \quad (4.3)$$

$$O_3 = \alpha \left[m_{cx} + m_{sx} + m_{sw} - \rho_{air} (V_{cx} + (m_{sx} + m_{sw})/\rho_s) - W_{zero} \right] \quad (4.4)$$

$$O_4 = \alpha \left[m_{ct} + m_{sy} + m_{sw} - \rho_{air} (V_{ct} + (m_{sy} + m_{sw})/\rho_s) - W_{zero} \right] \quad (4.5)$$

where

m = mass

O = observation (balance reading)

V = volume

W_{zero} = balance reading with no load on the balance pan

α = balance calibration factor

ρ_{air} = mass density of ambient air in the balance chamber

ρ_s = mass density of standard masses and sensitivity mass

subscripts: ct: tare cylinder

cx: sample cylinder

sy: standard mass(es) used in weighings 1 and 4

sx: standard mass(es) used in weighings 2 and 3

sw: sensitivity mass (20 g was used here)

The assumptions implicit in Eqs. (4.2–4.5) are that the balance reading is linear with the applied load over the limited range of the weighings and that all quantities are constant over the time needed for a complete set of weighings.

The standard masses m_{sy} and m_{sx} were selected to give approximately the same total balance loading for weighings 1 and 2. By keeping the balance loading nearly the same, the effects of any non-linear balance response are greatly reduced; that is, the balance is assumed to be linear over only a limited range. The W_{zero} is the reading with nothing on the balance pan. A direct-reading balance can be tared to give a W_{zero} of zero; for a mass-comparator-type balance W_{zero} is the minimum load needed to bring the balance into its weighing range. In either case, it is the same for each weighing.

Equations (4.2–4.5) form a system of four equations in the unknowns α , m_{ct} , m_{cx} , and W_{zero} . The air density ρ_{air} was calculated from the ambient temperature, pressure, and humidity measured in the balance chamber using a barometer (Vaisala PTB220) and humidity and temperature transmitter (Vaisala HMP237) together with the equations of Picard et al. [53], and ρ_s was obtained from the calibration certificate for the standard masses. The cylinder volumes V_{ct} and V_{cx} were obtained by filling each cylinder with water and determining the water weight; knowing the density of water and also the mass and density of the cylinder itself, the total volume was calculated.

Equations (4.3 and 4.4) are solved for α :

$$\alpha = \frac{O_3 - O_2}{m_{sw} (1 - \rho_{air}/\rho_s)}. \quad (4.6)$$

Equations (4.2 and 4.5) yield a similar expression for α and these can be averaged to obtain:

$$\alpha = \frac{(O_3 - O_2) + (O_4 - O_1)}{2m_{sw} (1 - \rho_{air}/\rho_s)}. \quad (4.7)$$

The parameter α is a calibration factor for the balance. The advantage of using a sensitivity mass and calibrating the balance in this manner is that the balance was calibrated over the same limited range as the cylinder weighings. This contrasts to assuming a linear (or perhaps quadratic) response over the entire balance range, as is the case when the built-in calibration function available on many balances is used.

Equations (4.2 and 4.3) are solved for the difference between the sample and tare cylinders:

$$(m_{\text{cx}} - m_{\text{ct}}) = \frac{O_2 - O_1}{\alpha} + (m_{\text{sy}} - m_{\text{sx}}) + \rho_{\text{air}} \left[(V_{\text{cx}} - V_{\text{ct}}) - \frac{m_{\text{sy}} - m_{\text{sx}}}{\rho_s} \right]. \quad (4.8)$$

A similar result is obtained by solving Eqs. (4.4 and 4.5) and these are combined to yield

$$(m_{\text{cx}} - m_{\text{ct}}) = \frac{(O_2 - O_1) + (O_3 - O_4)}{2\alpha} + (m_{\text{sy}} - m_{\text{sx}}) + \rho_{\text{air}} \left[(V_{\text{cx}} - V_{\text{ct}}) - \frac{m_{\text{sy}} - m_{\text{sx}}}{\rho_s} \right]. \quad (4.9)$$

The key advantage in this approach is that the air buoyancy effect reduces to the (small) difference in volumes of the tare and sample cylinders and the relatively small effect of the standard masses. Also note that W_{zero} and any other constant loads cancel out.

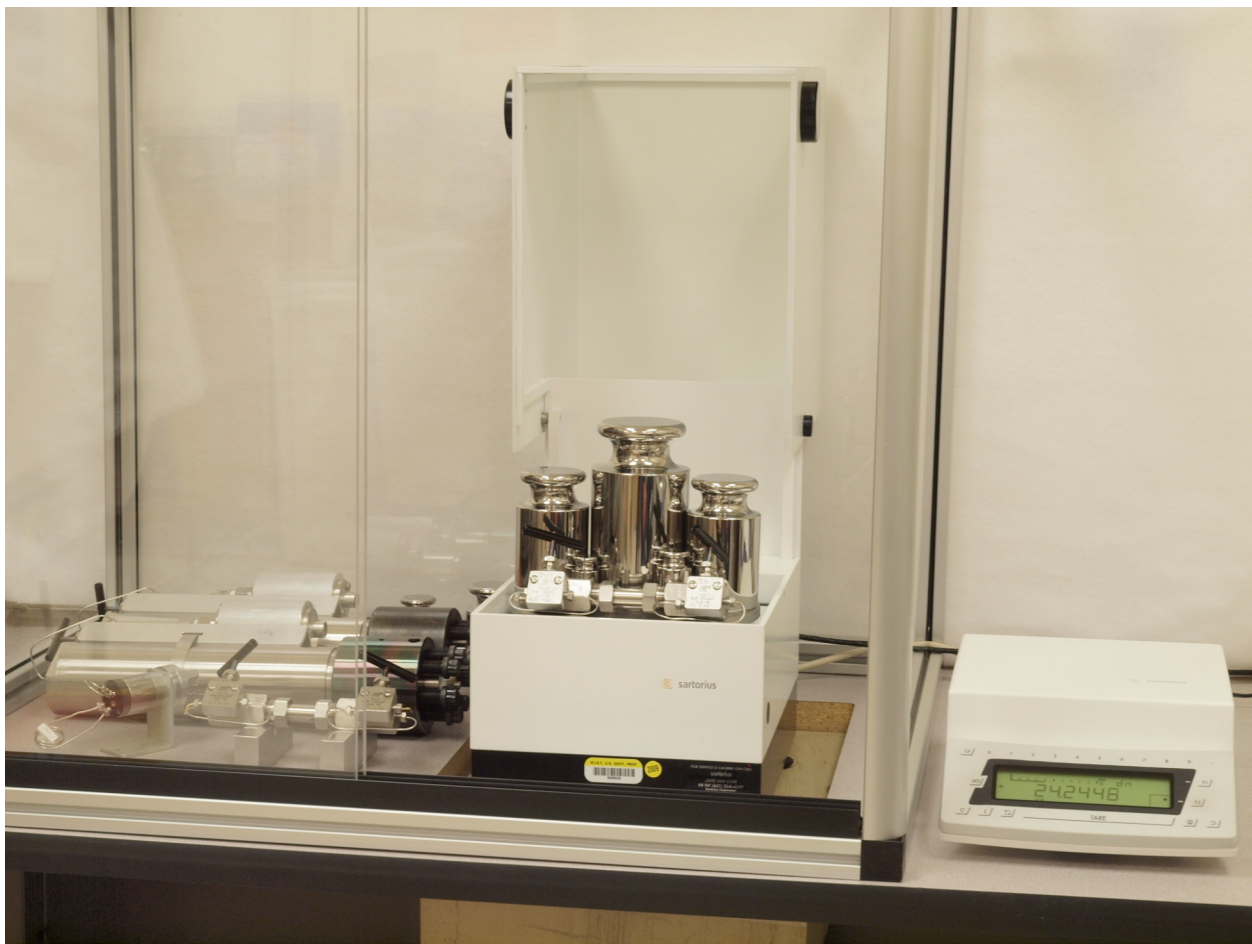


Figure 4.1. Water cylinder and standard masses shown on 10 kg mass comparator during the weighing process for gravimetric preparation of humid-gas mixtures; the “tare” water cylinder and the gas-charge cylinders (large cylinders with 1 valve and pressure transducer) are to the left of the balance; for clarity the draft shields have been opened.

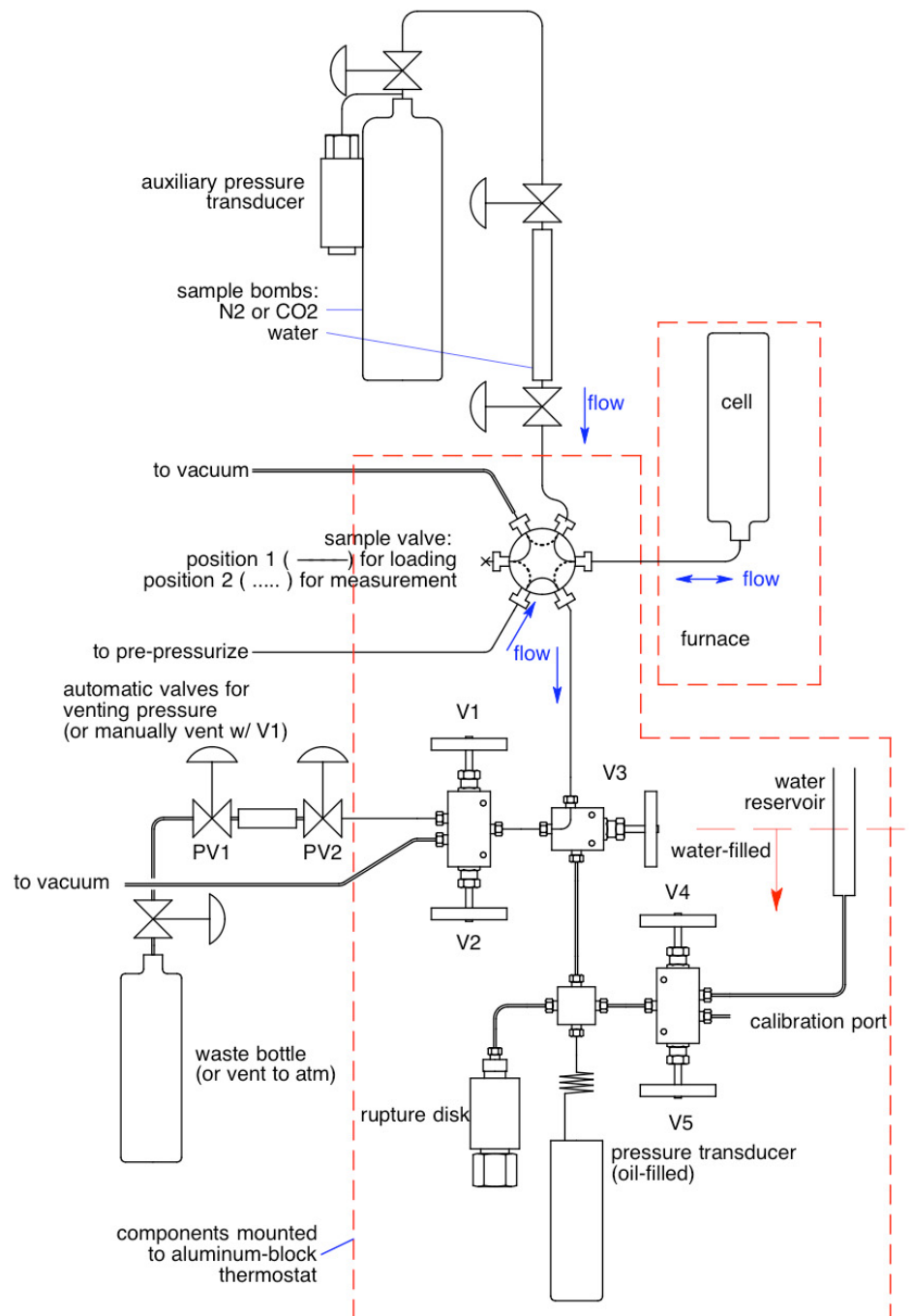


Figure 4.2. Sample and pressure system for high-temperature measurements on water + (nitrogen or carbon dioxide) systems.

CONCLUSIONS AND FUTURE DIRECTIONS

For the modeling part of the work, we have incorporated our molecular modeling results to produce a complete description of the gas-phase thermodynamics of the main components of combustion gases. These results have been integrated into a mixture equation-of-state model and implemented in software based on the NIST REFPROP database [1].

On the experimental side, density measurements have been performed for the H₂O/N₂ and H₂O/CO₂ systems at $T = 500$ K, 560 K, and 620 K. The results are consistent with the modeling work. Measurements of the thermal conductivity of pure H₂O, N₂ and CO₂ and the binary H₂O/N₂ and H₂O/CO₂ mixtures have been completed at temperatures of 500 K, 560 K, 620 K, 680 K, and 740 K with pressures up to 40 MPa.

While this completes the present project, there are related areas of need that could be considered as extensions to this work. These would include:

- (1) Extension of the thermodynamic framework to allow prediction of condensation of water and of vapor-liquid equilibria more generally.
- (2) Experimental measurements for saturated vapor composition for the H₂O/CO₂ mixture at low temperatures (where the uncertainty of our theoretical results becomes larger) in order to provide data for separation and sequestration of CO₂ from combustion gases.
- (3) Measurements and correlation work for improving the knowledge of the viscosity and thermal conductivity of pure CO₂.
- (4) Measurements and modeling for better characterizing the interactions between CO₂ and N₂.

REFERENCES

1. Lemmon, E.W., Huber, M.L., McLinden, M.O. 2010. NIST Standard Reference Database 23, NIST Reference Fluid Thermodynamic and Transport Properties--REFPROP, version 9.0. Gaithersburg, MD: Standard Reference Data Program, National Institute of Standards and Technology
2. Tulegenov, A.S., Wheatley, R.J., Hodges, M.P., Harvey, A.H. 2007. Intermolecular potential and second virial coefficient of the water–nitrogen complex. *J. Chem. Phys.* 126: 094305
3. Rigby, M., Prausnitz, J.M. 1968. Solubility of water in compressed nitrogen, argon, and methane. *J. Phys. Chem.* 72: 330
4. Kosyakov, N.E., Ivchenko, B.I., Krishtopa, P.P. 1977. Moisture contents of compressed nitrogen and hydrogen at low temperatures. *J. Appl. Chem. USSR* 50: 2436
5. Gillespie, P.C., Wilson, G.M. 1980. *Technical Report No. RR-41*, Gas Processors Association, Tulsa, OK
6. Oellrich, L.R., Althaus, K. 2001. *GERG Technical Monograph 14, Fortschr.-Ber. VDI, Series 3, No. 679*, VDI Verlag, Düsseldorf
7. Podmurnaya, O.A., Gudkov, O., Dubovikov, N. 2004. Equilibrium composition of nitrogen-water mixtures at pressures below 10 MPa. *Russ. J. Phys. Chem.* 78: 300
8. Mohammadi, A.H., Chapoy, A., Tohidi, B., Richon, D. 2005. Water content measurement and modeling in the nitrogen plus water system. *J. Chem. Eng. Data* 50: 541
9. Wilson, G.M., Brady, C.J. 1983. *Heats of Mixing of Steam with N₂, CO₂, H₂, CH₄ and CO at High Temperatures and Pressures Using a New High Temperature Calorimeter, Technical Report No. RR-73*, Gas Processors Association, Tulsa, OK
10. Wormald, C.J., Lancaster, N.M. 1988. Excess Enthalpies and Cross-term 2nd Virial Coefficients for Mixtures Containing Water Vapor. *J. Chem. Soc., Faraday Trans. 1* 84: 3141
11. Lancaster, N.M., Wormald, C.J. 1990. Excess molar enthalpies of 9 binary steam mixtures – New and corrected values. *J. Chem. Eng. Data* 35: 11
12. Blanco, S.T., Velasco, I., Otin, S. 2002. Dew points of binary nitrogen plus water mixtures. *Phys. Chem. Liquids* 40: 167
13. Abdulagatov, I.M., Bazaev, A.R., Gasanov, R.K., Ramazanova, A.E. 1996. Measurements of the (p,q,T) properties and virial coefficients of pure water, methane, n-hexane, n-octane, benzene, and of their aqueous mixtures in the supercritical region. *J. Chem. Thermodyn.* 28: 1037
14. Gillespie, P.C., Wilson, G.M. 1982. *Vapor-Liquid and Liquid-Liquid Equilibria, Technical Report No. RR-48*, Gas Processors Association, Tulsa, OK
15. Bamberger, A., Sieder, G., Maurer, G. 2000. High-pressure (vapor + liquid) equilibrium in binary mixtures of (carbon dioxide + water or acetic acid) at temperatures from 313 to 353 K. *J. Supercrit. Fluids* 17: 97
16. Coan, C.R., King Jr., A.D. 1971. Solubility of water in compressed carbon dioxide, nitrous oxide, and ethane. Evidence for hydration of carbon dioxide and nitrous oxide in the gas phase. *J. Am. Chem. Soc.* 93: 1857

17. Vanderzee, C.E., Haas, N.C. 1981. Second cross virial coefficients B12 for the gas mixture (carbon dioxide + water) from 300 to 1000 K. *J. Chem. Thermodyn.* 13: 203
18. Patel, M.R., Holste, J.C., Hall, K.R., Eubank, P.T. 1987. Thermophysical properties of gaseous carbon dioxide-water mixtures. *Fluid Phase Equil.* 36: 279
19. Valtz, A., Chapoy, A., Coquelet, C., Paricaud, P., Richon, D. 2004. Vapour-liquid equilibria in the carbon dioxide-water system, measurement and modeling from 278.2 to 318.2 K. *Fluid Phase Equil.* 226: 333
20. Wheatley, R.J., Harvey, A.H. 2011. Intermolecular potential energy surface and second virial coefficients for the water-CO₂ dimer. *J. Chem. Phys.* 134: 134309
21. Hodges, M.P., Wheatley, R.J., Harvey, A.H. 2002. Intermolecular potentials and second virial coefficients of the water-neon and water-argon complexes. *J. Chem. Phys.* 117: 7169-7179
22. Akin-Ojo, O., Harvey, A.H., Szalewicz, K. 2006. Calculations of the cross second virial coefficient with quantum corrections for the methane-water system using an *ab initio* potential energy surface. *J. Chem. Phys.* 125: 014314
23. Wheatley, R.J., Harvey, A.H. 2007. The water-oxygen dimer: first-principles calculation of an extrapolated potential energy surface and second virial coefficients. *J. Chem. Phys.* 127: 074303
24. Wheatley, R.J., Harvey, A.H. 2009. Intermolecular potential energy surface and second virial coefficients for the nonrigid water-CO dimer. *J. Chem. Phys.* 131: 154305
25. Wagner, W., Kleinrahm, R. 2004. Densimeters for very accurate density measurements of fluids over large ranges of temperature, pressure, and density. *Metrologia* 41: S24-S39
26. McLinden, M.O., Kleinrahm, R., Wagner, W. 2007. Force transmission errors in magnetic suspension densimeters. *Int. J. Thermophys.* 28: 429-448
27. Hust, J.G., Filla, J., Smith, D.R. 1987. A modified digital PID temperature controller for thermal property measurements. *J. Thermal Insulation* 11: 102-107
28. Span, R., Lemmon, E.W., Jacobsen, R.T., Wagner, W., Yokozeki, A. 2000. A reference equation of state for the thermodynamic properties of nitrogen for temperatures from 63.151 to 1000 K and pressures to 2200 MPa. *J. Phys. Chem. Ref. Data* 29: 1361-1433
29. Span, R., Wagner, W. 1996. A new equation of state for carbon dioxide covering the fluid region from the triple-point temperature to 1100 K at pressures up to 800 MPa. *J. Phys. Chem. Ref. Data* 26: 1509-1596
30. Harris, G.L., Torres, J.A. 2003. *Selected laboratory and measurement practices and procedures, to support basic mass calibrations*. NISTIR 6969, National Institute of Standards and Technology
31. Bowman, H.A., Schoonover, R.M., Carroll, C.L. 1973. A density scale based on solid objects. *J. Res. Natl. Bur. Stand.* 78A: 13-40
32. Bowman, H.A., Schoonover, R.M., Carroll, C.L. 1974. The utilization of solid objects as reference standards in density measurements. *Metrologia* 10: 117-121
33. McLinden, M.O., Splett, J.D. 2008. A liquid density standard over wide ranges of temperature and pressure based on toluene. *J. Res. Natl. Inst. Stand. Technol.* 113: 29-67
34. Swenson, C.A. 1983. Recommended values for the thermal expansivity of silicon from 0 to 1000 K. *J. Phys. Chem. Ref. Data* 12: 179-182
35. Smithells, C.J. 1997. *Smithells Metals Reference Book*. Boston: Butterworth-Heinemann
36. Haynes, W.M., (Editor). 2010. *CRC Handbook of Chemistry and Physics, 91st Edition*. Boca Raton, FL: CRC Press

37. Boggs, P.T., Byrd, R.H., Rogers, J.E., Schnabel, R.B. 1992. *User's reference guide for ODRPACK version 2.01 software for weighted orthogonal distance regression. Rep. NISTIR 4834; code is available at <http://www.netlib.org/odrpack/>*, National Institute of Standards and Technology
38. Perkins, R.A., Roder, H.M., Nieto De Castro, C.A. 1991. A High-Temperature Transient Hot-Wire Thermal Conductivity Apparatus for Fluids. *J. Res. Natl. Inst. Stand. Technol.* 96: 247-269
39. Healy, J., Degroot, J.J., Kestin, J. 1976. The Theory of the Transient Hot-Wire Method for Measuring the Thermal Conductivity. *Physica* C82: 392-408
40. Assael, M.J., Karagiannidis, L., Richardson, S.M., Wakeham, W.A. 1992. Compression Work using the Transient Hot-Wire Method. *Int. J. Thermophys.* 13: 223-235
41. Taxis, B., Stephan, K. 1994. The Measurement of the Thermal Conductivity of Gases at Low Density by the Transient Hot-Wire Technique. *High Temp. High Press.* 15: 141-153
42. Li, S.F.Y., Papadaki, M., Wakeham, W.A. 1993. The measurement of the Thermal Conductivity of Gases at Low Density by the Transient Hot-Wire Technique. *High Temp. High Press.* 25: 451-458
43. Li, S.F.Y., Papadaki, M., Wakeham, W.A. 1994. Thermal Conductivity of Low-Density Polyatomic Gases. In *Thermal Conductivity* 22, ed. Tong, T.W., pp. 531-542. Lancaster, PA: Technomic Publishing
44. Kierkus, W.T., Mani, N., Venart, J.E.S. 1973. Radial-Axial Transient Heat Conduction in a Region Bounded Internally by a Circular Cylinder of Finite Length and Appreciable Heat Capacity. *Canadian J. Phys.* 51: 1182-1186
45. Woodfield, P.L., Fukai, J., Fujii, M., Takata, Y., Shinzato, K. 2008. A Two-Dimensional Analytical Solution for the Transient Short-Hot-Wire Method. *Int. J. Thermophys.* 29: 1278-1298
46. Roder, H.M., Perkins, R.A., Laesecke, A., Nieto De Castro, C.A. 2000. Absolute steady-state thermal conductivity measurements by use of a transient hot-wire system. *J. Res. Natl. Inst. Stand. Technol.* 105: 221-253
47. Lemmon, E.W., Jacobsen, R.T. 2004. Viscosity and thermal conductivity equations for nitrogen, oxygen, argon, and air. *Int. J. Thermophys.* 25: 21-69
48. Vesovic, V., Wakeham, W.A., Olchowy, G.A., Sengers, J.V., Watson, J.T.R., Millat, J. 1990. The transport properties of carbon dioxide. *J. Phys. Chem. Ref. Data* 19: 763-808
49. International Association for the Properties of Water and Steam. 1998. *Revised release on the IAPS formulation 1985 for the thermal conductivity of ordinary water substance.*
50. Gruss, H., Schmick, H. 1928. Über die Wärmeleitfähigkeit von Gasgemischen. *Wissenschaftliche Veröffentlichungen aus dem Siemens-Konzern*: 202-224
51. Timrot, D.L., Vargaftik, N.B. 1952. *Heat conductivity, viscosity, and thermodynamical properties of steam at high temperatures and pressures*. Presented at Fourth World Power Conference, London
52. Frohn, A., Westerdorf, M. 1981. *Measurements of the conduction of heat in water vapor, nitrogen and mixtures of these gases in a wide knudsen-number range*. Presented at 17th International Thermal Conductivity Conference, Gaithersburg, MD
53. Picard, A., Davis, R.S., Gläser, M., Fujii, K. 2008. Revised formula for the density of moist air (CIPM-2007). *Metrologia* 45: 149-155

APPENDIX

Thermal Conductivity Data Tables

Nomenclature

- Run Point – Unique measurement identification number.
- p_e – Measured pressure of fluid in hot-wire cell. (Uncertainty[†] of 7 kPa)
- q – Applied heating power per unit length of wire. (Relative Uncertainty[†] of 0.01 %)
- T_e – Measured temperature associated with the thermal conductivity. (Uncertainty[†] of 5 mK)
- ρ_e – Mass density of fluid in hot-wire cell calculated with an equation of state at measured T_e and P_e . (Uncertainty[†] varies with state point and is largest in the critical region, where small changes T_e and p_e lead to large changes in ρ_e)
- λ_e – Measured thermal conductivity of fluid in hot-wire cell. (Uncertainty[†] less than 1 % for measurements away from the critical point and for gas at pressures above 1 MPa, increasing to 4 % at temperatures above 500 K and for gas at pressure below 1 MPa)
- STAT – Reproducibility of thermal conductivity from the uncertainty[†] in the slope of the line fit to ideal temperature rise versus the logarithm of elapsed time. (0.001 corresponds to 0.1 %)
- T_i – Measured temperature of hot-wire cell. (Uncertainty[†] of 5 mK)
- ΔT_a – Average rise in temperature during the steady-state measurement. (Uncertainty[†] of 5 mK)
- t_s – Start time for averaging of steady-state temperature rise. (Uncertainty[†] of 2.5 μ s)
- t_e – End time for averaging of steady-state temperature rise. (Uncertainty[†] of 2.5 μ s)
- Ra – Rayleigh number (values of $Ra < 17,000$ require convection corrections of less than 1 %).

[†] Coverage factor of $k=2$ (approximately 95 % confidence interval).

List of Tables

	<u>Page</u>
Table A1. Thermal conductivity data for nitrogen from transient measurements at temperatures from 500 K to 740 K.	A3
Table A2. Thermal conductivity data for nitrogen from steady-state measurements at temperatures from 500 K to 740 K.	A11
Table A3. Thermal conductivity data for carbon dioxide from transient measurements at temperatures from 500 K to 740 K.	A15
Table A4. Thermal conductivity data for carbon dioxide from steady-state measurements at temperatures from 500 K to 740 K.	A26
Table A5. Thermal conductivity data for water from transient measurements at temperatures from 500 K to 740 K.	A28
Table A6. Thermal conductivity data for water from steady-state measurements at temperatures from 500 K to 740 K.	A34
Table A7. Thermal conductivity data for mixtures of water with nitrogen from transient measurements at temperatures from 500 K to 740 K.	A40
Table A8. Thermal conductivity data for mixtures of water with nitrogen from steady-state measurements at temperatures from 500 K to 740 K.	A45
Table A9. Thermal conductivity data for the mixtures of water with carbon dioxide from transient measurements at temperatures from 500 K to 740 K.	A54
Table A10. Thermal conductivity data for mixtures of water with carbon dioxide from steady-state measurements at temperatures from 500 K to 740 K.	A65

Table A1. Thermal conductivity data for nitrogen from transient measurements at temperatures from 500 K to 740 K.

Run Point	$\frac{p_e}{\text{MPa}}$	$\frac{q}{\text{W} \cdot \text{m}^{-1}}$	T_e K	$\frac{\rho_e}{\text{kg} \cdot \text{m}^{-3}}$	$\frac{\lambda_e}{\text{W} \cdot \text{m}^{-1} \cdot \text{K}^{-1}}$	STAT	$\frac{T_i}{\text{K}}$
5001	35.679	0.16167	503.727	200.180	0.04860	0.003	501.573
5002	35.641	0.18131	503.986	199.910	0.04838	0.003	501.573
5003	35.606	0.20209	504.265	199.640	0.04786	0.003	501.573
5004	35.571	0.22401	504.563	199.370	0.04783	0.003	501.579
5005	35.534	0.24707	504.865	199.100	0.04772	0.003	501.574
5006	35.365	0.16195	503.717	198.750	0.04943	0.003	501.582
5007	35.284	0.18149	503.978	198.280	0.04944	0.002	501.577
5008	35.199	0.20239	504.258	197.790	0.04924	0.002	501.587
5009	35.122	0.22397	504.559	197.330	0.04927	0.002	501.595
5010	35.044	0.24712	504.876	196.860	0.04911	0.002	501.593
5011	30.115	0.16197	503.895	173.980	0.04768	0.003	501.599
5012	30.055	0.18151	504.165	173.600	0.04755	0.003	501.601
5013	29.997	0.20240	504.458	173.220	0.04776	0.002	501.598
5014	29.941	0.22400	504.767	172.850	0.04768	0.002	501.601
5015	29.882	0.24717	505.097	172.450	0.04779	0.002	501.601
5016	29.825	0.16160	503.895	172.570	0.04674	0.003	501.602
5017	29.801	0.18125	504.179	172.360	0.04665	0.003	501.604
5018	29.775	0.20201	504.457	172.140	0.04619	0.003	501.594
5019	29.750	0.22396	504.765	171.920	0.04608	0.004	501.601
5020	29.724	0.24697	505.092	171.680	0.04610	0.003	501.599
5021	25.045	0.16162	504.011	148.580	0.04512	0.005	501.592
5022	25.029	0.18126	504.303	148.410	0.04509	0.003	501.585
5023	25.012	0.20203	504.598	148.240	0.04520	0.004	501.585
5024	24.995	0.22396	504.939	148.050	0.04519	0.004	501.592
5025	24.974	0.24701	505.252	147.850	0.04460	0.003	501.584
5026	24.887	0.16200	503.971	147.770	0.04606	0.003	501.587
5027	24.848	0.18153	504.263	147.490	0.04603	0.002	501.587
5028	24.816	0.20243	504.581	147.230	0.04610	0.003	501.582
5029	24.780	0.22403	504.911	146.950	0.04618	0.003	501.585
5030	24.740	0.24718	505.257	146.650	0.04632	0.003	501.586
5031	20.382	0.14338	503.826	123.920	0.04462	0.003	501.593
5032	20.354	0.16201	504.113	123.700	0.04475	0.003	501.589
5033	20.326	0.18157	504.426	123.470	0.04481	0.003	501.596
5034	20.298	0.20247	504.754	123.240	0.04505	0.003	501.596
5035	20.270	0.22406	505.089	123.000	0.04492	0.003	501.592
5036	20.229	0.14316	503.826	123.090	0.04422	0.004	501.596
5037	20.215	0.16166	504.120	122.940	0.04421	0.003	501.600
5038	20.201	0.18133	504.421	122.790	0.04400	0.004	501.599
5039	20.189	0.20209	504.750	122.650	0.04389	0.003	501.600

Run Point	$\frac{p_e}{\text{MPa}}$	$\frac{q}{\text{W} \cdot \text{m}^{-1}}$	$\frac{T_e}{\text{K}}$	$\frac{\rho_e}{\text{kg} \cdot \text{m}^{-3}}$	$\frac{\lambda_e}{\text{W} \cdot \text{m}^{-1} \cdot \text{K}^{-1}}$	STAT	$\frac{T_i}{\text{K}}$
5040	20.176	0.22404	505.087	122.490	0.04390	0.004	501.596
5041	15.299	0.12578	503.712	95.460	0.04341	0.005	501.590
5042	15.292	0.14316	504.004	95.360	0.04334	0.004	501.593
5043	15.285	0.16166	504.310	95.260	0.04305	0.005	501.592
5044	15.276	0.18132	504.634	95.150	0.04306	0.004	501.590
5045	15.267	0.20209	504.972	95.030	0.04310	0.004	501.592
5046	15.170	0.12606	503.657	94.730	0.04367	0.004	501.596
5047	15.156	0.14340	503.950	94.590	0.04358	0.003	501.602
5048	15.141	0.16204	504.256	94.440	0.04357	0.003	501.595
5049	15.126	0.18159	504.595	94.290	0.04365	0.003	501.595
5050	15.108	0.20249	504.955	94.120	0.04384	0.003	501.595
5051	10.104	0.10986	503.584	64.670	0.04275	0.005	501.602
5052	10.094	0.12608	503.871	64.570	0.04299	0.005	501.599
5053	10.083	0.14341	504.184	64.460	0.04285	0.004	501.604
5054	10.076	0.16206	504.519	64.380	0.04294	0.004	501.601
5055	10.067	0.18160	504.869	64.280	0.04313	0.004	501.600
5056	10.055	0.10952	503.567	64.370	0.04302	0.006	501.604
5057	10.052	0.12579	503.845	64.310	0.04303	0.006	501.595
5058	10.048	0.14317	504.155	64.250	0.04267	0.007	501.596
5059	10.043	0.16169	504.494	64.180	0.04265	0.005	501.598
5060	10.039	0.18138	504.840	64.110	0.04271	0.005	501.593
5106	36.604	0.16025	563.127	184.250	0.05190	0.003	561.067
5107	36.556	0.17860	563.372	183.980	0.05192	0.003	561.073
5108	36.507	0.19798	563.616	183.700	0.05182	0.003	561.069
5109	36.459	0.21835	563.887	183.420	0.05141	0.003	561.073
5110	36.409	0.23968	564.153	183.130	0.05154	0.003	561.071
5111	36.051	0.16034	563.091	181.970	0.05163	0.003	561.093
5112	35.936	0.17880	563.339	181.420	0.05244	0.003	561.090
5113	35.832	0.19787	563.575	180.910	0.05148	0.003	561.086
5114	35.737	0.21831	563.835	180.440	0.05177	0.002	561.082
5115	35.633	0.23975	564.092	179.930	0.05180	0.002	561.075
5116	29.938	0.16030	563.176	155.690	0.05019	0.003	561.025
5117	29.882	0.17873	563.455	155.360	0.05017	0.003	561.032
5118	29.814	0.19783	563.736	154.990	0.04994	0.003	561.031
5119	29.748	0.21827	564.020	154.620	0.04997	0.002	561.034
5120	29.677	0.23959	564.315	154.230	0.05015	0.002	561.046
5121	29.513	0.16021	563.263	153.770	0.04975	0.003	561.060
5122	29.483	0.17856	563.527	153.570	0.04972	0.003	561.066
5123	29.453	0.19796	563.777	153.370	0.04995	0.003	561.063
5124	29.417	0.21829	564.072	153.130	0.04977	0.002	561.066
5125	29.386	0.23965	564.364	152.920	0.04975	0.003	561.070

Run Point	$\frac{p_e}{\text{MPa}}$	$\frac{q}{\text{W} \cdot \text{m}^{-1}}$	$\frac{T_e}{\text{K}}$	$\frac{\rho_e}{\text{kg} \cdot \text{m}^{-3}}$	$\frac{\lambda_e}{\text{W} \cdot \text{m}^{-1} \cdot \text{K}^{-1}}$	STAT	$\frac{T_i}{\text{K}}$
5126	24.914	0.14285	563.088	132.800	0.04893	0.004	561.040
5127	24.888	0.16021	563.333	132.620	0.04874	0.003	561.038
5128	24.866	0.17856	563.599	132.460	0.04875	0.003	561.041
5129	24.844	0.19796	563.865	132.300	0.04872	0.003	561.033
5130	24.822	0.21833	564.150	132.130	0.04849	0.002	561.028
5131	24.694	0.14309	563.054	131.780	0.04874	0.003	561.041
5132	24.646	0.16033	563.310	131.490	0.04878	0.003	561.040
5133	24.593	0.17877	563.590	131.190	0.04868	0.003	561.046
5134	24.548	0.19787	563.868	130.910	0.04875	0.003	561.046
5135	24.496	0.21828	564.172	130.600	0.04881	0.002	561.050
5136	19.618	0.12662	562.968	107.320	0.04728	0.004	561.042
5137	19.585	0.14307	563.228	107.110	0.04744	0.003	561.042
5138	19.555	0.16035	563.420	106.920	0.04743	0.003	561.043
5139	19.520	0.17881	563.698	106.700	0.04757	0.003	561.038
5140	19.488	0.19785	563.991	106.490	0.04730	0.003	561.041
5141	19.457	0.12652	562.956	106.520	0.04717	0.004	561.043
5142	19.442	0.14287	563.205	106.410	0.04735	0.003	561.041
5143	19.428	0.16025	563.465	106.290	0.04741	0.003	561.045
5144	19.413	0.17861	563.750	106.160	0.04738	0.003	561.045
5145	19.399	0.19799	564.039	106.040	0.04742	0.003	561.047
5146	15.003	0.12653	563.086	83.890	0.04670	0.004	561.058
5147	14.994	0.14288	563.350	83.800	0.04625	0.004	561.062
5148	14.985	0.16028	563.626	83.720	0.04646	0.003	561.063
5149	14.976	0.17861	563.916	83.630	0.04649	0.003	561.063
5150	14.966	0.19800	564.232	83.530	0.04654	0.003	561.069
5151	14.901	0.12664	563.078	83.360	0.04644	0.004	561.060
5152	14.880	0.14309	563.337	83.220	0.04659	0.004	561.061
5153	14.860	0.16035	563.591	83.070	0.04635	0.003	561.056
5154	14.840	0.17881	563.885	82.930	0.04639	0.003	561.060
5155	14.820	0.19789	564.194	82.780	0.04659	0.003	561.064
5156	9.952	0.12666	563.227	56.960	0.04569	0.005	561.055
5158	9.927	0.14309	563.515	56.800	0.04588	0.004	561.060
5160	9.902	0.16035	563.812	56.630	0.04600	0.004	561.066
5162	9.878	0.17880	564.134	56.470	0.04602	0.004	561.068
5164	9.853	0.19795	564.396	56.310	0.04610	0.004	561.074
5196	40.638	0.17671	622.418	183.190	0.05597	0.003	620.297
5197	40.541	0.19489	622.624	182.770	0.05598	0.003	620.294
5198	40.440	0.21393	622.874	182.340	0.05561	0.003	620.299
5199	40.344	0.23385	623.110	181.920	0.05569	0.002	620.297
5200	40.250	0.25473	623.376	181.500	0.05577	0.002	620.301
5201	39.798	0.17639	622.425	180.080	0.05525	0.003	620.318

Run Point	$\frac{p_e}{\text{MPa}}$	$\frac{q}{\text{W} \cdot \text{m}^{-1}}$	$\frac{T_e}{\text{K}}$	$\frac{\rho_e}{\text{kg} \cdot \text{m}^{-3}}$	$\frac{\lambda_e}{\text{W} \cdot \text{m}^{-1} \cdot \text{K}^{-1}}$	STAT	$\frac{T_i}{\text{K}}$
5202	39.601	0.19461	622.635	179.290	0.05517	0.003	620.311
5203	39.409	0.21372	622.872	178.520	0.05501	0.002	620.309
5204	39.228	0.23335	623.127	177.780	0.05504	0.002	620.301
5205	39.045	0.25424	623.409	177.020	0.05478	0.002	620.297
5206	34.328	0.17671	622.581	159.190	0.05418	0.003	620.298
5207	34.275	0.19491	622.823	158.930	0.05437	0.003	620.305
5208	34.217	0.21395	623.060	158.650	0.05424	0.002	620.301
5209	34.157	0.23387	623.310	158.350	0.05422	0.002	620.306
5210	34.103	0.25474	623.590	158.070	0.05412	0.002	620.309
5211	33.767	0.17641	622.490	157.010	0.05369	0.003	620.311
5212	33.636	0.19464	622.719	156.440	0.05347	0.003	620.312
5213	33.514	0.21375	622.968	155.910	0.05350	0.003	620.315
5214	33.402	0.23338	623.234	155.400	0.05342	0.003	620.305
5215	33.283	0.25429	623.505	154.870	0.05348	0.002	620.299
5216	29.569	0.15943	622.384	140.180	0.05240	0.003	620.301
5217	29.471	0.17642	622.625	139.720	0.05235	0.003	620.307
5218	29.375	0.19466	622.872	139.280	0.05233	0.003	620.306
5219	29.282	0.21379	623.118	138.840	0.05231	0.003	620.302
5220	29.186	0.23341	623.388	138.390	0.05253	0.002	620.308
5221	29.078	0.15945	622.400	138.150	0.05314	0.003	620.300
5222	29.041	0.17676	622.639	137.950	0.05319	0.003	620.304
5223	29.001	0.19494	622.872	137.740	0.05284	0.002	620.295
5224	28.962	0.21401	623.126	137.530	0.05283	0.002	620.297
5225	28.923	0.23392	623.385	137.310	0.05301	0.002	620.295
5226	24.951	0.15945	622.478	120.790	0.05210	0.004	620.280
5227	24.922	0.17676	622.715	120.620	0.05219	0.003	620.279
5228	24.894	0.19494	622.967	120.460	0.05183	0.003	620.280
5229	24.870	0.21400	623.236	120.300	0.05190	0.002	620.282
5230	24.844	0.23391	623.516	120.140	0.05197	0.002	620.283
5231	24.708	0.15944	622.403	119.760	0.05155	0.003	620.294
5232	24.640	0.17644	622.645	119.430	0.05147	0.003	620.299
5233	24.568	0.19468	622.903	119.070	0.05133	0.003	620.307
5234	24.501	0.21382	623.192	118.730	0.05125	0.003	620.314
5235	24.434	0.23345	623.465	118.390	0.05156	0.003	620.314
5236	20.002	0.15945	622.557	99.040	0.05061	0.003	620.286
5237	19.948	0.17646	622.779	98.760	0.05039	0.003	620.278
5238	19.902	0.19469	623.017	98.520	0.05048	0.003	620.273
5239	19.854	0.21382	623.263	98.260	0.05037	0.003	620.262
5240	19.802	0.23345	623.522	97.990	0.05057	0.002	620.256
5241	19.750	0.15948	622.532	97.910	0.05087	0.005	620.250
5242	19.733	0.17679	622.759	97.800	0.05083	0.005	620.246

Run Point	$\frac{p_e}{\text{MPa}}$	$\frac{q}{\text{W} \cdot \text{m}^{-1}}$	$\frac{T_e}{\text{K}}$	$\frac{\rho_e}{\text{kg} \cdot \text{m}^{-3}}$	$\frac{\lambda_e}{\text{W} \cdot \text{m}^{-1} \cdot \text{K}^{-1}}$	STAT	$\frac{T_i}{\text{K}}$
5243	19.710	0.19497	623.022	97.650	0.05088	0.003	620.245
5244	19.689	0.21406	623.288	97.520	0.05086	0.004	620.241
5245	19.669	0.23398	623.575	97.380	0.05080	0.003	620.240
5246	15.161	0.15948	622.650	76.730	0.04957	0.006	620.237
5247	15.150	0.17679	622.912	76.650	0.04968	0.004	620.233
5248	15.139	0.19498	623.187	76.560	0.04981	0.004	620.235
5249	15.127	0.21404	623.490	76.470	0.05004	0.003	620.236
5250	15.115	0.23397	623.789	76.380	0.04965	0.004	620.236
5251	15.019	0.15948	622.631	76.060	0.04941	0.003	620.291
5252	14.991	0.17648	622.918	75.890	0.04943	0.003	620.311
5253	14.961	0.19472	623.240	75.720	0.04943	0.003	620.321
5254	14.933	0.21386	623.547	75.550	0.04943	0.003	620.332
5255	14.904	0.23349	623.840	75.380	0.04952	0.003	620.341
5256	9.969	0.15947	622.745	51.640	0.04881	0.004	620.252
5258	9.933	0.17648	622.974	51.440	0.04873	0.004	620.231
5260	9.906	0.19472	623.299	51.280	0.04868	0.004	620.242
5262	9.876	0.21386	623.670	51.100	0.04876	0.003	620.252
5264	9.846	0.23348	624.028	50.930	0.04885	0.003	620.279
5296	39.438	0.19271	681.732	164.610	0.05860	0.003	679.460
5297	39.325	0.21154	681.964	164.170	0.05845	0.003	679.466
5298	39.213	0.23124	682.204	163.730	0.05843	0.002	679.466
5299	39.099	0.25185	682.446	163.280	0.05848	0.002	679.459
5300	38.989	0.27334	682.703	162.830	0.05829	0.002	679.464
5301	38.439	0.19277	681.749	161.120	0.05782	0.003	679.467
5302	38.202	0.21171	681.977	160.240	0.05765	0.003	679.459
5303	37.966	0.23111	682.205	159.360	0.05760	0.002	679.455
5304	37.733	0.25184	682.455	158.480	0.05774	0.002	679.460
5305	37.511	0.27294	682.729	157.640	0.05759	0.002	679.459
5306	32.399	0.19275	681.878	139.310	0.05606	0.003	679.452
5307	32.241	0.21168	682.111	138.680	0.05607	0.003	679.450
5308	32.080	0.23116	682.369	138.030	0.05625	0.003	679.458
5309	31.922	0.25177	682.623	137.400	0.05629	0.002	679.455
5310	31.762	0.27295	682.896	136.750	0.05610	0.002	679.459
5311	31.182	0.19273	681.864	134.780	0.05642	0.003	679.462
5312	31.108	0.21158	682.101	134.460	0.05639	0.003	679.462
5313	31.040	0.23130	682.339	134.160	0.05655	0.002	679.456
5314	30.971	0.25194	682.589	133.850	0.05660	0.002	679.456
5315	30.908	0.27338	682.874	133.570	0.05656	0.002	679.457
5316	24.844	0.17477	681.676	110.380	0.05512	0.004	679.393
5317	24.799	0.19276	681.914	110.160	0.05509	0.003	679.394
5318	24.753	0.21159	682.156	109.950	0.05523	0.003	679.393

Run Point	$\frac{p_e}{\text{MPa}}$	$\frac{q}{\text{W} \cdot \text{m}^{-1}}$	$\frac{T_e}{\text{K}}$	$\frac{\rho_e}{\text{kg} \cdot \text{m}^{-3}}$	$\frac{\lambda_e}{\text{W} \cdot \text{m}^{-1} \cdot \text{K}^{-1}}$	STAT	$\frac{T_i}{\text{K}}$
5319	24.713	0.23129	682.420	109.740	0.05511	0.002	679.395
5320	24.673	0.25195	682.665	109.550	0.05516	0.002	679.386
5321	24.485	0.17473	681.621	108.960	0.05480	0.003	679.369
5322	24.405	0.19280	681.870	108.610	0.05460	0.003	679.371
5323	24.319	0.21174	682.154	108.220	0.05469	0.003	679.372
5324	24.230	0.23116	682.416	107.820	0.05451	0.002	679.375
5325	24.143	0.25186	682.701	107.440	0.05448	0.002	679.386
5326	19.443	0.17473	681.851	88.400	0.05333	0.003	679.418
5327	19.379	0.19281	682.064	88.110	0.05329	0.003	679.404
5328	19.316	0.21172	682.327	87.810	0.05335	0.003	679.395
5329	19.256	0.23112	682.571	87.530	0.05349	0.003	679.391
5330	19.197	0.25185	682.842	87.260	0.05337	0.003	679.382
5331	19.129	0.17479	681.792	87.100	0.05407	0.003	679.378
5332	19.104	0.19276	682.036	86.970	0.05390	0.003	679.378
5333	19.079	0.21160	682.286	86.830	0.05412	0.003	679.374
5334	19.058	0.23129	682.567	86.710	0.05406	0.002	679.377
5335	19.035	0.25192	682.868	86.570	0.05395	0.002	679.382
5336	14.924	0.17478	681.980	69.180	0.05295	0.004	679.421
5337	14.908	0.19277	682.130	69.100	0.05307	0.003	679.426
5338	14.892	0.21165	682.463	68.990	0.05326	0.003	679.438
5339	14.875	0.23135	682.744	68.900	0.05327	0.002	679.437
5340	14.859	0.25197	683.071	68.790	0.05336	0.002	679.453
5341	14.784	0.17480	681.977	68.580	0.05264	0.003	679.487
5342	14.746	0.19286	682.249	68.380	0.05290	0.003	679.489
5343	14.708	0.21177	682.528	68.190	0.05285	0.003	679.490
5344	14.669	0.23124	682.830	67.990	0.05266	0.003	679.509
5345	14.626	0.25192	683.127	67.780	0.05288	0.002	679.503
5346	9.890	0.15794	681.915	46.860	0.05214	0.004	679.491
5348	9.840	0.17479	682.143	46.610	0.05194	0.004	679.466
5350	9.794	0.19284	682.348	46.390	0.05192	0.003	679.429
5352	9.745	0.21182	682.594	46.150	0.05224	0.003	679.409
5354	9.699	0.23125	682.874	45.920	0.05225	0.003	679.408
5386	40.201	0.20869	742.309	154.930	0.06297	0.003	739.999
5387	39.996	0.22811	742.523	154.220	0.06284	0.003	740.005
5388	39.799	0.24845	742.769	153.540	0.06251	0.002	740.017
5389	39.602	0.26962	743.015	152.850	0.06275	0.002	740.018
5390	39.414	0.29078	743.262	152.190	0.06281	0.002	740.021
5391	38.331	0.20861	742.379	148.810	0.06150	0.003	740.034
5392	37.941	0.22774	742.602	147.480	0.06198	0.003	740.021
5393	37.560	0.24814	742.834	146.180	0.06171	0.003	740.026
5394	37.189	0.26897	743.065	144.910	0.06158	0.002	740.012

Run Point	$\frac{p_e}{\text{MPa}}$	$\frac{q}{\text{W} \cdot \text{m}^{-1}}$	$\frac{T_e}{\text{K}}$	$\frac{\rho_e}{\text{kg} \cdot \text{m}^{-3}}$	$\frac{\lambda_e}{\text{W} \cdot \text{m}^{-1} \cdot \text{K}^{-1}}$	STAT	$\frac{T_i}{\text{K}}$
5395	36.835	0.29109	743.330	143.680	0.06134	0.002	740.007
5396	35.192	0.20870	742.521	138.320	0.06180	0.003	740.054
5397	35.054	0.22813	742.755	137.810	0.06187	0.003	740.058
5398	34.915	0.24848	743.005	137.300	0.06161	0.003	740.068
5399	34.780	0.26965	743.253	136.800	0.06151	0.002	740.073
5400	34.646	0.29081	743.498	136.300	0.06169	0.002	740.065
5401	33.921	0.20860	742.381	134.020	0.06075	0.003	740.059
5402	33.624	0.22773	742.610	132.970	0.06102	0.003	740.049
5403	33.334	0.24814	742.810	131.950	0.06082	0.003	740.037
5404	33.058	0.26898	743.052	130.960	0.06092	0.002	740.025
5405	32.782	0.29108	743.316	129.970	0.06071	0.002	740.006
5406	29.354	0.19005	742.271	118.150	0.06010	0.004	740.023
5407	29.258	0.20862	742.500	117.770	0.06032	0.003	740.028
5408	29.164	0.22803	742.744	117.400	0.06055	0.003	740.033
5409	29.070	0.24837	742.997	117.040	0.06053	0.003	740.042
5410	28.976	0.26952	743.266	116.660	0.06051	0.002	740.053
5411	28.554	0.18995	742.310	115.300	0.05983	0.003	740.071
5412	28.344	0.20861	742.556	114.510	0.05973	0.003	740.073
5413	28.144	0.22774	742.808	113.760	0.05993	0.003	740.080
5414	27.945	0.24813	743.047	113.010	0.05969	0.003	740.074
5415	27.744	0.26897	743.287	112.260	0.05986	0.002	740.063
5416	24.176	0.19004	742.383	99.360	0.05954	0.003	740.046
5417	24.109	0.20863	742.624	99.080	0.05954	0.003	740.046
5418	24.044	0.22803	742.857	98.810	0.05967	0.003	740.045
5419	23.977	0.24833	743.097	98.530	0.05940	0.002	740.044
5420	23.896	0.26955	743.361	98.200	0.05949	0.002	740.033
5421	23.573	0.18996	742.237	97.140	0.05869	0.003	740.007
5422	23.421	0.20862	742.446	96.550	0.06048	0.003	739.989
5423	23.307	0.22776	742.644	96.100	0.05898	0.003	739.968
5424	23.182	0.24818	743.007	95.590	0.05898	0.003	739.959
5425	23.054	0.26900	743.260	95.080	0.05895	0.002	739.943
5426	19.893	0.19010	742.458	83.200	0.05882	0.003	739.971
5427	19.850	0.20868	742.703	83.000	0.05832	0.004	739.974
5428	19.806	0.22808	742.982	82.810	0.05851	0.003	739.990
5429	19.764	0.24840	743.260	82.610	0.05865	0.002	740.007
5430	19.719	0.26960	743.549	82.410	0.05868	0.003	740.021
5431	19.465	0.18995	742.486	81.550	0.05809	0.003	740.081
5432	19.365	0.20863	742.757	81.130	0.05810	0.003	740.099
5433	19.265	0.22777	743.012	80.720	0.05827	0.003	740.106
5434	19.167	0.24816	743.278	80.310	0.05806	0.003	740.104
5435	19.067	0.26899	743.524	79.900	0.05806	0.003	740.095

Run Point	$\frac{p_e}{\text{MPa}}$	$\frac{q}{\text{W} \cdot \text{m}^{-1}}$	$\frac{T_e}{\text{K}}$	$\frac{\rho_e}{\text{kg} \cdot \text{m}^{-3}}$	$\frac{\lambda_e}{\text{W} \cdot \text{m}^{-1} \cdot \text{K}^{-1}}$	STAT	$\frac{T_i}{\text{K}}$
5436	14.976	0.17233	742.300	63.920	0.05734	0.004	740.002
5437	14.949	0.19005	742.533	63.800	0.05758	0.004	739.995
5438	14.922	0.20860	742.763	63.670	0.05765	0.004	739.982
5439	14.895	0.22800	743.009	63.540	0.05800	0.003	739.974
5440	14.867	0.24834	743.270	63.400	0.05801	0.002	739.968
5441	14.734	0.17217	742.236	62.960	0.05731	0.004	739.967
5442	14.672	0.18995	742.465	62.690	0.05746	0.004	739.965
5443	14.611	0.20861	742.719	62.420	0.05727	0.003	739.974
5444	14.552	0.22775	743.013	62.160	0.05755	0.003	739.984
5445	14.492	0.24814	743.284	61.900	0.05736	0.003	739.984
5446	10.006	0.17218	742.429	43.590	0.05682	0.004	739.983
5448	9.931	0.18997	742.689	43.250	0.05699	0.004	739.982
5450	9.857	0.20862	742.945	42.930	0.05684	0.004	739.975
5452	9.782	0.22777	743.212	42.610	0.05710	0.004	739.980
5454	9.711	0.24817	743.508	42.290	0.05688	0.004	739.982
5486	9.005	0.17220	742.570	39.380	0.05725	0.005	740.124
5488	9.014	0.18999	742.839	39.400	0.05730	0.004	740.131
5490	9.023	0.20864	743.125	39.430	0.05737	0.004	740.153
5492	9.031	0.22778	743.417	39.450	0.05741	0.004	740.169
5494	9.038	0.24817	743.704	39.460	0.05740	0.004	740.173
5496	7.903	0.17214	742.638	34.710	0.05705	0.005	740.152
5498	7.851	0.18995	742.911	34.480	0.05733	0.004	740.162
5500	7.799	0.20862	743.210	34.250	0.05714	0.004	740.178
5502	7.748	0.22772	743.483	34.020	0.05727	0.004	740.175
5504	7.697	0.24815	743.780	33.790	0.05744	0.004	740.173

Table A2. Thermal conductivity data for nitrogen from steady-state measurements at temperatures from 500 K to 740 K.

Run Point	$\frac{p_e}{\text{MPa}}$	$\frac{q}{\text{W} \cdot \text{m}^{-1}}$	$\frac{T_e}{\text{K}}$	$\frac{\rho_e}{\text{kg} \cdot \text{m}^{-3}}$	$\frac{\lambda_e}{\text{W} \cdot \text{m}^{-1} \cdot \text{K}^{-1}}$	$\frac{\Delta T_a}{\text{K}}$	$\frac{t_s}{\text{s}}$	$\frac{t_e}{\text{s}}$	Ra
5071	5.068	0.09478	502.715	33.247	0.04136	2.247	29.04	60.00	1319
5072	5.063	0.10988	502.891	33.205	0.04139	2.601	29.04	60.00	1522
5073	5.059	0.12610	503.086	33.167	0.04151	2.976	26.64	60.00	1735
5074	5.056	0.14345	503.285	33.132	0.04155	3.381	26.64	60.00	1966
5075	5.051	0.16209	503.501	33.086	0.04158	3.815	26.64	60.00	2210
5077	3.076	0.09478	502.753	20.355	0.03994	2.330	29.04	60.00	517
5079	3.072	0.10989	502.936	20.318	0.04025	2.680	26.64	60.00	592
5081	3.067	0.12612	503.141	20.279	0.04023	3.077	26.64	60.00	677
5083	3.063	0.14346	503.358	20.241	0.04018	3.504	29.04	60.00	767
5085	3.058	0.16211	503.577	20.201	0.04027	3.949	29.04	60.00	860
5087	1.533	0.09478	502.753	10.210	0.04023	2.314	26.64	60.00	130
5089	1.531	0.10988	502.932	10.195	0.04021	2.685	26.64	60.00	150
5091	1.530	0.12609	503.146	10.179	0.04003	3.094	26.64	60.00	172
5093	1.528	0.14342	503.349	10.162	0.04020	3.505	24.24	60.00	194
5095	1.526	0.16210	503.570	10.146	0.04027	3.953	26.64	60.00	218
5097	0.426	0.09478	502.763	2.849	0.03989	2.335	24.24	60.00	10
5099	0.425	0.10988	502.938	2.844	0.04011	2.692	24.24	60.00	12
5101	0.425	0.12611	503.127	2.843	0.04023	3.080	26.64	60.00	13
5103	0.425	0.14343	503.329	2.839	0.04033	3.495	26.64	60.00	15
5105	0.424	0.16211	503.550	2.834	0.04039	3.944	26.64	60.00	17
5157	9.940	0.12663	562.401	56.984	0.04584	2.698	26.64	60.00	3438
5159	9.915	0.14306	562.577	56.832	0.04575	3.051	26.64	60.00	3866
5161	9.891	0.16037	562.756	56.678	0.04613	3.389	26.64	60.00	4268
5163	9.867	0.17881	562.946	56.529	0.04615	3.775	24.24	60.00	4725
5165	9.841	0.19792	563.086	56.373	0.04767	4.044	19.44	60.00	5032
5167	4.963	0.12668	562.457	29.100	0.04441	2.798	29.04	60.00	961
5169	4.954	0.14315	562.625	29.038	0.04448	3.156	29.04	60.00	1079
5171	4.943	0.16044	562.803	28.968	0.04470	3.519	24.24	60.00	1196
5173	4.933	0.17889	562.985	28.899	0.04488	3.908	26.64	60.00	1321
5175	4.923	0.19799	563.197	28.832	0.04493	4.319	24.24	60.00	1452
5177	2.582	0.12666	562.441	15.300	0.04398	2.828	24.24	60.00	272
5179	2.578	0.14318	562.616	15.268	0.04401	3.195	26.64	60.00	305
5181	2.573	0.16042	562.806	15.238	0.04393	3.586	24.24	60.00	341
5183	2.569	0.17888	563.002	15.205	0.04413	3.980	26.64	60.00	377
5185	2.567	0.19792	563.236	15.188	0.04368	4.448	26.64	60.00	419
5187	0.539	0.12670	562.524	3.219	0.04248	2.930	24.24	60.00	13
5189	0.539	0.14311	562.727	3.217	0.04206	3.342	24.24	60.00	14
5191	0.538	0.16041	562.919	3.212	0.04224	3.730	21.84	60.00	16
5193	0.537	0.17890	563.134	3.208	0.04240	4.145	21.84	60.00	18
5195	0.537	0.19794	563.360	3.203	0.04244	4.582	24.24	60.00	19
5257	9.953	0.15950	621.790	51.637	0.05049	3.090	21.84	60.00	2560
5259	9.917	0.17651	621.934	51.448	0.05067	3.407	21.84	60.00	2801

Run Point	$\frac{p_e}{\text{MPa}}$	$\frac{q}{\text{W} \cdot \text{m}^{-1}}$	$\frac{T_e}{\text{K}}$	$\frac{\rho_e}{\text{kg} \cdot \text{m}^{-3}}$	$\frac{\lambda_e}{\text{W} \cdot \text{m}^{-1} \cdot \text{K}^{-1}}$	$\frac{\Delta T_a}{\text{K}}$	$\frac{t_s}{\text{s}}$	$\frac{t_e}{\text{s}}$	Ra
5261	9.893	0.19474	622.137	51.312	0.04996	3.809	24.24	60.00	3114
5263	9.862	0.21389	622.359	51.142	0.04957	4.214	21.84	60.00	3420
5265	9.828	0.23355	622.587	50.956	0.04958	4.598	17.04	60.00	3701
5267	5.174	0.15952	621.983	27.408	0.04682	3.342	24.24	60.00	804
5269	5.160	0.17653	622.117	27.332	0.04711	3.676	21.84	60.00	879
5271	5.146	0.19477	622.283	27.253	0.04737	4.033	24.24	60.00	958
5273	5.131	0.21391	622.457	27.165	0.04759	4.408	24.24	60.00	1040
5275	5.117	0.23356	622.654	27.085	0.04771	4.801	24.24	60.00	1125
5277	3.024	0.15950	621.940	16.170	0.04622	3.388	21.84	60.00	287
5279	3.017	0.17652	622.143	16.131	0.04626	3.747	21.84	60.00	315
5281	3.011	0.19477	622.366	16.091	0.04609	4.149	21.84	60.00	347
5283	3.005	0.21392	622.596	16.053	0.04603	4.562	21.84	60.00	380
5285	2.998	0.23357	622.770	16.015	0.04692	4.888	21.84	60.00	404
5287	1.035	0.14305	621.870	5.582	0.04562	3.080	21.84	60.00	31
5289	1.033	0.15951	622.046	5.569	0.04580	3.421	19.44	60.00	35
5291	1.031	0.17654	622.216	5.560	0.04586	3.782	19.44	60.00	38
5293	1.030	0.19478	622.402	5.549	0.04595	4.164	21.84	60.00	42
5295	1.028	0.21393	622.591	5.539	0.04595	4.574	21.84	60.00	46
5347	9.870	0.15798	680.961	46.829	0.05190	2.982	21.84	60.00	1653
5349	9.820	0.17483	681.074	46.595	0.05235	3.271	21.84	60.00	1795
5351	9.771	0.19288	681.189	46.366	0.05295	3.567	19.44	60.00	1938
5353	9.724	0.21183	681.344	46.142	0.05315	3.902	19.44	60.00	2099
5355	9.678	0.23128	681.514	45.922	0.05331	4.246	19.44	60.00	2262
5357	5.744	0.15798	680.925	27.741	0.05088	3.048	21.84	60.00	608
5359	5.722	0.17483	681.096	27.631	0.05078	3.379	21.84	60.00	669
5361	5.701	0.19287	681.267	27.523	0.05078	3.727	19.44	60.00	731
5363	5.678	0.21186	681.456	27.411	0.05078	4.094	24.24	60.00	796
5365	5.657	0.23128	681.652	27.302	0.05083	4.464	19.44	60.00	861
5367	3.009	0.15795	680.976	14.699	0.05021	3.090	21.84	60.00	175
5369	2.999	0.17480	681.134	14.647	0.05023	3.418	21.84	60.00	193
5371	2.989	0.19285	681.299	14.598	0.05036	3.762	17.04	60.00	210
5373	2.979	0.21177	681.474	14.544	0.05036	4.130	19.44	60.00	229
5375	2.969	0.23126	681.653	14.492	0.05061	4.488	19.44	60.00	247
5377	0.571	0.15790	680.982	2.818	0.04901	3.165	17.04	60.00	7
5379	0.570	0.17476	681.140	2.810	0.04920	3.490	19.44	60.00	7
5381	0.568	0.19286	681.312	2.803	0.04934	3.840	19.44	60.00	8
5383	0.567	0.21179	681.506	2.794	0.04928	4.222	19.44	60.00	9
5385	0.565	0.23130	681.687	2.787	0.04950	4.591	17.04	60.00	9
5447	9.973	0.17219	741.469	43.503	0.05638	2.995	21.84	60.00	1183
5449	9.897	0.18998	741.621	43.177	0.05639	3.303	17.04	60.00	1285
5451	9.823	0.20863	741.785	42.855	0.05636	3.629	19.44	60.00	1391
5453	9.751	0.22779	741.951	42.544	0.05648	3.953	19.44	60.00	1493
5455	9.678	0.24818	742.106	42.233	0.05656	4.300	19.44	60.00	1601
5457	5.972	0.17219	741.533	26.482	0.05418	3.120	17.04	60.00	467
5459	5.936	0.18996	741.627	26.319	0.05620	3.319	21.84	60.00	491

Run Point	$\frac{p_e}{\text{MPa}}$	$\frac{q}{\text{W} \cdot \text{m}^{-1}}$	$\frac{T_e}{\text{K}}$	$\frac{\rho_e}{\text{kg} \cdot \text{m}^{-3}}$	$\frac{\lambda_e}{\text{W} \cdot \text{m}^{-1} \cdot \text{K}^{-1}}$	$\frac{\Delta T_a}{\text{K}}$	$\frac{t_s}{\text{s}}$	$\frac{t_e}{\text{s}}$	Ra
5461	5.900	0.20863	741.788	26.158	0.05624	3.643	21.84	60.00	532
5463	5.865	0.22777	741.960	26.001	0.05612	3.985	19.44	60.00	575
5465	5.830	0.24816	742.149	25.842	0.05594	4.355	19.44	60.00	621
5467	3.001	0.17220	741.572	13.468	0.05416	3.124	24.24	60.00	123
5469	2.986	0.18998	741.721	13.399	0.05421	3.443	19.44	60.00	134
5471	2.971	0.20864	741.890	13.329	0.05420	3.782	17.04	60.00	146
5473	2.956	0.22779	742.065	13.260	0.05429	4.122	19.44	60.00	157
5475	2.941	0.24819	742.262	13.191	0.05427	4.493	17.04	60.00	169
5477	0.987	0.17218	741.583	4.466	0.05380	3.145	12.24	60.00	14
5479	0.983	0.18999	741.739	4.447	0.05386	3.466	17.04	60.00	15
5481	0.979	0.20860	741.905	4.429	0.05384	3.807	17.04	60.00	16
5483	0.975	0.22779	742.064	4.409	0.05405	4.141	14.64	60.00	18
5485	0.971	0.24815	742.221	4.391	0.05425	4.495	17.04	60.00	19
5487	9.009	0.17220	741.612	39.447	0.05665	2.983	21.84	60.00	974
5489	9.019	0.18999	741.782	39.477	0.05659	3.293	19.44	60.00	1077
5491	9.027	0.20865	741.954	39.504	0.05649	3.622	19.44	60.00	1185
5493	9.035	0.22779	742.132	39.526	0.05659	3.947	19.44	60.00	1292
5495	9.042	0.24813	742.298	39.547	0.05668	4.292	19.44	60.00	1406
5497	7.880	0.17217	741.650	34.663	0.05630	3.001	17.04	60.00	762
5499	7.828	0.18990	741.816	34.432	0.05615	3.319	21.84	60.00	831
5501	7.776	0.20855	741.978	34.205	0.05615	3.644	19.44	60.00	900
5503	7.725	0.22773	742.157	33.979	0.05615	3.979	17.04	60.00	970
5505	7.675	0.24798	742.332	33.757	0.05613	4.334	21.84	60.00	1042
5507	5.935	0.17209	741.703	26.312	0.05501	3.072	17.04	60.00	454
5509	5.899	0.18989	741.851	26.153	0.05519	3.379	21.84	60.00	493
5511	5.863	0.20859	742.019	25.993	0.05520	3.710	19.44	60.00	535
5513	5.828	0.22769	742.195	25.835	0.05516	4.053	21.84	60.00	577
5515	5.793	0.24806	742.366	25.677	0.05522	4.410	19.44	60.00	620
5517	3.992	0.17214	741.714	17.842	0.05459	3.098	17.04	60.00	213
5519	3.971	0.18978	741.832	17.746	0.05543	3.364	21.84	60.00	228
5521	3.951	0.20855	741.995	17.653	0.05562	3.683	19.44	60.00	247
5523	3.929	0.22750	742.169	17.554	0.05536	4.037	17.04	60.00	268
5525	3.908	0.24780	742.366	17.455	0.05530	4.402	19.44	60.00	289
5527	2.011	0.17205	741.725	9.061	0.05440	3.108	14.64	60.00	56
5529	2.002	0.18979	741.858	9.016	0.05474	3.407	19.44	60.00	60
5531	1.992	0.20854	741.990	8.971	0.05523	3.711	17.04	60.00	65
5533	1.982	0.22752	742.111	8.927	0.05563	4.020	19.44	60.00	70
5535	1.973	0.24791	742.248	8.886	0.05598	4.352	17.04	60.00	75
5537	0.986	0.17211	741.619	4.462	0.05408	3.127	19.44	60.00	14
5539	0.982	0.18989	741.783	4.442	0.05395	3.459	17.04	60.00	15
5541	0.978	0.20862	741.946	4.424	0.05414	3.787	19.44	60.00	16
5543	0.974	0.22769	742.117	4.405	0.05414	4.132	17.04	60.00	18
5545	0.970	0.24802	742.311	4.385	0.05407	4.508	17.04	60.00	19
5547	0.141	0.15551	741.502	0.639	0.05251	2.910	14.64	60.00	0
5549	0.141	0.17209	741.639	0.638	0.05281	3.202	14.64	60.00	0

Run Point	$\frac{p_e}{\text{MPa}}$	$\frac{q}{\text{W} \cdot \text{m}^{-1}}$	$\frac{T_e}{\text{K}}$	$\frac{\rho_e}{\text{kg} \cdot \text{m}^{-3}}$	$\frac{\lambda_e}{\text{W} \cdot \text{m}^{-1} \cdot \text{K}^{-1}}$	$\frac{\Delta T_a}{\text{K}}$	$\frac{t_s}{\text{s}}$	$\frac{t_e}{\text{s}}$	Ra
5551	0.140	0.18986	741.808	0.637	0.05295	3.523	14.64	60.00	0
5553	0.140	0.20859	741.964	0.635	0.05305	3.863	17.04	60.00	0
5555	0.140	0.22773	742.136	0.634	0.05309	4.215	17.04	60.00	0

Table A3. Thermal conductivity data for carbon dioxide from transient measurements at temperatures from 500 K to 740 K.

Run Point	$\frac{p_e}{\text{MPa}}$	$\frac{q}{\text{W} \cdot \text{m}^{-1}}$	$\frac{T_e}{\text{K}}$	$\frac{\rho_e}{\text{kg} \cdot \text{m}^{-3}}$	$\frac{\lambda_e}{\text{W} \cdot \text{m}^{-1} \cdot \text{K}^{-1}}$	STAT	$\frac{T_i}{\text{K}}$
8001	34.597	0.24645	741.382	233.550	0.06463	0.006	738.809
8002	34.505	0.26581	741.594	232.920	0.06395	0.007	738.814
8003	34.405	0.28673	741.807	232.230	0.06498	0.007	738.799
8004	34.324	0.30837	742.052	231.650	0.06463	0.004	738.802
8005	34.230	0.33094	742.257	231.000	0.06395	0.006	738.797
8006	33.576	0.24551	741.357	227.320	0.06303	0.003	738.789
8007	33.379	0.26576	741.575	226.030	0.06317	0.003	738.789
8008	33.173	0.28671	741.805	224.680	0.06302	0.003	738.792
8009	32.978	0.30799	742.030	223.400	0.06294	0.003	738.789
8010	32.787	0.33056	742.292	222.130	0.06325	0.003	738.777
8011	28.836	0.24524	742.623	197.260	0.06207	0.007	738.767
8012	28.688	0.26541	742.862	196.240	0.06127	0.004	738.776
8013	28.196	0.24554	741.413	193.550	0.06137	0.004	738.771
8014	28.058	0.26585	741.653	192.590	0.06182	0.004	738.783
8015	27.916	0.28679	741.901	191.610	0.06153	0.003	738.783
8016	27.778	0.30832	742.136	190.650	0.06181	0.006	738.783
8017	27.634	0.33108	742.259	189.690	0.06148	0.011	738.786
8018	31.489	0.24639	741.251	214.420	0.06310	0.006	738.662
8019	31.415	0.26573	741.489	213.880	0.06348	0.007	738.645
8020	31.327	0.28660	741.717	213.260	0.06378	0.005	738.640
8021	31.264	0.30830	741.976	212.770	0.06287	0.005	738.656
8022	31.186	0.33088	742.234	212.200	0.06344	0.004	738.660
8023	30.778	0.24560	741.367	209.930	0.06234	0.003	738.708
8024	30.609	0.26559	741.624	208.780	0.06193	0.004	738.712
8025	30.445	0.28669	741.889	207.670	0.06191	0.003	738.732
8026	30.274	0.30792	742.161	206.510	0.06222	0.003	738.751
8027	30.115	0.33061	742.444	205.410	0.06192	0.003	738.771
8028	23.979	0.24649	741.668	166.120	0.06094	0.008	738.836
8029	23.929	0.26587	741.901	165.730	0.06111	0.005	738.838
8030	23.887	0.28674	742.132	165.400	0.06178	0.006	738.845
8031	23.835	0.30841	742.389	164.990	0.06139	0.004	738.832
8032	23.796	0.33102	742.681	164.650	0.06083	0.004	738.839
8033	23.506	0.24566	741.624	163.010	0.06041	0.004	738.835
8034	23.399	0.26576	741.853	162.250	0.06016	0.003	738.840
8035	23.293	0.28688	742.106	161.490	0.06031	0.003	738.839
8036	23.197	0.30818	742.367	160.790	0.06043	0.003	738.840
8037	23.104	0.33077	742.618	160.120	0.06030	0.003	738.839
8038	19.775	0.24649	741.835	138.110	0.05955	0.008	738.839
8039	19.746	0.26581	742.086	137.850	0.06021	0.005	738.852

Run Point	$\frac{p_e}{\text{MPa}}$	$\frac{q}{\text{W} \cdot \text{m}^{-1}}$	$\frac{T_e}{\text{K}}$	$\frac{\rho_e}{\text{kg} \cdot \text{m}^{-3}}$	$\frac{\lambda_e}{\text{W} \cdot \text{m}^{-1} \cdot \text{K}^{-1}}$	STAT	$\frac{T_i}{\text{K}}$
8040	19.711	0.28674	742.342	137.560	0.06031	0.004	738.844
8041	19.676	0.30845	742.629	137.270	0.06032	0.005	738.849
8042	19.629	0.33101	742.848	136.910	0.05996	0.004	738.853
8044	19.463	0.24563	741.800	136.010	0.05925	0.004	738.862
8045	19.390	0.26578	742.035	135.470	0.05939	0.003	738.860
8046	19.311	0.28701	742.313	134.880	0.05918	0.003	738.867
8047	19.241	0.30821	742.559	134.360	0.05907	0.003	738.864
8048	19.153	0.33067	742.849	133.710	0.05896	0.003	738.860
8049	15.170	0.24577	741.922	106.750	0.05843	0.003	738.830
8050	15.124	0.26578	742.164	106.390	0.05847	0.003	738.827
8051	15.079	0.28669	742.405	106.040	0.05836	0.003	738.828
8052	15.030	0.30822	742.735	105.650	0.05809	0.003	738.820
8053	14.974	0.33066	743.016	105.230	0.05802	0.003	738.825
8054	14.862	0.24651	741.945	104.620	0.05846	0.008	738.813
8055	14.839	0.26586	742.177	104.430	0.05976	0.007	738.806
8056	14.817	0.28681	742.454	104.240	0.05849	0.005	738.812
8057	14.809	0.30844	742.730	104.140	0.05958	0.006	738.802
8058	14.834	0.33103	743.025	104.260	0.05870	0.004	738.805
8059	9.245	0.19091	741.590	65.580	0.05878	0.008	738.976
8060	9.239	0.20868	741.833	65.510	0.05898	0.008	738.977
8061	9.220	0.22730	742.103	65.350	0.05747	0.007	738.983
8062	9.207	0.24666	742.363	65.240	0.05762	0.008	738.983
8063	9.204	0.26603	742.650	65.190	0.05903	0.008	738.993
8064	9.188	0.19063	741.579	65.180	0.05742	0.004	738.984
8065	9.169	0.20821	741.795	65.020	0.05729	0.004	738.980
8066	9.151	0.22685	742.049	64.880	0.05745	0.004	738.986
8067	9.123	0.24582	742.335	64.650	0.05759	0.004	738.995
8068	9.092	0.26593	742.597	64.410	0.05737	0.004	738.988
8069	5.974	0.19075	741.428	42.510	0.05762	0.005	738.854
8070	5.966	0.20824	741.668	42.440	0.05751	0.005	738.838
8071	5.949	0.22663	742.100	42.300	0.05782	0.005	738.828
8072	5.944	0.24586	742.375	42.240	0.05748	0.005	738.823
8073	5.936	0.26599	742.628	42.170	0.05839	0.005	738.810
8074	5.935	0.19087	741.584	42.230	0.05935	0.009	738.798
8075	5.937	0.20864	741.845	42.230	0.05768	0.012	738.805
8076	5.924	0.22722	742.123	42.120	0.05823	0.007	738.796
8077	5.935	0.24662	742.392	42.180	0.05865	0.007	738.792
8078	5.933	0.26594	742.654	42.150	0.05889	0.008	738.793
8129	4.964	0.15949	681.968	38.600	0.05244	0.009	679.422
8130	4.962	0.17590	682.226	38.570	0.05255	0.007	679.421
8131	4.962	0.19312	682.515	38.550	0.05266	0.007	679.428

Run Point	$\frac{p_e}{\text{MPa}}$	$\frac{q}{\text{W} \cdot \text{m}^{-1}}$	$\frac{T_e}{\text{K}}$	$\frac{\rho_e}{\text{kg} \cdot \text{m}^{-3}}$	$\frac{\lambda_e}{\text{W} \cdot \text{m}^{-1} \cdot \text{K}^{-1}}$	STAT	$\frac{T_i}{\text{K}}$
8132	4.960	0.21107	682.807	38.520	0.05166	0.010	679.428
8133	4.959	0.22990	683.127	38.490	0.05172	0.006	679.430
8134	4.941	0.15942	682.002	38.420	0.05166	0.005	679.448
8135	4.933	0.17590	682.272	38.340	0.05209	0.005	679.456
8136	4.929	0.19318	682.550	38.290	0.05194	0.005	679.455
8137	4.925	0.21091	682.825	38.250	0.05188	0.004	679.456
8138	4.924	0.22981	683.120	38.220	0.05195	0.004	679.449
8139	38.032	0.24885	681.875	280.750	0.06123	0.003	679.238
8140	37.846	0.26933	682.155	279.390	0.06120	0.003	679.252
8141	37.660	0.29062	682.423	278.050	0.06107	0.003	679.284
8142	37.481	0.31228	682.690	276.750	0.06115	0.003	679.302
8143	37.298	0.33517	682.735	275.530	0.06120	0.003	679.321
8144	37.047	0.24930	682.012	274.230	0.06181	0.007	679.353
8145	36.966	0.26888	682.235	273.590	0.06151	0.004	679.357
8146	36.890	0.29003	682.458	272.980	0.06085	0.006	679.365
8147	36.807	0.31197	682.713	272.320	0.06081	0.004	679.365
8148	36.736	0.33482	682.975	271.720	0.06118	0.004	679.371
8149	31.422	0.22976	682.006	236.300	0.05957	0.006	679.401
8150	31.380	0.24937	682.191	235.930	0.05867	0.007	679.396
8151	31.327	0.26894	682.432	235.470	0.05882	0.005	679.399
8152	31.273	0.29010	682.671	234.990	0.05862	0.006	679.403
8153	31.224	0.31203	682.929	234.540	0.05958	0.005	679.402
8154	30.976	0.22966	682.044	233.200	0.05852	0.003	679.444
8155	30.852	0.24897	682.303	232.230	0.05898	0.003	679.467
8156	30.724	0.26946	682.566	231.230	0.05879	0.003	679.499
8157	30.596	0.29077	682.872	230.210	0.05844	0.003	679.529
8158	30.461	0.31243	683.129	229.170	0.05841	0.003	679.552
8159	25.599	0.21101	682.002	195.110	0.05730	0.006	679.508
8160	25.560	0.22986	682.215	194.750	0.05750	0.006	679.500
8161	25.519	0.24945	682.436	194.380	0.05660	0.005	679.489
8162	25.488	0.26900	682.661	194.080	0.05700	0.005	679.475
8163	25.446	0.29017	682.899	193.690	0.05719	0.005	679.467
8164	25.273	0.21084	681.898	192.780	0.05650	0.003	679.423
8165	25.193	0.22972	682.119	192.130	0.05664	0.003	679.413
8166	25.104	0.24901	682.332	191.410	0.05667	0.003	679.418
8167	25.029	0.26949	682.562	190.790	0.05622	0.003	679.412
8168	24.934	0.29080	682.858	190.000	0.05676	0.003	679.427
8169	20.050	0.21087	682.162	154.260	0.05502	0.003	679.444
8170	19.988	0.22973	682.374	153.740	0.05490	0.003	679.445
8171	19.938	0.24904	682.633	153.300	0.05498	0.003	679.454
8172	19.880	0.26953	682.903	152.790	0.05486	0.003	679.452

Run Point	$\frac{p_e}{\text{MPa}}$	$\frac{q}{\text{W} \cdot \text{m}^{-1}}$	$\frac{T_e}{\text{K}}$	$\frac{\rho_e}{\text{kg} \cdot \text{m}^{-3}}$	$\frac{\lambda_e}{\text{W} \cdot \text{m}^{-1} \cdot \text{K}^{-1}}$	STAT	$\frac{T_i}{\text{K}}$
8173	19.821	0.29082	683.170	152.280	0.05509	0.003	679.444
8174	19.498	0.21100	682.137	150.140	0.05450	0.006	679.429
8175	19.481	0.22982	682.376	149.950	0.05480	0.007	679.435
8176	19.450	0.24941	682.630	149.650	0.05514	0.005	679.436
8177	19.424	0.26900	682.887	149.390	0.05495	0.004	679.434
8178	19.402	0.29020	683.142	149.160	0.05466	0.006	679.439
8179	15.314	0.21101	682.340	118.470	0.05395	0.006	679.446
8180	15.302	0.22985	682.595	118.330	0.05314	0.006	679.444
8181	15.269	0.24940	682.873	118.020	0.05341	0.005	679.456
8182	15.255	0.26903	683.131	117.860	0.05383	0.005	679.450
8183	15.250	0.29018	683.394	117.770	0.05363	0.005	679.448
8184	15.155	0.21087	682.219	117.280	0.05344	0.003	679.454
8185	15.105	0.22975	682.501	116.840	0.05349	0.003	679.448
8186	15.122	0.24905	682.774	116.920	0.05346	0.003	679.449
8187	15.108	0.26955	683.062	116.750	0.05351	0.003	679.449
8188	15.084	0.29086	683.359	116.520	0.05353	0.003	679.452
8189	10.132	0.19318	682.379	78.660	0.05220	0.004	679.544
8190	10.104	0.21091	682.625	78.420	0.05182	0.003	679.532
8191	10.090	0.22980	682.897	78.280	0.05275	0.003	679.536
8192	10.100	0.24910	683.138	78.320	0.05256	0.003	679.528
8193	10.049	0.26961	683.425	77.890	0.05194	0.003	679.510
8194	10.000	0.19308	682.280	77.650	0.05243	0.009	679.473
8195	9.996	0.21106	682.559	77.590	0.05321	0.008	679.463
8196	9.986	0.22991	682.829	77.480	0.05237	0.005	679.459
8197	9.980	0.24951	683.044	77.400	0.05293	0.005	679.450
8198	9.965	0.26910	683.376	77.250	0.05192	0.004	679.450
8199	5.177	0.17589	682.231	40.240	0.05264	0.008	679.431
8200	5.176	0.19310	682.500	40.210	0.05158	0.011	679.431
8201	5.174	0.21110	682.795	40.180	0.05177	0.007	679.429
8202	5.170	0.22992	683.121	40.130	0.05230	0.007	679.434
8203	5.171	0.24948	683.418	40.120	0.05260	0.007	679.427
8204	5.153	0.17590	682.257	40.050	0.05193	0.005	679.448
8205	5.147	0.19318	682.536	39.990	0.05175	0.005	679.443
8206	5.142	0.21092	682.813	39.930	0.05200	0.004	679.447
8207	5.144	0.22980	683.104	39.930	0.05194	0.004	679.448
8219	37.153	0.25072	622.613	308.530	0.05895	0.006	619.871
8220	37.101	0.27044	622.845	308.000	0.05865	0.004	619.872
8221	37.048	0.29170	623.105	307.440	0.05861	0.004	619.884
8222	36.993	0.31380	623.348	306.870	0.05793	0.005	619.898
8223	36.938	0.33674	623.620	306.300	0.05802	0.003	619.898
8224	36.540	0.25040	622.698	303.960	0.05761	0.003	619.963

Run Point	$\frac{p_e}{\text{MPa}}$	$\frac{q}{\text{W} \cdot \text{m}^{-1}}$	$\frac{T_e}{\text{K}}$	$\frac{\rho_e}{\text{kg} \cdot \text{m}^{-3}}$	$\frac{\lambda_e}{\text{W} \cdot \text{m}^{-1} \cdot \text{K}^{-1}}$	STAT	$\frac{T_i}{\text{K}}$
8225	36.433	0.27100	622.958	303.010	0.05760	0.003	619.977
8226	36.306	0.29243	623.217	301.910	0.05741	0.003	619.993
8227	36.185	0.31421	623.469	300.850	0.05748	0.003	619.996
8228	36.072	0.33726	623.728	299.860	0.05767	0.003	620.000
8229	31.314	0.23101	622.653	264.370	0.05496	0.003	619.998
8230	31.224	0.25042	622.897	263.520	0.05514	0.003	620.000
8231	31.144	0.27105	623.155	262.760	0.05523	0.003	620.002
8232	31.053	0.29247	623.407	261.910	0.05491	0.003	620.007
8233	30.972	0.31427	623.685	261.130	0.05499	0.003	620.013
8234	30.815	0.23112	622.717	260.440	0.05538	0.004	620.013
8235	30.773	0.25080	622.947	259.980	0.05554	0.004	620.018
8236	30.736	0.27054	623.197	259.560	0.05479	0.004	620.019
8237	30.699	0.29181	623.453	259.120	0.05515	0.004	620.016
8238	30.663	0.31387	623.711	258.700	0.05505	0.004	620.020
8239	25.270	0.21207	622.715	215.990	0.05237	0.003	620.029
8240	25.214	0.23107	622.960	215.420	0.05250	0.003	620.033
8241	25.162	0.25049	623.204	214.890	0.05258	0.003	620.038
8242	25.092	0.27109	623.471	214.190	0.05238	0.003	620.036
8243	25.029	0.29253	623.741	213.560	0.05242	0.003	620.033
8244	24.972	0.21221	622.692	213.560	0.05279	0.005	620.026
8245	24.949	0.23113	622.948	213.250	0.05214	0.005	620.028
8246	24.926	0.25087	623.216	212.950	0.05252	0.004	620.032
8247	24.900	0.27059	623.444	212.630	0.05235	0.005	620.026
8248	24.875	0.29187	623.734	212.300	0.05282	0.005	620.023
8249	20.300	0.19415	622.647	174.630	0.05099	0.006	620.022
8250	20.280	0.21223	622.879	174.380	0.05023	0.008	620.018
8251	20.259	0.23118	623.153	174.100	0.05046	0.005	620.023
8252	20.239	0.25086	623.426	173.840	0.05061	0.004	620.027
8253	20.226	0.27059	623.681	173.640	0.05038	0.005	620.021
8254	20.032	0.19427	622.611	172.380	0.05008	0.003	620.023
8255	19.998	0.21210	622.854	172.010	0.05031	0.003	620.027
8256	19.970	0.23110	623.111	171.680	0.05056	0.003	620.021
8257	19.921	0.25052	623.373	171.180	0.05037	0.003	620.028
8258	19.875	0.27113	623.647	170.690	0.05015	0.003	620.019
8259	15.215	0.19429	622.862	131.170	0.04828	0.003	620.028
8260	15.185	0.21213	623.154	130.840	0.04875	0.003	620.037
8261	15.163	0.23114	623.443	130.580	0.04859	0.003	620.048
8262	15.142	0.25057	623.732	130.320	0.04839	0.003	620.054
8263	15.123	0.27119	624.019	130.080	0.04833	0.003	620.048
8264	15.035	0.19419	622.846	129.620	0.04860	0.008	620.045
8265	15.022	0.21227	623.122	129.440	0.04863	0.005	620.044

Run Point	$\frac{p_e}{\text{MPa}}$	$\frac{q}{\text{W} \cdot \text{m}^{-1}}$	$\frac{T_e}{\text{K}}$	$\frac{\rho_e}{\text{kg} \cdot \text{m}^{-3}}$	$\frac{\lambda_e}{\text{W} \cdot \text{m}^{-1} \cdot \text{K}^{-1}}$	STAT	$\frac{T_i}{\text{K}}$
8266	15.011	0.23121	623.406	129.280	0.04899	0.005	620.045
8267	15.004	0.25095	623.682	129.150	0.04818	0.006	620.047
8268	14.994	0.27067	623.998	128.980	0.04848	0.004	620.050
8269	10.188	0.17690	622.851	87.730	0.04624	0.007	620.034
8270	10.190	0.19417	623.089	87.710	0.04681	0.006	620.030
8271	10.186	0.21229	623.408	87.620	0.04712	0.007	620.032
8272	10.181	0.23124	623.712	87.530	0.04725	0.004	620.032
8273	10.164	0.25098	624.026	87.330	0.04716	0.004	620.037
8274	10.135	0.17692	622.760	87.290	0.04659	0.003	620.041
8275	10.135	0.19432	623.042	87.240	0.04671	0.003	620.043
8276	10.122	0.21216	623.340	87.080	0.04683	0.003	620.040
8277	10.114	0.23117	623.628	86.960	0.04683	0.003	620.036
8278	10.099	0.25060	623.949	86.780	0.04681	0.003	620.037
8279	5.505	0.16037	622.793	47.200	0.04592	0.004	620.022
8280	5.502	0.17694	623.080	47.160	0.04585	0.004	620.028
8281	5.498	0.19434	623.385	47.100	0.04597	0.004	620.019
8282	5.496	0.21218	623.692	47.050	0.04590	0.004	620.027
8283	5.500	0.23119	624.064	47.060	0.04585	0.003	620.026
8284	5.500	0.16044	622.821	47.160	0.04629	0.007	620.029
8285	5.499	0.17694	623.107	47.130	0.04646	0.007	620.028
8286	5.496	0.19423	623.407	47.080	0.04547	0.007	620.030
8287	5.495	0.21235	623.747	47.040	0.04553	0.006	620.043
8288	5.495	0.23129	624.090	47.010	0.04590	0.005	620.045
8299	37.753	0.23901	563.337	359.100	0.05646	0.006	560.729
8300	37.707	0.26126	563.592	358.480	0.05635	0.004	560.734
8301	37.664	0.28458	563.868	357.870	0.05634	0.004	560.752
8302	37.622	0.30886	564.136	357.280	0.05568	0.003	560.751
8303	37.578	0.33317	564.425	356.650	0.05602	0.003	560.760
8304	37.323	0.23898	563.441	355.450	0.05525	0.003	560.796
8305	37.234	0.26090	563.706	354.470	0.05553	0.003	560.808
8306	37.141	0.28429	563.962	353.470	0.05522	0.003	560.814
8307	37.050	0.30819	564.215	352.480	0.05523	0.003	560.818
8308	36.959	0.33356	564.517	351.450	0.05546	0.003	560.831
8309	30.120	0.21778	563.578	292.720	0.05171	0.006	560.830
8310	30.096	0.23903	563.851	292.300	0.05190	0.004	560.837
8311	30.072	0.26130	564.130	291.870	0.05136	0.005	560.836
8312	30.050	0.28460	564.425	291.450	0.05152	0.004	560.840
8313	30.026	0.30951	564.626	291.080	0.05185	0.003	560.846
8314	29.873	0.21771	563.435	290.590	0.05129	0.003	560.861
8315	29.808	0.23911	563.707	289.780	0.05102	0.003	560.862
8316	29.760	0.26105	564.000	289.130	0.05125	0.003	560.864

Run Point	$\frac{p_e}{\text{MPa}}$	$\frac{q}{\text{W} \cdot \text{m}^{-1}}$	$\frac{T_e}{\text{K}}$	$\frac{\rho_e}{\text{kg} \cdot \text{m}^{-3}}$	$\frac{\lambda_e}{\text{W} \cdot \text{m}^{-1} \cdot \text{K}^{-1}}$	STAT	$\frac{T_i}{\text{K}}$
8317	29.706	0.28445	564.321	288.400	0.05107	0.003	560.865
8318	29.652	0.30833	564.627	287.680	0.05111	0.003	560.864
8319	25.081	0.19734	563.485	245.800	0.04848	0.003	560.877
8320	25.046	0.21773	563.772	245.290	0.04843	0.003	560.880
8321	25.007	0.23913	564.052	244.740	0.04842	0.003	560.874
8322	24.965	0.26106	564.330	244.170	0.04846	0.003	560.872
8323	24.913	0.28447	564.641	243.480	0.04863	0.003	560.875
8324	24.771	0.19760	563.488	242.840	0.04813	0.005	560.877
8325	24.753	0.21792	563.757	242.500	0.04863	0.005	560.875
8326	24.737	0.23923	564.041	242.180	0.04887	0.004	560.874
8327	24.721	0.26150	564.335	241.840	0.04852	0.005	560.874
8328	24.703	0.28483	564.667	241.460	0.04871	0.004	560.878
8329	20.241	0.19759	563.736	198.710	0.04581	0.005	560.870
8330	20.228	0.21789	563.968	198.470	0.04605	0.006	560.873
8331	20.211	0.23920	564.284	198.150	0.04653	0.004	560.872
8332	20.192	0.26148	564.614	197.800	0.04657	0.004	560.884
8333	20.177	0.28481	564.954	197.490	0.04628	0.004	560.880
8334	20.108	0.19736	563.693	197.420	0.04598	0.003	560.891
8335	20.083	0.21776	564.005	197.020	0.04612	0.003	560.890
8336	20.054	0.23916	564.318	196.580	0.04595	0.003	560.883
8337	20.031	0.26111	564.640	196.200	0.04596	0.003	560.883
8338	20.007	0.28450	564.961	195.810	0.04608	0.003	560.878
8339	15.223	0.17824	563.669	148.970	0.04393	0.006	560.876
8340	15.216	0.19758	563.965	148.790	0.04410	0.005	560.871
8341	15.204	0.21792	564.291	148.560	0.04419	0.005	560.876
8342	15.200	0.23923	564.645	148.400	0.04379	0.004	560.879
8343	15.198	0.26150	564.982	148.260	0.04391	0.005	560.874
8344	15.166	0.17835	563.643	148.410	0.04376	0.003	560.878
8345	15.149	0.19737	563.927	148.140	0.04380	0.003	560.878
8346	15.117	0.21776	564.227	147.710	0.04371	0.003	560.876
8347	15.097	0.23919	564.548	147.410	0.04366	0.003	560.876
8348	15.083	0.26114	564.894	147.150	0.04395	0.003	560.883
8349	10.102	0.17822	563.964	97.900	0.04124	0.009	560.871
8350	10.096	0.19758	564.316	97.760	0.04171	0.005	560.876
8351	10.090	0.21795	564.682	97.620	0.04212	0.006	560.874
8352	10.085	0.23921	565.051	97.500	0.04212	0.004	560.875
8353	10.085	0.26152	565.435	97.410	0.04172	0.004	560.873
8354	10.061	0.17835	563.992	97.480	0.04167	0.003	560.876
8355	10.059	0.19739	564.322	97.390	0.04161	0.003	560.871
8356	10.054	0.21779	564.696	97.260	0.04178	0.003	560.876
8357	10.052	0.23920	565.063	97.170	0.04157	0.003	560.879

Run Point	$\frac{p_e}{\text{MPa}}$	$\frac{q}{\text{W} \cdot \text{m}^{-1}}$	$\frac{T_e}{\text{K}}$	$\frac{\rho_e}{\text{kg} \cdot \text{m}^{-3}}$	$\frac{\lambda_e}{\text{W} \cdot \text{m}^{-1} \cdot \text{K}^{-1}}$	STAT	$\frac{T_i}{\text{K}}$
8358	10.041	0.26116	565.420	96.980	0.04168	0.003	560.872
8359	5.169	0.15991	564.015	49.420	0.04011	0.008	560.866
8360	5.168	0.17823	564.360	49.370	0.04038	0.008	560.861
8361	5.167	0.19759	564.752	49.320	0.04075	0.005	560.866
8362	5.166	0.21793	565.152	49.270	0.04039	0.007	560.870
8363	5.163	0.23924	565.575	49.210	0.04060	0.004	560.866
8364	5.160	0.15997	563.939	49.340	0.04049	0.004	560.872
8365	5.160	0.17838	564.319	49.290	0.04054	0.003	560.879
8366	5.159	0.19741	564.709	49.250	0.04046	0.004	560.882
8367	5.157	0.21781	565.118	49.190	0.04053	0.004	560.880
8368	5.154	0.23924	565.533	49.120	0.04058	0.003	560.884
8379	42.160	0.22504	503.645	466.620	0.05896	0.005	501.430
8380	42.120	0.24817	503.870	465.950	0.05794	0.007	501.430
8381	42.077	0.27245	504.131	465.190	0.05791	0.004	501.440
8382	42.036	0.29782	504.386	464.470	0.05767	0.006	501.443
8383	41.993	0.32439	504.659	463.700	0.05797	0.005	501.451
8384	41.817	0.22486	503.735	463.540	0.05914	0.003	501.482
8385	41.732	0.24804	504.005	462.400	0.05937	0.003	501.501
8386	41.649	0.27229	504.269	461.290	0.05927	0.003	501.513
8387	41.569	0.29740	504.445	460.340	0.05914	0.003	501.532
8388	41.479	0.32431	504.725	459.150	0.05905	0.003	501.541
8389	41.238	0.22508	503.787	458.410	0.05730	0.007	501.569
8390	41.195	0.24823	504.035	457.660	0.05791	0.006	501.572
8391	41.159	0.27251	504.286	456.990	0.05752	0.005	501.577
8392	41.126	0.29788	504.541	456.330	0.05688	0.006	501.578
8393	41.094	0.32445	504.816	455.640	0.05675	0.004	501.578
8394	40.561	0.22487	503.854	452.330	0.05825	0.003	501.604
8395	40.469	0.24811	504.091	451.170	0.05825	0.003	501.610
8396	40.396	0.27236	504.350	450.150	0.05839	0.003	501.612
8397	40.322	0.29743	504.626	449.090	0.05820	0.003	501.620
8398	40.243	0.32398	504.907	447.980	0.05798	0.003	501.622
8399	35.397	0.20273	503.811	403.940	0.05449	0.003	501.617
8400	35.335	0.22420	504.057	402.990	0.05452	0.003	501.618
8401	35.273	0.24743	504.308	402.050	0.05432	0.003	501.625
8402	35.209	0.27175	504.577	401.050	0.05460	0.003	501.630
8403	35.145	0.29671	504.852	400.060	0.05461	0.003	501.630
8404	35.091	0.20232	503.807	400.910	0.05363	0.007	501.628
8405	35.065	0.22428	504.057	400.320	0.05318	0.005	501.630
8406	35.043	0.24736	504.304	399.770	0.05264	0.006	501.633
8407	35.017	0.27158	504.577	399.160	0.05236	0.005	501.633
8408	34.992	0.29681	504.857	398.530	0.05245	0.004	501.639

Run Point	$\frac{p_e}{\text{MPa}}$	$\frac{q}{\text{W} \cdot \text{m}^{-1}}$	$\frac{T_e}{\text{K}}$	$\frac{\rho_e}{\text{kg} \cdot \text{m}^{-3}}$	$\frac{\lambda_e}{\text{W} \cdot \text{m}^{-1} \cdot \text{K}^{-1}}$	STAT	$\frac{T_i}{\text{K}}$
8409	29.636	0.20234	504.059	343.690	0.04936	0.006	501.628
8410	29.621	0.22428	504.334	343.200	0.04910	0.005	501.633
8411	29.604	0.24739	504.601	342.710	0.04855	0.007	501.632
8412	29.585	0.27155	504.899	342.160	0.04849	0.007	501.633
8413	29.564	0.29685	505.205	341.580	0.04838	0.005	501.630
8414	29.434	0.18181	503.819	341.760	0.05011	0.003	501.633
8415	29.392	0.20275	504.081	340.990	0.05020	0.003	501.639
8416	29.346	0.22440	504.336	340.200	0.05009	0.003	501.640
8417	29.296	0.24754	504.618	339.330	0.05025	0.003	501.650
8418	29.250	0.27190	504.910	338.480	0.05035	0.003	501.649
8419	25.281	0.16219	503.772	294.950	0.04677	0.003	501.639
8420	25.242	0.18185	504.038	294.250	0.04694	0.003	501.646
8421	25.208	0.20269	504.323	293.560	0.04689	0.003	501.647
8422	25.174	0.22431	504.609	292.890	0.04703	0.003	501.650
8423	25.150	0.24760	504.911	292.320	0.04715	0.003	501.644
8424	25.090	0.16190	503.762	292.760	0.04556	0.009	501.641
8425	25.078	0.18157	504.035	292.340	0.04587	0.006	501.647
8426	25.064	0.20237	504.307	291.920	0.04625	0.007	501.649
8427	25.050	0.22436	504.592	291.480	0.04593	0.005	501.645
8428	25.036	0.24743	504.903	291.010	0.04535	0.005	501.646
8429	19.906	0.14337	503.772	231.230	0.04275	0.010	501.645
8430	19.896	0.16191	504.056	230.910	0.04272	0.006	501.649
8431	19.888	0.18161	504.339	230.600	0.04196	0.009	501.646
8432	19.880	0.20239	504.644	230.280	0.04209	0.005	501.639
8433	19.871	0.22437	504.972	229.930	0.04206	0.007	501.643
8434	19.800	0.14363	503.774	229.960	0.04333	0.003	501.644
8435	19.779	0.16228	504.038	229.500	0.04298	0.003	501.640
8436	19.748	0.18187	504.318	228.930	0.04315	0.003	501.642
8437	19.719	0.20284	504.627	228.350	0.04329	0.003	501.641
8438	19.696	0.22439	504.952	227.840	0.04307	0.003	501.647
8439	15.146	0.12623	503.771	173.560	0.04003	0.003	501.646
8440	15.135	0.14353	504.043	173.290	0.03999	0.003	501.647
8441	15.121	0.16232	504.356	172.960	0.04003	0.003	501.646
8442	15.094	0.18176	504.687	172.460	0.03997	0.003	501.642
8443	15.082	0.20269	505.021	172.150	0.04026	0.003	501.644
8444	15.073	0.12599	503.735	172.700	0.03926	0.009	501.642
8445	15.070	0.14340	504.015	172.510	0.03945	0.009	501.638
8446	15.060	0.16195	504.320	172.240	0.03975	0.006	501.637
8447	15.058	0.18163	504.647	172.050	0.03913	0.008	501.635
8448	15.052	0.20244	505.010	171.790	0.03940	0.005	501.640
8449	10.224	0.10969	503.707	114.590	0.03767	0.010	501.635

Run Point	$\frac{p_e}{\text{MPa}}$	$\frac{q}{\text{W} \cdot \text{m}^{-1}}$	$\frac{T_e}{\text{K}}$	$\frac{\rho_e}{\text{kg} \cdot \text{m}^{-3}}$	$\frac{\lambda_e}{\text{W} \cdot \text{m}^{-1} \cdot \text{K}^{-1}}$	STAT	$\frac{T_i}{\text{K}}$
8450	10.219	0.12600	503.992	114.450	0.03651	0.009	501.638
8451	10.218	0.14341	504.339	114.330	0.03701	0.007	501.638
8452	10.207	0.16196	504.715	114.080	0.03749	0.008	501.639
8453	10.208	0.18166	505.060	113.990	0.03716	0.005	501.640
8454	10.213	0.10994	503.648	114.480	0.03718	0.004	501.635
8455	10.195	0.12618	503.934	114.180	0.03693	0.003	501.640
8456	10.191	0.14356	504.287	114.030	0.03731	0.003	501.633
8457	10.177	0.16216	504.612	113.760	0.03727	0.003	501.625
8458	10.182	0.18172	505.001	113.710	0.03748	0.003	501.632
8459	5.129	0.10994	504.039	55.760	0.03573	0.005	501.636
8460	5.124	0.12618	504.388	55.650	0.03567	0.004	501.643
8461	5.121	0.14353	504.771	55.580	0.03569	0.004	501.646
8462	5.119	0.16220	505.188	55.490	0.03584	0.004	501.652
8463	5.120	0.18179	505.628	55.450	0.03595	0.004	501.656
8464	5.116	0.10968	504.049	55.610	0.03513	0.011	501.653
8465	5.115	0.12599	504.398	55.560	0.03521	0.012	501.652
8466	5.115	0.14339	504.793	55.500	0.03589	0.006	501.656
8467	5.114	0.16194	505.188	55.440	0.03537	0.010	501.655
8468	5.114	0.18166	505.630	55.380	0.03565	0.006	501.654
8504	36.154	0.20186	503.590	411.660	0.05453	0.005	501.404
8505	36.127	0.22378	503.845	411.050	0.05383	0.004	501.404
8506	36.104	0.24682	504.099	410.480	0.05363	0.004	501.402
8507	36.080	0.27094	504.367	409.880	0.05336	0.005	501.405
8508	36.053	0.29615	504.647	409.250	0.05313	0.005	501.409
8509	34.938	0.20202	503.782	399.430	0.05278	0.004	501.585
8510	34.914	0.22395	504.019	398.880	0.05230	0.005	501.586
8511	34.890	0.24701	504.275	398.300	0.05213	0.004	501.588
8512	34.861	0.27113	504.537	397.660	0.05201	0.004	501.592
8513	34.827	0.29634	504.813	396.950	0.05176	0.005	501.599
8514	34.721	0.20202	503.795	397.240	0.05275	0.008	501.603
8515	34.701	0.22396	504.044	396.710	0.05245	0.005	501.603
8516	34.670	0.24699	504.294	396.070	0.05154	0.008	501.605
8517	34.649	0.27115	504.568	395.500	0.05153	0.005	501.605
8518	34.621	0.29638	504.841	394.870	0.05127	0.006	501.609
8519	34.398	0.20238	503.847	393.940	0.05366	0.003	501.609
8520	34.344	0.22397	504.080	393.090	0.05367	0.003	501.612
8521	34.280	0.24711	504.331	392.110	0.05388	0.003	501.617
8522	34.217	0.27139	504.587	391.140	0.05368	0.003	501.611
8523	34.153	0.29631	504.878	390.110	0.05372	0.003	501.620
8524	33.721	0.20204	503.870	387.050	0.05172	0.003	501.615
8525	33.692	0.22397	504.114	386.430	0.05153	0.004	501.622

Run Point	$\frac{p_e}{\text{MPa}}$	$\frac{q}{\text{W} \cdot \text{m}^{-1}}$	$\frac{T_e}{\text{K}}$	$\frac{\rho_e}{\text{kg} \cdot \text{m}^{-3}}$	$\frac{\lambda_e}{\text{W} \cdot \text{m}^{-1} \cdot \text{K}^{-1}}$	STAT	$\frac{T_i}{\text{K}}$
8526	33.662	0.24703	504.363	385.810	0.05144	0.004	501.619
8527	33.635	0.27118	504.640	385.170	0.05110	0.005	501.621
8528	33.605	0.29644	504.933	384.500	0.05095	0.004	501.621

Table A4. Thermal conductivity data for carbon dioxide from steady-state measurements at temperatures from 500 K to 740 K.

Run Point	$\frac{p_e}{\text{MPa}}$	$\frac{q}{\text{W} \cdot \text{m}^{-1}}$	$\frac{T_e}{\text{K}}$	$\frac{\rho_e}{\text{kg} \cdot \text{m}^{-3}}$	$\frac{\lambda_e}{\text{W} \cdot \text{m}^{-1} \cdot \text{K}^{-1}}$	$\frac{\Delta T_a}{\text{K}}$	$\frac{t_s}{\text{s}}$	$\frac{t_e}{\text{s}}$	Ra
8110	0.434	0.19087	740.547	3.098	0.05378	3.487	14.64	60.00	8
8112	0.433	0.20862	740.717	3.095	0.05348	3.834	14.64	60.00	9
8114	0.433	0.22725	740.895	3.095	0.05347	4.176	12.24	60.00	9
8116	0.435	0.24661	741.082	3.103	0.05331	4.545	17.04	60.00	10
8118	0.435	0.26599	741.251	3.102	0.05343	4.892	12.24	60.00	11
8120	0.433	0.19061	740.559	3.092	0.05334	3.512	14.64	60.00	8
8122	0.432	0.20823	740.692	3.085	0.05362	3.816	17.04	60.00	9
8124	0.431	0.22674	740.845	3.080	0.05355	4.161	14.64	60.00	9
8126	0.430	0.24573	741.016	3.074	0.05347	4.516	17.04	60.00	10
8128	0.430	0.26611	741.209	3.069	0.05348	4.889	17.04	60.00	11
8489	0.901	0.08080	502.830	9.543	0.03363	2.360	21.84	60.00	145
8490	0.900	0.09444	503.019	9.536	0.03359	2.761	24.24	60.00	169
8491	0.900	0.10961	503.245	9.530	0.03365	3.199	29.04	60.00	195
8492	0.900	0.12591	503.481	9.523	0.03371	3.668	24.24	60.00	224
8493	0.900	0.14330	503.737	9.515	0.03368	4.178	26.64	60.00	254
8495	0.417	0.08080	502.838	4.403	0.03329	2.384	17.04	60.00	31
8497	0.417	0.09445	503.043	4.400	0.03320	2.794	29.04	60.00	36
8499	0.417	0.10960	503.257	4.397	0.03335	3.228	24.24	60.00	41
8501	0.417	0.12589	503.499	4.395	0.03338	3.704	29.04	60.00	47
8503	0.417	0.14329	503.744	4.392	0.03346	4.206	29.04	60.00	54
8530	5.839	0.15533	741.489	41.556	0.05589	2.726	17.04	60.00	1148
8532	5.841	0.17186	741.633	41.562	0.05607	3.006	19.44	60.00	1265
8534	5.842	0.18966	741.836	41.555	0.05543	3.354	19.44	60.00	1410
8536	5.842	0.20826	742.026	41.546	0.05530	3.690	19.44	60.00	1550
8538	5.843	0.22741	742.193	41.541	0.05542	4.020	17.04	60.00	1687
8540	3.999	0.15530	741.457	28.496	0.05676	2.687	21.84	60.00	526
8542	3.986	0.17185	741.580	28.397	0.05718	2.951	19.44	60.00	574
8544	3.973	0.18961	741.804	28.302	0.05491	3.390	19.44	60.00	654
8546	3.963	0.20824	741.982	28.221	0.05478	3.731	24.24	60.00	716
8548	3.949	0.22748	742.146	28.115	0.05482	4.072	17.04	60.00	775
8550	2.034	0.15535	741.482	14.512	0.05427	2.812	17.04	60.00	141
8552	2.030	0.17190	741.595	14.481	0.05428	3.111	17.04	60.00	155
8554	2.025	0.18968	741.770	14.438	0.05410	3.444	19.44	60.00	171
8556	2.019	0.20829	741.988	14.392	0.05381	3.803	19.44	60.00	187
8558	2.012	0.22741	742.242	14.340	0.05326	4.194	19.44	60.00	205
8560	0.991	0.15534	741.560	7.071	0.05380	2.837	17.04	60.00	33
8562	0.988	0.17186	741.650	7.049	0.05462	3.092	14.64	60.00	36
8564	0.985	0.18962	741.748	7.028	0.05533	3.368	14.64	60.00	39
8566	0.982	0.20826	741.890	7.006	0.05558	3.683	19.44	60.00	43
8568	0.980	0.22734	742.058	6.985	0.05544	4.030	17.04	60.00	46
8570	0.163	0.15531	741.510	1.165	0.05201	2.934	17.04	60.00	1
8572	0.163	0.17190	741.688	1.165	0.05158	3.274	19.44	60.00	1

Run Point	$\frac{p_e}{\text{MPa}}$	$\frac{q}{\text{W} \cdot \text{m}^{-1}}$	$\frac{T_e}{\text{K}}$	$\frac{\rho_e}{\text{kg} \cdot \text{m}^{-3}}$	$\frac{\lambda_e}{\text{W} \cdot \text{m}^{-1} \cdot \text{K}^{-1}}$	$\frac{\Delta T_a}{\text{K}}$	$\frac{t_s}{\text{s}}$	$\frac{t_e}{\text{s}}$	Ra
8574	0.163	0.18962	741.899	1.164	0.05138	3.625	19.44	60.00	1
8576	0.163	0.20827	742.118	1.161	0.05123	3.994	14.64	60.00	1
8578	0.163	0.22737	742.322	1.161	0.05116	4.366	19.44	60.00	1
8580	5.832	0.15530	741.429	41.508	0.05612	2.714	31.44	60.00	1140
8582	5.832	0.17215	741.563	41.501	0.05638	2.995	17.04	60.00	1257
8584	5.832	0.18985	741.720	41.492	0.05634	3.304	12.24	60.00	1385
8586	5.832	0.20842	741.871	41.482	0.05638	3.623	19.44	60.00	1518
8588	5.832	0.22781	742.038	41.472	0.05641	3.957	19.44	60.00	1656
8590	4.048	0.15529	741.443	28.843	0.05503	2.770	21.84	60.00	556
8592	4.042	0.17215	741.584	28.799	0.05522	3.060	14.64	60.00	612
8594	4.037	0.18985	741.749	28.753	0.05509	3.382	17.04	60.00	674
8596	4.031	0.20842	741.916	28.708	0.05489	3.727	21.84	60.00	740
8598	4.025	0.22782	742.085	28.655	0.05508	4.059	17.04	60.00	803
8600	2.045	0.08112	504.058	21.784	0.03394	2.345	21.84	60.00	775
8602	2.044	0.09483	504.255	21.760	0.03398	2.737	24.24	60.00	901
8604	2.043	0.11005	504.469	21.740	0.03409	3.166	26.64	60.00	1039
8606	2.042	0.12641	504.704	21.722	0.03414	3.630	21.84	60.00	1187
8608	2.041	0.14389	504.964	21.701	0.03404	4.143	29.04	60.00	1350
8610	2.037	0.08114	504.081	21.699	0.03380	2.355	29.04	60.00	771
8612	2.036	0.09519	504.281	21.671	0.03396	2.749	26.64	60.00	897
8614	2.033	0.11037	504.494	21.628	0.03416	3.168	26.64	60.00	1028
8616	2.030	0.12666	504.730	21.589	0.03417	3.634	26.64	60.00	1174
8618	2.029	0.14409	504.982	21.568	0.03400	4.154	29.04	60.00	1337

Table A5. Thermal conductivity data for water from transient measurements at temperatures from 500 K to 740 K.

Run Point	$\frac{p_e}{\text{MPa}}$	$\frac{q}{\text{W} \cdot \text{m}^{-1}}$	$\frac{T_e}{\text{K}}$	$\frac{\rho_e}{\text{kg} \cdot \text{m}^{-3}}$	$\frac{\lambda_e}{\text{W} \cdot \text{m}^{-1} \cdot \text{K}^{-1}}$	STAT	$\frac{T_i}{\text{K}}$
3061	7.247	0.19770	563.944	37.390	0.06991	0.006	561.912
3063	7.251	0.21815	564.230	37.360	0.06989	0.006	561.937
3065	7.254	0.23959	564.453	37.330	0.06937	0.006	561.955
3067	7.256	0.26158	564.703	37.290	0.06954	0.006	561.975
3069	7.257	0.28503	564.965	37.250	0.06960	0.006	561.985
3071	6.088	0.19796	564.441	29.170	0.06281	0.006	561.979
3073	6.078	0.21843	564.742	29.070	0.06278	0.006	561.988
3075	6.068	0.23991	565.007	28.970	0.06267	0.006	561.997
3077	6.057	0.26194	565.307	28.870	0.06243	0.007	562.006
3079	6.047	0.28540	565.609	28.760	0.06255	0.007	562.007
3081	4.980	0.17892	564.619	22.580	0.05981	0.008	562.006
3083	4.972	0.19801	564.872	22.510	0.05974	0.008	562.005
3085	4.963	0.21849	565.186	22.430	0.05988	0.008	562.014
3087	4.953	0.23997	565.459	22.360	0.06012	0.008	562.015
3089	4.945	0.26198	565.772	22.290	0.06005	0.008	562.013
3171	15.575	0.19451	620.670	98.710	0.12898	0.007	619.779
3174	15.572	0.25738	620.974	98.190	0.12788	0.006	619.802
3175	15.566	0.28039	621.106	97.890	0.12747	0.006	619.806
3176	15.546	0.19457	620.757	98.070	0.12699	0.006	619.808
3177	15.540	0.21462	620.855	97.820	0.12705	0.006	619.808
3178	15.534	0.23565	620.950	97.580	0.12666	0.006	619.812
3179	15.528	0.25731	621.059	97.320	0.12646	0.006	619.813
3180	15.522	0.28036	621.180	97.040	0.12633	0.006	619.818
3181	12.957	0.19484	621.316	66.580	0.08913	0.005	619.818
3182	12.948	0.21495	621.491	66.420	0.08849	0.005	619.820
3183	12.939	0.23602	621.664	66.270	0.08839	0.005	619.825
3184	12.930	0.25768	621.835	66.110	0.08821	0.005	619.824
3185	12.921	0.28079	622.022	65.950	0.08800	0.005	619.824
3186	12.000	0.19485	621.503	58.600	0.08209	0.005	619.832
3187	11.991	0.21502	621.693	58.470	0.08175	0.005	619.835
3188	11.982	0.23611	621.884	58.340	0.08211	0.005	619.834
3189	11.973	0.25785	622.063	58.210	0.08167	0.005	619.835
3190	11.964	0.28085	622.271	58.080	0.08189	0.005	619.832
3191	10.974	0.19496	621.688	51.130	0.07673	0.005	619.825
3192	10.965	0.21505	621.883	51.020	0.07660	0.005	619.823
3193	10.957	0.23617	622.090	50.920	0.07634	0.005	619.818
3194	10.948	0.25784	622.282	50.810	0.07648	0.005	619.812
3195	10.939	0.28101	622.503	50.700	0.07632	0.005	619.814
3196	9.975	0.19502	621.826	44.660	0.07251	0.006	619.808

Run Point	$\frac{p_e}{\text{MPa}}$	$\frac{q}{\text{W} \cdot \text{m}^{-1}}$	$\frac{T_e}{\text{K}}$	$\frac{\rho_e}{\text{kg} \cdot \text{m}^{-3}}$	$\frac{\lambda_e}{\text{W} \cdot \text{m}^{-1} \cdot \text{K}^{-1}}$	STAT	$\frac{T_i}{\text{K}}$
3198	9.956	0.21517	622.037	44.500	0.07266	0.006	619.806
3200	9.938	0.23627	622.255	44.350	0.07246	0.006	619.802
3202	9.920	0.25795	622.473	44.200	0.07274	0.006	619.797
3204	9.900	0.28105	622.727	44.040	0.07221	0.006	619.802
3206	9.107	0.19507	621.941	39.510	0.07008	0.006	619.798
3208	9.088	0.21513	622.164	39.370	0.06961	0.006	619.803
3210	9.068	0.23636	622.406	39.220	0.06995	0.006	619.801
3212	9.049	0.25802	622.627	39.080	0.06952	0.006	619.794
3214	9.029	0.28108	622.877	38.940	0.06969	0.006	619.777
3216	7.981	0.19508	622.119	33.380	0.06755	0.007	619.785
3218	7.964	0.21521	622.358	33.260	0.06771	0.007	619.782
3220	7.946	0.23634	622.599	33.140	0.06777	0.007	619.771
3222	7.929	0.25795	622.864	33.020	0.06771	0.007	619.770
3224	7.911	0.28119	623.113	32.910	0.06756	0.007	619.761
3226	8.007	0.19506	622.085	33.510	0.06767	0.007	619.784
3228	7.989	0.21521	622.373	33.390	0.06779	0.007	619.787
3230	7.972	0.23631	622.633	33.270	0.06786	0.007	619.797
3232	7.954	0.25798	622.894	33.150	0.06757	0.007	619.808
3234	7.936	0.28104	623.178	33.030	0.06776	0.007	619.813
3401	23.366	0.38619	680.632	128.290	0.14282	0.005	679.087
3402	23.371	0.41202	680.682	128.290	0.14279	0.005	679.121
3403	23.375	0.43921	680.748	128.250	0.14298	0.005	679.166
3404	23.378	0.46672	680.817	128.210	0.14399	0.005	679.194
3405	23.381	0.49558	680.882	128.160	0.14402	0.005	679.218
3406	24.121	0.38522	680.754	137.350	0.15315	0.005	679.220
3407	24.121	0.41100	680.864	137.200	0.15270	0.005	679.228
3408	24.122	0.43815	680.966	137.060	0.15260	0.005	679.229
3409	24.122	0.46560	681.069	136.920	0.15211	0.005	679.231
3410	24.122	0.49444	681.179	136.760	0.15250	0.005	679.240
3421	23.724	0.38468	679.367	134.250	0.15063	0.005	678.010
3422	23.715	0.41035	679.303	134.230	0.15073	0.005	677.947
3423	23.707	0.43741	679.270	134.180	0.15187	0.005	677.901
3424	23.702	0.46479	679.258	134.130	0.15138	0.005	677.862
3425	23.697	0.49360	679.296	134.020	0.15137	0.006	677.835
3426	23.685	0.38445	679.298	133.860	0.15022	0.005	677.757
3427	23.683	0.41017	679.376	133.740	0.15133	0.005	677.739
3428	23.682	0.43724	679.444	133.620	0.15145	0.006	677.729
3429	23.680	0.46465	679.521	133.490	0.15053	0.006	677.716
3430	23.677	0.49342	679.582	133.380	0.15137	0.006	677.689
3431	23.667	0.38437	679.164	133.820	0.15038	0.006	677.621
3432	23.666	0.41007	679.238	133.700	0.15110	0.005	677.610

Run Point	$\frac{p_e}{\text{MPa}}$	$\frac{q}{\text{W} \cdot \text{m}^{-1}}$	$\frac{T_e}{\text{K}}$	$\frac{\rho_e}{\text{kg} \cdot \text{m}^{-3}}$	$\frac{\lambda_e}{\text{W} \cdot \text{m}^{-1} \cdot \text{K}^{-1}}$	STAT	$\frac{T_i}{\text{K}}$
3433	23.664	0.43712	679.317	133.580	0.15034	0.005	677.599
3434	23.663	0.46452	679.428	133.410	0.15070	0.006	677.594
3435	23.662	0.49332	679.516	133.280	0.15111	0.006	677.589
3436	23.800	0.38491	680.913	133.110	0.15025	0.005	679.389
3437	23.800	0.41068	681.039	132.950	0.14961	0.005	679.402
3438	23.800	0.43781	681.140	132.810	0.14937	0.005	679.395
3439	23.800	0.46523	681.256	132.660	0.14915	0.006	679.396
3440	23.799	0.49405	681.368	132.500	0.14965	0.006	679.386
3441	22.572	0.38503	681.155	118.950	0.13571	0.005	679.375
3442	22.572	0.41080	681.288	118.830	0.13554	0.005	679.382
3443	22.572	0.43793	681.421	118.700	0.13576	0.005	679.378
3444	22.572	0.46536	681.575	118.550	0.13500	0.005	679.385
3445	22.572	0.49422	681.706	118.420	0.13516	0.006	679.387
3446	21.635	0.38519	681.381	109.470	0.12603	0.005	679.378
3447	21.635	0.41096	681.527	109.350	0.12602	0.005	679.386
3448	21.635	0.43810	681.671	109.240	0.12639	0.005	679.392
3449	21.635	0.46556	681.808	109.130	0.12570	0.005	679.386
3450	21.635	0.49444	681.970	109.000	0.12639	0.005	679.393
3451	20.484	0.38534	681.606	99.090	0.11680	0.005	679.372
3452	20.484	0.41113	681.750	99.000	0.11707	0.005	679.375
3453	20.484	0.43829	681.920	98.900	0.11676	0.005	679.383
3454	20.484	0.46576	682.082	98.790	0.11736	0.005	679.387
3455	20.483	0.49464	682.234	98.700	0.11705	0.005	679.383
3456	19.259	0.38556	681.801	89.260	0.10889	0.005	679.380
3457	19.259	0.41134	681.975	89.170	0.10944	0.005	679.383
3458	19.259	0.43852	682.156	89.080	0.10923	0.005	679.381
3459	19.259	0.46600	682.338	88.990	0.10919	0.005	679.384
3460	19.258	0.49488	682.511	88.910	0.10900	0.005	679.384
3461	17.823	0.38577	682.036	78.950	0.10101	0.005	679.390
3462	17.823	0.41158	682.205	78.880	0.10163	0.005	679.389
3463	17.822	0.43877	682.401	78.800	0.10151	0.005	679.394
3464	17.822	0.46629	682.581	78.730	0.10118	0.005	679.389
3465	17.821	0.49519	682.781	78.660	0.10143	0.005	679.383
3466	16.198	0.38597	682.310	68.530	0.09423	0.005	679.364
3467	16.198	0.41180	682.500	68.470	0.09436	0.005	679.360
3468	16.197	0.43899	682.715	68.410	0.09445	0.005	679.358
3469	16.196	0.46652	682.907	68.350	0.09429	0.005	679.350
3470	16.196	0.49543	683.125	68.280	0.09469	0.005	679.349
3471	14.545	0.38613	682.573	59.010	0.08863	0.005	679.340
3472	14.545	0.41198	682.798	58.960	0.08920	0.005	679.342
3473	14.545	0.43920	683.023	58.910	0.08901	0.005	679.342

Run Point	$\frac{p_e}{\text{MPa}}$	$\frac{q}{\text{W} \cdot \text{m}^{-1}}$	$\frac{T_e}{\text{K}}$	$\frac{\rho_e}{\text{kg} \cdot \text{m}^{-3}}$	$\frac{\lambda_e}{\text{W} \cdot \text{m}^{-1} \cdot \text{K}^{-1}}$	STAT	$\frac{T_i}{\text{K}}$
3474	14.544	0.46673	683.264	58.860	0.08880	0.005	679.349
3475	14.544	0.49565	683.503	58.810	0.08910	0.005	679.342
3476	12.642	0.33618	682.442	49.170	0.08407	0.005	679.330
3477	12.641	0.36080	682.678	49.140	0.08409	0.006	679.333
3478	12.641	0.38629	682.909	49.100	0.08405	0.006	679.330
3479	12.641	0.41214	683.160	49.060	0.08383	0.006	679.338
3480	12.640	0.43940	683.396	49.020	0.08403	0.006	679.326
3601	40.353	0.38395	740.298	228.590	0.22727	0.006	739.186
3602	40.364	0.40964	740.468	228.350	0.22600	0.006	739.264
3603	40.373	0.43676	740.605	228.160	0.22539	0.006	739.315
3604	40.380	0.46396	740.741	227.950	0.22463	0.006	739.372
3605	40.385	0.49272	740.846	227.780	0.22522	0.006	739.403
3606	40.394	0.38404	740.531	228.560	0.22653	0.006	739.502
3607	40.394	0.40964	740.588	228.430	0.22530	0.005	739.509
3608	40.392	0.43677	740.636	228.310	0.22580	0.005	739.513
3609	40.390	0.46414	740.660	228.230	0.22702	0.005	739.517
3610	40.387	0.49290	740.694	228.130	0.22608	0.005	739.510
3611	39.578	0.38396	740.543	219.550	0.21593	0.005	739.508
3612	39.576	0.40965	740.593	219.440	0.21488	0.006	739.509
3613	39.575	0.43669	740.663	219.290	0.21476	0.005	739.516
3614	39.574	0.46403	740.719	219.160	0.21517	0.005	739.522
3615	39.572	0.49278	740.786	219.020	0.21584	0.005	739.518
3616	38.468	0.38394	740.739	207.380	0.20070	0.006	739.551
3617	38.467	0.40955	740.812	207.240	0.20207	0.005	739.545
3618	38.466	0.43664	740.915	207.040	0.20098	0.005	739.549
3619	38.464	0.46400	740.991	206.890	0.20112	0.005	739.545
3620	38.462	0.49269	741.083	206.700	0.20211	0.005	739.527
3621	37.553	0.38394	740.832	197.850	0.19238	0.005	739.537
3622	37.553	0.40963	740.919	197.700	0.19259	0.005	739.537
3623	37.552	0.43669	741.021	197.530	0.19266	0.005	739.538
3624	37.550	0.46386	741.077	197.420	0.19226	0.005	739.535
3625	37.549	0.49285	741.184	197.240	0.19246	0.005	739.541
3626	36.580	0.38399	740.904	188.150	0.18311	0.005	739.528
3627	36.579	0.40974	740.998	188.000	0.18264	0.005	739.532
3628	36.578	0.43686	741.118	187.810	0.18235	0.005	739.544
3629	36.577	0.46427	741.141	187.770	0.18282	0.005	739.538
3630	36.576	0.49303	741.262	187.580	0.18357	0.005	739.546
3631	35.585	0.38415	741.002	178.610	0.17402	0.005	739.545
3632	35.584	0.40983	741.120	178.450	0.17508	0.005	739.547
3633	35.583	0.43694	741.149	178.400	0.17507	0.005	739.554
3634	35.582	0.46434	741.258	178.250	0.17469	0.005	739.551

Run Point	$\frac{p_e}{\text{MPa}}$	$\frac{q}{\text{W} \cdot \text{m}^{-1}}$	$\frac{T_e}{\text{K}}$	$\frac{\rho_e}{\text{kg} \cdot \text{m}^{-3}}$	$\frac{\lambda_e}{\text{W} \cdot \text{m}^{-1} \cdot \text{K}^{-1}}$	STAT	$\frac{T_i}{\text{K}}$
3635	35.581	0.49312	741.401	178.050	0.17448	0.005	739.559
3636	34.551	0.38442	741.051	169.220	0.16643	0.005	739.559
3637	34.551	0.41014	741.172	169.070	0.16722	0.005	739.562
3638	34.549	0.43717	741.242	168.980	0.16755	0.005	739.561
3639	34.548	0.46460	741.368	168.820	0.16591	0.005	739.558
3640	34.546	0.49330	741.493	168.650	0.16656	0.005	739.551
3641	33.466	0.38462	741.067	159.860	0.15966	0.005	739.512
3642	33.464	0.41037	741.128	159.770	0.15885	0.005	739.508
3643	33.461	0.43748	741.254	159.620	0.15910	0.005	739.490
3644	33.459	0.46493	741.396	159.450	0.15880	0.005	739.484
3645	33.457	0.49375	741.540	159.290	0.15944	0.005	739.483
3646	32.139	0.38484	741.162	148.950	0.15105	0.005	739.478
3647	32.138	0.41053	741.317	148.800	0.15076	0.005	739.475
3648	32.137	0.43765	741.490	148.630	0.15120	0.004	739.489
3649	32.136	0.46527	741.412	148.700	0.15017	0.005	739.489
3650	32.135	0.49383	741.617	148.510	0.15037	0.005	739.491
3651	30.856	0.38511	741.317	138.970	0.14313	0.005	739.505
3652	30.855	0.41083	741.481	138.840	0.14319	0.005	739.500
3653	30.854	0.43782	741.663	138.690	0.14628	0.004	739.499
3654	30.853	0.46536	741.810	138.570	0.14443	0.004	739.496
3655	30.851	0.49388	741.984	138.420	0.14284	0.005	739.499
3656	29.413	0.38545	741.424	128.490	0.13657	0.004	739.499
3657	29.412	0.41117	741.602	128.370	0.13468	0.005	739.485
3658	29.411	0.43826	741.800	128.230	0.13759	0.004	739.490
3659	29.410	0.46600	741.796	128.220	0.13512	0.005	739.497
3660	29.409	0.49492	741.997	128.080	0.13709	0.004	739.488
3661	27.961	0.38580	741.546	118.600	0.12946	0.004	739.481
3662	27.960	0.41134	741.776	118.460	0.13143	0.004	739.492
3663	27.958	0.43873	741.817	118.430	0.12829	0.005	739.490
3664	27.957	0.46624	742.033	118.300	0.12902	0.004	739.484
3665	27.956	0.49508	742.253	118.170	0.13030	0.004	739.490
3666	26.367	0.38611	741.780	108.390	0.12090	0.005	739.475
3667	26.366	0.41196	741.975	108.290	0.12074	0.005	739.477
3668	26.364	0.43935	742.019	108.260	0.12096	0.005	739.477
3669	26.363	0.46690	742.239	108.150	0.12126	0.005	739.481
3670	26.362	0.49579	742.466	108.040	0.12096	0.005	739.475
3691	26.398	0.36064	741.355	108.780	0.11707	0.005	739.068
3692	26.404	0.38487	741.593	108.700	0.11718	0.005	739.125
3693	26.409	0.41016	741.850	108.610	0.11669	0.005	739.179
3694	26.412	0.43582	742.089	108.520	0.11705	0.005	739.232
3695	26.415	0.46275	742.338	108.420	0.11707	0.005	739.288

Run Point	$\frac{p_e}{\text{MPa}}$	$\frac{q}{\text{W} \cdot \text{m}^{-1}}$	$\frac{T_e}{\text{K}}$	$\frac{\rho_e}{\text{kg} \cdot \text{m}^{-3}}$	$\frac{\lambda_e}{\text{W} \cdot \text{m}^{-1} \cdot \text{K}^{-1}}$	STAT	$\frac{T_i}{\text{K}}$
3696	26.424	0.36133	741.645	108.800	0.11765	0.005	739.470
3697	26.424	0.38551	741.804	108.720	0.11751	0.005	739.476
3698	26.423	0.41098	741.966	108.640	0.11708	0.005	739.479
3699	26.422	0.43622	742.131	108.560	0.11686	0.005	739.483
3700	26.421	0.46354	742.304	108.470	0.11736	0.005	739.481
3701	24.812	0.36147	741.824	99.150	0.11119	0.005	739.482
3702	24.812	0.38550	742.000	99.080	0.11146	0.005	739.494
3703	24.811	0.41096	742.188	99.000	0.11162	0.005	739.500
3704	24.811	0.43668	742.302	98.950	0.11152	0.005	739.504
3705	24.810	0.46396	742.492	98.870	0.11145	0.005	739.514
3706	22.782	0.36146	741.971	87.870	0.10516	0.005	739.502
3707	22.781	0.38558	742.163	87.810	0.10539	0.005	739.505
3708	22.780	0.41122	742.318	87.750	0.10527	0.005	739.486
3709	22.778	0.43682	742.503	87.690	0.10507	0.005	739.484
3710	22.777	0.46380	742.686	87.620	0.10482	0.005	739.474
3711	21.058	0.36153	742.100	78.960	0.10087	0.005	739.446
3712	21.057	0.38564	742.286	78.900	0.10051	0.005	739.447
3713	21.055	0.41130	742.488	78.840	0.10067	0.005	739.446
3714	21.054	0.43707	742.668	78.790	0.10057	0.005	739.432
3715	21.053	0.46390	742.888	78.730	0.10082	0.005	739.439
3716	19.088	0.36179	742.292	69.400	0.09662	0.005	739.455
3717	19.087	0.38594	742.506	69.360	0.09676	0.005	739.459
3718	19.086	0.41144	742.720	69.310	0.09670	0.005	739.465
3719	19.085	0.43724	742.946	69.260	0.09629	0.005	739.467
3720	19.085	0.46425	743.167	69.210	0.09618	0.005	739.467
3721	16.666	0.36192	742.581	58.490	0.09207	0.006	739.461
3722	16.665	0.38616	742.801	58.450	0.09210	0.006	739.467
3723	16.665	0.41143	743.037	58.410	0.09176	0.006	739.469
3724	16.664	0.43740	743.261	58.370	0.09228	0.006	739.465
3725	16.663	0.46426	743.514	58.330	0.09198	0.006	739.465
3726	14.427	0.36214	742.743	49.120	0.08949	0.006	739.474
3727	14.426	0.38637	742.986	49.090	0.08901	0.006	739.475
3728	14.426	0.41190	743.244	49.050	0.08929	0.006	739.478
3729	14.425	0.43755	743.493	49.020	0.08957	0.006	739.482
3730	14.424	0.46422	743.753	48.990	0.08910	0.006	739.478

Table A6. Thermal conductivity data for water from steady-state measurements at temperatures from 500 K to 740 K.

Run Point	$\frac{P_e}{\text{MPa}}$	$\frac{q}{\text{W} \cdot \text{m}^{-1}}$	$\frac{T_e}{\text{K}}$	$\frac{\rho_e}{\text{kg} \cdot \text{m}^{-3}}$	$\frac{\lambda_e}{\text{W} \cdot \text{m}^{-1} \cdot \text{K}^{-1}}$	$\frac{\Delta T_a}{\text{K}}$	$\frac{t_s}{\text{s}}$	$\frac{t_e}{\text{s}}$	Ra
3002	2.533	0.11020	504.018	12.389	0.04502	2.399	24.24	60.00	1408
3004	2.526	0.12643	504.203	12.345	0.04518	2.741	24.24	60.00	1586
3006	2.521	0.14377	504.409	12.303	0.04513	3.120	24.24	60.00	1779
3008	2.515	0.16254	504.626	12.263	0.04493	3.541	26.64	60.00	1990
3010	2.510	0.18207	504.855	12.224	0.04476	3.981	24.24	60.00	2206
3012	2.001	0.11024	504.156	9.465	0.04271	2.533	24.24	60.00	673
3014	1.997	0.12651	504.349	9.438	0.04258	2.915	26.64	60.00	767
3016	1.993	0.14386	504.568	9.412	0.04230	3.336	21.84	60.00	869
3018	1.989	0.16249	504.771	9.386	0.04261	3.740	24.24	60.00	964
3020	1.985	0.18210	504.995	9.358	0.04268	4.183	24.24	60.00	1066
3022	1.516	0.11022	504.234	6.978	0.04084	2.650	24.24	60.00	319
3024	1.513	0.12653	504.427	6.960	0.04091	3.037	21.84	60.00	362
3026	1.510	0.14398	504.628	6.941	0.04116	3.434	24.24	60.00	406
3028	1.506	0.16265	504.851	6.916	0.04117	3.879	21.84	60.00	453
3030	1.504	0.18225	505.079	6.906	0.04112	4.351	26.64	60.00	505
3032	1.029	0.11020	504.299	4.622	0.03905	2.772	21.84	60.00	125
3034	1.028	0.12658	504.499	4.616	0.03927	3.166	24.24	60.00	142
3036	1.026	0.14401	504.711	4.601	0.03932	3.597	24.24	60.00	160
3038	1.026	0.16267	504.942	4.600	0.03935	4.060	24.24	60.00	180
3040	1.026	0.18222	505.191	4.598	0.03919	4.567	24.24	60.00	202
3042	0.489	0.11027	504.332	2.145	0.03828	2.831	24.24	60.00	24
3044	0.486	0.12655	504.541	2.130	0.03818	3.257	24.24	60.00	27
3046	0.484	0.14400	504.756	2.118	0.03827	3.697	24.24	60.00	30
3048	0.482	0.16274	505.002	2.109	0.03818	4.188	26.64	60.00	34
3050	0.481	0.18231	505.244	2.103	0.03828	4.680	24.24	60.00	37
3052	0.119	0.11028	504.391	0.515	0.03632	2.983	24.24	60.00	1
3054	0.121	0.12660	504.609	0.523	0.03636	3.421	26.64	60.00	2
3056	0.122	0.14390	504.851	0.528	0.03631	3.894	24.24	60.00	2
3058	0.123	0.16266	505.096	0.531	0.03647	4.382	26.64	60.00	2
3060	0.124	0.18226	505.358	0.533	0.03649	4.907	24.24	60.00	2
3062	7.249	0.19773	563.178	37.569	0.07423	2.511	31.44	60.00	23995
3064	7.253	0.21817	563.325	37.567	0.07441	2.753	21.84	60.00	26200
3066	7.255	0.23963	563.469	37.555	0.07435	3.014	21.84	60.00	28531
3068	7.257	0.26162	563.619	37.534	0.07418	3.285	21.84	60.00	30887
3070	7.258	0.28506	563.770	37.508	0.07408	3.569	21.84	60.00	33316
3072	6.084	0.19800	563.497	29.260	0.06316	3.023	24.24	60.00	10708
3074	6.074	0.21845	563.659	29.173	0.06311	3.333	21.84	60.00	11645
3076	6.063	0.23994	563.815	29.087	0.06326	3.646	17.04	60.00	12568
3078	6.053	0.26197	563.984	28.999	0.06336	3.968	17.04	60.00	13490
3080	6.042	0.28543	564.155	28.912	0.06343	4.311	17.04	60.00	14455
3082	4.977	0.17894	563.571	22.637	0.05564	3.134	21.84	60.00	4712
3084	4.967	0.19803	563.738	22.574	0.05574	3.459	21.84	60.00	5143

Run Point	$\frac{P_e}{\text{MPa}}$	$\frac{q}{\text{W} \cdot \text{m}^{-1}}$	$\frac{T_e}{\text{K}}$	$\frac{\rho_e}{\text{kg} \cdot \text{m}^{-3}}$	$\frac{\lambda_e}{\text{W} \cdot \text{m}^{-1} \cdot \text{K}^{-1}}$	$\frac{\Delta T_a}{\text{K}}$	$\frac{t_s}{\text{s}}$	$\frac{t_e}{\text{s}}$	Ra
3086	4.959	0.21850	563.888	22.513	0.05678	3.745	21.84	60.00	5510
3088	4.949	0.24000	564.071	22.448	0.05660	4.122	19.44	60.00	5996
3090	4.941	0.26202	564.250	22.386	0.05677	4.484	21.84	60.00	6450
3092	3.985	0.16051	563.525	17.383	0.05206	3.018	24.24	60.00	2078
3094	3.978	0.17897	563.696	17.336	0.05211	3.361	24.24	60.00	2292
3096	3.970	0.19808	563.829	17.289	0.05352	3.622	21.84	60.00	2447
3098	3.962	0.21855	564.004	17.243	0.05350	3.996	21.84	60.00	2675
3100	3.955	0.24003	564.190	17.200	0.05348	4.388	24.24	60.00	2910
3102	2.955	0.14324	563.432	12.411	0.04937	2.847	21.84	60.00	797
3104	2.949	0.16051	563.591	12.376	0.04951	3.181	21.84	60.00	883
3106	2.944	0.17899	563.745	12.350	0.04984	3.523	21.84	60.00	971
3108	2.940	0.19808	563.920	12.323	0.04991	3.893	24.24	60.00	1066
3110	2.935	0.21855	564.118	12.294	0.04987	4.298	21.84	60.00	1167
3112	1.972	0.14326	563.490	8.017	0.04697	2.995	24.24	60.00	290
3114	1.969	0.16053	563.692	8.002	0.04664	3.380	24.24	60.00	325
3116	1.967	0.17901	563.888	7.986	0.04688	3.750	21.84	60.00	358
3118	1.963	0.19810	564.064	7.969	0.04748	4.097	21.84	60.00	389
3120	1.960	0.21858	564.264	7.951	0.04751	4.518	21.84	60.00	426
3122	0.929	0.12678	563.374	3.662	0.04495	2.771	21.84	60.00	47
3124	0.928	0.14324	563.551	3.656	0.04509	3.121	24.24	60.00	53
3126	0.927	0.16053	563.744	3.653	0.04479	3.521	24.24	60.00	59
3128	0.926	0.17901	563.929	3.648	0.04516	3.895	24.24	60.00	65
3130	0.925	0.19811	564.138	3.640	0.04521	4.306	24.24	60.00	72
3132	0.126	0.11145	563.271	0.484	0.04242	2.581	24.24	60.00	1
3134	0.129	0.12677	563.445	0.499	0.04264	2.921	24.24	60.00	1
3136	0.131	0.14325	563.638	0.506	0.04233	3.325	24.24	60.00	1
3138	0.131	0.16054	563.824	0.505	0.04275	3.690	26.64	60.00	1
3140	0.131	0.17903	564.033	0.503	0.04283	4.107	24.24	60.00	1
3197	9.967	0.19506	621.038	44.749	0.07587	2.462	19.44	60.00	14593
3199	9.948	0.21519	621.157	44.613	0.07566	2.718	19.44	60.00	15912
3201	9.930	0.23628	621.288	44.474	0.07537	2.989	21.84	60.00	17279
3203	9.911	0.25805	621.420	44.335	0.07566	3.244	17.04	60.00	18524
3205	9.892	0.28102	621.555	44.195	0.07556	3.529	19.44	60.00	19897
3207	9.098	0.19498	621.109	39.583	0.07192	2.616	19.44	60.00	10333
3209	9.079	0.21519	621.235	39.454	0.07178	2.889	19.44	60.00	11269
3211	9.059	0.23634	621.369	39.323	0.07200	3.157	19.44	60.00	12165
3213	9.040	0.25807	621.499	39.195	0.07216	3.435	17.04	60.00	13071
3215	9.020	0.28118	621.651	39.062	0.07219	3.734	17.04	60.00	14029
3217	7.974	0.19504	621.203	33.433	0.06663	2.843	19.44	60.00	6624
3219	7.956	0.21515	621.336	33.327	0.06678	3.126	21.84	60.00	7203
3221	7.938	0.23632	621.474	33.220	0.06697	3.421	21.84	60.00	7792
3223	7.921	0.25810	621.629	33.112	0.06707	3.726	19.44	60.00	8389
3225	7.903	0.28130	621.777	33.005	0.06722	4.048	19.44	60.00	9009
3227	7.999	0.19516	621.196	33.567	0.06721	2.820	21.84	60.00	6652
3229	7.981	0.21518	621.359	33.457	0.06626	3.150	19.44	60.00	7342

Run Point	$\frac{p_e}{\text{MPa}}$	$\frac{q}{\text{W} \cdot \text{m}^{-1}}$	$\frac{T_e}{\text{K}}$	$\frac{\rho_e}{\text{kg} \cdot \text{m}^{-3}}$	$\frac{\lambda_e}{\text{W} \cdot \text{m}^{-1} \cdot \text{K}^{-1}}$	$\frac{\Delta T_a}{\text{K}}$	$\frac{t_s}{\text{s}}$	$\frac{t_e}{\text{s}}$	Ra
3231	7.964	0.23636	621.511	33.348	0.06691	3.424	19.44	60.00	7886
3233	7.946	0.25796	621.666	33.237	0.06710	3.722	19.44	60.00	8472
3235	7.928	0.28114	621.825	33.128	0.06715	4.049	19.44	60.00	9108
3237	6.973	0.17632	621.161	28.391	0.06373	2.701	21.84	60.00	3893
3239	6.957	0.19507	621.301	28.302	0.06389	2.978	21.84	60.00	4248
3241	6.942	0.21518	621.461	28.214	0.06332	3.312	21.84	60.00	4675
3243	6.926	0.23637	621.615	28.126	0.06331	3.636	19.44	60.00	5078
3245	6.910	0.25804	621.766	28.037	0.06373	3.941	19.44	60.00	5445
3247	5.968	0.17623	621.242	23.641	0.05945	2.900	24.24	60.00	2509
3249	5.955	0.19502	621.389	23.571	0.05982	3.188	21.84	60.00	2732
3251	5.941	0.21524	621.555	23.499	0.06012	3.500	21.84	60.00	2970
3253	5.928	0.23636	621.729	23.426	0.06013	3.841	19.44	60.00	3226
3255	5.914	0.25801	621.893	23.354	0.06019	4.186	21.84	60.00	3482
3257	5.010	0.17624	621.286	19.369	0.05814	2.971	19.44	60.00	1518
3259	4.998	0.19502	621.450	19.312	0.05814	3.286	24.24	60.00	1664
3261	4.987	0.21514	621.615	19.255	0.05829	3.616	21.84	60.00	1814
3263	4.976	0.23636	621.793	19.200	0.05788	3.999	21.84	60.00	1989
3265	4.964	0.25806	621.938	19.144	0.05882	4.296	19.44	60.00	2118
3267	3.971	0.15808	621.189	14.987	0.05600	2.770	21.84	60.00	746
3269	3.962	0.17628	621.337	14.947	0.05636	3.069	21.84	60.00	820
3271	3.953	0.19503	621.509	14.905	0.05642	3.392	21.84	60.00	898
3273	3.944	0.21517	621.684	14.862	0.05645	3.740	19.44	60.00	982
3275	3.935	0.23637	621.862	14.820	0.05664	4.094	21.84	60.00	1066
3277	2.966	0.15805	621.237	10.951	0.05414	2.867	21.84	60.00	367
3279	2.959	0.17623	621.397	10.922	0.05453	3.174	21.84	60.00	403
3281	2.952	0.19500	621.570	10.891	0.05440	3.520	19.44	60.00	443
3283	2.946	0.21525	621.753	10.860	0.05453	3.876	21.84	60.00	484
3285	2.939	0.23634	621.928	10.829	0.05473	4.240	21.84	60.00	526
3287	1.962	0.15805	621.218	7.097	0.05448	2.851	21.84	60.00	137
3289	1.958	0.17627	621.374	7.080	0.05468	3.168	21.84	60.00	152
3291	1.954	0.19513	621.550	7.065	0.05445	3.521	21.84	60.00	168
3293	1.951	0.21530	621.764	7.048	0.05361	3.946	19.44	60.00	187
3295	1.947	0.23638	621.951	7.033	0.05365	4.329	19.44	60.00	204
3297	0.752	0.15806	621.315	2.657	0.05091	3.051	19.44	60.00	18
3299	0.757	0.17627	621.483	2.675	0.05107	3.392	21.84	60.00	21
3301	0.760	0.19506	621.676	2.685	0.05099	3.759	24.24	60.00	23
3303	0.762	0.21520	621.857	2.690	0.05116	4.134	21.84	60.00	25
3305	0.763	0.23642	622.050	2.694	0.05130	4.529	19.44	60.00	28
3306	2.036	0.15813	621.201	7.378	0.05424	2.865	17.04	60.00	150
3307	2.033	0.17635	621.365	7.363	0.05443	3.184	19.44	60.00	166
3308	2.030	0.19510	621.537	7.348	0.05418	3.538	19.44	60.00	184
3309	2.027	0.21529	621.720	7.335	0.05415	3.907	21.84	60.00	202
3310	2.024	0.23634	621.915	7.321	0.05405	4.297	17.04	60.00	221
3312	0.114	0.15803	621.368	0.397	0.04907	3.165	21.84	60.00	0
3314	0.115	0.17628	621.535	0.403	0.04929	3.514	17.04	60.00	0

Run Point	$\frac{p_e}{\text{MPa}}$	$\frac{q}{\text{W} \cdot \text{m}^{-1}}$	$\frac{T_e}{\text{K}}$	$\frac{\rho_e}{\text{kg} \cdot \text{m}^{-3}}$	$\frac{\lambda_e}{\text{W} \cdot \text{m}^{-1} \cdot \text{K}^{-1}}$	$\frac{\Delta T_a}{\text{K}}$	$\frac{t_s}{\text{s}}$	$\frac{t_e}{\text{s}}$	Ra
3316	0.116	0.19512	621.709	0.406	0.04929	3.889	21.84	60.00	1
3318	0.117	0.21524	621.898	0.408	0.04936	4.285	24.24	60.00	1
3320	0.117	0.23640	622.099	0.409	0.04948	4.694	21.84	60.00	1
3412	0.115	0.17179	680.573	0.367	0.05573	3.028	24.24	60.00	0
3414	0.112	0.18958	680.675	0.357	0.06044	3.084	19.44	60.00	0
3416	0.109	0.20824	680.879	0.347	0.06000	3.412	21.84	60.00	0
3418	0.104	0.22736	681.080	0.331	0.05934	3.767	17.04	60.00	0
3420	0.099	0.24772	681.266	0.315	0.05938	4.101	14.64	60.00	0
3482	10.446	0.31306	681.224	39.009	0.07974	3.811	5.04	60.00	7272
3484	10.446	0.33638	681.364	38.993	0.07983	4.087	5.04	60.00	7779
3486	10.445	0.36104	681.513	38.974	0.08009	4.369	5.04	60.00	8293
3488	10.445	0.38653	681.643	38.958	0.08048	4.650	2.64	60.00	8806
3490	10.444	0.41241	681.791	38.941	0.08062	4.948	2.64	60.00	9346
3492	8.062	0.31316	681.405	28.817	0.07369	4.153	19.44	60.00	3532
3494	8.061	0.33651	681.564	28.805	0.07353	4.470	19.44	60.00	3793
3496	8.061	0.36116	681.737	28.792	0.07343	4.801	17.04	60.00	4064
3498	8.061	0.38672	681.897	28.781	0.07347	5.136	19.44	60.00	4337
3500	8.060	0.41260	682.062	28.767	0.07350	5.475	17.04	60.00	4611
3502	5.576	0.31328	681.529	19.140	0.06978	4.405	17.04	60.00	1361
3504	5.576	0.33662	681.694	19.133	0.06968	4.738	17.04	60.00	1461
3506	5.576	0.36130	681.859	19.127	0.06979	5.078	19.44	60.00	1563
3508	5.575	0.38685	682.030	19.118	0.06974	5.439	19.44	60.00	1670
3510	5.575	0.41274	682.177	19.111	0.07038	5.750	9.84	60.00	1762
3512	5.929	0.26851	681.191	20.477	0.06868	3.834	19.44	60.00	1396
3514	5.929	0.29062	681.377	20.470	0.06859	4.155	17.04	60.00	1510
3516	5.929	0.31359	681.514	20.462	0.07022	4.379	17.04	60.00	1588
3518	5.928	0.33697	681.690	20.452	0.07007	4.715	19.44	60.00	1706
3520	5.927	0.36164	681.852	20.442	0.07011	5.056	17.04	60.00	1825
3522	4.977	0.26856	681.246	16.940	0.06806	3.874	19.44	60.00	899
3524	4.977	0.29065	681.413	16.933	0.06800	4.196	17.04	60.00	972
3526	4.977	0.31362	681.593	16.926	0.06783	4.538	17.04	60.00	1049
3528	4.977	0.33699	681.764	16.921	0.06780	4.878	17.04	60.00	1125
3530	4.976	0.36169	681.941	16.913	0.06778	5.236	19.44	60.00	1205
3532	3.963	0.26860	681.298	13.288	0.06684	3.948	17.04	60.00	524
3534	3.963	0.29071	681.467	13.282	0.06683	4.274	17.04	60.00	566
3536	3.962	0.31367	681.634	13.276	0.06681	4.612	17.04	60.00	609
3538	3.962	0.33705	681.807	13.271	0.06664	4.968	19.44	60.00	655
3540	3.962	0.36175	681.994	13.266	0.06645	5.347	17.04	60.00	704
3542	2.952	0.26864	681.320	9.757	0.06658	3.967	17.04	60.00	264
3544	2.951	0.29075	681.468	9.750	0.06664	4.289	14.64	60.00	285
3546	2.950	0.31373	681.622	9.743	0.06669	4.624	17.04	60.00	307
3548	2.948	0.33709	681.776	9.735	0.06672	4.966	19.44	60.00	329
3550	2.947	0.36179	681.926	9.729	0.06697	5.311	17.04	60.00	351
3552	1.970	0.26865	681.296	6.425	0.06512	4.057	17.04	60.00	110
3554	1.970	0.29074	681.473	6.423	0.06497	4.400	17.04	60.00	119

Run Point	$\frac{P_e}{\text{MPa}}$	$\frac{q}{\text{W} \cdot \text{m}^{-1}}$	$\frac{T_e}{\text{K}}$	$\frac{\rho_e}{\text{kg} \cdot \text{m}^{-3}}$	$\frac{\lambda_e}{\text{W} \cdot \text{m}^{-1} \cdot \text{K}^{-1}}$	$\frac{\Delta T_a}{\text{K}}$	$\frac{t_s}{\text{s}}$	$\frac{t_e}{\text{s}}$	Ra
3556	1.969	0.31371	681.653	6.419	0.06488	4.754	17.04	60.00	128
3558	1.969	0.33708	681.833	6.418	0.06478	5.116	17.04	60.00	138
3560	1.968	0.36181	682.024	6.412	0.06480	5.490	17.04	60.00	147
3562	0.941	0.26867	681.408	3.028	0.06205	4.257	19.44	60.00	24
3564	0.940	0.29078	681.574	3.025	0.06211	4.603	17.04	60.00	26
3566	0.940	0.31376	681.753	3.023	0.06208	4.969	19.44	60.00	28
3568	0.939	0.33712	681.953	3.019	0.06208	5.340	14.64	60.00	30
3570	0.939	0.36185	682.139	3.018	0.06210	5.729	19.44	60.00	32
3572	0.477	0.26869	681.452	1.526	0.06087	4.340	17.04	60.00	6
3574	0.477	0.29080	681.626	1.525	0.06100	4.687	19.44	60.00	6
3576	0.478	0.31378	681.804	1.528	0.06097	5.060	19.44	60.00	7
3578	0.478	0.33716	681.990	1.527	0.06099	5.435	17.04	60.00	8
3580	0.478	0.36188	682.195	1.526	0.06097	5.836	14.64	60.00	8
3582	0.104	0.26871	681.534	0.332	0.05841	4.521	19.44	60.00	0
3584	0.107	0.29083	681.721	0.342	0.05851	4.886	19.44	60.00	0
3586	0.110	0.31382	681.908	0.350	0.05863	5.261	17.04	60.00	0
3588	0.113	0.33720	682.105	0.360	0.05863	5.653	19.44	60.00	0
3590	0.116	0.36190	682.309	0.370	0.05871	6.058	19.44	60.00	0
3596	9.755	0.26730	741.188	31.477	0.07858	3.331	31.44	60.00	2266
3597	9.739	0.28936	741.245	31.417	0.08253	3.434	26.64	60.00	2325
3598	9.723	0.31222	741.422	31.349	0.08065	3.790	29.04	60.00	2549
3599	9.707	0.33550	741.613	31.280	0.07903	4.153	26.64	60.00	2775
3600	9.691	0.36010	741.792	31.213	0.07780	4.526	24.24	60.00	3005
3732	11.929	0.31521	741.356	39.484	0.08217	3.741	17.04	60.00	4463
3734	11.928	0.33812	741.520	39.465	0.08101	4.067	21.84	60.00	4840
3736	11.926	0.36210	741.683	39.446	0.08014	4.400	17.04	60.00	5223
3738	11.925	0.38608	741.752	39.434	0.08305	4.527	9.84	60.00	5367
3740	11.923	0.41146	741.924	39.413	0.08214	4.874	7.44	60.00	5763
3742	9.313	0.31473	741.449	29.884	0.07836	3.932	21.84	60.00	2355
3744	9.311	0.33782	741.625	29.867	0.07731	4.276	19.44	60.00	2554
3746	9.309	0.36174	741.784	29.851	0.07664	4.617	19.44	60.00	2751
3748	9.307	0.38595	741.943	29.836	0.07610	4.959	17.04	60.00	2948
3750	9.305	0.41140	742.061	29.823	0.07780	5.170	19.44	60.00	3068
3752	6.169	0.27148	741.241	19.139	0.07524	3.543	14.64	60.00	748
3754	6.167	0.29293	741.402	19.127	0.07430	3.870	19.44	60.00	816
3756	6.165	0.31479	741.557	19.115	0.07363	4.197	17.04	60.00	882
3758	6.163	0.33783	741.667	19.104	0.07502	4.420	17.04	60.00	927
3760	6.161	0.36173	741.829	19.092	0.07439	4.772	17.04	60.00	999
3762	5.980	0.27054	741.179	18.519	0.07514	3.536	19.44	60.00	693
3764	5.978	0.29192	741.346	18.506	0.07435	3.855	21.84	60.00	754
3766	5.976	0.31368	741.511	18.494	0.07372	4.177	21.84	60.00	815
3768	5.974	0.33666	741.654	18.482	0.07426	4.450	19.44	60.00	866
3770	5.972	0.36046	741.832	18.469	0.07363	4.805	17.04	60.00	933
3772	3.881	0.27026	741.227	11.764	0.07446	3.568	14.64	60.00	256
3774	3.879	0.29144	741.391	11.755	0.07333	3.906	21.84	60.00	279

Run Point	$\frac{p_e}{\text{MPa}}$	$\frac{q}{\text{W} \cdot \text{m}^{-1}}$	$\frac{T_e}{\text{K}}$	$\frac{\rho_e}{\text{kg} \cdot \text{m}^{-3}}$	$\frac{\lambda_e}{\text{W} \cdot \text{m}^{-1} \cdot \text{K}^{-1}}$	$\frac{\Delta T_a}{\text{K}}$	$\frac{t_s}{\text{s}}$	$\frac{t_e}{\text{s}}$	Ra
3776	3.877	0.31322	741.546	11.745	0.07266	4.236	17.04	60.00	302
3778	3.874	0.33605	741.705	11.735	0.07218	4.575	19.44	60.00	326
3780	3.873	0.35987	741.845	11.727	0.07252	4.876	19.44	60.00	346
3782	1.930	0.27001	741.271	5.741	0.07127	3.725	14.64	60.00	58
3784	1.930	0.29133	741.444	5.741	0.07043	4.067	14.64	60.00	64
3786	1.930	0.31305	741.614	5.740	0.06986	4.405	17.04	60.00	69
3788	1.931	0.33599	741.796	5.740	0.06935	4.763	21.84	60.00	74
3790	1.931	0.35974	741.976	5.739	0.06897	5.127	14.64	60.00	80
3792	0.953	0.23014	741.022	2.812	0.07015	3.226	14.64	60.00	12
3794	0.961	0.24949	741.188	2.834	0.06912	3.549	17.04	60.00	13
3796	0.967	0.27002	741.349	2.851	0.06842	3.879	21.84	60.00	14
3798	0.972	0.29134	741.523	2.865	0.06783	4.222	17.04	60.00	16
3800	0.975	0.31305	741.703	2.873	0.06740	4.565	17.04	60.00	17
3826	16.901	0.26992	740.825	59.786	0.09443	2.762	2.64	60.00	9841
3827	16.900	0.29117	740.947	59.763	0.09399	2.989	2.64	60.00	10627
3828	16.899	0.31281	741.061	59.741	0.09400	3.206	2.64	60.00	11376
3829	16.898	0.33586	741.177	59.719	0.09418	3.431	2.64	60.00	12151
3830	16.898	0.35954	741.299	59.696	0.09404	3.673	2.64	60.00	12979
3831	14.420	0.26943	740.985	49.297	0.08629	3.034	7.44	60.00	6438
3832	14.419	0.29073	741.115	49.279	0.08619	3.275	5.04	60.00	6934
3833	14.418	0.31238	741.233	49.261	0.08618	3.516	5.04	60.00	7431
3834	14.417	0.33526	741.290	49.250	0.08935	3.640	2.64	60.00	7683
3835	14.416	0.35895	741.410	49.232	0.08957	3.884	2.64	60.00	8182
3836	0.204	0.08857	503.144	0.886	0.03685	2.362	24.24	60.00	3
3837	0.204	0.10269	503.333	0.886	0.03680	2.741	24.24	60.00	4
3838	0.204	0.11786	503.529	0.884	0.03685	3.143	24.24	60.00	4
3839	0.204	0.13406	503.739	0.883	0.03685	3.574	24.24	60.00	5
3840	0.203	0.15150	503.966	0.882	0.03688	4.036	24.24	60.00	5
3842	2.203	0.08855	502.801	10.589	0.04729	1.839	21.84	60.00	684
3844	2.203	0.10272	503.030	10.585	0.04354	2.314	24.24	60.00	857
3846	2.205	0.11786	503.221	10.586	0.04313	2.680	24.24	60.00	989
3848	2.206	0.13403	503.420	10.584	0.04315	3.045	21.84	60.00	1120
3850	2.237	0.15147	503.623	10.749	0.04337	3.423	21.84	60.00	1313

Table A7. Thermal conductivity data for mixtures of water with nitrogen from transient measurements at temperatures from 500 K to 740 K.

Run Point	$\frac{p_e}{\text{MPa}}$	$\frac{q}{\text{W} \cdot \text{m}^{-1}}$	$\frac{T_e}{\text{K}}$	$\frac{\rho_e}{\text{kg} \cdot \text{m}^{-3}}$	$\frac{\lambda_e}{\text{W} \cdot \text{m}^{-1} \cdot \text{K}^{-1}}$	STAT	$\frac{T_i}{\text{K}}$
500 K, 0.6172 Mole Fraction Water							
No Transient Data							
500 K, 0.2497 Mole Fraction Water							
2021	9.331	0.11722	503.660	56.770	0.04859	0.006	501.773
2023	9.337	0.13334	503.930	56.770	0.04850	0.006	501.773
2025	9.343	0.15067	504.223	56.770	0.04895	0.006	501.774
2027	9.348	0.16886	504.528	56.760	0.04899	0.006	501.776
2029	9.352	0.18832	504.842	56.750	0.04907	0.006	501.780
2031	9.389	0.11724	503.614	57.120	0.04921	0.006	501.778
2033	9.393	0.13336	503.877	57.120	0.04936	0.006	501.777
2035	9.397	0.15070	504.164	57.110	0.04923	0.006	501.779
2037	9.402	0.16889	504.463	57.090	0.04942	0.006	501.781
2039	9.406	0.18832	504.773	57.080	0.05009	0.006	501.778
2041	9.434	0.11733	503.683	57.390	0.04931	0.006	501.778
2043	9.434	0.13347	503.947	57.350	0.04936	0.006	501.786
2045	9.433	0.15081	504.219	57.320	0.04928	0.006	501.784
2047	9.433	0.16900	504.504	57.280	0.04931	0.006	501.783
2049	9.432	0.18846	504.807	57.240	0.04925	0.006	501.777
2051	7.940	0.11733	503.762	48.340	0.04926	0.007	501.763
2053	7.939	0.13347	504.028	48.300	0.04912	0.007	501.764
2055	7.938	0.15082	504.312	48.270	0.04906	0.007	501.754
2057	7.943	0.16903	504.613	48.270	0.04900	0.007	501.753
2059	7.943	0.18849	504.949	48.230	0.04907	0.007	501.757
560 K, 0.6200 Mole Fraction Water							
3021	10.305	0.19530	563.065	53.700	0.06427	0.006	560.743
3023	10.305	0.21549	563.315	53.660	0.06405	0.006	560.751
3025	10.304	0.23667	563.570	53.620	0.06422	0.006	560.747
3027	10.304	0.25840	563.831	53.570	0.06430	0.006	560.744
3029	10.304	0.28156	564.119	53.530	0.06408	0.006	560.753
3031	10.278	0.19536	563.135	53.530	0.06402	0.007	560.772
3033	10.277	0.21553	563.386	53.490	0.06391	0.007	560.783
3035	10.276	0.23672	563.633	53.440	0.06404	0.006	560.778
3037	10.275	0.25845	563.889	53.400	0.06429	0.006	560.774
3039	10.275	0.28160	564.155	53.350	0.06380	0.007	560.772
3041	7.957	0.19544	563.433	40.290	0.06181	0.008	560.749
3043	7.962	0.21565	563.709	40.290	0.06212	0.008	560.748
3045	7.962	0.23685	563.998	40.260	0.06173	0.008	560.751
3047	7.961	0.25859	564.287	40.220	0.06191	0.008	560.743

Run Point	$\frac{p_e}{\text{MPa}}$	$\frac{q}{\text{W} \cdot \text{m}^{-1}}$	$\frac{T_e}{\text{K}}$	$\frac{\rho_e}{\text{kg} \cdot \text{m}^{-3}}$	$\frac{\lambda_e}{\text{W} \cdot \text{m}^{-1} \cdot \text{K}^{-1}}$	STAT	$\frac{T_i}{\text{K}}$
3049	7.960	0.28175	564.612	40.180	0.06211	0.008	560.751
560 K, 0.2811 Mole Fraction Water							
No Transient Data							
620 K, 0.6263 Mole Fraction Water							
5001	23.686	0.27186	621.947	116.170	0.08519	0.005	619.766
5003	23.684	0.29424	622.109	116.090	0.08561	0.005	619.765
5005	23.685	0.31749	622.290	116.030	0.08555	0.005	619.763
5007	23.684	0.34112	622.494	115.950	0.08523	0.005	619.757
5009	23.684	0.36613	622.686	115.880	0.08517	0.006	619.752
5011	20.946	0.27196	622.171	100.850	0.08044	0.006	619.745
5013	20.949	0.29434	622.370	100.810	0.08025	0.006	619.747
5015	20.950	0.31759	622.595	100.750	0.08004	0.006	619.750
5017	20.947	0.34124	622.790	100.670	0.08039	0.005	619.743
5019	20.948	0.36626	623.019	100.610	0.08083	0.005	619.747
5021	18.102	0.27211	622.397	85.490	0.07599	0.006	619.748
5023	18.102	0.29451	622.604	85.440	0.07632	0.006	619.742
5025	18.104	0.31779	622.835	85.400	0.07625	0.006	619.747
5027	18.100	0.34148	623.053	85.330	0.07614	0.006	619.742
5029	18.106	0.36647	623.311	85.300	0.07629	0.006	619.742
5031	15.017	0.27224	622.640	69.450	0.07263	0.007	619.732
5033	15.014	0.29465	622.888	69.390	0.07250	0.007	619.739
5035	15.021	0.31793	623.150	69.380	0.07283	0.007	619.739
5037	15.022	0.34163	623.395	69.340	0.07250	0.007	619.738
5039	15.022	0.36666	623.660	69.290	0.07269	0.007	619.740
620 K, 0.2881 Mole Fraction Water							
6001	34.442	0.27220	622.449	155.820	0.07086	0.005	619.741
6003	34.441	0.29459	622.670	155.760	0.07068	0.005	619.741
6005	34.441	0.31788	622.898	155.690	0.07094	0.005	619.739
6007	34.440	0.34155	623.123	155.630	0.07096	0.005	619.729
6009	34.441	0.36658	623.376	155.560	0.07073	0.005	619.730
6011	34.308	0.27223	622.432	155.280	0.07027	0.005	619.780
6013	34.308	0.29464	622.636	155.220	0.07078	0.005	619.777
6015	34.308	0.31789	622.854	155.160	0.07053	0.005	619.772
6017	34.309	0.34161	623.097	155.100	0.07069	0.005	619.768
6019	34.308	0.36664	623.386	155.020	0.07047	0.005	619.774
6021	30.001	0.27225	622.565	137.390	0.06883	0.005	619.771
6023	30.003	0.29466	622.807	137.340	0.06887	0.005	619.772
6025	30.007	0.31796	623.057	137.300	0.06852	0.005	619.771
6027	30.002	0.34165	623.320	137.210	0.06856	0.006	619.772
6029	30.006	0.36669	623.567	137.170	0.06847	0.006	619.772
6031	26.016	0.25120	622.539	120.400	0.06709	0.006	619.774

Run Point	$\frac{p_e}{\text{MPa}}$	$\frac{q}{\text{W} \cdot \text{m}^{-1}}$	$\frac{T_e}{\text{K}}$	$\frac{\rho_e}{\text{kg} \cdot \text{m}^{-3}}$	$\frac{\lambda_e}{\text{W} \cdot \text{m}^{-1} \cdot \text{K}^{-1}}$	STAT	$\frac{T_i}{\text{K}}$
6033	26.013	0.27229	622.752	120.340	0.06707	0.006	619.768
6035	26.016	0.29470	622.989	120.300	0.06718	0.006	619.759
6037	26.016	0.31798	623.242	120.250	0.06729	0.006	619.759
6039	26.019	0.34166	623.536	120.200	0.06747	0.006	619.759
6041	21.931	0.25122	622.707	102.480	0.06571	0.007	619.768
6043	21.936	0.27233	622.962	102.450	0.06576	0.006	619.776
6045	21.933	0.29473	623.200	102.400	0.06575	0.006	619.766
6047	21.942	0.31802	623.446	102.390	0.06580	0.006	619.759
6049	21.941	0.34170	623.722	102.340	0.06614	0.006	619.755
6051	18.034	0.25124	622.817	84.990	0.06537	0.007	619.759
6053	18.040	0.27236	623.088	84.980	0.06483	0.007	619.753
6055	18.038	0.29477	623.345	84.930	0.06519	0.007	619.755
6057	18.034	0.31806	623.623	84.870	0.06511	0.007	619.752
6059	18.035	0.34178	623.901	84.830	0.06521	0.007	619.754
6061	13.703	0.21124	622.408	65.190	0.06492	0.008	619.748
6063	13.706	0.23063	622.661	65.180	0.06475	0.008	619.754
6065	13.702	0.25129	622.906	65.130	0.06475	0.009	619.747
6067	13.707	0.27240	623.172	65.130	0.06506	0.008	619.747
6069	13.711	0.29481	623.477	65.110	0.06468	0.009	619.737
680 K, 0.6489 Mole Fraction Water							
7001	33.681	0.35317	681.369	146.180	0.09806	0.005	678.984
7003	33.682	0.37680	681.530	146.120	0.09794	0.005	678.978
7005	33.682	0.40168	681.727	146.030	0.09815	0.005	678.968
7007	33.680	0.42688	681.870	145.970	0.09831	0.005	678.980
7009	33.677	0.45334	682.048	145.880	0.09807	0.005	678.979
7011	30.066	0.35323	681.717	128.880	0.09263	0.005	678.980
7013	30.073	0.37689	681.895	128.850	0.09246	0.005	678.980
7015	30.083	0.40176	682.088	128.830	0.09289	0.005	678.972
7017	30.084	0.42695	682.264	128.770	0.09279	0.005	678.965
7019	30.078	0.45341	682.453	128.680	0.09253	0.005	678.962
7021	26.111	0.35331	681.949	110.330	0.08826	0.006	678.974
7023	26.110	0.37695	682.133	110.270	0.08777	0.006	678.978
7025	26.107	0.40186	682.339	110.200	0.08794	0.005	678.980
7027	26.104	0.42705	682.542	110.130	0.08799	0.006	678.979
7029	26.114	0.45352	682.756	110.120	0.08811	0.006	678.974
7031	21.871	0.35340	682.148	90.910	0.08405	0.006	678.968
7033	21.866	0.37707	682.380	90.840	0.08373	0.006	678.979
7035	21.869	0.40199	682.596	90.800	0.08371	0.006	678.981
7037	21.869	0.42720	682.822	90.750	0.08403	0.006	678.980
7039	21.878	0.45367	683.076	90.740	0.08373	0.007	678.972
7041	17.905	0.35349	682.331	73.230	0.08070	0.007	678.962

Run Point	$\frac{p_e}{\text{MPa}}$	$\frac{q}{\text{W} \cdot \text{m}^{-1}}$	$\frac{T_e}{\text{K}}$	$\frac{\rho_e}{\text{kg} \cdot \text{m}^{-3}}$	$\frac{\lambda_e}{\text{W} \cdot \text{m}^{-1} \cdot \text{K}^{-1}}$	STAT	$\frac{T_i}{\text{K}}$
7043	17.905	0.37717	682.578	73.190	0.08079	0.007	678.971
7045	17.906	0.40207	682.836	73.160	0.08111	0.007	678.968
7047	17.906	0.42727	683.091	73.110	0.08118	0.007	678.971
7049	17.905	0.45379	683.357	73.070	0.08105	0.007	678.977
680 K, 0.2809 Mole Fraction Water							
8001	38.593	0.28601	681.576	156.390	0.07664	0.005	678.931
8003	38.593	0.30732	681.828	156.330	0.07613	0.005	678.939
8005	38.590	0.32985	682.025	156.270	0.07634	0.005	678.936
8007	38.588	0.35317	682.237	156.220	0.07658	0.005	678.938
8009	38.586	0.37682	682.457	156.150	0.07664	0.005	678.942
8011	34.097	0.28603	681.780	139.950	0.07482	0.005	678.938
8013	34.096	0.30735	681.983	139.900	0.07473	0.006	678.941
8015	34.089	0.32986	682.211	139.830	0.07471	0.005	678.947
8017	34.082	0.35319	682.437	139.750	0.07514	0.005	678.948
8019	34.082	0.37684	682.672	139.700	0.07466	0.006	678.947
8021	30.200	0.26511	681.633	125.360	0.07354	0.006	678.938
8023	30.195	0.28607	681.854	125.300	0.07353	0.006	678.940
8025	30.198	0.30739	682.077	125.260	0.07353	0.006	678.951
8027	30.204	0.32992	682.314	125.240	0.07382	0.006	678.950
8029	30.201	0.35323	682.531	125.180	0.07372	0.006	678.940
8031	26.005	0.26513	681.754	109.160	0.07262	0.006	678.931
8033	26.009	0.28607	682.010	109.130	0.07245	0.006	678.942
8035	26.005	0.30739	682.214	109.080	0.07237	0.006	678.936
8037	26.001	0.32993	682.467	109.030	0.07245	0.006	678.950
8039	26.004	0.35325	682.707	109.000	0.07242	0.006	678.953
8041	22.059	0.24500	681.625	93.570	0.07202	0.007	678.938
8043	22.053	0.26517	681.859	93.510	0.07181	0.007	678.947
8045	22.051	0.28610	682.096	93.470	0.07212	0.007	678.952
8047	22.054	0.30743	682.308	93.450	0.07198	0.007	678.940
8049	22.061	0.32996	682.544	93.450	0.07171	0.007	678.941
8051	17.974	0.24502	681.766	77.000	0.07126	0.008	678.940
8053	17.977	0.26518	681.995	76.990	0.07131	0.007	678.943
8055	17.980	0.28613	682.251	76.970	0.07137	0.007	678.948
8057	17.981	0.30744	682.500	76.940	0.07114	0.008	678.956
8059	17.976	0.32999	682.755	76.890	0.07136	0.008	678.965
740 K, 0.6356 Mole Fraction Water							
9001	21.785	0.28411	741.754	80.010	0.08889	0.006	739.221
9003	21.694	0.30533	741.975	79.630	0.08907	0.006	739.224
9005	21.604	0.32768	742.198	79.250	0.08903	0.006	739.227
9007	21.515	0.35077	742.430	78.880	0.08926	0.006	739.234
9009	21.427	0.37426	742.657	78.510	0.08894	0.006	739.241

Run Point	$\frac{p_e}{\text{MPa}}$	$\frac{q}{\text{W} \cdot \text{m}^{-1}}$	$\frac{T_e}{\text{K}}$	$\frac{\rho_e}{\text{kg} \cdot \text{m}^{-3}}$	$\frac{\lambda_e}{\text{W} \cdot \text{m}^{-1} \cdot \text{K}^{-1}}$	STAT	$\frac{T_i}{\text{K}}$
740 K, 0.2754 Mole Fraction Water							
10021	29.844	0.26380	741.895	113.600	0.07761	0.006	739.281
10023	29.533	0.28465	742.131	112.470	0.07757	0.006	739.291
10025	29.227	0.30587	742.376	111.370	0.07751	0.006	739.303
10027	28.930	0.32821	742.608	110.290	0.07774	0.006	739.296
10029	28.641	0.35148	742.857	109.240	0.07774	0.006	739.296
10031	28.118	0.24378	741.758	107.560	0.07735	0.006	739.297
10033	27.848	0.26385	741.970	106.570	0.07761	0.006	739.300
10035	27.584	0.28470	742.194	105.610	0.07738	0.006	739.302
10037	27.326	0.30589	742.425	104.660	0.07775	0.006	739.302
10039	27.074	0.32832	742.672	103.730	0.07769	0.006	739.303
10041	24.195	0.24373	741.917	93.520	0.07688	0.006	739.294
10043	24.007	0.26387	742.116	92.810	0.07677	0.006	739.284
10045	23.821	0.28470	742.343	92.110	0.07659	0.006	739.282
10047	23.639	0.30573	742.560	91.420	0.07672	0.006	739.272
10049	23.460	0.32836	742.805	90.750	0.07648	0.007	739.276
10051	23.163	0.24382	741.934	89.780	0.07659	0.007	739.272
10053	22.993	0.26387	742.143	89.130	0.07650	0.007	739.265
10055	22.826	0.28466	742.367	88.500	0.07637	0.007	739.261
10057	22.662	0.30567	742.608	87.870	0.07627	0.006	739.268
10059	22.499	0.32834	742.847	87.250	0.07677	0.006	739.265
10061	18.273	0.24352	742.292	71.690	0.07535	0.007	739.307
10063	18.172	0.26345	742.512	71.290	0.07515	0.007	739.307
10065	18.073	0.28445	742.753	70.900	0.07545	0.007	739.306
10067	17.974	0.30577	742.981	70.500	0.07566	0.007	739.302
10069	17.876	0.32777	743.244	70.110	0.07574	0.007	739.306
10071	15.610	0.24404	741.958	61.680	0.07546	0.007	739.294
10073	15.535	0.26410	742.171	61.380	0.07567	0.007	739.284
10075	15.462	0.28496	742.434	61.080	0.07559	0.007	739.295
10077	15.389	0.30620	742.699	60.780	0.07537	0.007	739.302
10079	15.315	0.32864	742.982	60.480	0.07575	0.007	739.311

Table A8. Thermal conductivity data for mixtures of water with nitrogen from steady-state measurements at temperatures from 500 K to 740 K.

Run Point	$\frac{p_e}{\text{MPa}}$	$\frac{q}{\text{W} \cdot \text{m}^{-1}}$	$\frac{T_e}{\text{K}}$	$\frac{\rho_e}{\text{kg} \cdot \text{m}^{-3}}$	$\frac{\lambda_e}{\text{W} \cdot \text{m}^{-1} \cdot \text{K}^{-1}}$	$\frac{\Delta T_a}{\text{K}}$	$\frac{t_s}{\text{s}}$	$\frac{t_e}{\text{s}}$	Ra
500 K, 0.6172 Mole Fraction Water									
1042	3.670	0.11733	502.975	20.470	0.04810	2.392	26.64	60.00	1384
1044	3.670	0.13347	503.133	20.461	0.04811	2.720	24.24	60.00	1569
1046	3.670	0.15082	503.298	20.450	0.04823	3.065	26.64	60.00	1762
1048	3.670	0.16903	503.480	20.438	0.04830	3.428	24.24	60.00	1964
1050	3.670	0.18850	503.674	20.427	0.04824	3.826	24.24	60.00	2185
1052	3.579	0.11737	503.005	19.926	0.04797	2.400	24.24	60.00	1298
1054	3.580	0.13351	503.170	19.920	0.04791	2.732	26.64	60.00	1475
1056	3.581	0.15087	503.352	19.914	0.04784	3.091	24.24	60.00	1664
1058	3.579	0.16909	503.540	19.895	0.04790	3.459	24.24	60.00	1854
1060	3.578	0.18856	503.726	19.879	0.04804	3.845	24.24	60.00	2052
1062	3.106	0.11738	503.063	17.130	0.04585	2.512	24.24	60.00	940
1064	3.108	0.13354	503.230	17.133	0.04599	2.849	26.64	60.00	1065
1066	3.108	0.15089	503.407	17.128	0.04605	3.214	24.24	60.00	1198
1068	3.109	0.16909	503.589	17.123	0.04616	3.592	24.24	60.00	1336
1070	3.109	0.18858	503.793	17.115	0.04624	3.998	24.24	60.00	1482
1072	2.499	0.11742	503.088	13.629	0.04470	2.579	26.64	60.00	562
1074	2.499	0.13357	503.246	13.625	0.04535	2.892	24.24	60.00	629
1076	2.499	0.15094	503.433	13.614	0.04542	3.262	24.24	60.00	707
1078	2.498	0.16916	503.620	13.607	0.04546	3.653	24.24	60.00	789
1080	2.498	0.18864	503.827	13.597	0.04555	4.064	24.24	60.00	875
1082	2.053	0.11744	503.084	11.103	0.04462	2.585	24.24	60.00	352
1084	2.053	0.13358	503.264	11.099	0.04465	2.938	24.24	60.00	399
1086	2.053	0.15096	503.446	11.095	0.04468	3.318	24.24	60.00	449
1088	2.053	0.16916	503.647	11.089	0.04477	3.710	24.24	60.00	501
1090	2.053	0.18866	503.859	11.083	0.04477	4.138	24.24	60.00	557
1092	1.497	0.11744	503.122	8.017	0.04331	2.664	24.24	60.00	175
1094	1.497	0.13358	503.306	8.015	0.04335	3.027	24.24	60.00	199
1096	1.497	0.15095	503.493	8.010	0.04350	3.409	24.24	60.00	223
1098	1.497	0.16918	503.693	8.005	0.04358	3.813	24.24	60.00	249
1100	1.496	0.18866	503.906	7.998	0.04363	4.247	24.24	60.00	276
1102	1.015	0.11744	503.133	5.391	0.04259	2.709	24.24	60.00	75
1104	1.015	0.13359	503.310	5.389	0.04267	3.076	24.24	60.00	86
1106	1.015	0.15096	503.509	5.386	0.04278	3.467	24.24	60.00	96
1108	1.015	0.16918	503.714	5.384	0.04282	3.882	24.24	60.00	107
1110	1.015	0.18867	503.942	5.381	0.04286	4.324	24.24	60.00	119
1112	0.540	0.11744	503.154	2.843	0.04175	2.764	24.24	60.00	20
1114	0.540	0.13360	503.338	2.843	0.04188	3.134	24.24	60.00	23
1116	0.540	0.15097	503.547	2.841	0.04191	3.539	24.24	60.00	26
1118	0.540	0.16919	503.749	2.839	0.04197	3.961	24.24	60.00	29
1120	0.540	0.18866	503.985	2.838	0.04197	4.416	24.24	60.00	32
1122	0.254	0.11745	503.162	1.332	0.04162	2.773	24.24	60.00	4

Run Point	$\frac{p_e}{\text{MPa}}$	$\frac{q}{\text{W} \cdot \text{m}^{-1}}$	$\frac{T_e}{\text{K}}$	$\frac{\rho_e}{\text{kg} \cdot \text{m}^{-3}}$	$\frac{\lambda_e}{\text{W} \cdot \text{m}^{-1} \cdot \text{K}^{-1}}$	$\frac{\Delta T_a}{\text{K}}$	$\frac{t_s}{\text{s}}$	$\frac{t_e}{\text{s}}$	Ra
1124	0.254	0.13360	503.353	1.332	0.04160	3.155	24.24	60.00	5
1126	0.254	0.15097	503.554	1.332	0.04161	3.565	24.24	60.00	5
1128	0.254	0.16920	503.770	1.331	0.04163	3.993	24.24	60.00	6
1130	0.254	0.18868	504.003	1.331	0.04166	4.450	26.64	60.00	7
1132	0.095	0.11744	503.197	0.496	0.04076	2.831	26.64	60.00	1
1134	0.095	0.13361	503.390	0.496	0.04084	3.214	24.24	60.00	1
1136	0.095	0.15097	503.595	0.496	0.04089	3.628	24.24	60.00	1
1138	0.095	0.16921	503.809	0.496	0.04095	4.059	26.64	60.00	1
1140	0.095	0.18870	504.045	0.496	0.04099	4.523	26.64	60.00	1
500 K, 0.2497 Mole Fraction Water									
2062	6.886	0.11737	502.975	42.017	0.04735	2.424	26.64	60.00	2394
2064	6.886	0.13351	503.133	41.999	0.04753	2.745	24.24	60.00	2707
2066	6.887	0.15088	503.302	41.990	0.04765	3.093	24.24	60.00	3045
2068	6.887	0.16908	503.480	41.976	0.04782	3.451	24.24	60.00	3392
2070	6.887	0.18855	503.667	41.957	0.04789	3.840	21.84	60.00	3767
2072	5.942	0.11738	502.991	36.262	0.04628	2.482	24.24	60.00	1817
2074	5.942	0.13352	503.162	36.249	0.04643	2.813	24.24	60.00	2056
2076	5.941	0.15088	503.342	36.233	0.04646	3.175	24.24	60.00	2317
2078	5.941	0.16909	503.527	36.217	0.04652	3.552	26.64	60.00	2586
2080	5.941	0.18857	503.715	36.201	0.04674	3.941	24.24	60.00	2864
2082	4.999	0.11739	503.019	30.515	0.04516	2.546	26.64	60.00	1312
2084	4.999	0.13354	503.191	30.502	0.04529	2.887	24.24	60.00	1485
2086	4.998	0.15089	503.372	30.488	0.04544	3.251	24.24	60.00	1669
2088	4.998	0.16911	503.555	30.476	0.04557	3.631	24.24	60.00	1861
2090	4.999	0.18858	503.759	30.465	0.04571	4.036	24.24	60.00	2064
2092	3.934	0.11740	503.016	24.019	0.04510	2.552	24.24	60.00	808
2094	3.935	0.13355	503.208	24.012	0.04489	2.916	26.64	60.00	922
2096	3.935	0.15092	503.397	24.002	0.04495	3.290	24.24	60.00	1039
2098	3.934	0.16913	503.604	23.990	0.04499	3.683	24.24	60.00	1160
2100	3.934	0.18862	503.809	23.979	0.04508	4.099	24.24	60.00	1288
2102	2.942	0.11742	503.065	17.957	0.04393	2.622	26.64	60.00	460
2104	2.941	0.13356	503.234	17.949	0.04402	2.975	24.24	60.00	521
2106	2.941	0.15092	503.429	17.941	0.04409	3.357	24.24	60.00	587
2108	2.941	0.16914	503.627	17.933	0.04421	3.752	24.24	60.00	654
2110	2.941	0.18861	503.840	17.923	0.04422	4.182	24.24	60.00	728
2112	1.999	0.11741	503.085	12.202	0.04312	2.672	24.24	60.00	214
2114	1.999	0.13357	503.254	12.197	0.04358	3.008	24.24	60.00	241
2116	1.999	0.15094	503.443	12.191	0.04366	3.392	24.24	60.00	271
2118	2.001	0.16915	503.654	12.197	0.04356	3.810	24.24	60.00	304
2120	2.003	0.18864	503.884	12.204	0.04347	4.257	26.64	60.00	340
2122	0.980	0.11742	503.115	5.979	0.04271	2.699	26.64	60.00	51
2124	0.980	0.13358	503.293	5.978	0.04281	3.063	26.64	60.00	58
2126	0.980	0.15094	503.485	5.974	0.04300	3.445	24.24	60.00	65
2128	0.980	0.16916	503.685	5.972	0.04307	3.856	24.24	60.00	73
2130	0.980	0.18864	503.896	5.969	0.04308	4.298	24.24	60.00	81

Run Point	$\frac{P_e}{\text{MPa}}$	$\frac{q}{\text{W} \cdot \text{m}^{-1}}$	$\frac{T_e}{\text{K}}$	$\frac{\rho_e}{\text{kg} \cdot \text{m}^{-3}}$	$\frac{\lambda_e}{\text{W} \cdot \text{m}^{-1} \cdot \text{K}^{-1}}$	$\frac{\Delta T_a}{\text{K}}$	$\frac{t_s}{\text{s}}$	$\frac{t_e}{\text{s}}$	Ra
2132	0.238	0.11743	503.157	1.452	0.04167	2.766	26.64	60.00	3
2134	0.238	0.13359	503.345	1.453	0.04175	3.140	24.24	60.00	3
2136	0.238	0.15095	503.542	1.453	0.04184	3.541	26.64	60.00	4
2138	0.238	0.16917	503.749	1.452	0.04194	3.959	26.64	60.00	4
2140	0.238	0.18865	503.971	1.452	0.04195	4.414	24.24	60.00	5
560 K, 0.6200 Mole Fraction Water									
3042	7.958	0.19546	562.364	40.407	0.05881	3.235	21.84	60.00	5580
3044	7.962	0.21567	562.533	40.411	0.05885	3.563	19.44	60.00	6138
3046	7.961	0.23687	562.698	40.387	0.05899	3.901	21.84	60.00	6698
3048	7.961	0.25863	562.859	40.374	0.05931	4.232	19.44	60.00	7249
3050	7.960	0.28180	563.037	40.349	0.05945	4.595	19.44	60.00	7845
3052	5.714	0.15846	562.163	28.296	0.05479	2.833	24.24	60.00	2049
3054	5.715	0.17671	562.324	28.292	0.05494	3.149	21.84	60.00	2274
3056	5.716	0.19556	562.492	28.285	0.05497	3.481	24.24	60.00	2509
3058	5.715	0.21577	562.666	28.271	0.05503	3.835	24.24	60.00	2756
3060	5.716	0.23697	562.847	28.262	0.05520	4.198	21.84	60.00	3010
3062	3.899	0.15851	562.232	18.932	0.05230	2.974	21.84	60.00	846
3064	3.899	0.17675	562.404	18.926	0.05234	3.313	21.84	60.00	940
3066	3.900	0.19561	562.570	18.923	0.05249	3.656	21.84	60.00	1036
3068	3.900	0.21584	562.757	18.915	0.05254	4.029	24.24	60.00	1139
3070	3.901	0.23704	562.947	18.911	0.05267	4.414	21.84	60.00	1246
3072	2.494	0.15853	562.273	11.933	0.05103	3.052	21.84	60.00	312
3074	2.495	0.17678	562.447	11.930	0.05099	3.405	21.84	60.00	347
3076	2.495	0.19563	562.629	11.928	0.05105	3.764	24.24	60.00	383
3078	2.495	0.21587	562.813	11.925	0.05117	4.143	21.84	60.00	421
3080	2.496	0.23709	563.022	11.921	0.05113	4.553	21.84	60.00	462
3082	1.089	0.12520	562.011	5.139	0.04867	2.527	24.24	60.00	43
3084	1.089	0.14147	562.174	5.139	0.04867	2.856	21.84	60.00	49
3086	1.090	0.15854	562.336	5.139	0.04882	3.190	24.24	60.00	55
3088	1.090	0.17679	562.527	5.137	0.04884	3.557	21.84	60.00	61
3090	1.090	0.19565	562.712	5.137	0.04888	3.932	21.84	60.00	67
3092	0.208	0.12520	562.068	0.975	0.04672	2.633	24.24	60.00	2
3094	0.209	0.14148	562.242	0.978	0.04672	2.975	24.24	60.00	2
3096	0.209	0.15854	562.418	0.979	0.04685	3.325	24.24	60.00	2
3098	0.210	0.17679	562.599	0.980	0.04698	3.697	24.24	60.00	2
3100	0.210	0.19566	562.787	0.980	0.04711	4.080	21.84	60.00	2
560 K, 0.2811 Mole Fraction Water									
4076	13.429	0.21578	562.605	71.492	0.05876	3.558	26.64	60.00	7638
4078	13.430	0.23698	562.760	71.474	0.05906	3.883	26.64	60.00	8323
4080	13.432	0.25874	562.926	71.461	0.05949	4.204	31.44	60.00	9000
4082	13.427	0.17671	562.295	71.525	0.05825	2.946	24.24	60.00	6339
4084	13.428	0.19557	562.435	71.510	0.05861	3.237	26.64	60.00	6958
4086	13.433	0.21576	562.594	71.512	0.05872	3.560	26.64	60.00	7646
4088	13.429	0.23697	562.758	71.470	0.05908	3.882	26.64	60.00	8321
4090	13.425	0.25873	562.914	71.427	0.05958	4.198	26.64	60.00	8979

Run Point	$\frac{p_e}{\text{MPa}}$	$\frac{q}{\text{W} \cdot \text{m}^{-1}}$	$\frac{T_e}{\text{K}}$	$\frac{\rho_e}{\text{kg} \cdot \text{m}^{-3}}$	$\frac{\lambda_e}{\text{W} \cdot \text{m}^{-1} \cdot \text{K}^{-1}}$	$\frac{\Delta T_a}{\text{K}}$	$\frac{t_s}{\text{s}}$	$\frac{t_e}{\text{s}}$	Ra
4092	10.007	0.17675	562.363	53.538	0.05532	3.117	24.24	60.00	3766
4094	10.007	0.19560	562.520	53.523	0.05542	3.440	24.24	60.00	4151
4096	10.009	0.21581	562.699	53.512	0.05537	3.796	24.24	60.00	4574
4098	10.010	0.23703	562.884	53.502	0.05540	4.165	24.24	60.00	5011
4100	10.008	0.25880	563.086	53.470	0.05547	4.537	21.84	60.00	5448
4102	7.475	0.15851	562.277	40.107	0.05326	2.913	21.84	60.00	1968
4104	7.477	0.17677	562.436	40.104	0.05342	3.237	24.24	60.00	2185
4106	7.481	0.19562	562.608	40.113	0.05328	3.590	24.24	60.00	2422
4108	7.481	0.21584	562.790	40.100	0.05349	3.944	24.24	60.00	2657
4110	7.477	0.23707	562.992	40.062	0.05346	4.332	24.24	60.00	2909
4112	5.011	0.15854	562.328	26.938	0.05172	3.006	21.84	60.00	907
4114	5.011	0.17681	562.500	26.932	0.05163	3.357	21.84	60.00	1012
4116	5.013	0.19565	562.672	26.934	0.05159	3.717	24.24	60.00	1119
4118	5.015	0.21588	562.862	26.932	0.05153	4.105	24.24	60.00	1235
4120	5.014	0.23710	563.062	26.919	0.05174	4.489	24.24	60.00	1348
4122	2.562	0.14149	562.219	13.800	0.05028	2.762	24.24	60.00	215
4124	2.564	0.15855	562.377	13.802	0.05030	3.094	24.24	60.00	241
4126	2.565	0.17681	562.566	13.807	0.04986	3.480	24.24	60.00	271
4128	2.565	0.19567	562.750	13.798	0.05026	3.821	24.24	60.00	297
4130	2.565	0.21589	562.942	13.795	0.05030	4.212	24.24	60.00	327
4132	1.053	0.14149	562.255	5.675	0.04878	2.848	24.24	60.00	37
4134	1.054	0.15856	562.434	5.677	0.04863	3.201	24.24	60.00	42
4136	1.054	0.17682	562.615	5.676	0.04859	3.572	21.84	60.00	46
4138	1.054	0.19568	562.804	5.673	0.04879	3.938	21.84	60.00	51
4140	1.053	0.21590	563.006	5.669	0.04880	4.343	24.24	60.00	56
4142	0.193	0.14149	562.315	1.043	0.04701	2.954	21.84	60.00	1
4144	0.194	0.15856	562.485	1.043	0.04721	3.296	24.24	60.00	1
4146	0.194	0.17681	562.670	1.043	0.04725	3.673	24.24	60.00	2
4148	0.194	0.19567	562.860	1.043	0.04747	4.047	24.24	60.00	2
4150	0.194	0.21590	563.065	1.042	0.04742	4.469	24.24	60.00	2
620 K, 0.6263 Mole Fraction Water									
5042	11.987	0.23062	621.286	54.509	0.06985	3.207	21.84	60.00	6890
5044	11.989	0.25128	621.425	54.502	0.07013	3.476	19.44	60.00	7458
5046	11.992	0.27239	621.569	54.500	0.06964	3.790	19.44	60.00	8120
5048	11.993	0.29481	621.736	54.481	0.06970	4.094	21.84	60.00	8751
5050	11.993	0.31811	621.880	54.465	0.07024	4.379	19.44	60.00	9344
5052	8.993	0.23068	621.426	40.080	0.06507	3.463	21.84	60.00	3597
5054	8.994	0.25130	621.586	40.072	0.06468	3.793	21.84	60.00	3933
5056	8.996	0.27244	621.726	40.068	0.06513	4.081	19.44	60.00	4227
5058	8.995	0.29486	621.885	40.051	0.06539	4.397	19.44	60.00	4544
5060	8.995	0.31817	622.060	40.035	0.06546	4.737	21.84	60.00	4884
5062	6.039	0.23071	621.533	26.397	0.06158	3.673	19.44	60.00	1474
5064	6.039	0.25137	621.706	26.390	0.06143	4.011	24.24	60.00	1607
5066	6.039	0.27248	621.870	26.379	0.06148	4.343	21.84	60.00	1736
5068	6.041	0.29492	622.051	26.378	0.06132	4.712	21.84	60.00	1882

Run Point	$\frac{P_e}{\text{MPa}}$	$\frac{q}{\text{W} \cdot \text{m}^{-1}}$	$\frac{T_e}{\text{K}}$	$\frac{\rho_e}{\text{kg} \cdot \text{m}^{-3}}$	$\frac{\lambda_e}{\text{W} \cdot \text{m}^{-1} \cdot \text{K}^{-1}}$	$\frac{\Delta T_a}{\text{K}}$	$\frac{t_s}{\text{s}}$	$\frac{t_e}{\text{s}}$	Ra
5070	6.041	0.31823	622.221	26.373	0.06159	5.060	21.84	60.00	2018
5072	2.961	0.19242	621.330	12.699	0.05786	3.267	24.24	60.00	268
5074	2.962	0.21133	621.499	12.697	0.05784	3.589	19.44	60.00	294
5076	2.962	0.23074	621.659	12.695	0.05810	3.901	19.44	60.00	319
5078	2.960	0.25140	621.824	12.684	0.05833	4.234	21.84	60.00	346
5080	2.961	0.27253	621.993	12.684	0.05835	4.588	21.84	60.00	374
5082	0.992	0.19243	621.371	4.202	0.05668	3.337	21.84	60.00	28
5084	0.992	0.21136	621.538	4.200	0.05678	3.658	24.24	60.00	30
5086	0.992	0.23076	621.695	4.201	0.05680	3.993	21.84	60.00	33
5088	0.993	0.25143	621.891	4.201	0.05636	4.384	19.44	60.00	36
5090	0.993	0.27255	622.075	4.200	0.05639	4.749	21.84	60.00	39
5092	0.168	0.17442	621.277	0.708	0.05456	3.141	24.24	60.00	1
5094	0.168	0.19244	621.442	0.709	0.05456	3.466	21.84	60.00	1
5096	0.168	0.21135	621.612	0.710	0.05421	3.831	21.84	60.00	1
5098	0.169	0.23076	621.791	0.710	0.05428	4.177	21.84	60.00	1
5100	0.169	0.25144	621.971	0.710	0.05448	4.535	21.84	60.00	1
620 K, 0.2881 Mole Fraction Water									
6052	18.040	0.25127	621.605	85.196	0.06555	3.709	26.64	60.00	8463
6054	18.040	0.27239	621.753	85.178	0.06570	4.007	26.64	60.00	9133
6056	18.036	0.29480	621.894	85.138	0.06635	4.289	26.64	60.00	9761
6058	18.032	0.31810	622.048	85.097	0.06667	4.600	31.44	60.00	10452
6060	18.037	0.34179	622.204	85.094	0.06687	4.922	33.84	60.00	11174
6062	13.706	0.21127	621.362	65.325	0.06384	3.226	21.84	60.00	4389
6064	13.704	0.23065	621.504	65.297	0.06401	3.510	21.84	60.00	4769
6066	13.703	0.25132	621.646	65.278	0.06428	3.806	21.84	60.00	5165
6068	13.711	0.27243	621.808	65.296	0.06389	4.147	21.84	60.00	5626
6070	13.710	0.29485	621.973	65.275	0.06400	4.477	19.44	60.00	6066
6072	10.291	0.21127	621.433	49.342	0.06103	3.385	24.24	60.00	2637
6074	10.297	0.23067	621.589	49.358	0.06084	3.705	21.84	60.00	2887
6076	10.299	0.25133	621.760	49.352	0.06086	4.033	21.84	60.00	3140
6078	10.298	0.27246	621.919	49.334	0.06112	4.352	21.84	60.00	3383
6080	10.295	0.29486	622.097	49.308	0.06113	4.707	21.84	60.00	3652
6082	6.097	0.17436	621.220	29.436	0.05756	2.971	19.44	60.00	820
6084	6.099	0.19237	621.385	29.439	0.05722	3.296	21.84	60.00	909
6086	6.099	0.21128	621.531	29.434	0.05771	3.589	19.44	60.00	989
6088	6.097	0.23069	621.662	29.415	0.05864	3.856	21.84	60.00	1061
6090	6.097	0.25136	621.832	29.408	0.05890	4.183	21.84	60.00	1150
6092	3.257	0.17437	621.267	15.786	0.05581	3.067	21.84	60.00	240
6094	3.258	0.19240	621.430	15.784	0.05593	3.377	21.84	60.00	265
6096	3.258	0.21130	621.597	15.783	0.05589	3.710	21.84	60.00	290
6098	3.259	0.23070	621.759	15.781	0.05610	4.036	21.84	60.00	316
6100	3.259	0.25138	621.936	15.779	0.05616	4.393	21.84	60.00	343
6102	1.107	0.17439	621.302	5.380	0.05495	3.116	19.44	60.00	28
6104	1.107	0.19241	621.461	5.380	0.05495	3.438	24.24	60.00	31
6106	1.108	0.21132	621.617	5.379	0.05504	3.770	21.84	60.00	34

Run Point	$\frac{P_e}{\text{MPa}}$	$\frac{q}{\text{W} \cdot \text{m}^{-1}}$	$\frac{T_e}{\text{K}}$	$\frac{\rho_e}{\text{kg} \cdot \text{m}^{-3}}$	$\frac{\lambda_e}{\text{W} \cdot \text{m}^{-1} \cdot \text{K}^{-1}}$	$\frac{\Delta T_a}{\text{K}}$	$\frac{t_s}{\text{s}}$	$\frac{t_e}{\text{s}}$	Ra
6108	1.108	0.23071	621.795	5.380	0.05472	4.140	21.84	60.00	37
6110	1.108	0.25139	621.960	5.379	0.05508	4.481	19.44	60.00	40
6112	0.183	0.17438	621.327	0.888	0.05366	3.190	21.84	60.00	1
6114	0.183	0.19241	621.496	0.888	0.05358	3.526	21.84	60.00	1
6116	0.183	0.21133	621.663	0.890	0.05366	3.866	21.84	60.00	1
6118	0.183	0.23071	621.837	0.890	0.05367	4.220	24.24	60.00	1
6120	0.183	0.25139	622.037	0.890	0.05338	4.623	21.84	60.00	1
680 K, 0.6489 Mole Fraction Water									
7052	14.076	0.30767	680.902	56.831	0.07752	3.858	19.44	60.00	6285
7054	14.078	0.33023	681.052	56.823	0.07732	4.148	17.04	60.00	6748
7056	14.077	0.35359	681.192	56.806	0.07733	4.438	19.44	60.00	7207
7058	14.074	0.37724	681.329	56.775	0.07773	4.707	17.04	60.00	7627
7060	14.078	0.40218	681.464	56.778	0.07793	5.001	17.04	60.00	8096
7062	9.977	0.28639	680.938	39.581	0.07136	3.925	17.04	60.00	2827
7064	9.975	0.30773	681.066	39.566	0.07164	4.200	17.04	60.00	3020
7066	9.970	0.33028	681.218	39.533	0.07178	4.497	17.04	60.00	3225
7068	9.967	0.35365	681.369	39.510	0.07191	4.805	17.04	60.00	3438
7070	9.966	0.37730	681.525	39.495	0.07186	5.128	17.04	60.00	3662
7072	6.855	0.24524	680.731	26.844	0.06811	3.532	19.44	60.00	1085
7074	6.855	0.26543	680.881	26.837	0.06806	3.825	19.44	60.00	1173
7076	6.858	0.28639	681.020	26.841	0.06834	4.110	17.04	60.00	1259
7078	6.859	0.30773	681.175	26.840	0.06859	4.399	17.04	60.00	1347
7080	6.860	0.33031	681.312	26.837	0.06884	4.704	17.04	60.00	1439
7082	4.104	0.20766	680.499	15.888	0.06628	3.078	19.44	60.00	308
7084	4.105	0.22627	680.627	15.888	0.06655	3.340	17.04	60.00	334
7086	4.105	0.24527	680.775	15.885	0.06654	3.621	17.04	60.00	362
7088	4.105	0.26545	680.923	15.881	0.06650	3.921	19.44	60.00	391
7090	4.103	0.28644	681.076	15.871	0.06650	4.231	17.04	60.00	421
7092	2.004	0.20763	680.517	7.689	0.06559	3.112	17.04	60.00	69
7094	2.003	0.22623	680.637	7.685	0.06614	3.362	19.44	60.00	74
7096	2.003	0.24524	680.784	7.683	0.06613	3.646	17.04	60.00	80
7098	2.003	0.26541	680.927	7.682	0.06624	3.939	19.44	60.00	87
7100	2.004	0.28640	681.098	7.682	0.06559	4.292	19.44	60.00	94
7102	1.010	0.20763	680.564	3.858	0.06398	3.190	21.84	60.00	17
7104	1.010	0.22623	680.706	3.859	0.06410	3.469	19.44	60.00	19
7106	1.011	0.24525	680.859	3.860	0.06370	3.784	19.44	60.00	20
7108	1.008	0.26542	681.009	3.848	0.06369	4.096	19.44	60.00	22
7110	1.008	0.28639	681.173	3.849	0.06381	4.412	19.44	60.00	24
7112	0.168	0.20763	680.621	0.639	0.06126	3.330	21.84	60.00	0
7114	0.168	0.22625	680.789	0.640	0.06094	3.648	19.44	60.00	1
7116	0.168	0.24524	680.920	0.640	0.06151	3.918	17.04	60.00	1
7118	0.168	0.26543	681.093	0.640	0.06133	4.253	19.44	60.00	1
7120	0.168	0.28641	681.254	0.640	0.06143	4.582	19.44	60.00	1
680 K, 0.2809 Mole Fraction Water									
8062	13.728	0.22609	680.564	59.506	0.06773	3.263	21.84	60.00	2878

Run Point	$\frac{p_e}{\text{MPa}}$	$\frac{q}{\text{W} \cdot \text{m}^{-1}}$	$\frac{T_e}{\text{K}}$	$\frac{\rho_e}{\text{kg} \cdot \text{m}^{-3}}$	$\frac{\lambda_e}{\text{W} \cdot \text{m}^{-1} \cdot \text{K}^{-1}}$	$\frac{\Delta T_a}{\text{K}}$	$\frac{t_s}{\text{s}}$	$\frac{t_e}{\text{s}}$	Ra
8064	13.729	0.24507	680.702	59.498	0.06765	3.539	19.44	60.00	3119
8066	13.728	0.26523	680.851	59.479	0.06780	3.820	17.04	60.00	3363
8068	13.723	0.28620	681.006	59.447	0.06803	4.107	19.44	60.00	3610
8070	13.727	0.30753	681.172	59.446	0.06791	4.418	19.44	60.00	3881
8072	10.066	0.22609	680.642	43.976	0.06597	3.357	17.04	60.00	1621
8074	10.066	0.24509	680.778	43.968	0.06610	3.631	17.04	60.00	1752
8076	10.067	0.26526	680.899	43.964	0.06652	3.905	17.04	60.00	1883
8078	10.065	0.28623	681.019	43.948	0.06687	4.190	17.04	60.00	2018
8080	10.065	0.30752	681.153	43.938	0.06709	4.486	19.44	60.00	2159
8082	6.072	0.20752	680.493	26.750	0.06407	3.178	17.04	60.00	565
8084	6.072	0.22610	680.647	26.743	0.06395	3.469	19.44	60.00	616
8086	6.072	0.24510	680.791	26.739	0.06421	3.745	19.44	60.00	664
8088	6.072	0.26527	680.943	26.734	0.06411	4.059	21.84	60.00	719
8090	6.072	0.28624	681.109	26.726	0.06420	4.374	17.04	60.00	774
8092	3.009	0.20753	680.577	13.331	0.06139	3.319	17.04	60.00	145
8094	3.009	0.22612	680.706	13.329	0.06165	3.601	17.04	60.00	157
8096	3.009	0.24512	680.859	13.327	0.06163	3.904	19.44	60.00	170
8098	3.009	0.26528	681.022	13.324	0.06181	4.213	17.04	60.00	183
8100	3.009	0.28626	681.187	13.320	0.06180	4.548	17.04	60.00	197
8102	1.062	0.19007	680.490	4.722	0.05919	3.152	19.44	60.00	17
8104	1.062	0.20753	680.638	4.719	0.05936	3.432	19.44	60.00	18
8106	1.062	0.22611	680.787	4.718	0.05935	3.740	19.44	60.00	20
8108	1.062	0.24512	680.939	4.718	0.05939	4.052	19.44	60.00	22
8110	1.062	0.26529	681.098	4.718	0.05961	4.369	17.04	60.00	23
8112	1.046	0.18990	680.342	4.653	0.06149	3.033	21.84	60.00	16
8114	1.047	0.20734	680.480	4.654	0.06120	3.327	19.44	60.00	17
8116	1.047	0.22591	680.637	4.653	0.06126	3.621	17.04	60.00	19
8118	1.046	0.24489	680.792	4.651	0.06141	3.916	17.04	60.00	20
8120	1.046	0.26503	680.971	4.650	0.06094	4.270	19.44	60.00	22
8122	0.155	0.18991	680.430	0.689	0.05852	3.186	19.44	60.00	0
8124	0.155	0.20734	680.575	0.688	0.05839	3.486	17.04	60.00	0
8126	0.155	0.22591	680.722	0.689	0.05847	3.793	19.44	60.00	0
8128	0.155	0.24489	680.881	0.689	0.05841	4.116	19.44	60.00	0
8130	0.155	0.26503	681.046	0.688	0.05844	4.452	21.84	60.00	1
740 K, 0.6356 Mole Fraction Water									
9002	21.744	0.28413	740.774	79.995	0.08838	3.120	17.04	60.00	7018
9004	21.654	0.30529	740.898	79.633	0.08799	3.364	14.64	60.00	7489
9006	21.564	0.32772	741.038	79.268	0.08759	3.625	14.64	60.00	7983
9008	21.476	0.35088	741.163	78.914	0.08766	3.875	12.24	60.00	8446
9010	21.387	0.37431	741.293	78.558	0.08792	4.118	9.84	60.00	8883
9012	17.551	0.28425	740.871	64.075	0.08437	3.284	17.04	60.00	4589
9014	17.490	0.30531	740.988	63.833	0.08440	3.525	19.44	60.00	4881
9016	17.432	0.32781	741.123	63.600	0.08413	3.794	17.04	60.00	5209
9018	17.374	0.35096	741.274	63.362	0.08377	4.077	17.04	60.00	5548
9020	17.318	0.37436	741.426	63.135	0.08331	4.370	12.24	60.00	5897

Run Point	$\frac{p_e}{\text{MPa}}$	$\frac{q}{\text{W} \cdot \text{m}^{-1}}$	$\frac{T_e}{\text{K}}$	$\frac{\rho_e}{\text{kg} \cdot \text{m}^{-3}}$	$\frac{\lambda_e}{\text{W} \cdot \text{m}^{-1} \cdot \text{K}^{-1}}$	$\frac{\Delta T_a}{\text{K}}$	$\frac{t_s}{\text{s}}$	$\frac{t_e}{\text{s}}$	Ra
9022	14.018	0.28422	740.975	50.815	0.08066	3.445	21.84	60.00	2927
9024	13.979	0.30539	741.105	50.661	0.08041	3.712	19.44	60.00	3131
9026	13.940	0.32784	741.264	50.501	0.07993	4.007	17.04	60.00	3354
9028	13.901	0.35103	741.411	50.346	0.07985	4.293	17.04	60.00	3567
9030	13.862	0.37437	741.546	50.190	0.07987	4.575	17.04	60.00	3774
9032	10.049	0.26349	740.897	36.134	0.07974	3.241	17.04	60.00	1332
9034	10.020	0.28437	741.027	36.019	0.07944	3.510	14.64	60.00	1432
9036	9.996	0.30557	741.167	35.926	0.07936	3.775	19.44	60.00	1530
9038	9.973	0.32797	741.327	35.832	0.07866	4.087	17.04	60.00	1646
9040	9.948	0.35115	741.475	35.733	0.07852	4.383	17.04	60.00	1754
9042	7.042	0.26361	740.955	25.156	0.07728	3.350	17.04	60.00	641
9044	7.027	0.28444	741.099	25.095	0.07689	3.632	19.44	60.00	691
9046	7.009	0.30562	741.243	25.026	0.07649	3.923	17.04	60.00	742
9048	6.993	0.32801	741.386	24.963	0.07650	4.209	19.44	60.00	791
9050	6.974	0.35121	741.535	24.887	0.07631	4.518	19.44	60.00	843
9052	4.113	0.24352	740.900	14.598	0.07354	3.254	19.44	60.00	201
9054	4.103	0.26362	741.032	14.559	0.07368	3.516	14.64	60.00	216
9056	4.093	0.28440	741.170	14.519	0.07355	3.799	17.04	60.00	232
9058	4.085	0.30562	741.320	14.489	0.07328	4.098	14.64	60.00	249
9060	4.075	0.32796	741.469	14.449	0.07334	4.393	17.04	60.00	265
9062	1.093	0.22468	740.876	3.851	0.06865	3.216	17.04	60.00	13
9064	1.093	0.24355	741.022	3.851	0.06837	3.500	14.64	60.00	14
9066	1.093	0.26359	741.156	3.853	0.06865	3.773	17.04	60.00	15
9068	1.092	0.28447	741.321	3.848	0.06848	4.082	14.64	60.00	17
9070	1.088	0.30567	741.457	3.833	0.06873	4.370	14.64	60.00	18
9072	0.122	0.22477	740.949	0.430	0.06582	3.355	24.24	60.00	0
9074	0.123	0.24364	741.083	0.431	0.06592	3.631	17.04	60.00	0
9076	0.123	0.26369	741.246	0.432	0.06578	3.938	19.44	60.00	0
9078	0.123	0.28453	741.407	0.432	0.06566	4.257	19.44	60.00	0
9080	0.123	0.30572	741.566	0.433	0.06560	4.578	17.04	60.00	0
740 K, 0.2754 Mole Fraction Water									
10082	11.331	0.24400	740.962	45.305	0.07173	3.334	19.44	60.00	1374
10084	11.286	0.26413	741.109	45.122	0.07135	3.628	17.04	60.00	1483
10086	11.241	0.28494	741.251	44.935	0.07149	3.905	19.44	60.00	1582
10088	11.193	0.30604	741.390	44.739	0.07153	4.191	14.64	60.00	1682
10090	11.150	0.32862	741.558	44.564	0.07129	4.515	17.04	60.00	1797
10092	8.179	0.22500	740.903	32.946	0.06830	3.232	21.84	60.00	702
10094	8.149	0.24381	741.036	32.823	0.06828	3.503	19.44	60.00	755
10096	8.120	0.26402	741.184	32.700	0.06820	3.797	19.44	60.00	811
10098	8.092	0.28477	741.343	32.584	0.06805	4.104	17.04	60.00	870
10100	8.064	0.30612	741.491	32.466	0.06851	4.381	17.04	60.00	922
10102	4.965	0.22510	740.963	20.142	0.06693	3.301	14.64	60.00	265
10104	4.953	0.24392	741.101	20.092	0.06681	3.584	17.04	60.00	286
10106	4.940	0.26413	741.253	20.034	0.06677	3.883	19.44	60.00	308
10108	4.926	0.28488	741.400	19.974	0.06668	4.193	19.44	60.00	331

Run Point	$\frac{p_e}{\text{MPa}}$	$\frac{q}{\text{W} \cdot \text{m}^{-1}}$	$\frac{T_e}{\text{K}}$	$\frac{\rho_e}{\text{kg} \cdot \text{m}^{-3}}$	$\frac{\lambda_e}{\text{W} \cdot \text{m}^{-1} \cdot \text{K}^{-1}}$	$\frac{\Delta T_a}{\text{K}}$	$\frac{t_s}{\text{s}}$	$\frac{t_e}{\text{s}}$	Ra
10110	4.911	0.30615	741.554	19.911	0.06650	4.518	19.44	60.00	354
10112	3.014	0.20660	740.825	12.280	0.06684	3.035	17.04	60.00	90
10114	3.006	0.22515	740.955	12.248	0.06671	3.314	14.64	60.00	97
10116	2.997	0.24407	741.096	12.207	0.06673	3.591	14.64	60.00	105
10118	2.990	0.26408	741.234	12.176	0.06662	3.892	17.04	60.00	113
10120	2.982	0.28506	741.382	12.143	0.06658	4.204	19.44	60.00	121
10132	0.171	0.20668	740.845	0.700	0.06593	3.078	17.04	60.00	0
10134	0.183	0.22509	740.979	0.750	0.06616	3.341	17.04	60.00	0
10136	0.186	0.24415	741.125	0.763	0.06614	3.625	19.44	60.00	0
10138	0.189	0.26425	741.266	0.774	0.06616	3.922	17.04	60.00	0
10140	0.190	0.28502	741.427	0.780	0.06635	4.218	17.04	60.00	0

Table A9. Thermal conductivity data for the mixtures of water with carbon dioxide from transient measurements at temperatures from 500 K to 740 K.

Run Point	$\frac{p_e}{\text{MPa}}$	$\frac{q}{\text{W} \cdot \text{m}^{-1}}$	T_e K	$\frac{\rho_e}{\text{kg} \cdot \text{m}^{-3}}$	$\frac{\lambda_e}{\text{W} \cdot \text{m}^{-1} \cdot \text{K}^{-1}}$	STAT	$\frac{T_i}{\text{K}}$
500 K, 0.6536 Mole Fraction Water							
11001	3.459	0.10967	504.456	24.350	0.04606	0.006	502.399
11003	3.457	0.12584	504.711	24.320	0.04604	0.005	502.372
11005	3.458	0.14317	504.974	24.310	0.04617	0.005	502.332
11007	3.456	0.16183	505.273	24.280	0.04638	0.005	502.307
11009	3.456	0.18137	505.611	24.250	0.04652	0.005	502.302
11011	3.456	0.10970	504.275	24.340	0.04701	0.006	502.290
11013	3.455	0.12587	504.554	24.310	0.04652	0.006	502.281
11015	3.455	0.14319	504.866	24.290	0.04661	0.005	502.275
11017	3.455	0.16181	505.192	24.270	0.04672	0.005	502.271
11019	3.451	0.18127	505.544	24.210	0.04674	0.005	502.262
500 K, 0.6380 Mole Fraction Water							
21001	4.193	0.10943	503.488	30.600	0.04747	0.004	501.584
21003	4.194	0.12566	503.750	30.580	0.04762	0.004	501.579
21005	4.202	0.14290	504.039	30.620	0.04738	0.004	501.575
21007	4.200	0.16149	504.357	30.570	0.04783	0.004	501.569
21009	4.199	0.18097	504.680	30.530	0.04785	0.004	501.569
21011	4.205	0.10950	503.402	30.700	0.04796	0.005	501.547
21013	4.204	0.12571	503.638	30.680	0.04798	0.004	501.542
21015	4.204	0.14299	503.902	30.650	0.04840	0.005	501.531
21017	4.204	0.16158	504.156	30.620	0.04821	0.004	501.510
21019	4.202	0.18108	504.426	30.580	0.04811	0.005	501.487
21021	4.200	0.10944	503.287	30.680	0.04783	0.005	501.422
21023	4.208	0.12565	503.615	30.710	0.04804	0.005	501.433
21025	4.200	0.14286	503.935	30.610	0.04798	0.005	501.453
21027	4.208	0.16140	504.296	30.650	0.04798	0.005	501.479
21029	4.209	0.18088	504.694	30.620	0.04895	0.004	501.507
21031	4.188	0.10955	503.361	30.570	0.04792	0.005	501.539
21033	4.186	0.12571	503.645	30.530	0.04800	0.005	501.552
21035	4.182	0.14301	503.914	30.470	0.04787	0.005	501.542
21037	4.187	0.16161	504.234	30.480	0.04791	0.005	501.537
21039	4.187	0.18111	504.578	30.450	0.04805	0.005	501.537
500 K, 0.2052 Mole Fraction Water							
2031	8.460	0.10943	503.984	85.140	0.04282	0.005	502.095
2033	8.439	0.12559	504.269	84.850	0.04294	0.004	502.109
2035	8.420	0.14286	504.548	84.570	0.04291	0.004	502.099
2037	8.409	0.16141	504.844	84.390	0.04301	0.004	502.082
2039	8.390	0.18091	505.201	84.090	0.04332	0.004	502.088

Run Point	$\frac{p_e}{\text{MPa}}$	$\frac{q}{\text{W} \cdot \text{m}^{-1}}$	T_e K	ρ_e $\text{kg} \cdot \text{m}^{-3}$	λ_e $\text{W} \cdot \text{m}^{-1} \cdot \text{K}^{-1}$	STAT	T_i K
2041	7.130	0.10952	503.952	70.790	0.04309	0.005	502.001
2043	7.120	0.12567	504.161	70.650	0.04240	0.005	501.969
2045	7.113	0.14301	504.432	70.530	0.04248	0.005	501.959
2047	7.097	0.16157	504.777	70.280	0.04244	0.004	501.954
2049	7.088	0.18105	505.130	70.130	0.04252	0.004	501.962
2051	7.075	0.10957	503.948	70.210	0.04239	0.005	501.967
2053	7.076	0.12575	504.234	70.170	0.04228	0.005	501.965
2055	7.077	0.14301	504.552	70.120	0.04242	0.005	501.959
2057	7.060	0.16166	504.874	69.880	0.04253	0.004	501.956
2059	7.059	0.18119	505.231	69.800	0.04247	0.005	501.958
2061	5.979	0.10954	504.028	58.660	0.04175	0.005	501.961
2063	5.963	0.12572	504.333	58.450	0.04174	0.005	501.964
2065	6.014	0.14302	504.666	58.930	0.04175	0.005	501.961
2067	5.987	0.16165	505.021	58.590	0.04164	0.004	501.960
2069	5.976	0.18115	505.388	58.430	0.04183	0.004	501.965
2073	5.125	0.12573	504.391	49.800	0.04131	0.005	501.951
2075	5.160	0.14297	504.738	50.110	0.04122	0.005	501.942
2077	5.212	0.16163	505.087	50.600	0.04157	0.004	501.950
2079	5.234	0.18112	505.474	50.780	0.04167	0.005	501.958
2081	3.765	0.10952	504.252	36.090	0.04061	0.006	501.970
2083	3.765	0.12570	504.605	36.060	0.04074	0.005	501.977
2085	3.766	0.14301	504.966	36.030	0.04065	0.005	501.974
2087	3.765	0.16156	505.352	35.990	0.04087	0.005	501.974
2089	3.755	0.18108	505.772	35.860	0.04077	0.005	501.985
500 K, 0.2363 Mole Fraction Water							
12021	10.819	0.10957	503.518	110.260	0.04519	0.004	501.765
12023	10.816	0.12578	503.772	110.130	0.04509	0.004	501.774
12025	10.819	0.14308	504.054	110.080	0.04530	0.004	501.773
12027	10.820	0.16161	504.347	109.990	0.04520	0.004	501.769
12029	10.819	0.18119	504.655	109.860	0.04526	0.004	501.770
12031	10.036	0.10955	503.574	101.390	0.04451	0.004	501.761
12033	9.999	0.12580	503.846	100.890	0.04437	0.004	501.771
12035	10.020	0.14308	504.118	101.040	0.04461	0.004	501.766
12037	10.026	0.16163	504.414	101.020	0.04463	0.004	501.765
12039	10.029	0.18122	504.726	100.950	0.04459	0.004	501.753
12041	9.009	0.10956	503.627	89.970	0.04367	0.004	501.755
12043	9.031	0.12581	503.865	90.150	0.04377	0.004	501.736
12045	9.036	0.14303	504.144	90.130	0.04371	0.004	501.720
12047	9.033	0.16164	504.457	90.010	0.04377	0.004	501.716
12049	9.040	0.18108	504.806	90.000	0.04372	0.004	501.726
12051	7.969	0.10958	503.681	78.660	0.04272	0.004	501.745

Run Point	$\frac{p_e}{\text{MPa}}$	$\frac{q}{\text{W} \cdot \text{m}^{-1}}$	$\frac{T_e}{\text{K}}$	$\frac{\rho_e}{\text{kg} \cdot \text{m}^{-3}}$	$\frac{\lambda_e}{\text{W} \cdot \text{m}^{-1} \cdot \text{K}^{-1}}$	STAT	$\frac{T_i}{\text{K}}$
12053	7.965	0.12574	503.969	78.550	0.04275	0.004	501.746
12055	7.949	0.14305	504.264	78.310	0.04301	0.004	501.744
12057	7.951	0.16166	504.548	78.270	0.04308	0.004	501.726
12059	7.951	0.18118	504.858	78.200	0.04318	0.004	501.712
12061	7.002	0.10957	503.651	68.380	0.04228	0.004	501.646
12063	6.993	0.12571	503.912	68.240	0.04229	0.004	501.633
12065	6.997	0.14306	504.205	68.220	0.04222	0.004	501.617
12067	7.001	0.16167	504.507	68.210	0.04242	0.004	501.609
12069	7.015	0.18105	504.882	68.290	0.04238	0.004	501.602
12071	5.938	0.10955	503.762	57.290	0.04162	0.004	501.664
12073	5.951	0.12578	504.073	57.380	0.04171	0.004	501.658
12075	5.989	0.14299	504.373	57.720	0.04165	0.004	501.635
12077	6.023	0.16164	504.678	58.020	0.04177	0.004	501.619
12079	6.053	0.18111	505.062	58.270	0.04172	0.004	501.623
12081	4.762	0.10953	503.912	45.320	0.04094	0.005	501.688
12083	4.761	0.12570	504.179	45.290	0.04110	0.004	501.654
12085	4.759	0.14301	504.486	45.230	0.04107	0.004	501.637
12087	4.759	0.16168	504.831	45.190	0.04124	0.004	501.623
12089	4.758	0.18121	505.205	45.150	0.04112	0.004	501.620
12091	3.683	0.10963	503.999	34.630	0.04061	0.005	501.710
12093	3.678	0.12577	504.323	34.560	0.04041	0.005	501.716
12095	3.677	0.14309	504.647	34.520	0.04073	0.004	501.709
12097	3.675	0.16175	504.964	34.480	0.04086	0.004	501.685
12099	3.675	0.18127	505.280	34.450	0.04090	0.004	501.645
560 K, 0.5669 Mole Fraction Water							
3011	12.046	0.15119	562.067	90.160	0.06287	0.005	560.380
3013	12.038	0.17845	562.344	90.010	0.06310	0.005	560.374
3015	12.032	0.20773	562.582	89.880	0.06328	0.004	560.338
3017	12.041	0.23923	562.806	89.880	0.06328	0.005	560.284
3019	12.042	0.27271	563.069	89.810	0.06334	0.005	560.240
3021	12.045	0.15034	561.935	90.190	0.06283	0.005	560.238
3023	12.036	0.17742	562.289	90.000	0.06282	0.005	560.268
3025	12.047	0.20649	562.660	89.990	0.06278	0.005	560.297
3027	12.037	0.23792	563.033	89.780	0.06314	0.005	560.313
3029	12.037	0.27106	563.382	89.670	0.06296	0.005	560.304
3033	10.149	0.17738	562.430	73.500	0.05922	0.005	560.209
3035	10.132	0.20654	562.812	73.270	0.05894	0.005	560.220
3037	10.084	0.23787	563.227	72.770	0.05906	0.005	560.231
3039	10.094	0.27113	563.648	72.760	0.05907	0.005	560.234
3041	8.074	0.15038	562.433	56.570	0.05592	0.005	560.218
3043	8.074	0.17749	562.840	56.510	0.05579	0.005	560.227

Run Point	$\frac{p_e}{\text{MPa}}$	$\frac{q}{\text{W} \cdot \text{m}^{-1}}$	$\frac{T_e}{\text{K}}$	$\frac{\rho_e}{\text{kg} \cdot \text{m}^{-3}}$	$\frac{\lambda_e}{\text{W} \cdot \text{m}^{-1} \cdot \text{K}^{-1}}$	STAT	$\frac{T_i}{\text{K}}$
3045	8.071	0.20662	563.204	56.420	0.05606	0.005	560.259
3047	8.072	0.23800	563.717	56.360	0.05615	0.005	560.304
3049	8.066	0.27111	564.271	56.220	0.05737	0.004	560.346
3051	8.063	0.15040	562.529	56.470	0.05601	0.005	560.404
3053	8.066	0.17753	562.906	56.430	0.05592	0.005	560.405
3055	8.040	0.20666	563.291	56.170	0.05597	0.005	560.395
3057	8.033	0.23811	563.654	56.060	0.05587	0.005	560.366
3059	8.028	0.27113	564.009	55.960	0.05610	0.005	560.323
3061	5.991	0.15041	562.624	40.650	0.05370	0.005	560.281
3063	5.992	0.17748	563.092	40.620	0.05324	0.005	560.312
3065	5.979	0.20660	563.562	40.480	0.05393	0.005	560.317
3067	5.976	0.23804	564.003	40.410	0.05412	0.005	560.290
3069	5.990	0.27127	564.443	40.470	0.05395	0.005	560.247
560 K, 0.3029 Mole Fraction Water							
4001	23.630	0.17747	562.091	213.760	0.06265	0.004	560.278
4003	23.630	0.19640	562.263	213.640	0.06292	0.004	560.267
4005	23.631	0.21668	562.469	213.500	0.06266	0.005	560.254
4007	23.631	0.23793	562.682	213.340	0.06288	0.005	560.247
4009	23.628	0.25978	562.912	213.140	0.06312	0.005	560.251
4011	21.009	0.17742	562.216	187.630	0.05973	0.005	560.228
4013	20.977	0.19635	562.420	187.180	0.05977	0.004	560.232
4015	20.979	0.21671	562.656	187.060	0.06002	0.005	560.238
4017	20.977	0.23797	562.885	186.900	0.06009	0.005	560.229
4019	21.003	0.25984	563.117	187.020	0.05992	0.005	560.219
4021	18.016	0.15032	562.107	158.310	0.05679	0.005	560.234
4023	18.009	0.17750	562.370	158.120	0.05704	0.005	560.225
4025	18.016	0.20660	562.696	158.030	0.05712	0.004	560.209
4027	18.008	0.23798	563.034	157.790	0.05709	0.005	560.187
4029	18.030	0.27114	563.439	157.810	0.05709	0.005	560.190
4031	15.007	0.15043	562.279	129.360	0.05433	0.004	560.251
4033	15.028	0.17735	562.572	129.450	0.05407	0.005	560.227
4035	15.004	0.20654	562.920	129.100	0.05450	0.005	560.206
4037	15.022	0.23777	563.319	129.120	0.05443	0.005	560.198
4039	15.033	0.27104	563.768	129.070	0.05447	0.005	560.202
4041	12.022	0.15029	562.471	101.510	0.05207	0.005	560.256
4043	12.023	0.17734	562.849	101.420	0.05213	0.005	560.243
4045	12.016	0.20640	563.179	101.280	0.05218	0.005	560.256
4047	11.993	0.23770	563.648	100.940	0.05226	0.005	560.265
4049	12.021	0.27080	564.142	101.070	0.05244	0.005	560.277
4051	8.909	0.15022	562.616	73.550	0.05019	0.005	560.268
4053	8.919	0.17727	563.013	73.570	0.05034	0.005	560.252

Run Point	$\frac{p_e}{\text{MPa}}$	$\frac{q}{\text{W} \cdot \text{m}^{-1}}$	T_e K	ρ_e $\text{kg} \cdot \text{m}^{-3}$	λ_e $\text{W} \cdot \text{m}^{-1} \cdot \text{K}^{-1}$	STAT	T_i K
4055	8.919	0.20639	563.432	73.500	0.05033	0.005	560.234
4057	8.936	0.23772	563.905	73.560	0.05027	0.005	560.224
4059	8.917	0.27083	564.446	73.300	0.05031	0.005	560.239
4061	7.001	0.15022	562.750	56.980	0.04924	0.005	560.262
4063	7.001	0.17731	563.154	56.930	0.04950	0.005	560.233
4065	7.043	0.20641	563.604	57.230	0.04967	0.005	560.213
4067	7.046	0.23774	564.140	57.190	0.04944	0.005	560.218
4069	7.020	0.27086	564.718	56.890	0.04954	0.005	560.254
620 K, 0.6132 Mole Fraction Water							
5011	27.763	0.29566	620.528	201.850	0.10519	0.005	618.738
5013	27.757	0.33224	620.662	201.670	0.10514	0.005	618.705
5015	27.746	0.37093	620.736	201.510	0.10521	0.005	618.652
5017	27.741	0.41171	620.763	201.430	0.10590	0.006	618.589
5019	27.734	0.45462	620.855	201.290	0.10632	0.006	618.555
5021	27.727	0.29565	620.184	201.830	0.10520	0.005	618.520
5023	27.725	0.33226	620.308	201.690	0.10528	0.005	618.516
5025	27.725	0.37115	620.460	201.560	0.10544	0.005	618.513
5027	27.727	0.41194	620.595	201.450	0.10572	0.006	618.504
5029	27.728	0.45503	620.777	201.300	0.10605	0.006	618.497
5031	24.993	0.29552	620.416	176.800	0.09768	0.005	618.498
5033	24.988	0.33205	620.624	176.590	0.09715	0.005	618.509
5035	25.001	0.37096	620.849	176.550	0.09730	0.005	618.517
5037	24.995	0.41187	621.076	176.330	0.09788	0.005	618.528
5039	25.018	0.45493	621.327	176.360	0.09834	0.006	618.548
5041	22.032	0.29551	620.749	150.810	0.08972	0.005	618.553
5043	22.016	0.33213	620.959	150.560	0.08966	0.005	618.556
5045	22.027	0.37082	621.198	150.520	0.08959	0.005	618.559
5047	22.029	0.41192	621.426	150.400	0.09021	0.006	618.563
5049	22.034	0.45476	621.674	150.300	0.09045	0.006	618.563
5051	19.053	0.29548	620.994	126.110	0.08312	0.005	618.547
5053	19.072	0.33198	621.249	126.150	0.08287	0.005	618.545
5055	19.072	0.37101	621.489	126.060	0.08333	0.006	618.535
5057	19.080	0.41173	621.746	126.010	0.08320	0.006	618.534
5059	19.068	0.45482	622.020	125.800	0.08348	0.006	618.527
5061	15.991	0.29539	621.247	102.240	0.07724	0.005	618.516
5063	16.007	0.33195	621.538	102.270	0.07752	0.005	618.514
5065	16.009	0.37063	621.859	102.190	0.07717	0.006	618.517
5067	16.011	0.41178	622.174	102.110	0.07809	0.006	618.514
5071	13.096	0.29540	621.476	81.070	0.07334	0.005	618.518
5073	13.079	0.33201	621.835	80.870	0.07341	0.006	618.522
5075	13.112	0.37065	622.196	81.030	0.07357	0.006	618.523

Run Point	$\frac{p_e}{\text{MPa}}$	$\frac{q}{\text{W} \cdot \text{m}^{-1}}$	$\frac{T_e}{\text{K}}$	$\frac{\rho_e}{\text{kg} \cdot \text{m}^{-3}}$	$\frac{\lambda_e}{\text{W} \cdot \text{m}^{-1} \cdot \text{K}^{-1}}$	STAT	$\frac{T_i}{\text{K}}$
5077	13.105	0.41152	622.621	80.890	0.07373	0.006	618.529
5079	13.091	0.45449	623.106	80.680	0.07463	0.006	618.560
5081	13.084	0.22861	620.956	81.100	0.07335	0.005	618.633
5083	13.083	0.26032	621.290	81.020	0.07332	0.006	618.647
5085	13.086	0.29471	621.620	80.970	0.07377	0.005	618.649
5087	13.087	0.33130	621.961	80.900	0.07354	0.006	618.646
5089	13.087	0.36984	622.313	80.820	0.07360	0.006	618.638
5091	10.012	0.22872	620.820	60.070	0.07052	0.006	618.589
5093	9.986	0.26048	621.365	59.820	0.07068	0.006	618.587
5095	9.997	0.29469	621.725	59.840	0.07081	0.006	618.573
5097	9.985	0.33129	622.114	59.700	0.07077	0.006	618.566
5099	9.987	0.36984	622.520	59.660	0.07093	0.006	618.559
5101	7.975	0.22836	621.362	46.790	0.06963	0.007	618.565
5103	7.985	0.26015	621.743	46.810	0.06934	0.007	618.558
5105	7.964	0.29460	622.033	46.650	0.07002	0.007	618.560
5107	7.991	0.33112	622.479	46.780	0.07021	0.007	618.569
5109	7.984	0.36973	622.950	46.680	0.06980	0.007	618.579
620 K, 0.6443 Mole Fraction Water							
15001	25.734	0.30265	619.963	184.120	0.10414	0.005	618.146
15003	25.741	0.34004	620.115	184.060	0.10414	0.005	618.146
15005	25.696	0.37983	620.266	183.510	0.10499	0.006	618.143
15007	25.715	0.42139	620.640	183.370	0.10470	0.006	618.142
15009	25.734	0.46546	620.874	183.360	0.10465	0.006	618.143
15011	22.796	0.30252	620.269	157.070	0.09475	0.005	618.129
15013	22.789	0.33995	620.513	156.860	0.09527	0.005	618.132
15015	22.770	0.37956	620.772	156.520	0.09506	0.006	618.148
15017	22.761	0.42135	621.042	156.260	0.09502	0.006	618.162
15019	22.786	0.46537	621.314	156.310	0.09553	0.006	618.150
15021	19.978	0.30253	620.530	132.700	0.08744	0.005	618.175
15023	20.006	0.33996	620.816	132.800	0.08695	0.005	618.173
15025	19.992	0.37959	621.084	132.540	0.08735	0.006	618.175
15027	19.947	0.42143	621.333	132.050	0.08746	0.006	618.178
15029	19.982	0.46542	621.621	132.200	0.08757	0.006	618.170
15031	16.886	0.30251	620.910	107.730	0.08083	0.005	618.175
15033	16.910	0.34002	621.140	107.830	0.08020	0.006	618.175
15035	16.938	0.37959	621.489	107.930	0.08043	0.006	618.172
15037	16.933	0.42141	621.815	107.770	0.08075	0.006	618.171
15039	16.890	0.46545	622.153	107.320	0.08063	0.006	618.180
15041	13.978	0.30250	621.101	85.980	0.07521	0.006	618.178
15043	13.956	0.34004	621.442	85.730	0.07524	0.006	618.176
15045	13.946	0.37965	621.802	85.580	0.07535	0.006	618.178

Run Point	$\frac{p_e}{\text{MPa}}$	$\frac{q}{\text{W} \cdot \text{m}^{-1}}$	$\frac{T_e}{\text{K}}$	$\frac{\rho_e}{\text{kg} \cdot \text{m}^{-3}}$	$\frac{\lambda_e}{\text{W} \cdot \text{m}^{-1} \cdot \text{K}^{-1}}$	STAT	$\frac{T_i}{\text{K}}$
15047	13.992	0.42151	622.194	85.810	0.07520	0.006	618.175
15049	14.007	0.46558	622.623	85.810	0.07552	0.007	618.171
15051	11.001	0.30261	621.465	65.240	0.07172	0.006	618.183
15053	11.012	0.34004	621.906	65.240	0.07192	0.006	618.183
15055	10.993	0.37969	622.330	65.050	0.07175	0.007	618.188
15057	10.959	0.42152	622.776	64.750	0.07178	0.007	618.197
620 K, 0.3030 Mole Fraction Water							
6001	27.938	0.19512	620.844	214.650	0.06738	0.004	618.974
6003	27.938	0.22550	621.103	214.490	0.06770	0.005	618.964
6005	27.935	0.25810	621.361	214.330	0.06769	0.005	618.935
6007	27.934	0.29288	621.784	214.090	0.06740	0.005	618.929
6009	27.931	0.32986	622.097	213.890	0.06770	0.005	618.924
6011	24.961	0.19506	621.017	190.820	0.06514	0.005	618.936
6013	24.983	0.22545	621.333	190.840	0.06543	0.005	618.939
6015	24.959	0.25806	621.633	190.510	0.06566	0.005	618.915
6017	24.980	0.29286	621.951	190.520	0.06560	0.005	618.891
6019	24.960	0.32985	622.270	190.200	0.06569	0.005	618.871
6021	21.955	0.19508	621.048	166.800	0.06323	0.005	618.886
6023	21.932	0.22548	621.427	166.460	0.06338	0.005	618.917
6025	21.954	0.25808	621.806	166.470	0.06338	0.005	618.924
6027	21.940	0.29288	622.167	166.220	0.06343	0.005	618.911
6029	21.953	0.32981	622.561	166.160	0.06355	0.005	618.899
6031	19.034	0.19509	621.235	143.460	0.06143	0.005	618.892
6033	19.063	0.22545	621.421	143.630	0.06137	0.005	618.870
6035	19.034	0.25811	621.803	143.270	0.06135	0.005	618.857
6037	19.018	0.29290	622.236	142.990	0.06180	0.005	618.871
6039	19.055	0.32991	622.663	143.140	0.06154	0.005	618.861
6041	15.984	0.19510	621.274	119.360	0.05962	0.005	618.851
6043	15.993	0.22552	621.631	119.330	0.05972	0.005	618.842
6045	16.024	0.25810	622.035	119.470	0.05998	0.005	618.821
6047	15.990	0.29292	622.437	119.100	0.05994	0.005	618.811
6049	15.996	0.32992	622.913	119.010	0.06031	0.005	618.828
6051	12.984	0.19508	621.359	95.940	0.05861	0.005	618.813
6053	13.005	0.22554	621.817	96.010	0.05847	0.005	618.823
6055	13.005	0.25815	622.216	95.930	0.05845	0.005	618.807
6057	13.016	0.29296	622.639	95.930	0.05877	0.005	618.781
6059	13.015	0.32986	623.123	95.820	0.05846	0.006	618.767
6061	9.946	0.19519	621.572	72.620	0.05764	0.006	618.845
6063	9.944	0.22561	622.001	72.540	0.05761	0.005	618.852
6065	9.938	0.25826	622.420	72.430	0.05781	0.005	618.821
6067	9.966	0.29306	622.849	72.590	0.05777	0.006	618.778

Run Point	$\frac{p_e}{\text{MPa}}$	$\frac{q}{\text{W} \cdot \text{m}^{-1}}$	$\frac{T_e}{\text{K}}$	$\frac{\rho_e}{\text{kg} \cdot \text{m}^{-3}}$	$\frac{\lambda_e}{\text{W} \cdot \text{m}^{-1} \cdot \text{K}^{-1}}$	STAT	$\frac{T_i}{\text{K}}$
6069	9.971	0.33007	623.351	72.550	0.05759	0.006	618.760
6071	7.965	0.19532	621.700	57.680	0.05719	0.006	618.850
6073	7.938	0.22576	622.124	57.420	0.05698	0.006	618.835
6075	7.976	0.25843	622.545	57.670	0.05718	0.006	618.808
6077	7.964	0.29334	623.007	57.520	0.05714	0.006	618.780
6079	7.975	0.33028	623.573	57.540	0.05718	0.006	618.792
680 K, 0.5962 Mole Fraction Water							
7001	34.625	0.34160	678.726	212.130	0.10698	0.005	676.713
7003	34.617	0.37936	678.808	212.020	0.10772	0.005	676.713
7005	34.613	0.41881	679.154	211.760	0.10747	0.005	676.721
7007	34.606	0.46041	679.304	211.610	0.10811	0.005	676.709
7009	34.602	0.50393	679.391	211.530	0.10794	0.006	676.685
7011	29.847	0.34138	679.022	179.070	0.09951	0.005	676.697
7013	29.905	0.37895	679.241	179.360	0.09919	0.005	676.706
7015	29.946	0.41849	679.497	179.500	0.09980	0.005	676.709
7017	29.941	0.46007	679.739	179.340	0.10023	0.005	676.718
7019	29.893	0.50366	679.963	178.900	0.09983	0.006	676.740
7021	27.081	0.30565	679.006	160.350	0.09599	0.005	676.747
7023	27.032	0.34127	679.252	159.910	0.09529	0.005	676.759
7025	27.031	0.37883	679.490	159.790	0.09485	0.006	676.767
7027	27.034	0.41839	679.738	159.710	0.09563	0.005	676.760
7029	27.025	0.45988	679.961	159.540	0.09555	0.006	676.741
7031	24.173	0.30561	679.066	140.960	0.09106	0.006	676.722
7033	24.170	0.34124	679.366	140.830	0.09078	0.006	676.739
7035	24.164	0.37881	679.657	140.690	0.09105	0.006	676.757
7037	24.135	0.41851	679.923	140.400	0.09196	0.006	676.769
7039	24.162	0.45998	680.204	140.470	0.09153	0.006	676.760
7041	20.430	0.30562	679.381	116.600	0.08629	0.006	676.750
7043	20.417	0.34125	679.705	116.420	0.08647	0.006	676.781
7045	20.436	0.37883	679.957	116.470	0.08681	0.006	676.781
7047	20.439	0.41839	680.318	116.390	0.08701	0.006	676.777
7049	20.440	0.45987	680.659	116.290	0.08706	0.006	676.783
7051	17.246	0.27198	679.144	96.670	0.08334	0.006	676.744
7053	17.242	0.30570	679.398	96.590	0.08332	0.006	676.723
7055	17.237	0.34140	679.670	96.500	0.08370	0.006	676.702
7057	17.237	0.37886	679.976	96.430	0.08345	0.006	676.682
7059	17.235	0.41841	680.308	96.350	0.08439	0.006	676.677
7061	14.049	0.27200	679.405	77.210	0.08180	0.006	676.715
7063	14.057	0.30569	679.685	77.210	0.08122	0.007	676.738
7065	14.045	0.34131	680.047	77.070	0.08094	0.007	676.755
7067	14.039	0.37892	680.418	76.980	0.08114	0.007	676.770

Run Point	$\frac{p_e}{\text{MPa}}$	$\frac{q}{\text{W} \cdot \text{m}^{-1}}$	$\frac{T_e}{\text{K}}$	$\frac{\rho_e}{\text{kg} \cdot \text{m}^{-3}}$	$\frac{\lambda_e}{\text{W} \cdot \text{m}^{-1} \cdot \text{K}^{-1}}$	STAT	$\frac{T_i}{\text{K}}$
7069	14.062	0.41849	680.804	77.050	0.08113	0.007	676.763
680 K, 0.2596 Mole Fraction Water							
8001	31.631	0.27231	679.185	215.730	0.07585	0.004	676.775
8003	31.640	0.30606	679.507	215.650	0.07608	0.004	676.766
8005	31.658	0.34168	679.865	215.610	0.07616	0.004	676.778
8007	31.672	0.37936	680.243	215.530	0.07585	0.004	676.797
8009	31.681	0.41890	680.650	215.410	0.07623	0.004	676.831
8011	31.507	0.27237	679.337	214.840	0.07786	0.005	676.906
8013	31.501	0.30608	679.637	214.660	0.07771	0.005	676.917
8015	31.497	0.34176	679.957	214.490	0.07760	0.005	676.913
8017	31.497	0.37939	680.275	214.350	0.07776	0.006	676.895
8019	31.495	0.41902	680.613	214.190	0.07777	0.006	676.888
8021	29.017	0.27239	679.418	198.070	0.07594	0.005	676.877
8023	28.991	0.30612	679.645	197.800	0.07670	0.005	676.878
8025	28.975	0.34180	679.985	197.550	0.07630	0.006	676.883
8027	28.962	0.37946	680.328	197.330	0.07632	0.006	676.887
8029	29.003	0.41912	680.691	197.460	0.07657	0.006	676.877
8031	26.041	0.27240	679.479	177.820	0.07490	0.006	676.882
8033	26.035	0.30620	679.767	177.680	0.07489	0.006	676.856
8035	26.033	0.34185	680.068	177.560	0.07496	0.006	676.833
8037	26.024	0.37942	680.385	177.390	0.07520	0.006	676.805
8039	26.045	0.41905	680.747	177.400	0.07539	0.006	676.797
8041	22.979	0.27248	679.424	156.850	0.07332	0.006	676.785
8043	22.988	0.30615	679.776	156.800	0.07346	0.006	676.786
8045	22.999	0.34183	680.157	156.760	0.07355	0.006	676.795
8047	23.021	0.37949	680.547	156.790	0.07335	0.006	676.806
8049	23.021	0.41912	680.966	156.660	0.07383	0.006	676.822
8051	19.971	0.24074	679.215	136.170	0.07162	0.006	676.747
8053	19.976	0.27250	679.594	136.100	0.07207	0.006	676.773
8055	19.979	0.30625	679.973	136.020	0.07205	0.006	676.796
8057	19.981	0.34197	680.396	135.920	0.07218	0.006	676.836
8059	19.985	0.37964	680.785	135.850	0.07197	0.006	676.841
8061	17.035	0.21139	679.138	115.880	0.07042	0.006	676.850
8063	17.037	0.24081	679.470	115.820	0.07054	0.006	676.861
8065	17.048	0.27259	679.820	115.820	0.07047	0.006	676.867
8067	17.048	0.30634	680.174	115.740	0.07060	0.006	676.860
8069	17.047	0.34204	680.567	115.650	0.07081	0.006	676.857
8071	13.939	0.17474	678.784	94.540	0.06995	0.006	676.829
8073	13.946	0.20196	679.089	94.540	0.06961	0.006	676.801
8075	13.942	0.23117	679.447	94.450	0.06946	0.007	676.813
8077	13.926	0.26235	679.797	94.280	0.06959	0.006	676.819

Run Point	$\frac{p_e}{\text{MPa}}$	$\frac{q}{\text{W} \cdot \text{m}^{-1}}$	$\frac{T_e}{\text{K}}$	$\frac{\rho_e}{\text{kg} \cdot \text{m}^{-3}}$	$\frac{\lambda_e}{\text{W} \cdot \text{m}^{-1} \cdot \text{K}^{-1}}$	STAT	$\frac{T_i}{\text{K}}$
8079	13.917	0.29548	680.164	94.160	0.07003	0.006	676.818
740 K, 0.5824 Mole Fraction Water							
9001	29.402	0.28236	741.562	151.580	0.09494	0.006	739.314
9003	29.379	0.31529	741.807	151.370	0.09499	0.006	739.319
9005	29.353	0.35006	742.157	151.120	0.09558	0.006	739.319
9007	29.337	0.38662	742.510	150.910	0.09581	0.005	739.305
9009	29.321	0.42510	742.686	150.770	0.09688	0.005	739.296
9011	29.287	0.28261	741.501	150.960	0.09481	0.006	739.295
9013	29.266	0.31560	741.861	150.730	0.09718	0.005	739.304
9015	29.255	0.35039	742.082	150.600	0.09463	0.006	739.302
9017	29.241	0.38704	742.372	150.430	0.09499	0.006	739.302
9019	29.220	0.42550	742.664	150.220	0.09504	0.006	739.311
9021	27.192	0.25176	741.465	139.460	0.09344	0.006	739.294
9023	27.110	0.28296	741.784	138.910	0.09593	0.005	739.288
9025	27.104	0.31597	742.125	138.780	0.09512	0.006	739.288
9027	27.067	0.35076	742.455	138.480	0.09315	0.006	739.282
9029	27.144	0.38742	742.821	138.800	0.09357	0.006	739.268
9031	23.984	0.25211	741.095	122.040	0.09142	0.006	739.277
9033	24.012	0.28333	741.728	122.030	0.09145	0.006	739.274
9035	24.018	0.31638	742.110	121.980	0.09144	0.006	739.280
9037	23.964	0.35131	742.357	121.620	0.09320	0.006	739.291
9039	23.950	0.38803	742.728	121.460	0.09218	0.006	739.287
9041	21.001	0.25244	741.469	105.850	0.08959	0.006	739.283
9045	20.975	0.31685	742.023	105.600	0.09011	0.006	739.289
9047	21.004	0.35181	742.451	105.670	0.09014	0.006	739.290
9049	20.998	0.38855	742.853	105.550	0.08958	0.006	739.291
9051	17.959	0.25278	741.567	89.650	0.08863	0.007	739.297
9053	17.923	0.28410	741.932	89.390	0.08848	0.007	739.280
9055	17.909	0.31730	742.046	89.300	0.08864	0.007	739.263
9057	17.898	0.35227	742.457	89.180	0.08884	0.007	739.233
9059	17.892	0.38907	742.844	89.080	0.08854	0.007	739.209
9061	15.077	0.22366	740.783	74.650	0.08782	0.007	739.179
9063	15.079	0.25316	741.692	74.540	0.08748	0.007	739.177
9065	15.075	0.28451	742.089	74.470	0.08727	0.007	739.188
9067	15.079	0.31770	742.496	74.440	0.08728	0.007	739.190
9069	15.061	0.35282	742.622	74.330	0.08744	0.007	739.191
740 K, 0.2963 Mole Fraction Water							
10011	35.052	0.27416	741.510	208.120	0.08653	0.006	739.196
10013	35.047	0.30606	741.841	207.970	0.08658	0.006	739.196
10015	35.037	0.34014	742.024	207.850	0.08700	0.006	739.220
10017	35.022	0.37544	742.390	207.630	0.08669	0.006	739.235

Run Point	$\frac{p_e}{\text{MPa}}$	$\frac{q}{\text{W} \cdot \text{m}^{-1}}$	$\frac{T_e}{\text{K}}$	$\frac{\rho_e}{\text{kg} \cdot \text{m}^{-3}}$	$\frac{\lambda_e}{\text{W} \cdot \text{m}^{-1} \cdot \text{K}^{-1}}$	STAT	$\frac{T_i}{\text{K}}$
10019	35.008	0.41258	742.741	207.410	0.08657	0.006	739.238
10021	32.124	0.27458	741.500	191.280	0.08557	0.006	739.226
10023	32.108	0.30664	741.891	191.060	0.08557	0.006	739.255
10025	32.112	0.34027	742.187	190.980	0.08543	0.006	739.247
10027	32.116	0.37554	742.540	190.880	0.08541	0.006	739.238
10029	32.106	0.41315	742.764	190.750	0.08536	0.006	739.229
10031	29.063	0.24461	741.022	173.590	0.08490	0.006	739.213
10033	29.038	0.27488	741.333	173.350	0.08427	0.006	739.193
10035	29.047	0.30695	741.686	173.290	0.08449	0.006	739.172
10037	29.061	0.34070	742.155	173.240	0.08382	0.006	739.179
10039	29.026	0.37611	742.509	172.930	0.08437	0.006	739.203
10041	25.982	0.24463	741.416	155.320	0.08281	0.006	739.207
10043	25.958	0.27487	741.747	155.090	0.08282	0.006	739.219
10045	25.955	0.30697	741.908	155.030	0.08308	0.006	739.230
10047	25.947	0.34088	742.331	154.870	0.08282	0.006	739.243
10049	25.930	0.37622	742.703	154.670	0.08278	0.006	739.238
10051	22.812	0.24492	741.399	136.480	0.08168	0.007	739.175
10053	22.831	0.27515	741.798	136.500	0.08159	0.006	739.186
10055	22.838	0.30705	742.199	136.460	0.08154	0.006	739.216
10057	22.817	0.34080	742.466	136.270	0.08175	0.006	739.243
10059	22.813	0.37663	742.873	136.150	0.08196	0.006	739.268
10061	20.029	0.24518	741.551	119.810	0.08093	0.007	739.240
10063	20.033	0.27532	741.968	119.760	0.08056	0.006	739.247
10065	20.002	0.30769	742.059	119.550	0.08098	0.007	739.268
10067	19.996	0.34141	742.520	119.420	0.08073	0.007	739.281
10069	19.998	0.37693	742.939	119.350	0.08091	0.007	739.268
10071	16.957	0.24531	741.469	101.390	0.08008	0.007	739.204
10073	16.991	0.27563	741.916	101.520	0.07959	0.007	739.203
10075	17.000	0.30786	742.264	101.520	0.07992	0.007	739.230
10077	16.990	0.34161	742.708	101.380	0.07992	0.007	739.263
10079	16.992	0.37723	743.124	101.330	0.07967	0.007	739.277

Table A10. Thermal conductivity data for mixtures of water with carbon dioxide from steady-state measurements at temperatures from 500 K to 740 K.

Run Point	$\frac{P_e}{\text{MPa}}$	$\frac{q}{\text{W} \cdot \text{m}^{-1}}$	$\frac{T_e}{\text{K}}$	$\frac{\rho_e}{\text{kg} \cdot \text{m}^{-3}}$	$\frac{\lambda_e}{\text{W} \cdot \text{m}^{-1} \cdot \text{K}^{-1}}$	$\frac{\Delta T_a}{\text{K}}$	$\frac{t_s}{\text{s}}$	$\frac{t_e}{\text{s}}$	Ra
500 K, 0.6536 Mole Fraction Water									
11012	3.456	0.10969	503.472	24.393	0.04524	2.375	19.44	60.00	2141
11014	3.455	0.12590	503.635	24.379	0.04533	2.719	21.84	60.00	2444
11016	3.456	0.14317	503.813	24.371	0.04544	3.083	19.44	60.00	2763
11018	3.453	0.16180	503.995	24.336	0.04563	3.468	17.04	60.00	3091
11020	3.452	0.18137	504.194	24.316	0.04574	3.876	17.04	60.00	3441
11022	3.082	0.10967	503.555	21.512	0.04352	2.471	17.04	60.00	1632
11024	3.078	0.12590	503.748	21.474	0.04350	2.836	21.84	60.00	1862
11026	3.081	0.14319	503.925	21.488	0.04365	3.213	17.04	60.00	2110
11028	3.085	0.16184	504.118	21.503	0.04377	3.620	19.44	60.00	2376
11030	3.086	0.18124	504.328	21.500	0.04382	4.047	19.44	60.00	2650
11032	2.609	0.10966	503.628	17.968	0.04162	2.585	21.84	60.00	1108
11034	2.607	0.12588	503.813	17.947	0.04185	2.950	17.04	60.00	1259
11036	2.603	0.14315	504.019	17.910	0.04199	3.343	19.44	60.00	1417
11038	2.602	0.16176	504.227	17.888	0.04209	3.767	19.44	60.00	1589
11040	2.605	0.18132	504.433	17.902	0.04224	4.206	19.44	60.00	1774
11042	2.065	0.10969	503.666	14.016	0.04066	2.648	21.84	60.00	637
11044	2.069	0.12586	503.864	14.035	0.04055	3.046	21.84	60.00	734
11046	2.073	0.14324	504.076	14.055	0.04053	3.468	21.84	60.00	837
11048	2.074	0.16177	504.321	14.056	0.04057	3.913	19.44	60.00	942
11050	2.070	0.18132	504.579	14.023	0.04069	4.372	19.44	60.00	1045
11052	1.913	0.10969	503.477	12.937	0.04092	2.633	19.44	60.00	529
11054	1.912	0.12586	503.615	12.926	0.04145	2.982	19.44	60.00	597
11062	1.512	0.10973	503.438	10.120	0.04055	2.659	19.44	60.00	308
11064	1.513	0.12591	503.640	10.124	0.04038	3.063	19.44	60.00	355
11066	1.516	0.14321	503.834	10.142	0.04040	3.482	21.84	60.00	405
11068	1.518	0.16177	504.049	10.149	0.04033	3.940	21.84	60.00	458
11070	1.516	0.18135	504.286	10.127	0.04056	4.391	21.84	60.00	507
11072	1.001	0.10967	503.467	6.617	0.03917	2.752	21.84	60.00	127
11074	1.000	0.12586	503.673	6.604	0.03924	3.151	19.44	60.00	145
11076	0.998	0.14320	503.912	6.588	0.03931	3.579	21.84	60.00	163
11078	0.997	0.16181	504.145	6.582	0.03937	4.038	19.44	60.00	183
11080	0.999	0.18136	504.374	6.590	0.03935	4.529	19.44	60.00	206
11082	0.527	0.10972	503.548	3.440	0.03811	2.829	21.84	60.00	33
11084	0.527	0.12587	503.757	3.443	0.03801	3.254	19.44	60.00	38
11086	0.528	0.14323	503.970	3.445	0.03814	3.690	19.44	60.00	43
11088	0.528	0.16184	504.196	3.446	0.03819	4.165	19.44	60.00	49
11090	0.528	0.18135	504.445	3.443	0.03831	4.652	19.44	60.00	54
11092	0.313	0.10965	503.557	2.034	0.03738	2.883	24.24	60.00	11
11094	0.313	0.12588	503.770	2.034	0.03751	3.298	19.44	60.00	13
11096	0.313	0.14314	504.006	2.033	0.03760	3.741	19.44	60.00	15
11098	0.313	0.16184	504.250	2.032	0.03769	4.219	19.44	60.00	17

Run Point	$\frac{P_e}{\text{MPa}}$	$\frac{q}{\text{W} \cdot \text{m}^{-1}}$	$\frac{T_e}{\text{K}}$	$\frac{\rho_e}{\text{kg} \cdot \text{m}^{-3}}$	$\frac{\lambda_e}{\text{W} \cdot \text{m}^{-1} \cdot \text{K}^{-1}}$	$\frac{\Delta T_a}{\text{K}}$	$\frac{t_s}{\text{s}}$	$\frac{t_e}{\text{s}}$	Ra
11100	0.314	0.18133	504.493	2.035	0.03771	4.725	21.84	60.00	19
11102	0.097	0.10965	503.613	0.627	0.03656	2.947	21.84	60.00	1
11104	0.098	0.12590	503.824	0.632	0.03664	3.376	21.84	60.00	1
11106	0.099	0.14315	504.042	0.638	0.03664	3.839	19.44	60.00	1
11108	0.099	0.16174	504.301	0.640	0.03669	4.331	19.44	60.00	2
11110	0.100	0.18133	504.590	0.644	0.03663	4.864	21.84	60.00	2
500 K, 0.6380 Mole Fraction Water									
21042	3.030	0.10954	502.761	21.428	0.04353	2.467	21.84	60.00	1564
21044	3.026	0.12576	502.934	21.387	0.04375	2.818	19.44	60.00	1775
21046	3.020	0.14306	503.118	21.334	0.04395	3.189	19.44	60.00	1993
21048	3.018	0.16167	503.302	21.310	0.04418	3.584	17.04	60.00	2230
21050	3.026	0.18112	503.515	21.352	0.04405	4.024	17.04	60.00	2511
21052	2.038	0.10953	502.853	14.035	0.04043	2.660	21.84	60.00	626
21054	2.036	0.12575	503.038	14.015	0.04069	3.034	17.04	60.00	710
21056	2.033	0.14301	503.239	13.988	0.04088	3.434	19.44	60.00	799
21058	2.037	0.16162	503.453	14.006	0.04093	3.875	19.44	60.00	903
21060	2.038	0.18114	503.684	14.005	0.04096	4.339	19.44	60.00	1009
21062	1.508	0.10948	502.857	10.246	0.04018	2.677	17.04	60.00	312
21064	1.507	0.12564	503.032	10.237	0.04017	3.073	21.84	60.00	357
21066	1.507	0.14294	503.229	10.230	0.04043	3.473	19.44	60.00	402
21068	1.506	0.16158	503.437	10.221	0.04052	3.917	19.44	60.00	451
21070	1.506	0.18106	503.686	10.214	0.04050	4.391	24.24	60.00	504
21082	1.016	0.10955	502.788	6.822	0.03906	2.756	24.24	60.00	133
21084	1.018	0.12569	503.018	6.834	0.03876	3.186	19.44	60.00	154
21086	1.018	0.14292	503.263	6.829	0.03868	3.630	21.84	60.00	175
21088	1.018	0.16149	503.522	6.824	0.03873	4.096	21.84	60.00	197
21090	1.018	0.18095	503.772	6.820	0.03884	4.578	19.44	60.00	220
21092	1.026	0.10955	502.884	6.892	0.03924	2.743	19.44	60.00	135
21094	1.026	0.12571	503.069	6.887	0.03933	3.141	19.44	60.00	155
21096	1.027	0.14297	503.281	6.888	0.03933	3.572	19.44	60.00	176
21098	1.026	0.16151	503.512	6.881	0.03923	4.045	19.44	60.00	198
21100	1.025	0.18107	503.754	6.873	0.03938	4.517	21.84	60.00	220
21102	0.556	0.10955	502.927	3.694	0.03792	2.839	21.84	60.00	38
21104	0.556	0.12570	503.136	3.689	0.03819	3.234	19.44	60.00	43
21106	0.555	0.14298	503.344	3.681	0.03832	3.667	21.84	60.00	48
21108	0.556	0.16157	503.572	3.686	0.03841	4.133	21.84	60.00	55
21110	0.556	0.18104	503.815	3.687	0.03841	4.632	19.44	60.00	61
21112	0.309	0.10954	502.947	2.041	0.03764	2.860	19.44	60.00	11
21114	0.309	0.12569	503.147	2.041	0.03766	3.280	19.44	60.00	13
21116	0.309	0.14300	503.341	2.039	0.03797	3.701	21.84	60.00	15
21118	0.309	0.16156	503.552	2.037	0.03817	4.160	19.44	60.00	16
21120	0.309	0.18108	503.757	2.034	0.03862	4.609	21.84	60.00	18
21128	0.203	0.16170	503.486	1.335	0.03768	4.217	21.84	60.00	7
21130	0.203	0.18122	503.735	1.333	0.03764	4.732	19.44	60.00	8
21132	0.203	0.10961	502.801	1.340	0.03753	2.870	21.84	60.00	5

Run Point	$\frac{P_e}{\text{MPa}}$	$\frac{q}{\text{W} \cdot \text{m}^{-1}}$	$\frac{T_e}{\text{K}}$	$\frac{\rho_e}{\text{kg} \cdot \text{m}^{-3}}$	$\frac{\lambda_e}{\text{W} \cdot \text{m}^{-1} \cdot \text{K}^{-1}}$	$\frac{\Delta T_a}{\text{K}}$	$\frac{t_s}{\text{s}}$	$\frac{t_e}{\text{s}}$	Ra
21134	0.204	0.12580	503.010	1.341	0.03758	3.290	21.84	60.00	6
21136	0.203	0.14307	503.236	1.339	0.03762	3.737	19.44	60.00	6
21138	0.204	0.16167	503.474	1.341	0.03768	4.217	19.44	60.00	7
21140	0.204	0.18123	503.722	1.342	0.03771	4.723	19.44	60.00	8
21142	0.097	0.10959	502.815	0.640	0.03709	2.904	19.44	60.00	1
21144	0.098	0.12579	503.023	0.643	0.03720	3.323	19.44	60.00	1
21146	0.098	0.14310	503.244	0.644	0.03732	3.769	19.44	60.00	1
21148	0.098	0.16168	503.489	0.643	0.03726	4.264	21.84	60.00	2
21150	0.098	0.18123	503.761	0.644	0.03703	4.809	21.84	60.00	2
21152	0.115	0.10967	502.977	0.754	0.03765	2.863	24.24	60.00	2
21154	0.115	0.12587	503.193	0.755	0.03752	3.297	19.44	60.00	2
21156	0.115	0.14315	503.422	0.753	0.03759	3.743	21.84	60.00	2
21158	0.115	0.16180	503.672	0.753	0.03759	4.230	21.84	60.00	2
21160	0.115	0.18133	503.921	0.753	0.03766	4.732	21.84	60.00	2
500 K, 0.2052 Mole Fraction Water									
2082	3.765	0.10953	503.323	36.163	0.03956	2.707	21.84	60.00	2778
2084	3.765	0.12571	503.519	36.150	0.03953	3.107	19.44	60.00	3182
2086	3.765	0.14300	503.728	36.131	0.03971	3.516	14.64	60.00	3591
2088	3.759	0.16156	503.951	36.049	0.03991	3.950	7.44	60.00	4009
2090	3.751	0.18108	504.186	35.954	0.04006	4.407	5.04	60.00	4440
2092	3.001	0.10954	503.409	28.598	0.03867	2.775	21.84	60.00	1721
2094	3.001	0.12572	503.605	28.586	0.03882	3.171	19.44	60.00	1963
2096	2.997	0.14302	503.812	28.527	0.03887	3.601	21.84	60.00	2216
2098	2.986	0.16164	504.033	28.409	0.03901	4.054	19.44	60.00	2469
2100	2.972	0.18117	504.272	28.254	0.03912	4.529	21.84	60.00	2722
2102	2.019	0.10959	503.432	19.041	0.03783	2.842	21.84	60.00	748
2104	2.018	0.12577	503.610	19.026	0.03822	3.229	21.84	60.00	847
2106	2.018	0.14309	503.800	19.017	0.03842	3.654	21.84	60.00	956
2108	2.021	0.16163	504.025	19.039	0.03828	4.140	19.44	60.00	1085
2110	2.019	0.18115	504.283	19.008	0.03823	4.646	21.84	60.00	1211
2112	1.038	0.10956	503.542	9.692	0.03618	2.973	24.24	60.00	193
2114	1.039	0.12573	503.765	9.696	0.03615	3.415	24.24	60.00	222
2116	1.039	0.14304	503.983	9.693	0.03621	3.878	24.24	60.00	252
2118	1.039	0.16162	504.232	9.684	0.03625	4.378	21.84	60.00	283
2120	1.038	0.18115	504.507	9.670	0.03640	4.885	19.44	60.00	315
2122	1.037	0.10963	503.592	9.683	0.03660	2.942	21.84	60.00	191
2124	1.036	0.12583	503.800	9.662	0.03685	3.353	21.84	60.00	216
2126	1.034	0.14314	504.010	9.645	0.03706	3.794	19.44	60.00	244
2128	1.033	0.16175	504.213	9.630	0.03734	4.254	19.44	60.00	272
2138	0.557	0.16166	504.183	5.172	0.03607	4.401	21.84	60.00	79
2140	0.558	0.18120	504.438	5.174	0.03616	4.922	21.84	60.00	89
2142	0.558	0.10956	503.470	5.181	0.03599	2.990	19.44	60.00	54
2144	0.558	0.12577	503.688	5.180	0.03599	3.432	24.24	60.00	62
2146	0.557	0.14304	503.918	5.173	0.03608	3.894	21.84	60.00	70
2148	0.557	0.16165	504.180	5.170	0.03607	4.402	21.84	60.00	79

Run Point	$\frac{p_e}{\text{MPa}}$	$\frac{q}{\text{W} \cdot \text{m}^{-1}}$	$\frac{T_e}{\text{K}}$	$\frac{\rho_e}{\text{kg} \cdot \text{m}^{-3}}$	$\frac{\lambda_e}{\text{W} \cdot \text{m}^{-1} \cdot \text{K}^{-1}}$	$\frac{\Delta T_a}{\text{K}}$	$\frac{t_s}{\text{s}}$	$\frac{t_e}{\text{s}}$	Ra
2150	0.557	0.18119	504.448	5.165	0.03612	4.928	21.84	60.00	89
2152	0.311	0.10956	503.531	2.884	0.03519	3.058	19.44	60.00	17
2154	0.311	0.12576	503.754	2.885	0.03536	3.493	19.44	60.00	19
2156	0.312	0.14305	504.002	2.886	0.03536	3.973	21.84	60.00	22
2158	0.312	0.16161	504.266	2.886	0.03541	4.483	21.84	60.00	25
2160	0.313	0.18114	504.532	2.892	0.03554	5.006	19.44	60.00	28
2162	0.095	0.10957	503.584	0.874	0.03483	3.090	21.84	60.00	2
2164	0.095	0.12574	503.810	0.876	0.03487	3.542	21.84	60.00	2
2166	0.095	0.14303	504.042	0.878	0.03500	4.014	19.44	60.00	2
2168	0.096	0.16172	504.284	0.885	0.03516	4.518	21.84	60.00	2
2170	0.096	0.18117	504.529	0.884	0.03529	5.042	19.44	60.00	3
500 K, 0.2363 Mole Fraction Water									
12102	2.993	0.10957	502.959	28.003	0.03912	2.744	19.44	60.00	1672
12104	2.995	0.12575	503.155	28.010	0.03916	3.144	19.44	60.00	1914
12106	2.996	0.14302	503.358	28.002	0.03918	3.574	19.44	60.00	2171
12108	2.996	0.16162	503.589	27.989	0.03919	4.034	21.84	60.00	2445
12110	2.996	0.18113	503.832	27.978	0.03925	4.512	21.84	60.00	2728
12112	2.055	0.09450	502.845	19.033	0.03744	2.477	21.84	60.00	667
12114	2.054	0.10956	503.039	19.015	0.03752	2.865	21.84	60.00	769
12116	2.053	0.12576	503.234	18.995	0.03775	3.268	24.24	60.00	874
12118	2.060	0.14304	503.457	19.050	0.03766	3.725	21.84	60.00	1000
12120	2.061	0.16158	503.693	19.053	0.03768	4.204	21.84	60.00	1128
12122	1.012	0.09449	502.894	9.270	0.03624	2.560	17.04	60.00	155
12124	1.013	0.10955	503.079	9.270	0.03643	2.953	24.24	60.00	179
12126	1.013	0.12581	503.267	9.269	0.03675	3.362	19.44	60.00	203
12128	1.014	0.14299	503.480	9.269	0.03684	3.811	19.44	60.00	230
12130	1.014	0.16167	503.705	9.269	0.03702	4.288	19.44	60.00	259
12132	0.538	0.09453	502.808	4.898	0.03627	2.560	24.24	60.00	42
12134	0.539	0.10958	503.019	4.905	0.03622	2.972	19.44	60.00	49
12136	0.539	0.12575	503.257	4.908	0.03603	3.428	21.84	60.00	57
12138	0.540	0.14303	503.508	4.911	0.03604	3.898	21.84	60.00	65
12140	0.540	0.16167	503.773	4.911	0.03603	4.408	19.44	60.00	73
12142	0.327	0.09448	502.857	2.968	0.03563	2.604	19.44	60.00	16
12144	0.327	0.10952	503.052	2.973	0.03583	3.002	21.84	60.00	18
12146	0.328	0.12578	503.260	2.977	0.03591	3.440	21.84	60.00	21
12148	0.328	0.14307	503.483	2.981	0.03605	3.898	21.84	60.00	24
12150	0.329	0.16162	503.730	2.982	0.03609	4.400	19.44	60.00	27
12152	0.106	0.09452	502.835	0.962	0.03558	2.609	21.84	60.00	2
12154	0.107	0.10958	503.046	0.969	0.03551	3.031	19.44	60.00	2
12156	0.107	0.12581	503.254	0.972	0.03567	3.464	21.84	60.00	2
12158	0.110	0.14303	503.496	0.995	0.03555	3.952	21.84	60.00	3
12160	0.110	0.16164	503.780	0.998	0.03526	4.503	21.84	60.00	3
560 K, 0.5669 Mole Fraction Water									
3062	5.990	0.15040	561.692	40.741	0.05272	2.785	7.44	60.00	4107
3064	5.981	0.17752	561.956	40.650	0.05278	3.279	5.04	60.00	4800

Run Point	$\frac{P_e}{\text{MPa}}$	$\frac{q}{\text{W} \cdot \text{m}^{-1}}$	$\frac{T_e}{\text{K}}$	$\frac{\rho_e}{\text{kg} \cdot \text{m}^{-3}}$	$\frac{\lambda_e}{\text{W} \cdot \text{m}^{-1} \cdot \text{K}^{-1}}$	$\frac{\Delta T_a}{\text{K}}$	$\frac{t_s}{\text{s}}$	$\frac{t_e}{\text{s}}$	Ra
3066	5.975	0.20662	562.183	40.581	0.05331	3.774	5.04	60.00	5493
3068	5.976	0.23804	562.411	40.563	0.05401	4.287	2.64	60.00	6221
3070	5.977	0.27116	562.655	40.548	0.05455	4.828	2.64	60.00	6986
3072	4.832	0.15040	561.662	32.316	0.05070	2.904	17.04	60.00	2498
3074	4.834	0.17750	561.919	32.315	0.05088	3.412	17.04	60.00	2929
3076	4.834	0.20668	562.191	32.294	0.05089	3.969	17.04	60.00	3395
3078	4.839	0.23807	562.470	32.309	0.05125	4.536	9.84	60.00	3876
3080	4.842	0.27127	562.762	32.310	0.05158	5.131	5.04	60.00	4375
3082	3.937	0.15047	561.734	25.999	0.04946	2.983	17.04	60.00	1565
3084	3.935	0.17761	561.984	25.971	0.04968	3.504	17.04	60.00	1831
3086	3.935	0.20672	562.234	25.950	0.05006	4.045	17.04	60.00	2106
3088	3.938	0.23819	562.507	25.957	0.05041	4.626	19.44	60.00	2405
3090	3.936	0.27131	562.793	25.931	0.05061	5.245	17.04	60.00	2716
3092	3.016	0.15048	561.684	19.664	0.04851	3.045	19.44	60.00	861
3094	3.017	0.17754	561.965	19.658	0.04837	3.602	17.04	60.00	1016
3096	3.016	0.20674	562.254	19.638	0.04838	4.192	17.04	60.00	1177
3098	3.015	0.23817	562.565	19.620	0.04850	4.816	17.04	60.00	1347
3100	3.016	0.27125	562.896	19.615	0.04845	5.489	19.44	60.00	1531
3102	1.958	0.15049	561.753	12.587	0.04663	3.170	17.04	60.00	343
3104	1.958	0.17758	562.032	12.580	0.04666	3.739	17.04	60.00	403
3106	1.959	0.20676	562.343	12.577	0.04670	4.349	19.44	60.00	468
3108	1.960	0.23818	562.669	12.573	0.04679	4.999	19.44	60.00	536
3110	1.960	0.27132	563.010	12.564	0.04677	5.696	17.04	60.00	608
3112	1.052	0.15049	561.807	6.681	0.04516	3.275	17.04	60.00	94
3114	1.055	0.17759	562.101	6.697	0.04507	3.872	19.44	60.00	112
3116	1.057	0.20677	562.427	6.705	0.04505	4.510	19.44	60.00	130
3118	1.058	0.23807	562.795	6.710	0.04496	5.203	19.44	60.00	150
3120	1.060	0.27129	563.182	6.718	0.04487	5.940	19.44	60.00	171
3122	0.503	0.15042	562.026	3.168	0.04311	3.429	19.44	60.00	21
3124	0.504	0.17738	562.359	3.174	0.04307	4.046	19.44	60.00	25
3126	0.504	0.20654	562.689	3.175	0.04308	4.710	19.44	60.00	29
3128	0.505	0.23794	563.025	3.175	0.04343	5.383	17.04	60.00	33
3130	0.504	0.27108	563.381	3.171	0.04367	6.100	17.04	60.00	38
3132	0.306	0.15046	561.805	1.923	0.04463	3.314	17.04	60.00	8
3134	0.306	0.17756	562.110	1.927	0.04455	3.917	17.04	60.00	9
3136	0.307	0.20672	562.465	1.931	0.04428	4.588	19.44	60.00	10
3138	0.307	0.23817	562.829	1.930	0.04421	5.294	17.04	60.00	12
3140	0.308	0.27123	563.214	1.931	0.04410	6.044	19.44	60.00	14
3142	0.114	0.15043	561.878	0.714	0.04352	3.397	17.04	60.00	1
3144	0.114	0.17761	562.185	0.718	0.04353	4.009	19.44	60.00	1
3146	0.115	0.20678	562.516	0.721	0.04351	4.670	19.44	60.00	1
3148	0.115	0.23816	562.870	0.722	0.04346	5.384	19.44	60.00	2
3150	0.115	0.27132	563.245	0.722	0.04347	6.133	19.44	60.00	2
560 K, 0.3029 Mole Fraction Water									
4062	7.018	0.15024	561.704	57.253	0.04989	2.928	7.44	60.00	6068

Run Point	$\frac{p_e}{\text{MPa}}$	$\frac{q}{\text{W} \cdot \text{m}^{-1}}$	$\frac{T_e}{\text{K}}$	$\frac{\rho_e}{\text{kg} \cdot \text{m}^{-3}}$	$\frac{\lambda_e}{\text{W} \cdot \text{m}^{-1} \cdot \text{K}^{-1}}$	$\frac{\Delta T_a}{\text{K}}$	$\frac{t_s}{\text{s}}$	$\frac{t_e}{\text{s}}$	Ra
4064	7.042	0.17730	561.925	57.437	0.05023	3.425	5.04	60.00	7139
4066	7.044	0.20642	562.186	57.422	0.05053	3.957	5.04	60.00	8227
4068	7.050	0.23777	562.500	57.425	0.05052	4.549	2.64	60.00	9439
4070	7.020	0.27095	562.843	57.125	0.05088	5.137	2.64	60.00	10515
4072	4.915	0.12552	561.482	39.489	0.04777	2.571	21.84	60.00	2384
4074	4.913	0.15019	561.698	39.455	0.04820	3.048	19.44	60.00	2816
4076	4.924	0.17728	561.957	39.526	0.04821	3.593	19.44	60.00	3328
4078	4.925	0.20635	562.238	39.514	0.04833	4.168	14.64	60.00	3851
4080	4.922	0.23769	562.541	39.461	0.04871	4.759	9.84	60.00	4377
4082	3.027	0.12554	561.524	23.969	0.04590	2.684	17.04	60.00	861
4084	3.025	0.15019	561.775	23.944	0.04597	3.205	19.44	60.00	1025
4086	3.029	0.17726	562.047	23.963	0.04619	3.764	19.44	60.00	1204
4088	3.031	0.20636	562.337	23.963	0.04620	4.379	19.44	60.00	1398
4090	3.032	0.23773	562.667	23.956	0.04607	5.056	19.44	60.00	1610
4092	2.006	0.12551	561.577	15.762	0.04412	2.793	17.04	60.00	374
4094	2.003	0.15020	561.859	15.728	0.04419	3.337	21.84	60.00	444
4096	2.004	0.17726	562.171	15.732	0.04417	3.939	21.84	60.00	524
4098	2.008	0.20638	562.509	15.748	0.04408	4.595	19.44	60.00	611
4100	2.007	0.23774	562.856	15.732	0.04421	5.277	21.84	60.00	699
4102	1.032	0.12552	561.638	8.045	0.04320	2.855	17.04	60.00	96
4104	1.032	0.15021	561.913	8.045	0.04355	3.388	19.44	60.00	114
4106	1.033	0.17727	562.221	8.045	0.04339	4.013	19.44	60.00	135
4108	1.034	0.20644	562.531	8.049	0.04365	4.645	19.44	60.00	156
4110	1.035	0.23774	562.859	8.056	0.04378	5.334	19.44	60.00	179
4112	0.504	0.12553	561.619	3.914	0.04308	2.863	21.84	60.00	22
4114	0.505	0.15021	561.924	3.919	0.04269	3.457	21.84	60.00	27
4116	0.505	0.17727	562.238	3.921	0.04281	4.068	21.84	60.00	32
4118	0.506	0.20647	562.569	3.927	0.04282	4.738	21.84	60.00	37
4120	0.507	0.23775	562.916	3.933	0.04290	5.444	19.44	60.00	43
4122	0.314	0.12553	561.656	2.432	0.04232	2.914	19.44	60.00	9
4124	0.315	0.15021	561.948	2.444	0.04238	3.482	21.84	60.00	11
4126	0.316	0.17731	562.259	2.446	0.04249	4.099	19.44	60.00	12
4128	0.316	0.20641	562.572	2.450	0.04266	4.754	19.44	60.00	14
4130	0.318	0.23776	562.900	2.458	0.04279	5.459	19.44	60.00	17
4132	0.101	0.12553	561.624	0.778	0.04247	2.904	19.44	60.00	1
4134	0.102	0.15024	561.929	0.790	0.04211	3.505	19.44	60.00	1
4136	0.103	0.17733	562.252	0.795	0.04194	4.153	19.44	60.00	1
4138	0.104	0.20640	562.596	0.800	0.04185	4.844	19.44	60.00	2
4140	0.104	0.23776	562.978	0.803	0.04196	5.566	19.44	60.00	2
620 K, 0.6132 Mole Fraction Water									
5104	7.978	0.26033	620.356	46.912	0.07039	3.608	5.04	60.00	5235
5106	7.969	0.29472	620.579	46.828	0.07095	4.048	5.04	60.00	5841
5108	7.989	0.33131	620.844	46.932	0.07081	4.553	5.04	60.00	6591
5110	7.974	0.36990	621.099	46.807	0.07117	5.052	2.64	60.00	7255
5112	6.014	0.22843	620.264	34.668	0.06562	3.411	19.44	60.00	2485

Run Point	$\frac{p_e}{\text{MPa}}$	$\frac{q}{\text{W} \cdot \text{m}^{-1}}$	$\frac{T_e}{\text{K}}$	$\frac{\rho_e}{\text{kg} \cdot \text{m}^{-3}}$	$\frac{\lambda_e}{\text{W} \cdot \text{m}^{-1} \cdot \text{K}^{-1}}$	$\frac{\Delta T_a}{\text{K}}$	$\frac{t_s}{\text{s}}$	$\frac{t_e}{\text{s}}$	Ra
5114	6.015	0.26038	620.480	34.660	0.06586	3.872	19.44	60.00	2815
5116	6.021	0.29471	620.726	34.677	0.06607	4.366	17.04	60.00	3173
5118	6.026	0.33102	621.018	34.688	0.06577	4.922	17.04	60.00	3573
5120	6.024	0.36978	621.323	34.657	0.06583	5.490	12.24	60.00	3969
5122	3.854	0.22850	620.457	21.742	0.06132	3.661	21.84	60.00	952
5124	3.854	0.26022	620.706	21.730	0.06190	4.129	19.44	60.00	1071
5126	3.853	0.29466	620.970	21.712	0.06204	4.664	17.04	60.00	1206
5128	3.853	0.33102	621.233	21.704	0.06218	5.226	19.44	60.00	1348
5130	3.851	0.36961	621.421	21.683	0.06407	5.665	2.64	60.00	1456
5132	2.059	0.18853	620.112	11.425	0.05961	3.111	21.84	60.00	206
5134	2.058	0.21789	620.361	11.414	0.05961	3.595	17.04	60.00	238
5136	2.059	0.24939	620.626	11.414	0.05951	4.122	19.44	60.00	272
5138	2.059	0.28304	620.900	11.408	0.05962	4.669	17.04	60.00	308
5140	2.059	0.31879	621.185	11.403	0.05972	5.250	19.44	60.00	345
5142	0.977	0.18853	620.180	5.366	0.05828	3.183	19.44	60.00	44
5144	0.977	0.21803	620.439	5.361	0.05827	3.681	19.44	60.00	51
5146	0.978	0.24943	620.742	5.368	0.05769	4.253	19.44	60.00	59
5148	0.979	0.28307	621.077	5.369	0.05736	4.855	17.04	60.00	67
5150	0.978	0.31893	621.443	5.361	0.05726	5.479	21.84	60.00	76
5152	0.984	0.18878	620.424	5.402	0.05818	3.192	19.44	60.00	45
5154	0.983	0.21824	620.639	5.395	0.05839	3.678	17.04	60.00	52
5156	0.982	0.24972	620.875	5.389	0.05881	4.178	17.04	60.00	58
5158	0.982	0.28339	621.138	5.387	0.05885	4.738	21.84	60.00	66
5160	0.983	0.31926	621.429	5.385	0.05889	5.334	19.44	60.00	74
5162	0.486	0.18878	620.396	2.654	0.05734	3.239	19.44	60.00	11
5164	0.485	0.21823	620.627	2.652	0.05739	3.742	19.44	60.00	12
5166	0.485	0.24984	620.878	2.649	0.05762	4.266	19.44	60.00	14
5168	0.485	0.28349	621.138	2.647	0.05780	4.825	19.44	60.00	16
5170	0.484	0.31932	621.412	2.643	0.05805	5.412	17.04	60.00	18
5172	0.278	0.18880	620.244	1.519	0.05844	3.179	19.44	60.00	3
5174	0.278	0.21830	620.483	1.519	0.05840	3.679	19.44	60.00	4
5176	0.278	0.24986	620.757	1.518	0.05818	4.226	17.04	60.00	5
5178	0.278	0.28348	621.046	1.516	0.05798	4.811	17.04	60.00	5
5180	0.278	0.31929	621.344	1.515	0.05804	5.413	17.04	60.00	6
5182	0.109	0.18885	620.335	0.593	0.05496	3.379	19.44	60.00	1
5184	0.109	0.21822	620.616	0.592	0.05483	3.915	19.44	60.00	1
5186	0.109	0.24976	620.909	0.593	0.05472	4.489	19.44	60.00	1
5188	0.109	0.28345	621.226	0.594	0.05467	5.099	19.44	60.00	1
5190	0.110	0.31927	621.545	0.596	0.05480	5.730	19.44	60.00	1
5192	0.110	0.18888	620.359	0.598	0.05615	3.309	19.44	60.00	1
5194	0.110	0.21826	620.620	0.601	0.05609	3.828	17.04	60.00	1
5196	0.111	0.24988	620.895	0.605	0.05601	4.388	19.44	60.00	1
5198	0.111	0.28348	621.197	0.606	0.05583	4.994	19.44	60.00	1
5200	0.112	0.31932	621.525	0.606	0.05558	5.651	19.44	60.00	1

Run Point	$\frac{P_e}{\text{MPa}}$	$\frac{q}{\text{W} \cdot \text{m}^{-1}}$	$\frac{T_e}{\text{K}}$	$\frac{\rho_e}{\text{kg} \cdot \text{m}^{-3}}$	$\frac{\lambda_e}{\text{W} \cdot \text{m}^{-1} \cdot \text{K}^{-1}}$	$\frac{\Delta T_a}{\text{K}}$	$\frac{t_s}{\text{s}}$	$\frac{t_e}{\text{s}}$	Ra
620 K, 0.6443 Mole Fraction Water									
15062	8.098	0.19372	619.628	46.650	0.06637	2.850	12.24	60.00	4387
15064	8.132	0.22392	619.841	46.846	0.06647	3.285	9.84	60.00	5098
15066	8.139	0.25629	620.067	46.864	0.06707	3.722	7.44	60.00	5772
15068	8.106	0.29085	620.285	46.636	0.06783	4.172	7.44	60.00	6387
15070	8.091	0.32759	620.540	46.515	0.06820	4.668	7.44	60.00	7089
15074	6.105	0.19374	619.715	34.395	0.06486	2.928	19.44	60.00	2227
15076	6.109	0.22393	619.939	34.400	0.06505	3.372	19.44	60.00	2562
15078	6.109	0.25631	620.185	34.384	0.06509	3.855	19.44	60.00	2920
15080	6.108	0.29087	620.442	34.360	0.06528	4.360	17.04	60.00	3291
15082	4.023	0.16574	619.577	22.171	0.06222	2.618	21.84	60.00	749
15084	4.019	0.19374	619.799	22.135	0.06219	3.061	19.44	60.00	871
15086	4.020	0.22393	620.039	22.131	0.06211	3.542	19.44	60.00	1006
15088	4.019	0.25631	620.286	22.115	0.06218	4.049	19.44	60.00	1146
15090	4.016	0.29088	620.544	22.089	0.06249	4.571	19.44	60.00	1289
15092	2.149	0.14011	619.413	11.619	0.05894	2.339	21.84	60.00	168
15094	2.148	0.16574	619.617	11.608	0.05932	2.749	21.84	60.00	196
15096	2.146	0.19375	619.836	11.595	0.05963	3.196	17.04	60.00	228
15098	2.149	0.22394	620.091	11.606	0.05944	3.706	17.04	60.00	264
15100	2.149	0.25633	620.348	11.600	0.05948	4.238	19.44	60.00	301
15102	1.062	0.14013	619.442	5.678	0.05693	2.421	19.44	60.00	39
15104	1.063	0.16577	619.677	5.682	0.05702	2.860	19.44	60.00	46
15106	1.060	0.19378	619.905	5.667	0.05750	3.315	19.44	60.00	53
15108	1.061	0.22398	620.164	5.666	0.05765	3.822	17.04	60.00	62
15110	1.062	0.25636	620.428	5.670	0.05767	4.373	17.04	60.00	70
15112	0.468	0.14013	619.458	2.486	0.05604	2.460	21.84	60.00	7
15114	0.468	0.16578	619.681	2.487	0.05630	2.897	19.44	60.00	9
15116	0.468	0.19378	619.915	2.488	0.05637	3.382	19.44	60.00	10
15118	0.469	0.22398	620.163	2.492	0.05655	3.897	17.04	60.00	12
15120	0.468	0.25637	620.429	2.485	0.05680	4.440	19.44	60.00	13
15122	0.275	0.14013	619.469	1.459	0.05533	2.491	19.44	60.00	3
15124	0.276	0.16577	619.681	1.465	0.05569	2.928	19.44	60.00	3
15126	0.278	0.19379	619.933	1.473	0.05550	3.434	21.84	60.00	4
15128	0.279	0.22399	620.188	1.480	0.05586	3.945	17.04	60.00	4
15130	0.280	0.25637	620.462	1.486	0.05604	4.500	19.44	60.00	5
15132	0.108	0.14014	619.494	0.570	0.05379	2.562	17.04	60.00	0
15134	0.109	0.16579	619.720	0.576	0.05444	2.995	17.04	60.00	0
15136	0.110	0.19380	619.968	0.582	0.05446	3.500	19.44	60.00	1
15138	0.112	0.22399	620.236	0.591	0.05427	4.059	21.84	60.00	1
15140	0.113	0.25637	620.523	0.596	0.05445	4.631	19.44	60.00	1
620 K, 0.3030 Mole Fraction Water									
6062	9.953	0.19521	620.447	72.834	0.05884	3.216	5.04	60.00	7793
6064	9.946	0.22563	620.680	72.746	0.05929	3.682	5.04	60.00	8887
6066	9.943	0.25827	620.878	72.697	0.05978	4.172	2.64	60.00	10044
6068	9.971	0.29307	621.110	72.879	0.06012	4.696	2.64	60.00	11351

Run Point	$\frac{p_e}{\text{MPa}}$	$\frac{q}{\text{W} \cdot \text{m}^{-1}}$	$\frac{T_e}{\text{K}}$	$\frac{\rho_e}{\text{kg} \cdot \text{m}^{-3}}$	$\frac{\lambda_e}{\text{W} \cdot \text{m}^{-1} \cdot \text{K}^{-1}}$	$\frac{\Delta T_a}{\text{K}}$	$\frac{t_s}{\text{s}}$	$\frac{t_e}{\text{s}}$	Ra
6070	9.963	0.33004	621.393	72.774	0.06012	5.276	2.64	60.00	12693
6072	7.938	0.19529	620.528	57.605	0.05652	3.366	9.84	60.00	4951
6074	7.955	0.22577	620.739	57.704	0.05710	3.848	5.04	60.00	5672
6076	7.977	0.25842	620.969	57.843	0.05763	4.357	5.04	60.00	6448
6078	7.980	0.29327	621.234	57.842	0.05787	4.917	5.04	60.00	7267
6080	7.980	0.33041	621.558	57.805	0.05795	5.524	2.64	60.00	8137
6082	6.003	0.19532	620.611	43.196	0.05377	3.552	19.44	60.00	2840
6084	6.001	0.22582	620.852	43.164	0.05398	4.087	21.84	60.00	3259
6086	6.036	0.25848	621.083	43.404	0.05467	4.616	12.24	60.00	3719
6088	6.038	0.29333	621.383	43.391	0.05489	5.214	9.84	60.00	4191
6090	6.013	0.33040	621.724	43.185	0.05493	5.863	9.84	60.00	4657
6092	4.052	0.19532	620.583	28.909	0.05266	3.637	19.44	60.00	1254
6094	4.052	0.22586	620.837	28.897	0.05293	4.183	17.04	60.00	1439
6096	4.053	0.25840	621.133	28.888	0.05288	4.789	19.44	60.00	1644
6098	4.054	0.29339	621.486	28.875	0.05270	5.453	19.44	60.00	1867
6100	4.054	0.33037	621.838	28.856	0.05321	6.080	7.44	60.00	2075
6102	2.120	0.19548	620.687	14.987	0.05201	3.692	17.04	60.00	328
6104	2.117	0.22585	620.985	14.962	0.05159	4.299	19.44	60.00	380
6106	2.116	0.25858	621.254	14.948	0.05199	4.885	21.84	60.00	430
6108	2.117	0.29329	621.582	14.949	0.05174	5.566	17.04	60.00	489
6110	2.118	0.33056	621.847	14.950	0.05335	6.085	2.64	60.00	534
6112	1.062	0.14967	620.248	7.478	0.05100	2.884	19.44	60.00	62
6114	1.062	0.17666	620.463	7.472	0.05146	3.374	17.04	60.00	73
6116	1.061	0.20568	620.708	7.463	0.05163	3.915	17.04	60.00	84
6118	1.060	0.23686	620.994	7.457	0.05149	4.520	19.44	60.00	97
6120	1.060	0.26987	621.299	7.448	0.05155	5.144	19.44	60.00	110
6122	0.520	0.14962	620.229	3.650	0.04897	3.002	17.04	60.00	15
6124	0.519	0.17653	620.527	3.642	0.04876	3.557	17.04	60.00	18
6126	0.519	0.20559	620.851	3.640	0.04877	4.141	19.44	60.00	21
6128	0.519	0.23674	621.195	3.638	0.04866	4.780	19.44	60.00	24
6130	0.518	0.26975	621.505	3.631	0.04888	5.421	17.04	60.00	27
6132	0.332	0.14947	620.285	2.330	0.04901	2.997	14.64	60.00	6
6134	0.332	0.17643	620.603	2.329	0.04877	3.555	19.44	60.00	7
6136	0.332	0.20539	620.941	2.329	0.04831	4.177	17.04	60.00	9
6138	0.332	0.23654	621.268	2.326	0.04821	4.820	17.04	60.00	10
6140	0.333	0.26947	621.613	2.330	0.04823	5.488	19.44	60.00	11
6142	0.331	0.14965	620.367	2.322	0.04902	2.999	14.64	60.00	6
6144	0.331	0.17657	620.647	2.323	0.04884	3.552	19.44	60.00	7
6146	0.331	0.20564	620.930	2.317	0.04919	4.108	17.04	60.00	8
6148	0.330	0.23680	621.210	2.315	0.04934	4.716	17.04	60.00	10
6150	0.331	0.26982	621.514	2.315	0.04945	5.361	17.04	60.00	11
6152	0.185	0.14969	620.342	1.300	0.04860	3.026	19.44	60.00	2
6154	0.186	0.17657	620.603	1.301	0.04866	3.565	17.04	60.00	2
6156	0.186	0.20556	620.896	1.301	0.04840	4.173	19.44	60.00	3
6158	0.186	0.23683	621.210	1.300	0.04869	4.779	19.44	60.00	3

Run Point	$\frac{P_e}{\text{MPa}}$	$\frac{q}{\text{W} \cdot \text{m}^{-1}}$	$\frac{T_e}{\text{K}}$	$\frac{\rho_e}{\text{kg} \cdot \text{m}^{-3}}$	$\frac{\lambda_e}{\text{W} \cdot \text{m}^{-1} \cdot \text{K}^{-1}}$	$\frac{\Delta T_a}{\text{K}}$	$\frac{t_s}{\text{s}}$	$\frac{t_e}{\text{s}}$	Ra
6160	0.186	0.26987	621.550	1.299	0.04874	5.440	17.04	60.00	3
6162	0.109	0.14963	620.351	0.763	0.04768	3.083	19.44	60.00	1
6164	0.109	0.17660	620.626	0.762	0.04769	3.638	21.84	60.00	1
6166	0.109	0.20564	620.920	0.762	0.04778	4.228	19.44	60.00	1
6168	0.109	0.23683	621.252	0.764	0.04762	4.886	19.44	60.00	1
6170	0.109	0.26981	621.595	0.764	0.04786	5.538	19.44	60.00	1
680 K, 0.5062 Mole Fraction Water									
7062	14.054	0.27202	678.320	77.411	0.08211	3.206	5.04	60.00	9494
7064	14.058	0.30571	678.473	77.413	0.08509	3.473	2.64	60.00	10275
7066	14.050	0.34135	678.686	77.331	0.08546	3.854	2.64	60.00	11359
7068	14.057	0.37894	678.885	77.340	0.08555	4.265	2.64	60.00	12556
7070	14.075	0.41850	679.099	77.411	0.08544	4.705	2.64	60.00	13861
7072	11.049	0.24039	678.441	59.730	0.07676	3.054	9.84	60.00	5057
7074	11.076	0.27211	678.558	59.875	0.08036	3.301	7.44	60.00	5491
7076	11.066	0.30579	678.753	59.793	0.08094	3.680	5.04	60.00	6095
7078	11.042	0.34151	678.965	59.633	0.08138	4.083	5.04	60.00	6713
7080	11.024	0.37914	679.166	59.502	0.08203	4.492	5.04	60.00	7341
7082	11.037	0.21104	678.178	59.695	0.07964	2.589	17.04	60.00	4287
7084	11.039	0.24048	678.367	59.686	0.07927	2.961	14.64	60.00	4895
7086	11.026	0.27216	678.564	59.585	0.07973	3.328	12.24	60.00	5476
7088	11.020	0.30584	678.763	59.525	0.08041	3.705	7.44	60.00	6074
7090	11.026	0.34143	678.969	59.540	0.08058	4.122	7.44	60.00	6754
7092	7.952	0.21107	678.333	42.184	0.07374	2.806	17.04	60.00	2157
7094	7.950	0.24044	678.522	42.160	0.07387	3.190	17.04	60.00	2446
7096	7.980	0.27214	678.718	42.313	0.07395	3.604	19.44	60.00	2783
7098	7.991	0.30582	678.944	42.356	0.07386	4.053	19.44	60.00	3132
7100	7.972	0.34146	679.175	42.233	0.07423	4.500	17.04	60.00	3451
7102	6.011	0.21107	678.326	31.508	0.07196	2.881	19.44	60.00	1176
7104	5.992	0.24047	678.482	31.399	0.07278	3.245	19.44	60.00	1314
7106	5.977	0.27218	678.662	31.305	0.07326	3.648	17.04	60.00	1466
7108	5.963	0.30581	678.857	31.222	0.07349	4.085	17.04	60.00	1630
7110	6.006	0.34150	679.105	31.439	0.07317	4.579	19.44	60.00	1853
7112	3.976	0.18328	678.185	20.588	0.07001	2.575	19.44	60.00	425
7114	3.978	0.21108	678.397	20.592	0.06936	2.992	14.64	60.00	494
7116	3.978	0.24045	678.607	20.586	0.06972	3.391	14.64	60.00	559
7118	3.974	0.27219	678.814	20.558	0.07025	3.809	19.44	60.00	625
7120	3.970	0.30587	679.037	20.531	0.07040	4.271	19.44	60.00	698
7122	1.887	0.18330	678.250	9.646	0.06683	2.699	14.64	60.00	92
7124	1.885	0.21109	678.455	9.633	0.06702	3.099	17.04	60.00	105
7126	1.884	0.24046	678.650	9.629	0.06725	3.518	19.44	60.00	120
7128	1.886	0.27223	678.878	9.633	0.06706	3.994	17.04	60.00	136
7130	1.887	0.30587	679.114	9.637	0.06718	4.479	14.64	60.00	152
7132	0.968	0.18328	678.261	4.920	0.06605	2.731	17.04	60.00	24
7134	0.968	0.21110	678.481	4.922	0.06586	3.154	17.04	60.00	27
7136	0.968	0.24052	678.667	4.920	0.06659	3.554	14.64	60.00	31

Run Point	$\frac{p_e}{\text{MPa}}$	$\frac{q}{\text{W} \cdot \text{m}^{-1}}$	$\frac{T_e}{\text{K}}$	$\frac{\rho_e}{\text{kg} \cdot \text{m}^{-3}}$	$\frac{\lambda_e}{\text{W} \cdot \text{m}^{-1} \cdot \text{K}^{-1}}$	$\frac{\Delta T_a}{\text{K}}$	$\frac{t_s}{\text{s}}$	$\frac{t_e}{\text{s}}$	Ra
7138	0.968	0.27220	678.883	4.918	0.06679	4.010	17.04	60.00	35
7140	0.968	0.30589	679.105	4.917	0.06689	4.500	17.04	60.00	39
7142	0.568	0.15748	678.164	2.883	0.06636	2.335	17.04	60.00	7
7144	0.568	0.18334	678.333	2.879	0.06649	2.713	12.24	60.00	8
7146	0.567	0.21115	678.503	2.876	0.06694	3.105	17.04	60.00	9
7148	0.567	0.24055	678.690	2.875	0.06725	3.520	17.04	60.00	10
7150	0.567	0.27229	678.914	2.874	0.06709	3.994	17.04	60.00	12
7152	0.336	0.15747	678.154	1.701	0.06464	2.397	17.04	60.00	2
7154	0.336	0.18332	678.339	1.701	0.06496	2.777	17.04	60.00	3
7156	0.336	0.21114	678.529	1.699	0.06504	3.194	14.64	60.00	3
7158	0.336	0.24052	678.728	1.698	0.06536	3.621	19.44	60.00	4
7160	0.335	0.27230	678.939	1.697	0.06558	4.086	17.04	60.00	4
7162	0.212	0.15746	678.139	1.072	0.06380	2.428	17.04	60.00	1
7164	0.212	0.18332	678.354	1.074	0.06377	2.828	14.64	60.00	1
7166	0.212	0.21113	678.558	1.073	0.06407	3.242	17.04	60.00	1
7168	0.212	0.24053	678.765	1.072	0.06422	3.685	17.04	60.00	1
7170	0.212	0.27227	678.981	1.072	0.06453	4.151	14.64	60.00	2
7172	0.108	0.15746	678.132	0.547	0.06258	2.475	14.64	60.00	0
7174	0.109	0.18332	678.349	0.551	0.06289	2.867	17.04	60.00	0
7176	0.107	0.21115	678.582	0.539	0.06288	3.303	17.04	60.00	0
7178	0.106	0.24055	678.798	0.535	0.06306	3.752	17.04	60.00	0
7180	0.106	0.27232	679.008	0.535	0.06352	4.217	17.04	60.00	0
680 K, 0.2596 Mole Fraction Water									
8072	13.942	0.17475	677.990	94.695	0.07195	2.359	5.04	60.00	7017
8074	13.946	0.20203	678.161	94.699	0.07175	2.730	5.04	60.00	8113
8076	13.934	0.23119	678.372	94.577	0.07156	3.126	5.04	60.00	9255
8078	13.925	0.26236	678.575	94.479	0.07206	3.516	2.64	60.00	10378
8080	13.934	0.29551	678.780	94.509	0.07221	3.943	2.64	60.00	11635
8082	10.917	0.17477	678.035	73.813	0.06938	2.459	14.64	60.00	4380
8084	10.934	0.20200	678.239	73.903	0.06895	2.856	12.24	60.00	5095
8086	10.938	0.23121	678.432	73.908	0.06893	3.265	7.44	60.00	5821
8088	10.940	0.26240	678.639	73.896	0.06917	3.688	5.04	60.00	6565
8090	10.912	0.29556	678.867	73.676	0.06964	4.121	5.04	60.00	7283
8094	7.894	0.20208	678.342	53.063	0.06724	2.942	17.04	60.00	2644
8096	7.873	0.23131	678.568	52.904	0.06698	3.379	19.44	60.00	3014
8098	7.870	0.26251	678.786	52.859	0.06705	3.828	19.44	60.00	3406
8100	7.888	0.29567	679.030	52.964	0.06680	4.324	17.04	60.00	3858
8102	6.054	0.14958	678.008	40.573	0.06435	2.281	21.84	60.00	1179
8104	6.068	0.17486	678.203	40.656	0.06436	2.666	19.44	60.00	1382
8106	6.025	0.20219	678.415	40.347	0.06475	3.063	14.64	60.00	1562
8108	6.026	0.23134	678.649	40.337	0.06426	3.529	19.44	60.00	1797
8110	6.062	0.26255	678.879	40.570	0.06418	4.008	19.44	60.00	2063
8112	3.794	0.14963	678.058	25.302	0.06273	2.344	26.64	60.00	458
8114	3.791	0.17493	678.254	25.277	0.06268	2.743	17.04	60.00	535
8116	3.797	0.20216	678.481	25.306	0.06199	3.204	19.44	60.00	625

Run Point	$\frac{P_e}{\text{MPa}}$	$\frac{q}{\text{W} \cdot \text{m}^{-1}}$	$\frac{T_e}{\text{K}}$	$\frac{\rho_e}{\text{kg} \cdot \text{m}^{-3}}$	$\frac{\lambda_e}{\text{W} \cdot \text{m}^{-1} \cdot \text{K}^{-1}}$	$\frac{\Delta T_a}{\text{K}}$	$\frac{t_s}{\text{s}}$	$\frac{t_e}{\text{s}}$	Ra
8118	3.797	0.23140	678.714	25.296	0.06199	3.666	17.04	60.00	714
8120	3.793	0.26262	678.969	25.260	0.06226	4.142	17.04	60.00	804
8122	1.983	0.14966	678.074	13.172	0.06215	2.368	17.04	60.00	122
8124	1.981	0.17496	678.280	13.154	0.06201	2.774	17.04	60.00	143
8126	1.983	0.20222	678.503	13.161	0.06145	3.235	19.44	60.00	166
8128	1.983	0.23145	678.730	13.158	0.06131	3.711	17.04	60.00	191
8130	1.983	0.26267	678.991	13.154	0.06109	4.227	17.04	60.00	217
8132	1.023	0.12656	677.909	6.777	0.06028	2.065	14.64	60.00	28
8134	1.024	0.14971	678.094	6.781	0.05952	2.473	19.44	60.00	33
8136	1.024	0.17500	678.310	6.779	0.05913	2.910	21.84	60.00	39
8138	1.024	0.20225	678.561	6.780	0.05914	3.362	17.04	60.00	45
8140	1.024	0.23148	678.828	6.780	0.05909	3.851	14.64	60.00	52
8142	0.429	0.12675	677.867	2.840	0.05970	2.088	26.64	60.00	5
8144	0.429	0.14992	678.054	2.841	0.05945	2.479	14.64	60.00	6
8146	0.429	0.17525	678.269	2.840	0.05962	2.891	17.04	60.00	7
8148	0.429	0.20257	678.499	2.838	0.05955	3.345	19.44	60.00	8
8150	0.429	0.23185	678.729	2.837	0.05958	3.826	19.44	60.00	9
8152	0.318	0.12674	677.903	2.101	0.05782	2.155	17.04	60.00	3
8154	0.317	0.14994	678.101	2.099	0.05780	2.550	19.44	60.00	3
8156	0.318	0.17527	678.308	2.101	0.05780	2.981	19.44	60.00	4
8158	0.318	0.20258	678.529	2.101	0.05793	3.438	17.04	60.00	4
8160	0.318	0.23188	678.769	2.102	0.05826	3.913	19.44	60.00	5
8162	0.196	0.12681	677.827	1.297	0.06152	2.027	17.04	60.00	1
8164	0.197	0.14995	678.042	1.299	0.06032	2.445	17.04	60.00	1
8166	0.197	0.17533	678.257	1.301	0.06029	2.860	17.04	60.00	1
8168	0.197	0.20261	678.485	1.303	0.06012	3.314	17.04	60.00	2
8170	0.197	0.23192	678.734	1.303	0.05971	3.819	17.04	60.00	2
8172	0.103	0.12678	677.924	0.681	0.05754	2.166	17.04	60.00	0
8174	0.103	0.14997	678.112	0.684	0.05777	2.552	21.84	60.00	0
8176	0.104	0.17532	678.298	0.686	0.05814	2.965	17.04	60.00	0
8178	0.104	0.20262	678.505	0.686	0.05824	3.420	19.44	60.00	0
8180	0.104	0.23193	678.733	0.688	0.05839	3.905	17.04	60.00	1
740 K, 0.5824 Mole Fraction Water									
9052	17.931	0.25282	740.660	89.649	0.08879	2.764	5.04	60.00	7506
9054	17.917	0.28415	740.864	89.542	0.08603	3.198	2.64	60.00	8655
9058	17.895	0.35229	741.134	89.382	0.08892	3.827	2.64	60.00	10300
9060	17.888	0.38911	741.344	89.306	0.08715	4.302	2.64	60.00	11544
9062	15.097	0.22367	740.493	74.795	0.08341	2.615	12.24	60.00	4832
9070	15.062	0.35287	741.230	74.513	0.08358	4.098	5.04	60.00	7480
9072	12.037	0.22398	740.608	58.993	0.07791	2.811	26.64	60.00	3127
9082	11.871	0.22486	740.632	58.141	0.07944	2.769	24.24	60.00	2986
9084	11.852	0.25469	740.782	58.032	0.08188	3.042	29.04	60.00	3265
9086	11.847	0.28595	741.010	57.981	0.07994	3.495	14.64	60.00	3739
9090	11.855	0.35475	741.368	57.986	0.08224	4.210	7.44	60.00	4496
9092	10.084	0.22488	740.674	49.073	0.07826	2.816	31.44	60.00	2115

Run Point	$\frac{p_e}{\text{MPa}}$	$\frac{q}{\text{W} \cdot \text{m}^{-1}}$	$\frac{T_e}{\text{K}}$	$\frac{\rho_e}{\text{kg} \cdot \text{m}^{-3}}$	$\frac{\lambda_e}{\text{W} \cdot \text{m}^{-1} \cdot \text{K}^{-1}}$	$\frac{\Delta T_a}{\text{K}}$	$\frac{t_s}{\text{s}}$	$\frac{t_e}{\text{s}}$	Ra
9094	10.086	0.25457	740.911	49.062	0.07604	3.278	21.84	60.00	2458
9096	10.051	0.28605	741.029	48.875	0.07980	3.510	26.64	60.00	2609
9098	10.049	0.31942	741.277	48.845	0.07838	3.987	31.44	60.00	2957
9100	10.069	0.35464	741.531	48.930	0.07669	4.520	19.44	60.00	3360
9102	7.997	0.22484	740.655	38.625	0.08001	2.759	26.64	60.00	1248
9104	8.030	0.25443	740.879	38.775	0.07679	3.250	26.64	60.00	1481
9106	8.032	0.28573	741.100	38.770	0.07511	3.730	21.84	60.00	1697
9114	8.022	0.25406	740.773	38.741	0.08061	3.094	21.84	60.00	1407
9116	7.994	0.28552	740.978	38.587	0.07987	3.508	31.44	60.00	1581
9118	8.000	0.31880	741.183	38.607	0.08016	3.901	21.84	60.00	1758
9120	7.999	0.35391	741.388	38.591	0.08073	4.299	24.24	60.00	1934
9122	6.099	0.19666	740.493	29.257	0.07915	2.443	29.04	60.00	616
9124	6.106	0.22405	740.660	29.284	0.08009	2.750	21.84	60.00	695
9126	6.099	0.25360	740.840	29.245	0.07926	3.144	31.44	60.00	792
9128	6.113	0.28498	741.043	29.302	0.07882	3.552	24.24	60.00	897
9130	6.111	0.31819	741.215	29.286	0.08016	3.900	29.04	60.00	983
9132	3.938	0.19668	740.531	18.739	0.07733	2.502	31.44	60.00	250
9134	3.932	0.22392	740.693	18.707	0.07848	2.807	19.44	60.00	279
9136	3.924	0.25347	740.863	18.663	0.07875	3.166	24.24	60.00	313
9138	3.919	0.28464	741.085	18.632	0.07740	3.617	29.04	60.00	356
9140	3.913	0.31761	741.240	18.600	0.07800	4.005	24.24	60.00	393
9142	1.661	0.19632	740.494	7.835	0.07544	2.561	26.64	60.00	43
9144	1.662	0.22365	740.666	7.840	0.07526	2.924	24.24	60.00	49
9146	1.661	0.25314	740.902	7.834	0.07357	3.385	19.44	60.00	57
9148	1.660	0.28449	741.110	7.828	0.07359	3.803	19.44	60.00	63
9150	1.659	0.31765	741.303	7.818	0.07461	4.189	24.24	60.00	70
9162	0.828	0.19369	740.630	3.892	0.07501	2.541	12.24	60.00	10
9164	0.827	0.22069	740.857	3.887	0.07183	3.022	21.84	60.00	12
9166	0.826	0.24980	741.059	3.882	0.07093	3.464	21.84	60.00	14
9168	0.825	0.28073	741.280	3.878	0.07068	3.906	19.44	60.00	16
9170	0.825	0.31347	741.504	3.873	0.07114	4.334	17.04	60.00	17
9172	0.455	0.19373	740.688	2.139	0.06977	2.731	21.84	60.00	3
9176	0.456	0.24983	741.070	2.141	0.06942	3.539	19.44	60.00	4
9178	0.456	0.28063	741.196	2.139	0.07292	3.786	24.24	60.00	5
9180	0.457	0.31337	741.487	2.143	0.07063	4.364	24.24	60.00	5
9182	0.113	0.19372	740.753	0.530	0.06667	2.856	21.84	60.00	0
9184	0.113	0.22068	740.937	0.532	0.06777	3.202	19.44	60.00	0
9186	0.115	0.24979	741.142	0.537	0.06745	3.641	21.84	60.00	0
9188	0.113	0.28065	741.327	0.530	0.06902	3.999	19.44	60.00	0
9190	0.113	0.31341	741.597	0.530	0.06794	4.536	24.24	60.00	0
740 K, 0.2963 Mole Fraction Water									
10078	16.986	0.34162	741.295	101.593	0.08123	4.060	2.64	60.00	10565
10080	16.974	0.37712	741.538	101.480	0.08010	4.535	2.64	60.00	11762
10082	13.948	0.24328	740.833	83.379	0.07798	3.040	7.44	60.00	5324
10084	13.959	0.27342	741.028	83.414	0.07709	3.451	5.04	60.00	6044

Run Point	$\frac{P_e}{\text{MPa}}$	$\frac{q}{\text{W} \cdot \text{m}^{-1}}$	$\frac{T_e}{\text{K}}$	$\frac{\rho_e}{\text{kg} \cdot \text{m}^{-3}}$	$\frac{\lambda_e}{\text{W} \cdot \text{m}^{-1} \cdot \text{K}^{-1}}$	$\frac{\Delta T_a}{\text{K}}$	$\frac{t_s}{\text{s}}$	$\frac{t_e}{\text{s}}$	Ra
10086	13.965	0.30530	741.169	83.436	0.07860	3.776	5.04	60.00	6614
10088	13.956	0.33896	741.383	83.353	0.07850	4.193	2.64	60.00	7321
10090	13.957	0.37436	741.616	83.325	0.07792	4.657	2.64	60.00	8120
10092	10.987	0.21498	740.721	65.560	0.07358	2.858	26.64	60.00	3069
10094	10.964	0.24332	740.834	65.416	0.07790	3.055	19.44	60.00	3266
10096	10.949	0.27345	741.038	65.306	0.07629	3.503	19.44	60.00	3727
10098	10.973	0.30534	741.245	65.429	0.07540	3.953	19.44	60.00	4220
10100	10.982	0.33896	741.438	65.463	0.07575	4.365	9.84	60.00	4660
10102	7.879	0.21499	740.722	46.891	0.07280	2.897	19.44	60.00	1566
10104	7.867	0.24333	740.856	46.811	0.07432	3.211	29.04	60.00	1730
10106	7.870	0.27344	741.032	46.815	0.07438	3.604	21.84	60.00	1940
10108	7.850	0.30535	741.249	46.684	0.07333	4.080	19.44	60.00	2182
10110	7.846	0.33889	741.487	46.642	0.07268	4.566	17.04	60.00	2435
10112	6.115	0.21464	740.754	36.326	0.06923	3.043	19.44	60.00	975
10114	6.069	0.24285	740.924	36.046	0.07191	3.316	21.84	60.00	1045
10116	6.039	0.27290	741.146	35.854	0.07232	3.704	19.44	60.00	1154
10120	6.010	0.33828	741.516	35.660	0.07383	4.496	21.84	60.00	1383
10122	3.082	0.21455	740.734	18.243	0.06937	3.040	17.04	60.00	239
10124	3.080	0.24283	740.922	18.226	0.07003	3.409	24.24	60.00	267
10126	3.078	0.27292	741.163	18.207	0.06893	3.892	19.44	60.00	304
10128	3.075	0.30473	741.388	18.184	0.06919	4.329	19.44	60.00	337
10130	3.071	0.33828	741.607	18.159	0.06983	4.762	21.84	60.00	370
10132	1.263	0.21455	740.762	7.461	0.06744	3.128	19.44	60.00	40
10134	1.261	0.24286	740.983	7.445	0.06701	3.563	19.44	60.00	46
10136	1.261	0.27295	741.233	7.441	0.06618	4.054	21.84	60.00	52
10138	1.261	0.30473	741.427	7.438	0.06734	4.449	21.84	60.00	57
10140	1.260	0.33817	741.689	7.430	0.06708	4.957	21.84	60.00	63
10142	0.312	0.21436	740.764	1.840	0.06762	3.117	21.84	60.00	2
10144	0.313	0.24250	741.001	1.844	0.06603	3.611	24.24	60.00	3
10146	0.313	0.27243	741.250	1.847	0.06487	4.128	19.44	60.00	3
10148	0.314	0.30427	741.507	1.849	0.06487	4.611	19.44	60.00	4
10150	0.314	0.33763	741.753	1.852	0.06514	5.096	19.44	60.00	4